Université de Montréal

Molecular mechanisms underlying deficient neurogenesis in Alzheimer's disease

Par

LAURA HAMILTON

Département de pathologie et biologie cellulaire

Faculté de Médecine

Thèse présentée à la Faculté des études supérieures

en vue de l'obtention du grade de Philosophiae Doctor (Ph.D.)

en pathologie et biologie cellulaire

Novembre 2014

Université de Montréal

Faculté des études supérieures et postdoctorales

Cette thèse de doctorat intitulée:

Molecular mechanisms underlying deficient neurogenesis in Alzheimer's disease

Présentée par:

LAURA HAMILTON

a été evaluée par un jury composé des personnes suivantes:

Guy Doucet, Ph.D.

Président-rapporteur

Karl J.L. Fernandes, Ph.D.

Directeur de recherche

Nicole Leclerc, Ph.D.

Membre du jury

Cindi Morshead, Ph.D.

Examinatrice externe

Alex Parker, Ph.D.

Représentant du doyen de la FESP

RÉSUMÉ

La neurogenèse est présente, dans le cerveau adulte, dans la zone sous-ventriculaire (ZSV) encadrant les ventricules latéraux et dans le gyrus dentelé (GD) de l'hippocampe, permettant l'apprentissage, la mémoire et la fonction olfactive. Ces micro-environnements possèdent des signaux contrôlant l'auto-renouvellement des cellules souches neurales (CSN), leur prolifération, leur destin et leur différenciation. Or, lors du vieillissement, les capacités régénératives et homéostatiques et la neurogenèse déclinent. Les patients atteints de la maladie d'Alzheimer (MA), comme le modèle animal reproduisant cette maladie (3xTg-AD), montrent une accélération des phénotypes liés au vieillissement dont une diminution de la neurogenèse. Notre hypothèse est que la découverte des mécanismes affectant la neurogenèse, lors du vieillissement et de la MA, pourrait fournir de nouvelles cibles thérapeutiques pour prévenir le déclin cognitif. Les études sur l'âge d'apparition et les mécanismes altérant la neurogenèse dans la MA sont contrastées et nous ont guidé vers deux études. L'examen des changements dans les étapes de la neurogenèse lors du vieillissement et du développement de la neuropathologie. Nous avons étudié la ZSV, les bulbes olfactifs et le GD de souris femelles de 11 et 18 mois, et l'apparition des deux pathologies associées à la MA : les plaques amyloïdes et les enchevêtrements neurofibrillaires. Nous avons découvert que les souris 3xTg-AD possèdent moins de cellules en prolifération, de progéniteurs et de neuroblastes, induisant une diminution de l'intégration de nouvelles cellules dans le GD et les bulbes olfactifs. Notons que le taux de neurogenèse chez ces souris de 11 mois est similaire à celui des souris de phénotype sauvage de 18 mois, indiquant une accélération des changements liés au vieillissement dans la MA. Dans la ZSV, nous avons aussi démontré une accumulation de gouttelettes lipidiques, suggérant des changements dans l'organisation et le métabolisme de la niche. Enfin, nous avons démontré que

le déficit de la neurogenèse apparait lors des premières étapes de la MA, avant l'apparition des plaques amyloïdes et des enchevêtrements neurofibrillaires. A l'examen des mécanismes inhibant la neurogenèse lors de la MA, nous voyons que chez des souris de 5 mois, le déficit de la neurogenèse dans la ZSV et le GD est corrélé avec l'accumulation de lipides, qui coïncide avec l'apparition du déclin cognitif. Nous avons aussi découvert que dans le cerveau humain de patients atteints de la MA et dans les 3xTg-AD, des gouttelettes lipidiques s'accumulaient dans les cellules épendymaires, représentant le principal soutien des CSN de la niche. Ces lipides sont des triglycérides enrichis en acide oléique qui proviennent de la niche et pas d'une défaillance du système périphérique. De plus, l'infusion locale d'acide oléique chez des souris de phénotype sauvage permet de reproduire l'accumulation de triglycérides dans les cellules épendymaires, comme dans la MA. Ces gouttelettes induisent un dérèglement de la voie de signalisation Akt-FoxO3 dans les CSN, menant à l'inhibition de leur activation *in vitro* et *in vivo*. Ces résultats permettent une meilleure compréhension de la régulation de la neurogenèse par le métabolisme lipidique. Nous avons démontré un nouveau mécanisme par lequel l'accumulation des lipides dans la ZSV induit une inhibition des capacités de prolifération et de régénération des CSN lors de la MA. Les travaux futurs permettront de comprendre comment et pourquoi le métabolisme lipidique du cerveau est altéré dans la MA, ce qui pourrait offrir de nouvelles voies thérapeutiques pour la prévention et la régénération.

Mots clefs : Maladie d'Alzheimer, vieillissement, cellules souches, neurogenèse, zone sous-ventriculaire, hippocampe, gyrus dentelé, lipide, acide gras, acide oléique.

SUMMARY

In the adult brain, neurogenesis continues in the subventricular zone (SVZ) surrounding the lateral ventricles and the dentate gyrus (DG) of the hippocampus where it plays a critical role in learning, memory, and olfactory function. Within these microenvironments, combinatorial signals control neural stem cell (NSC) self-renewal, proliferation, fate determination and differentiation. Unfortunately, during aging, neurogenesis declines along with many other homeostatic and regenerative capabilities. Furthermore, Alzheimer's disease (AD) patients and many AD models show an acceleration of several aging related phenotypes including neurogenesis. We hypothesize that uncovering how neurogenesis is affected during aging and in AD will provide novel targets for prevention of cognitive decline. However, conflicting findings including the age of onset and the mechanisms altering neurogenesis in AD propelled us to perform the two following studies. First, we examined the various steps of neurogenesis and how they change as a result of aging, neuropathology development, and neurogenic niches. We studied neurogenesis in the SVZ, olfactory bulb, and DG of 11- and 18-month-old female mice and simultaneously measured the stages of the two major AD-associated pathologies, amyloid plaques and neurofibrillary tangles. We found that, 3xTg-AD mice had fewer proliferating cells, neural progenitors and neuroblasts, resulting in decreased numbers of adult-born cells added to the dentate granule cell layer and the olfactory bulbs. Interestingly, the levels of neurogenesis in 11-month-old 3xTg mice were similar to those in 18-month-old WT mice, indicating an acceleration of aging-related changes in neurogenesis. Interestingly, we found that the deficits in neurogenesis appear at early stages of AD-associated pathologies, before the appearance of the hallmark Aβ plaques and neurofibrillary tangles. Instead, we found a pronounced accumulation of large lipid droplets, suggestive of significant organizational and metabolic changes (Chapter

2). Second, we examined the mechanisms inhibiting neurogenesis in AD. Studying young 5-month-old mice, we found that deficits in SVZ and DG neurogenesis still correlated with extensive lipid accumulation coinciding with the onset of cognitive decline. Importantly, we found that postmortem AD brains and 3xTg-AD mice accumulate neutral lipids within ependymal cells, the main support cell of the SVZ niche. Using novel mass spectrometry techniques, we identified these lipids as oleic acid-enriched triglycerides. Moreover, analysis of plasma, cerebrospinal fluid, and microdissected SVZs showed that these lipids originate from niche-derived rather than peripheral lipid metabolism defects. Remarkably, locally increasing oleic acid in wild-type mice was sufficient to recapitulate the AD-associated ependymal triglyceride phenotype and led to a de-regulation of the Akt-FoxO3 NSC preservation pathway, and inhibition of NSC activation in vitro and in vivo (Chapter 3). Together, this work suggests a novel mechanism of cognitive defects. Specifically, lipid accumulation within SVZ niche cells during early adulthood inhibits the proliferative and regenerative capacity of NSCs in AD. Future work aimed at understanding how and why brain lipid metabolism is altered in AD could provide therapeutic targets for preventative and regenerative strategies for those suffering from AD.

Keywords: Alzheimer's disease, aging, stem cell, neurogenesis, subventricular zone, hippocampus, dentate gyrus, lipid, fatty acid, oleic acid.

TABLE OF CONTENTS

LIST OF FIGURES

CHAPTER 1

CHAPTER 2

CHAPTER 3

LIST OF ABBREVIATIONS

AA	arachidonic acid
AD	Alzheimer's disease
AICD	amyloid precursor protein intracellular domain
ALDH	aldehyde dehydrogenase
aNSC	active neural stem cell
AP	alkaline phosphatase
Apo	apolipoprotein
APP	amyloid precursor protein
AraC	cystosine arabinoside
Ascl	achaete-scute homolog-1
ATP	adenosine triphosphate
Aβ	amyloid beta
BACE	beta site cleaving enzyme
BLBP	brain lipid binding protein
BMP	bone morphogenic protein
BrdU	bromodeoxyuridine
CAA	cerebral amyloid angiopathy
CNS	central nervous system
CSF	cerebral spinal fluid
CTF	c terminal fragment
DCX	doublecortin
DG	dentate gyrus

DHA	docosahexaenoic acid
DPA	docosapentaenoic acid
EA	eicosenoic acid
EDA	eicosadienoic acid
EGF	epidermal growth factor
EGFR	epidermal growth factor receptor
EPA	eicosapentaenoic acid
FABP	fatty acid binding protein
FASN	fatty acid synthase
FGF	fibroblastic growth factor
FoxO	forkhead
GABA	gamma-aminobutyric acid
GC	granule cell
GCL	granule cell layer
GFAP	glial fibrillary acid protein
ICV	intracerebroventricular
IGF	insulin-like growth factor
IL	interleukin
LeX	lewis X
LIF	leukemia inhibitory factor
LA	linoleic acid
MCI	mild cognitive impairment
mTOR	mammalian target of rapamycin

mTORC	mammalian target of rapamycin complex
NCI	non cognitively impaired
NEP	neuroepithelial cells
NeuroD	neuronal differentiation factor
NeuN	neuronal nuclei
NSC	neural stem cell
OA	oleic acid
OB	olfactory bulb
OCT4	octamer-binding transcription factor 4
PA	palmitic acid
PC	phosphatidylcholine
PCNA	proliferating cell nuclear antigen
PDGF	platelet-derived growth factor
PEDF	pigment epithelium-derived factor
PGC	periglomerular cells
POA	palmitoleic acid
PS	presenilin
PSA-NCAM	polysialylated-neural cell adhesion molecule
qNSC	quiescent neural stem cell
Rbpj	recombining binding protein suppressor of hairless
RGC	radial glial cells
RMS	rostral migratory stream
SA	stearic acid

sAPP	soluble amyloid precursor protein
SCD-1	sterol coA dehydrogenase
Shh	sonic hedgehog
Sox2	(sex-determining region y)-box-2
SVZ	subventricular zone
TAP	transit-amplifying progenitor
TGF	transforming growth factor beta
TNF	tumour necrosis factor
TUC	TOAD-64/Ulip/CRMP
TUNEL	terminal deoxynucleotidyl transferase dUTP nick end labelling
VEGF	vascular endothelial growth factor
VCAM	vascular cell adhesion protein
Wnt	wingless-integrin

ACKNOWLEDGEMENTS

I would like to express my deepest gratitude to my supervisor Dr. Karl Fernandes for his patient guidance, encouragement, and for believing in me. His critical thinking and love for science continue to inspire me.

I would like to thank the interns that worked on these projects, Christian Dugas, Alexandra Vadnais, Nita Avrith, and Carl Tamas. Thank you to our collaborators Dr. Frederic Calon and his student Dr. Carl Julien, Dr. Pierre Chaurand and his student Martin Dufresne, Dr. Martin Parent and his student Sarah Petryszyn and Dr. Alexandra Furtos for their esteemed contributions to this work.

Thank you to the former Fernandes lab members Meriem, Matt, Stef, Alex, and Greg. To the current lab members Catherine, Sandra, Loic, Louis-Charles, and Brianna, thank you for your wonderful presence, friendship, and inspiring conversations. I big thank you to Anne Aumont for her friendship and indispensible help.

I am grateful to my committee members Dr. Adriana Di Polo, Dr. Nicole Leclerc, and Dr. Diane Legace for insight and guidance and to my thesis committee members Dr. Guy Doucet, Dr. Alex Parker, and Dr. Cindi Morshead.

CHAPTER 1

I. GENERAL INTRODUCTION

I.1 NEUROGENESIS

Early neuroscientists believed the nervous system to be fixed and incapable of plasticity. However, the discovery of dividing cells in adult mammalian brains in the mid 1960's changed the way we look at the brain and importantly revealed potential for regeneration and plasticity that was thought to be impossible. It is now accepted that post-natal proliferation persists within the brains of virtually all species studied including rodents (Altman & Das, 1965), primates (Gould *et al.*, 1999; Kornack & Rakic, 1999) and humans (Eriksson *et al.*, 1998; Kukekov *et al.*, 1999), in two main brain regions, the subventricular zone (SVZ) of the lateral ventricles and the dentate gyrus (DG) of the hippocampus. In these locations, resident pools of slowly dividing glial neural stem cells (NSC) generate highly proliferative transit amplifying progenitors (TAP)s that give rise to fate-committed neuronal or glial precursors. These progenitors migrate to their final destinations and differentiate into functional post-mitotic neurons and glia important for various aspects of cerebral function and plasticity (Doetsch *et al.*, 1999a; Doetsch *et al.*, 1999b; Seri *et al.*, 2001; Imura *et al.*, 2003; Alvarez-Buylla & Lim, 2004).

In adulthood, neurogenesis is maintained by permissive microenvironments that provide key intrinsic and extrinsic factors that conserve pools of stem cells throughout life. The identification of adult NSCS and what regulates them has been a complex task, nevertheless important progress has been made in understanding what controls where, how, and why adult neurogenesis occurs.

Stem cells are functionally defined by their two cardinal properties: the ability to 1) self-renew by symmetric or asymmetric cell division and 2) differentiate into multiple cellular lineages. In mammals, there are two main types of stem cells: pluripotent embryonic stem cells

and lineage-restricted somatic stem cells. Embryonic stem cells are isolated from the inner cell mass of a blastocysts and give rise to all three germ lines: ectoderm, mesoderm and endoderm. Adult stem cells persist in various tissues including, for example, skin (epidermal) and brain (neural). These cells only give rise to cell types of the specific tissue in which they reside.

I.1.1 Development of neural stem cells

Prior to adopting their mature adult phenotype, NSCs evolve through several distinct developmental stages during which they possess different properties and perform different biological functions (Figure 1) (Alvarez-Buylla *et al.*, 2001). Throughout development of the central nervous system (CNS), the main biological function of the early NSCs precursors is *tissue growth*. In their first phase, the precursors of NSCs correspond to primitive neuroepithelial cells (NEPs). NEPs span the one cell-layer thick neural tube, contacting both the inner ventricular surface and the outer pial surface, and they divide symmetrically in order to rapidly expand their population. The onset of asymmetric cell divisions initiates a second phase, when the accumulation of differentiated progeny and consequent thickening of the neural tube cause NEPs to transition into radial glial cells (RGCs). Once thought to mainly serve a scaffolding function, it is now known that RGCs generate the neurons, astrocytes, and oligodendrocytes of the developing CNS, either directly or indirectly via intermediate progenitor cells (Noctor *et al.*, 2004; Kriegstein & Alvarez-Buylla, 2009; Hansen *et al.*, 2010). In the final stages of development, a subpopulation of RGCs begins assembling the SVZ niche that will maintain NSCs during adulthood. They do so by retracting their apical processes while maintaining ventricular contact at their basal surface, subsequently converting into either ventricle-lining

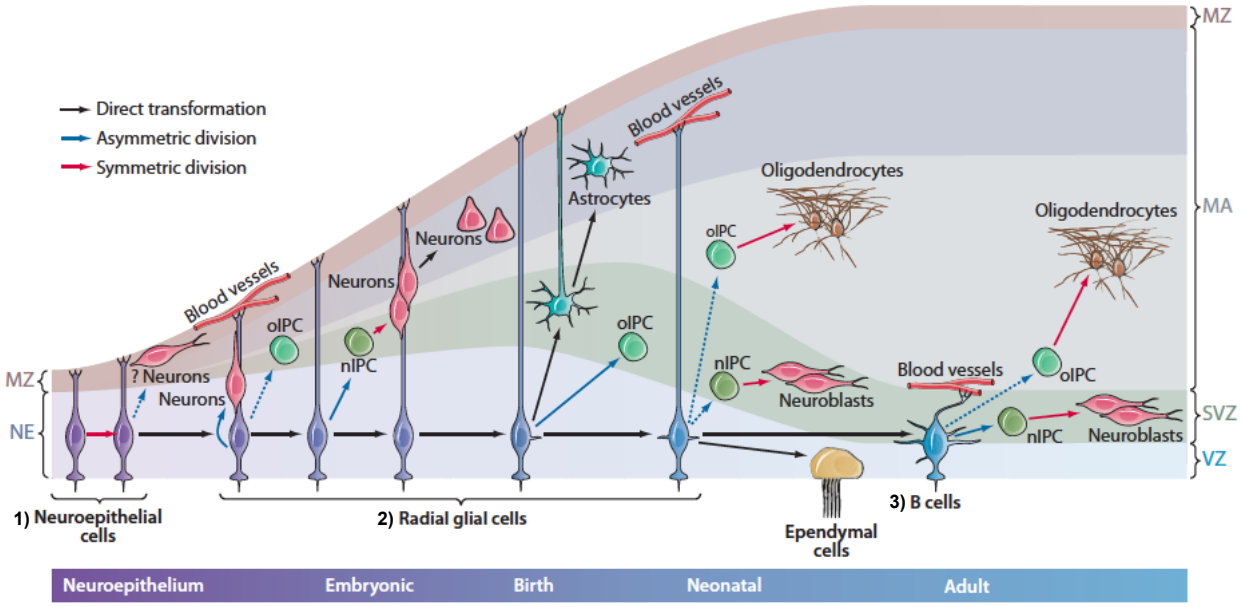

Figure 1. Development of adult neural stem cells.

Prior to adulthood, neural stem cells (NSCs) pass through three morphologically and functionally distinct phases. 1) Initially, neuroepithelial stem cells divide symmetrically to expand their numbers. As the neuroepithelium (NE) thickens, neuroepithelial cells elongate and convert into radial glial cells (RGC). 2) RGCs divide asymmetrically to generate neurons or intermediate progenitors (nIPCs). Oligodendrocytes are also derived from RGCs through oligodendrocyte progenitors (oIPCs). As the progeny from the RGCs and IPCs move into the mantel (MA) for differentiation, the brain thickens. RGCs have apical-basal polarity as they contact the ventricle via a single primary cilium and project basally to contact blood vessels, meninges and the basal lamina. A subpopulation of RGCs retain apical contact and function as NSCs in the neonate. As formation of the main populations of differentiated neural cell types nears completion, forebrain radial glial cells retract their peripheral radial process and differentiate into either ventricle-contacting subventricular zone (SVZ) astrocytes or ventricle-lining ependymal cells, setting up the SVZ niche. A subpopulation of SVZ astrocytes retains NSC characteristics postnatally and

into adulthood. 3) During adulthood, NSC function shifts to forebrain maintenance; aNSCs primarily divide asymmetrically, maintaining the size of the stem cell pool while generating new neuroblasts and glioblasts. Image originally from (Kreigsten and Alvarez-Buylla et al., 2009, Annual Review of Neuroscience), reproduced with permission from Annual Reviews © 2009. MZ, marginal zone, VZ, ventricular zone.

ependymal cells or ventricle-contacting SVZ astrocytes (Merkle *et al.*, 2004; Spassky *et al.*, 2005).

The biological function of NSCs undergoes a major change when they begin shifting into a mode dedicated to *tissue maintenance*. This maintenance phase begins in the postnatal period and continues throughout adulthood. In the forebrain, a subpopulation of SVZ astrocytes continues functioning as postnatal and adult NSCs (Doetsch *et al.*, 1999a; Imura *et al.*, 2003; Morshead *et al.*, 2003).

I.1.2 Identification of adult neural stem cells

Subventricular zone

Although new dividing cells were labelled in the brains of adult mammals in the 1960's (Altman & Das, 1965) this finding was met with significant scepticism, delaying the identification of adult NSCs for decades. In 1992, Reynolds and Weiss placed dissected adult striatum in culture in the presence of growth factors and discovered that a sub-population of cells grew into free-floating clonal colonies comprised of neural stem cells and progenitors, termed neurospheres (Reynolds & Weiss, 1992). Individual neurospheres were capable of serial self-renewal and multi-potency, as they differentiated into neurons, astrocytes and oligodendrocytes upon removal of growth factors (Vescovi *et al.*, 1993; Reynolds & Weiss, 1996). Elucidation of the appropriate culture conditions to isolate and propagate NSCs provided the first explicit demonstration of adult NSCs. Soon after, the van der Kooy lab showed that lateral ventricle subependymal cells were a necessary and sufficient source of neurospheres (Morshead *et al.*, 1994). Subsequently, neurospheres were isolated all along the ventricular system, including the spinal cord (Weiss *et al.*, 1996). Although this technique did not allow for the purification of

NSCs, the neurosphere assay did confirm their presence in the adult CNS and provided a much-needed tool for studying their properties.

Ablation techniques and lineage tracing experiments allowed for the identification of NSCs *in vivo*, their cellular lineage, and division kinetics under physiological and regenerative conditions. Morshead et al. used high doses of ^{3}H-thymidine to induce cell death in constitutively proliferating SVZ cells, depopulating the lateral ventricle sub-ependymal zone. Interestingly, a sub-population of cells persisted and displayed NSC characteristics both *in vitro* and *in vivo* (Morshead *et al.*, 1994). Clonal retroviral infection of SVZ cells demonstrated that NSCs mainly divide asymmetrically, allowing them to simultaneously maintain the stem cell pool and generate rapidly dividing TAPs. Newly generated cells remain in the SVZ for approximately 15 days before migrating to the olfactory bulb (25%) or dying (60%) (Morshead *et al.*, 1998). A related study used glial fibrillary acid protein (GFAP)-Tva mice that express the receptor for avian leukosis virus under the GFAP promoter to trace the fate of GFAP-expressing cells after infusion of fibroblastic growth factor (FGF). Injection of the avian leukosis virus encoding alkaline phosphatase (AP) into the SVZ resulted in specific labeling of GFAP-expressing cells and their progeny. After 1 day AP expression was limited to the SVZ. AP-positive migrating neuroblasts and olfactory bulb interneurons began to appear at 3.5 and 14 days after infection, respectively (Holland & Varmus, 1998). Similar findings were seen after SVZ ablation using the anti-mitotic chemotherapy drug cytosine arabinoside (AraC). After 6 days, all SVZ cells are depleted with exception of post-mitotic ependymal cells and GFAP-expressing putative NSCs. GFAP+ cells with a radial morphology resumed proliferation to first give rise to TAPs and neuroblasts, which migrate through the rostral migratory stream (RMS) to repopulate olfactory interneurons over a 14 day period (Doetsch *et al.*, 1999b). Furthermore, genetic ablation of GFAP-expressing cells

specifically, eliminated adult neurogenesis and neurosphere formation completely (Imura *et al.*, 2003; Morshead *et al.*, 2003; Garcia *et al.*, 2004). Together, these and other studies led to the conclusion that glial cells with NSC properties reside within the subependyma of the adult lateral ventricle and are the source of neurospheres in rodents. The development of whole mounts of the lateral ventricle walls aided the further characterization and localization of GFAP+ NSCs within the SVZ. NSCs were shown to send out two processes, one that projects apically through a pinwheel-like cluster of ependymal cells to contact the ventricle and the other reaching basally to touch niche blood vessels. These cells possess NSC properties, making new neurons in vivo and differentiating into neurons, astrocytes, and oligodendrocytes in vitro (Mirzadeh *et al.*, 2008). Further work by Ponti et al., revealed the proliferation dynamics of GFAP+ NSCs, achaete-scute homolog-1 (Ascl)+ TAPs, and doublecortin (DCX)+ neuroblasts *in vivo.* This study demonstrated that, following the initial division of NSCs, TAPs divide three times before turning into neuroblasts (which divided once or twice before leaving the SVZ (Ponti *et al.*, 2013). Together, these data established that glia NSCs are mainly quiescent, dividing only once every 2-3 weeks to generate TAPs that give rise to migratory, fate-committed neuroblasts and glioblasts *in vivo*.

Several succeeding studies attempted to selectively label NSCs using markers including (sex-determining region y)-box-2 (Sox2), GFAP, Nestin, Musashi 1 and 2, Prominin-1/CD133 and bromodeoxyuridine (BrdU) long-term retention (reviewed in (Basak & Taylor, 2009)). However, since NSCs are virtually identical to niche astrocytes, no specific combination of markers could definitively distinguish the two (reviewed by (Mamber *et al.*, 2013)). Many groups used flow cytometry to enrich for NSCs, using markers including Prominin-1/CD133 (Uchida *et al.*, 2000; Corti *et al.*, 2007; Obermair *et al.*, 2010), Lewis X (LeX) (Capela &

Temple, 2002), Aldehyde dehydrogenase (ALDH) (Obermair *et al.*, 2010) and peanut agglutinin (Rietze *et al.*, 2001). For example, Corti et al. showed that Prominin-1 is co-expressed with known NSC markers Sox1/2, Musashi, and Nestin and that the Prominin-1+ SVZ cells makeup the neurosphere-forming population. Moreover, transplantation experiments showed that Prominin-1-positive cells give rise to neurons and glial cells in vivo (Corti *et al.*, 2007). In a second study, Obermair et al. compared SVZ cells that expressed Prominin-1, ALDH, and LeX on both genetic and functional properties. They found that rarely dividing cells are LeX-positive, Prominin-1-positive, and express high levels of ALDH, while rapidly dividing cells are Prominin-1-negative, LeX-negative, and express low levels of ALDH. This suggested that expression of Prominin-1, Lewis X, and high levels of ALDH could be used to distinguish between quiescent, slowly dividing and active, rapidly dividing neural precursor populations. In addition, cells expressing Prominin-1, LeX, and high levels of ALDH also co-expressed high levels of the classic stem cell markers, Notch and Nestin, and expressed low levels of TAP markers such as PAX6 and Mash-1 and formed multi-potent neurospheres in vitro (Obermair *et al.*, 2010). Together, these and other studies uncovered NSCs in the adult CNS that are capable of multi-potent differentiation *in vitro*. The next step was to identify their properties and neurogenic lineage *in vivo*.

Using genetic markers and lineage tracing several sub-types of NSCs have been categorized (Figure 2). For example, three distinct Notch/Hes5-expressing NSC populations were identified in the SVZ 1) GFAP+/brain lipid binding protein (BLBP)-, 2) GFAP+/BLBP+, and 3) GFAP-/BLBP+. BLBP+ NSCs comprised a proliferating, epidermal growth factor receptor (EGFR)+, component of pinwheel structures, made up the majority of neurosphere-forming cells and persistently generated neurons in the adult (Giachino *et al.*, 2014). Using a

different set of markers, Codega et al. isolated a quiescent NSC population (qNSC) that were CD24-/GFAP+/CD133+, and an active NSC population (aNSC) that were CD24-/GFAP+/CD133+/EGFR+/Nestin+. They demonstrated that after transplantation both populations generated new neurons *in vivo*, however aNSCs generated significantly more new neurons than quiescent NSCs due to shorter cell cycles. Similarly, both qNSCs and aNSCs formed neurospheres, however aNSCs made up the vast majority of neurosphere colonies. Importantly, qNSCs could become activated in culture and upregulated Nestin and EGFR expression, suggesting that these cell types are interconvertible cell populations (Codega *et al.*, 2014). Intriguingly, the Morshead group has recently identified a novel NSC sub-population that is upstream of the classical adult GFAP-expressing NSCs. This population of NSCs is activated by leukemia inhibitor factor (LIF) and displays primitive NSC properties, such as octamer-binding transcription factor 4 (Oct4) expression and the ability to integrate into the inner cell mass of blastocysts. Moreover, these cells generate self-renewing, multi-potent neurosphere colonies that give rise to GFAP+ NSCs *in vitro*. In addition, when GFAP+ NSCs are eliminated *in vivo*, the remaining Oct4+ NSCs can fully repopulate the SVZ (Sachewsky *et al.*, 2014). Collectively, these experiments demonstrated up to four possible sub-types of adult NSCs reside within the SVZ and give rise to progenitors and neuroblasts during adulthood (Figure 2).

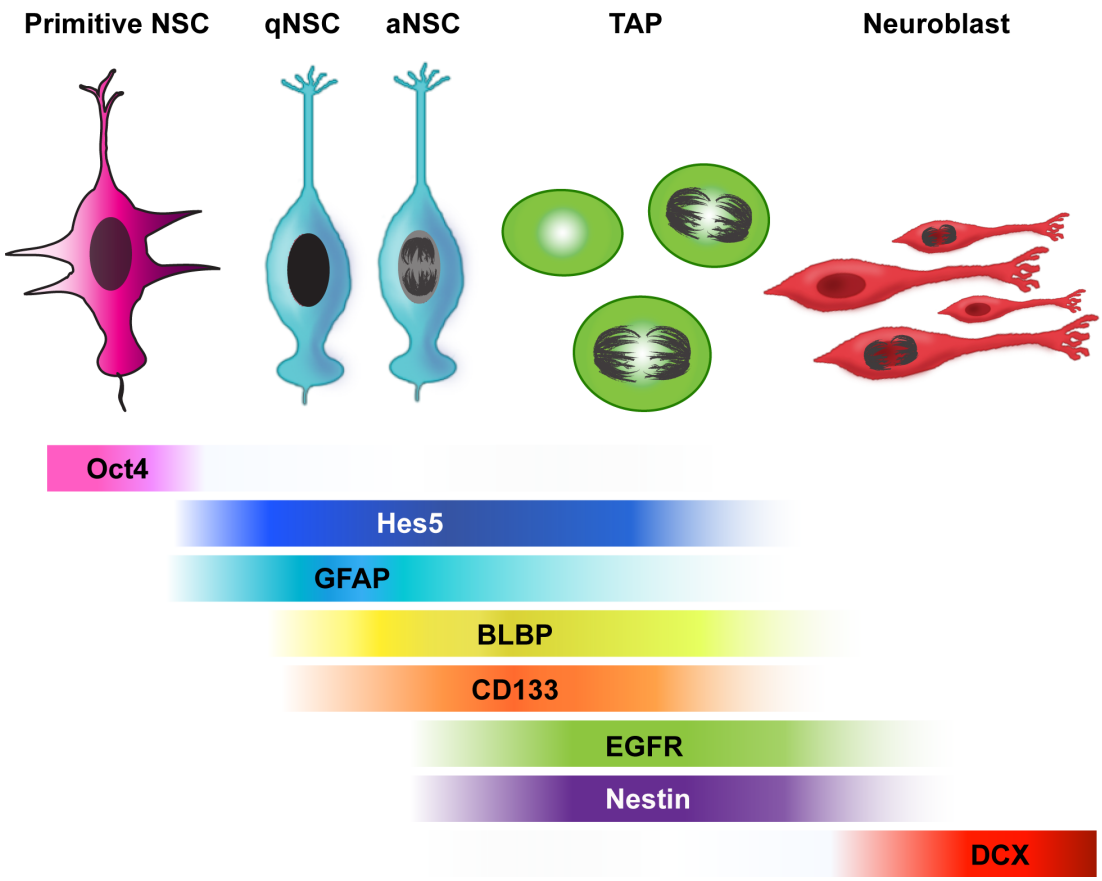

Figure 2. Summary of the neurogenic stem cell lineage and markers.

Primitive neural stem cells (NSCs) express Oct4 and respond to LIF but not EGF or FGF (Sachewsky. et al., 2014). Quiescent NSCs (qNSCs) express GFAP/CD133 but not EGFR or Nestin, while active NSCs (aNSCs) express GFAP/CD133/EGFR/Nestin (Codega et al., 2014) and Hes5/BLBP (Giachino et al., 2014). aNSCs divide to give rise to transit amplifying cells (TAPs) that begin to lose expression of immature NSC markers and become lineage specified to produce doublecortin (DCX)-expressing neuroblasts in the SVZ. (Image generated by Laura Hamilton and Loic Cochard).

Dentate gyrus

Hippocampal neurogenesis occurs in the subgranular zone located at the interface between the granule cell layer and the hilus of the DG (Altman & Das, 1965). In the prevailing model of adult hippocampal neurogenesis, similarly to the SVZ, quiescent radial glia-like (RGL) cells within the subgranular zone generate proliferative precursors known as intermediate progenitors, which give rise to neuroblasts. Within days, newborn neurons extend dendrites toward the molecular layer and project axons through the hilus toward the CA3 (Zhao *et al*., 2006). In the following weeks and months new neurons continue maturing and synaptic integration into the existing circuitry (reviewed by (Ge *et al*., 2008)).

The identification and characterization of NSCs in the dentate gyrus has not been without controversy and questions still remains as to whether definitive NSCs exist in the DG. The first study to characterize RGCs as the putative stem cells in the DG ablated dividing neural precursor cells in vivo by infusing the anti-mitotic drug AraC (Seri *et al.*, 2001). The authors followed up these initial results using viral transduction strategies to track the fate of nestin or GFAP+ cells and found that both populations give rise to adult-born hippocampal neurons (Seri *et al.*, 2004). Genetic ablation (Garcia *et al*., 2004; DeCarolis *et al*., 2013) and transgenic fate-mapping (Garcia *et al*., 2004; Seri *et al*., 2004; Ahn & Joyner, 2005; Lagace *et al*., 2007; Dranovsky *et al*., 2011; DeCarolis *et al*., 2013) further confirmed that RGC have stem cell properties. Based on these studies, it was presumed that the RGC was the stem cell that supported adult neurogenesis. In the following years, two keys studies aimed to untangling the self-renewal capacity and fate of RGCs. Importantly, one study proposed a self-renewing RGL, while the other found RGCs to have only short-term self-renewal. Two groups used in vivo clonal analysis to reveal that a single RGL undergoes several rounds of self-renewal and differentiation to produce both neurons and

astrocytes over a long duration, demonstrating characteristic stem cell properties by individual RGLs (Bonaguidi *et al*., 2011; Dranovsky *et al*., 2011). On the other hand, Encinas et al. proposed that RGLs do not possess long-term self-renewal. Instead, RGLs repeatedly entered the cell cycle once activated and generated only neurons before terminally differentiating into astrocytes (Encinas *et al*., 2011). A unifying theory can be reached if multiple subpopulations of NSCs are present within the DG and that these studies have looked at slightly different populations and thus found differing NSC properties.

I.1.3 Niche structure, cell types, and location

Adult NSCs reside in specialized niches that tightly regulate their behaviour to maintain a life-long pool. Within these niches, combinatorial extrinsic signals arising from adjacent NSCs, TAPs, neuroblasts, ependymal cells, microglia, extracellular matrix molecules, the cerebrospinal fluid (CSF), and the vasculature interact with cell-intrinsic mechanisms to control proliferation, self-renewal capacity, fate determination, migration, differentiation, and survival (Fuchs *et al.*, 2004; Morrison & Spradling, 2008; Suh *et al.*, 2009; Walker *et al.*, 2009). Insights into how the NSC niches are organized and the key regulators that promote or hinder neurogenesis are continually being uncovered.

Subventricular zone

In the lateral ventricle SVZ, NSCs are ideally positioned to be regulated by environmental signals. Systemic factors reach NSCs via their contacts with the CSF and SVZ blood vessels (Figure 3) (Mirzadeh *et al.*, 2008; Tavazoie *et al.*, 2008; Codega *et al.*, 2014). A

major source of local signals are the adjacent ependymal cells, which constitute approximately 25% of cells within this NSC niche (Doetsch *et al.*, 1997) and surround NSCs in pinwheel structures within the walls of the lateral ventricles (Mirzadeh *et al.*, 2008). Ependymal cells provide a critical barrier mediating the exchange of ions, macromolecules and immune cells between the brain and the circulating CSF, and also secrete a variety of molecules that regulate NSC activity. NSC cilia act as a mechanosensory (Singla & Reiter, 2006) and sensory organelle involved in the integration of multiple signalling pathways including sonic hedgehog (Shh), wingless-integrin (Wnt), and platelet-derived growth factor (PDGF) signalling (Corbit *et al.*, 2005; Jackson *et al.*, 2006; Rohatgi *et al.*, 2007; Corbit *et al.*, 2008). TAP cells are found closely apposed to their precursors and often in close proximity to blood vessels (Doetsch *et al.*, 1999a; Shen *et al.*, 2008; Tavazoie *et al.*, 2008). The motile cilia of ependymal cells contribute to CSF flow and are required to create gradients of Slit chemorepellents that guide neuroblast migration from the SVZ toward the olfactory bulb (Nguyen-Ba-Charvet *et al.*, 2004; Sawamoto *et al.*, 2006). Microglia, the resident immune cells of the brain, are also found scattered throughout the SVZ and although their exact role has not been identified, it is proposed that they secrete soluble factors within the niche.

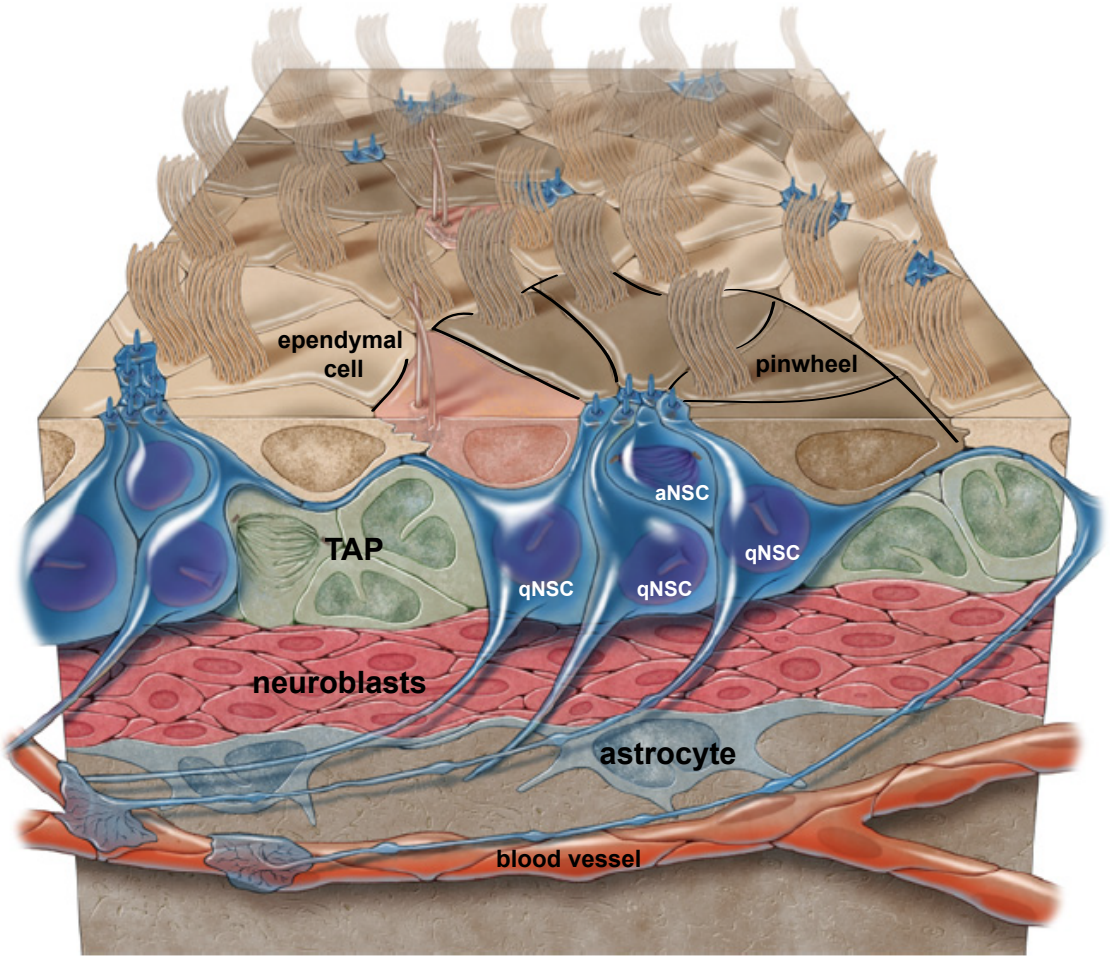

Figure 3. Cellular composition of the adult lateral ventricle niche.

Quiescent (qNSC) and active (aNSC) adult neural stem cells extend an apical extension to directly contact the ventricle cerebrospinal fluid and a long basal process ending on blood vessels. NSCs form the core of a pinwheel-like structure comprised of multi-ciliated ependymal cells. When activated, NSCs divide to produce transit-amplifying progenitors (TAPs) that differentiate into chains of migrating neuroblasts destined for the olfactory bulb. (Image originally from Mirzadeh et al., 2008, Cell Stem cell), modified and reproduced with permission from Elsevier © 2008.

Dentate gyrus

DG neurogenesis is tightly regulated by many of the same factors as the SVZ including adjacent cells, extracellular matrix molecules and the vasculature. However, unlike the SVZ ependymal and CSF factors do not border the DG. Instead, local innervations from cortical and hippocampal inputs are sources of key regulation that in addition to pre-programmed intrinsic mechanisms alter DG neurogenesis (Fuchs *et al.*, 2004; Morrison & Spradling, 2008; Suh *et al.*, 2009; Walker *et al.*, 2009; Hsieh, 2012; Aimone *et al.*, 2014).

I.1.4 Regulation of adult neural stem cells

Since adult NSCs are thought to be remnant radial glia cells from development, it is no surprise that major developmental signalling pathways including bone morphogenic protein (BMP), Shh, Notch and Wnt, continue to regulate the maintenance, activation, and fate choice of adult neural precursors.

I.1.4.1 Bone morphogenetic proteins

BMPs are a group of cytokines from the transforming growth factor (TGF)-β family, originally discovered for their ability to induce the formation of cartilage and bone (Urist, 1965). BMPs have since been shown to be essential for orchestrating tissue architecture throughout the nervous system (reviewed in (Bond *et al.*, 2012)). BMP2 and BMP4 and their downstream effectors Smad1/5/8 are present in the adult brain and NSCs and TAPs in the adult SVZ express

both these ligands and their receptors (Lim *et al.*, 2000; Peretto *et al.*, 2004). BMPs control a vast range of cellular behaviours largely due to the differential levels of BMP signalling within the niche. One explanation for this stems from the proximity of each cell type to the BMP inhibitor Noggin, expressed by ependymal cells. BMP signalling in neural progenitor cells leads to an inhibition of neural specification and promotion of glia differentiation (Lim *et al.*, 2000; Colak *et al.*, 2008). While, exogenous infusion of Noggin decreases neuroblast production in the SVZ and increases oligodendrogenesis (Colak *et al.*, 2008). It has also been suggested that NSCs express Noggin, implying additional cell autonomous regulation within the NSC population (Peretto *et al.*, 2004). Similarly, within the DG, BMP regulates NSC quiescence and activation (Bonaguidi *et al.*, 2008; Mira *et al.*, 2010). Taken together, these results suggest that the levels of BMP signalling within the adult neurogenic niches are tightly regulated to allow the production of differentiated progeny while preserving the stem cell population.

I.1.4.2 Sonic hedgehog

Shh was first identified in drosophila during a genetic screen looking for genes that regulate the patterning of embryonic segmentation. They discovered that one of their mutant embryos displayed a phenotype resembling a hedgehog and named the gene hedgehog (Nusslein-Volhard & Wieschaus, 1980). Shh signalling in the adult SVZ has been implicated in fate specification and NSCs proliferation (recently reviewed by (Alvarez-Buylla & Ihrie, 2014)). Shh has been detected in the CSF but is not prevalent in the SVZ, however, its downstream effectors are expressed throughout this region (Petrova *et al.*, 2013). Injection of Shh in the lateral ventricle in rodents, results in elevated BrdU+ proliferating cells and downstream transcription,

suggesting that Shh-responsive cells are indeed present in this region (Traiffort *et al.*, 1998). Moreover, exogenous administration of Shh has been shown to increase the number of multi-potent cells and enhance self-renewal capacity of neurospheres, indicating that this protein can activate proliferation and inhibit differentiation of NSCs (Palma *et al.*, 2005). Anti-mitotic AraC treatment revealed that it is the sub-population of remaining slow-dividing cells that display active Shh signalling (Ahn & Joyner, 2005) and this signalling is required for the establishment and maintenance of the adult SVZ (Balordi & Fishell, 2007b; a; Han *et al.*, 2008; Ihrie *et al.*, 2011). Indeed, recent studies have shown that Shh inhibits neurogenesis and leads to a decrease of proliferation and neurogenesis, and a gradual loss of NSCs, suggesting a role for Shh in NSC maintenance (Petrova *et al.*, 2013). Shh also regulates DG NSCs. Overexpression of Shh near the dentate gyrus increases proliferation and neurogenesis of SGZ cells. Additionally, in culture, Shh maintains proliferation of adult hippocampal neuronal progenitors (Lai *et al.*, 2003). Although the sources of Shh have not been clearly identified, there is evidence suggesting a role of lipophilic modification in Shh distribution. When bound to cholesterol, Shh is distributed over hundreds of micrometers. In contrast, when cholesterol is unbound, its distribution is greatly restricted, though it retained similar biological activity. Thus, lipid-modification may be one way of targeting secreted factors within the niche (Lewis *et al.*, 2001)

I.1.4.3 Notch-delta

The Notch signalling pathway is a critical regulator of lateral inhibition, a process involving cell-cell communication to control cell fate during embryonic and adult life. Several gain and loss of function experiments have shown that like Shh, Notch plays an essential role in

the preservation of the NSC pool. Indeed, Notch ligands Notch1,2,3, Jagged1 and Delta1 are expressed by GFAP-expressing NSCs and astrocytes within the SVZ as well as in neuroblasts within the RMS (Givogri *et al.*, 2006; Basak *et al.*, 2012). Jagged1 treatments *in vitro* and *in vivo* have demonstrated that Notch signalling is required for NSC proliferation and self-renewal (Nyfeler *et al.*, 2005). Similarly, it has been shown that EGF signalling in TAP cells inhibited proliferation and self-renewal of NSCs by suppressing Notch signalling within NSCs (Aguirre *et al.*, 2010). Another study showed that when recombining binding protein suppressor of hairless (Rbpj) was deleted in the adult brain, all NSCs differentiated into TAPs and neurons. As a result, neurogenesis increased transiently, but 3 months later all neural stem cells were depleted and neurogenesis was extinguished (Imayoshi *et al.*, 2010). Moreover, Nestin promoter driven Notch-1 deletion results in a selective loss of active NSCs. In contrast, quiescent NSCs were unaffected after Notch1 ablation until induced to proliferate during regeneration or aging conditions, whereupon they became Notch1-dependent and failed to maintain neurogenesis (Basak *et al.*, 2012). However, since this study only inhibited Notch signalling in Nestin+ cells, which have since been shown to be the active NSCs (Codega *et al.*, 2014), it is not surprising that only active NSCs were affected. In another study, Notch-1 deletion in vivo resulted in increased NSCs leaving the SVZ niche toward the OB, while over-expression of Notch-1 in vitro led to the transformation of TAPs to NSCs (Piccin *et al.*, 2013). Lineage tracing experiments with *Hes5::CreER* transgenic mice demonstrated that NSCs with active canonical Notch signalling generate multiple neuron subtypes in the OB (Giachino *et al.*, 2014), implying that all adult NSC lineages need Notch signalling. Interestingly, Notch signalling also appears to regulate niche components through Ephrins to keep ependymal cells from differentiating into niche astrocytes in the adult SVZ (Nomura *et al.*, 2010). Indeed, many Ephrins and Ephrin

receptors regulate cell proliferation in the adult SVZ (Conover *et al.*, 2000; Holmberg *et al.*, 2005; Ricard *et al.*, 2006; Genander & Frisen, 2010). Neural precursors in the DG are also regulated by Notch. Briefly, Notch1 and Jagged, are expressed in the SGZ where they participate in many developmental cell fate decisions and in certain contexts promotes an undifferentiated, precursor cell state (Stump *et al.*, 2002). Moreover, two Notch ligands, Jag1 and Dll4, are prominently expressed in the vasculature, and it is possible that these vasculature-derived Notch-ligands might regulate Notch signalling activity in NSCs (High *et al.*, 2008). Overall, Notch balances NSC proliferation while keeping them in an undifferentiated state.

I.1.4.4 Wnt

The Wnt signalling pathway regulates crucial aspects of cell fate determination and proliferation. Using axin-reporter mice, Adachi et al. found active Wnt signalling in GFAP+ and Mash1+ cells, but not in DCX+ neuroblasts. Retroviral stabilization of downstream effectors of canonical Wnt signalling increased the number of Mash-1+ TAPs, while chemical inhibition of Wnt signalling led to increased proliferation and enhanced neurogenesis in the OB (Adachi *et al.*, 2007). SVZ regeneration studies suggest a role for Wnt in asymmetric NSC division. They observed an upregulation of Wnt signalling after antimitotic treatment, when NSCs are biased towards asymmetric division to repopulate the SVZ (Piccin & Morshead, 2011). Continuous live imaging in culture showed that NSCs produce either neurons and astrocytes or oligodendrocytes, but never all three. Importantly, only the oligodendrocytes lineage NSCs responded to canonical Wnt signalling. In vitro and in vivo increased or decreased Wnt3 altered the number of Olig2+ cells and platelet derived growth factor receptor (PDGFR)-α positive cells, but did not affect

neurogenesis and astrogliogenesis. This suggests that Wnt contributes to the fine-tuning of oligodendrogliogenesis in the adult SVZ (Ortega *et al.*, 2013). Wnt signalling is implicated in proliferation and differentiation during development and in adult DG NSCs (Lie *et al.*, 2005; Adachi *et al.*, 2007). In particular, two Wnt target genes NeuroD1 and Prox1 play important roles in neuronal differentiation (Gao *et al.*, 2009; Karalay *et al.*, 2011). Similarly to Shh, Wnt signalling can be regulated by lipidation (reviewed by (Steinhauer & Treisman, 2009)). Wnt3 has two lipid modification sites, specifically a palmitic acid (Willert *et al.*, 2003) and a palmitoleic acid (Takada *et al.*, 2006) that regulate the affinity of Wnt to bind to its receptor (Komekado *et al.*, 2007; Kurayoshi *et al.*, 2007; Franch-Marro *et al.*, 2008) and its secretion (Willert *et al.*, 2003; Takada *et al.*, 2006; Komekado *et al.*, 2007; Kurayoshi *et al.*, 2007).

I.1.4.5 Epidermal and fibroblast growth factor

Growth factors are major regulators of adult neurogenesis. In 1992, Reynolds and Weiss first isolated adult NSCs when they placed dissected striatum in culture with EGF (Reynolds *et al.*, 1992). Other groups performed similar culture studies using FGF (Richards *et al.*, 1992; Gritti *et al.*, 1996; Johe *et al.*, 1996). Further analyses indicated that FGF- and EGF-responsive cells corresponded to the same populations within the SVZ. SVZ cells where shown to co-express EGF and FGF receptors in vivo, and when placed in vitro the number of neurospheres isolated in the presence of FGF2 and/or EGF was the same (Gritti *et al.*, 1999). It is now accepted that EGFR is primarily expressed on a sub-population of activated NSCs and their immediate progeny, TAP cells (Vescovi *et al.*, 1993; Doetsch *et al.*, 2002; Pastrana *et al.*, 2009; Codega *et al.*, 2014). Exogenous stimulation of the EGFR by ventricular infusion of EGF

increases the number of NSCs contacting the ventricle (Doetsch *et al.*, 2002), the rate of proliferating oligodendrocyte progenitors, and the number of migrating cells into the surrounding parenchyma (Craig *et al.*, 1996; Doetsch *et al.*, 2002; Aguirre *et al.*, 2005; Aguirre & Gallo, 2007; Gonzalez-Perez *et al.*, 2009). It has been shown that the endogenous ligand for the EGF pathway is transforming growth factor (TGF)-α. TGF-α-deficient mice exhibit decreased proliferation within the adult SVZ, which is rescued in vitro by administration of EGF (Tropepe *et al.*, 1997). Infusion of FGF-2 similarly increases proliferation in the adult SVZ and results in fewer newly born neurons (Kuhn *et al.*, 1997; Holland & Varmus, 1998), while loss of FGF-2 decreases the slow-dividing stem cell pool (Zheng *et al.*, 2004), suggest that FGF-2 functions to maintain the neural precursor population.

I.1.4.6 Insulin-like Growth Factor

Insulin-like growth factors (IGFs) are a group of hormones with similar structural features to insulin and are produced by many tissues in the body including the brain (Bondy CA et al., 1993, GA Werther 1990). IGFs bind to IGF receptors to activate the PI3K-AKT signalling pathway and its downstream effectors FoxO transcription factors and –TOR kinase. Genetic manipulation of IGF effectors has established their critical role in NSCs maintenance. FoxO family members (FoxO1, FoxO3, FoxO4) have been shown to control NSC self-renewal (Paik *et al.*, 2009; Ro *et al.*, 2013). FoxO1/3/4 deficiency leads to an acute increase in NSC proliferation and neurogenesis, followed by premature NSC exhaustion and loss of neurogenesis (Paik *et al.*, 2009). Interestingly, this phenotype seems to be mainly due to loss of FoxO3, as it has been shown to be necessary and sufficient for NSC preservation (Renault *et al.*, 2009; Schmidt-

Strassburger *et al.*, 2012). Indeed, loss of FoxO3 in FoxO3- knockout mice results in a smaller NSC pool in vivo and NSCs/NPs from FoxO3- knockout mice generate fewer primary and secondary neurospheres and these sphere were no longer multi-potent, indicating a loss of both cardinal properties of NSC (Renault *et al.*, 2009). Similarly, constitutive activation of FoxO3 leads to NSC apoptosis and depletion (Schmidt-Strassburger *et al.*, 2012). Our group showed that Mammalian target of rapamycin (mTOR) signalling is central in determining proliferation versus quiescence in the adult forebrain NSC niche. Within the SVZ, mTOR complex-1 (mTORC1) activation is present in TAPs but not in GFAP+ NSCs. Inhibition of mTORC1 with Rapamycin depletes the TAP pool in vivo and suppresses EGF-induced proliferation in neurosphere cultures. Interestingly, mTORC1 inhibition reduced NSC proliferation that could be reversed with EGF infusion. In addition, the decrease of neural precursor proliferation seen during aging could be reactivated by EGF administration in an mTORC1-dependent manner (Paliouras *et al.*, 2012). These findings established links between mTOR signalling, proliferation, EGF-signalling and aging-associated quiescence in the adult forebrain NSC niche. Taken together, IGF-1-downstream effectors are needed for maintaining proliferation and retaining stem cell characteristics within SVZ niche throughout life.

I.1.4.7 Hippocampal circuitry

The hippocampus and DG receive and transmit signals that modify neurogenesis (Veena *et al.*, 2011). GABA-mediated excitation promotes neuronal differentiation of type 2, nonradial NSCs, and synaptic integration of immature neurons (Ge *et al.*, 2006; Ge *et al.*, 2007). Song et al. demonstrated that nestin-expressing RGCs in the SGZ were responsive to GABA through ɣ2

receptors (Song *et al.*, 2012). GABA, presumably from spill over from GABAergic synapses, suppressed the symmetric proliferation of RGLs, instead biasing them to quiescence (Song *et al.*, 2012). Glutamate also regulates proliferation within the DG (Cameron *et al.*, 1995) and is important for neuronal development and integration (Tashiro *et al.*, 2006). A lesion in the dorsal nuclei of raphe or inhibition of serotonin production like-wise decreases proliferation in the DG (Brezun & Daszuta, 1999; 2000) (Radley & Jacobs, 2002). In addition, denervation of dopaminergic neurons also decreases proliferation of NSCs in the SGZ (Hoglinger *et al.*, 2004). Consistent with this, neurogenesis is required for the benefits of antidepressant treatments (Gould *et al.*, 1999; Santarelli *et al.*, 2003).

I.1.4.8 Brain barriers

The brain is arguably the most critical organ in the body and thus is especially well protected from both physical and metabolic stress. These barriers additionally provide regulatory and instructive roles especially within the SVZ niche. The two barriers regulating the exchange of molecules between the CNS and the blood are the blood-brain and blood-CSF barriers. As another line of defense, the brain has elaborate clearance mechanisms provided by the blood, CSF, and billions of glial cells.

The blood-brain barrier

The blood-brain barrier is a selectively permeable interface comprised of astrocytes, endothelial cells, smooth muscle pericytes, and fibroblasts. Together, these cells provide physical

and chemical obstacles to the movement of macromolecules from the periphery into the central nervous system, controlling neuronal function and protecting the brain from injury and disease (Zlokovic, 2008). Blood vessel endothelial cells restrict the diffusion of microscopic substances and large or hydrophilic molecules, while allowing the diffusion of small hydrophobic molecules such as oxygen, carbon dioxide, hormones and lipids. However, the role of vessels in the CNS extends beyond restricting the influx of molecules into the brain. In both the SVZ and DG, endothelial cells release soluble factors that stimulate the self-renewal of NSCs, inhibit their differentiation, and stimulate neurogenesis (Shen *et al.*, 2004; Shen *et al.*, 2008; Tavazoie *et al.*, 2008). Indeed, 80% of proliferating cells in the SVZ are found within 10 mm of blood vessels, and 70% of NSCs lie within 5 mm (Tavazoie *et al.*, 2008). In addition, sources of vascular endothelial growth factor (VEGF), Notch, pigment epithelium-derived factor (PEDF) secreted by endothelial cells regulate the proliferation and commitment of NSCs to a neurogenic fate (Andreu-Agullo *et al.*, 2009; Pierfelice *et al.*, 2011), suggesting a tight association between blood-borne factors and neurogenesis. Astrocytes are an essential component of the neurovascular unit and directly regulate the properties of the blood-brain barrier. There are more than a billion astrocytes throughout the brain and SVZ niche that provide crucial structural and regulatory functions. Through endfeet surrounding blood vessels, astrocytes form gap junctions and are closely associated with the vasculature and its basal lamina. In addition, astrocytes play a major role in brain metabolism by controlling the concentrations of ions and nutrients of the interstitial fluid that surrounds neurons. At this level, astrocytes can regulate the neurogenic niche indirectly by determining the accessibility of endothelial and circulation-derived factors as well as the availability of cytokines and growth factors in the basal lamina (Barres, 2008; Saunders *et al.*, 2013; Siegenthaler *et al.*, 2013). Astroglial-derived soluble and membrane bound

factors promote proliferation and neuronal fate. Astrocytes regulate neurogenesis by the secretion of factors such as Wnt3 (Lie *et al.*, 2005), Shh (Jiao & Chen, 2008), interleukin-1b, interleukin-6, and IGF-binding protein 6 (Barkho *et al.*, 2006). Indeed, astrocytes derived from neurogenic niches (DG and SVZ), but not from non-neurogenic areas (spinal cord), promote proliferation and neuronal fate commitment of neural precursors in culture (Lim & Alvarez-Buylla, 1999; Song *et al.*, 2002a). In the adult SVZ, astrocytes express Robo receptors and regulate the migration of Slit1-expressing neuroblasts through the RMS (Kaneko *et al.*, 2010). SVZ astrocytes also release glutamate to regulate the survival of neuroblasts and are critical for the maturation and synaptogenesis of newly formed neurons (Platel *et al.*, 2010). In the DG resident astrocytes are critical for the maturation and synaptogenesis of newly formed neurons. Astroglial-derived soluble and membrane bound factors promote proliferation and neuronal fate for hippocampal NSCs (Song *et al.*, 2002a; Song *et al.*, 2002b; Nedergaard *et al.*, 2003; Ullian *et al.*, 2004; Ma *et al.*, 2005). Wnt3 has been examined extensively as a candidate that mediates astrocyte signals in NSCs (Lie *et al.*, 2005). Moreover, ATP production from astrocyte metabolism regulates NSC proliferation (Cao *et al.*, 2013a; Cao *et al.*, 2013b).

Microglia are the resident macrophages and primary immune cells of the brain where they serve multiple functions, ranging from phagocytosis to neuroprotection. In the adult DG, microglia are found in the hilus and along the border of the GC layer (Wirenfeldt *et al.*, 2003). Most newborn cells in the adult DG fail to survive past the first week (Sierra *et al.*, 2010) and after 3 to 4 weeks the number of surviving newborn cells stabilizes (Kempermann & Neumann, 2003; Sierra *et al.*, 2010). Microglia modify neurogenesis through apoptosis-coupled phagocytosis of new neurons that have not integrated (Ribak *et al.*, 2009; Sierra *et al.*, 2010). The contribution of microglia to the neurogenic niche appears to depend largely on their

secretion of cytokines and chemokines. Depending on the mode of activation, microglia release proinflammatory or anti-inflammatory cytokines that can support or suppress neurogenesis (Monje *et al.*, 2003; Butovsky *et al.*, 2006).

The brain-CSF interface

The brain-CSF interface is the lining of epithelial-like ependymal cells between the cerebral ventricles and parenchyma. These cells filter CSF factors and secrete signals that aid in the regulation of SVZ NSCs. CSF surrounds the brain, both internally and externally, and is secreted by the epithelial cells of the choroid plexus in the cerebral ventricles (lateral, 3rd, and 4th ventricles). CSF is propelled through the ventricular system by beating motile cilia of ependymal cells, allowing the long-range dissemination of local and systemic signals. Growth factors and ligands implicated in SVZ NSC regulation are also present in the CSF, including TGFs, IGFs, PDGFs, Shh, Wnts, BMPs, Slits and retinoic acid (Lehtinen *et al.*, 2011; Lee *et al.*, 2012; Zappaterra & Lehtinen, 2012). Interestingly, a recent study has shown that part of the restorative function of sleep may be due to the brain increasing the clearance of degradation products of neural activity via the rapid inflow of CSF (Xie *et al.*, 2013).

Additionally, ependymal cells create a neurogenic microenvironment by secreting diffusible factors such as noggin, a selective BMP-signalling inhibitor (Lim *et al.*, 2000). NSCs contact ependymal cells via adheren junctions, anchoring them within the niche and creating an apical domain that is directly exposed to the CSF (Mirzadeh *et al.*, 2008). Some receptors, such as vascular cell adhesion protein 1 (VCAM1), are differentially distributed on NSCs. VCAM1 is localized to the apical surface of NSCs at the center of pinwheels, and disruption of VCAM1

signalling causes activation and proliferation of quiescent stem cells, and their exit from the SVZ niche (Kokovay *et al.*, 2012). Although the sources of most niche signals remain to be fully characterized, it is clear that multiple factors and sources integrate to affect NSC activity and the number of new neurons and astrocytes they produce. This interplay sustains neurogenesis over a lifetime and allows for exquisite sensitivity to a wide-range of local and distal stimuli.

The SVZ and SGZ represent neurogenic niches or local microenvironments that permit and support neurogenesis. Studies have identified key components and factors of the two neurogenic niches. It is interesting to note that there are clear similarities and important differences between SVZ and DG neural precursors. SVZ NSCs have been shown to fulfill the two cardinal stem cell properties i.e. multi-potentiality and self-renewal. They generate both neurons (Doetsch *et al*., 1999b; Gheusi *et al*., 2013) and glia including astrocytes, oligodendrocytes and ependymal cells (Menn *et al*., 2006; Gonzalez-Perez *et al*., 2009) and have the capacity for self-renewal (Reynolds & Weiss, 1992; Doetsch *et al*., 1999a). On the other hand, in the DG there is still much debate over whether "true" NSCs even exist in the adult. Evidence supporting RGLs as NSCs comes from anti-mitotic regeneration assays (Seri *et al*., 2001), genetic ablation (Garcia *et al*., 2004), and transgenic fate-mapping (Ahn & Joyner, 2005; Lagace *et al*., 2007; Dranovsky *et al*., 2011). In vivo clonal analysis further revealed that a single RGL could go through several rounds of self-renewal and differentiation to produce both neurons and astrocytes over a long duration. However, oligodendrocytes were not produced from this process (Bonaguidi *et al*., 2011). In the same year, alternative RGL properties were postulated. Encinas et al. proposed that RGLs do not possess long-term maintenance instead RGLs repeatedly enter cell cycle once activated and generate only neurons before terminally

differentiating into astrocytes (Encinas *et al*., 2011). A clear similarity between putative NSCs in the SVZ and DG is the expression of genes such as GFAP, nestin and sox2 although lineage tracing suggests that these markers label slightly different but overlapping cell populations. Moreover, regulatory factors between these two niches share commonalities and differences. For example, a main difference is that the SVZ boarders the lateral ventricle that is lined with ependymal cells that play important regulatory roles in NSC behaviour as discussed previously above. While, innervations from the entorhinal cortex, raphe nuclei and hilus interneurons are important regulators of DG neurogenesis (Leranth & Hajszan, 2007). The types of neurons produced in these two areas are also different. New neurons born in the SVZ migrate the OB and differentiate into various types of GABAergic granule cells as well as small populations of glomerular cells that express GABA or TH (Merkle *et al*., 2007; Brill *et al*., 2009). In the DG, the majority of new neurons are glutamatergic granule neurons with a small percentage of newly born cells differentiating into GABAergic basket cells.

I.1.5 The function of adult born neurons

I.1.5.1 Rodents

Subventricular zone

Olfaction is a central sense for most vertebrates as it provides information about danger, food palatability, reproductive fitness, and innate or learned behavioural responses. With this in mind, the discovery of adult neurogenesis in the olfactory system is not entirely surprising.

However, determining the precise function of adult born OB neurons has fuelled years of research and still remains largely controversial in both rodents and humans.

More than 30,000 neuroblasts exit the rodent SVZ each day (Alvarez-Buylla *et al.*, 2001), where they migrate tangentially through the rostral migratory stream (Lois & Alvarez-Buylla, 1994; Jankovski & Sotelo, 1996) toward the olfactory bulb (OB) to differentiate into periglomerular and granule olfactory interneurons (Lois & Alvarez-Buylla, 1994). Newly generated OB neurons are mainly GABAergic granule cells (GCs) with a small percentage of dopaminergic periglomerular cells (PGCs). Experiments using viral targeting or genetic lineage tracing have revealed that distinct interneurons subtypes are made within discrete locations along adult SVZ (Figure 4). Specifically, superficial granule interneurons are mainly generated by NSCs in the dorsal SVZ while deep granule interneurons are primarily derived from the ventral SVZ. Distinct populations of PGCs also arise from distinct locations within the anterior and medial adult SVZ, and a population of glutamatergic olfactory bulb neurons is derived from the dorsal SVZ (Merkle *et al.*, 2007; Brill *et al.*, 2009). Newborn OB neurons have been morphologically and electrophysiologically characterized using retroviruses. GCs become morphologically mature by 2 weeks of age, forming elaborate dendrites that extend into the external plexiform layer of the bulb (Petreanu & Alvarez-Buylla, 2002). In contrast, PGCs take 4 weeks to fully develop their dendritic and axonal morphology (Belluzzi *et al.*, 2003). Functionally, as in the adult DG, the first synapses made onto new cells are gamma-aminobutyric acid (GABA)ergic, followed soon after by glutamatergic inputs. In periglomerular cells, the maturation of the voltage-dependent sodium current, and consequently the capacity of the newly generated cells to fire action potentials, seems to precede the appearance of synaptic contacts

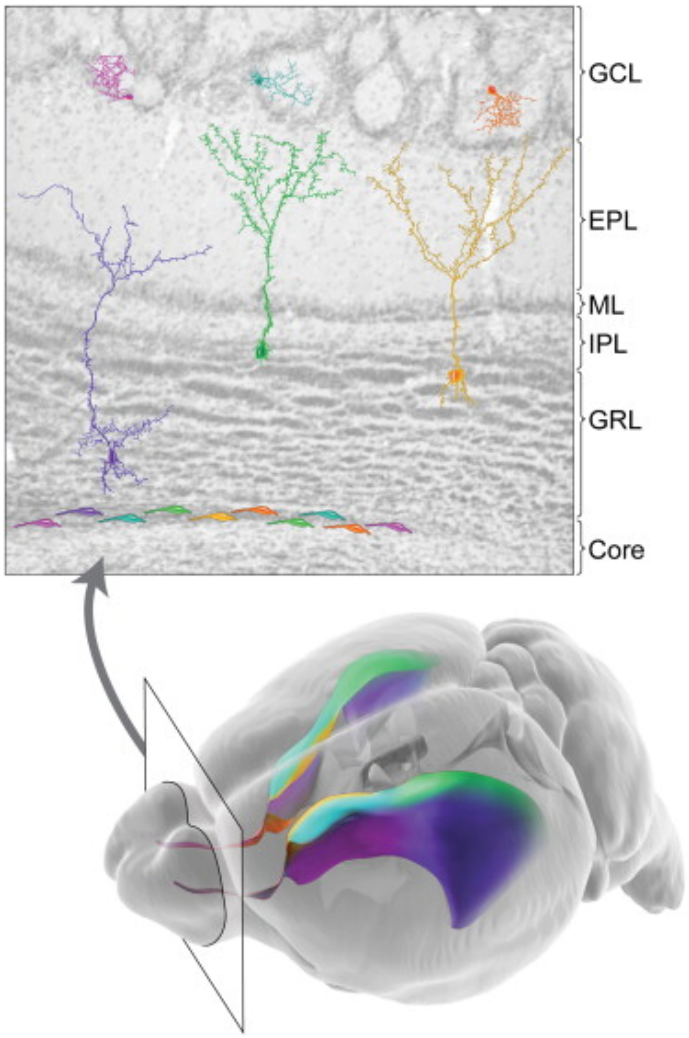

Figure 4. The adult SVZ is heterogeneous and produces discrete interneuron subtypes.

Neuroblasts derived from the subventricular zone (SVZ) enter the core of the olfactory bulb and migrate radially to populate the granular layer (GRL) and glomerular layer (GCL). Color gradients correspond to the site of origin of the differently coloured newly generated olfactory neurons. The ventral SVZ predominantly generates GABAergic deep granule cells (purple) and periglomerular cells (magenta). The dorsal SVZ, by contrast, produces superficial granule cells (green) and dopaminergic periglomerular cells (teal). The medial face of the SVZ generates glutamatergic superficial granule cells (yellow) and periglomerular cells (orange). Image from (Ihrie and Alvarez-Buylla, Neuron 2011), reproduced with permission from Elsevier © 2011.

(Belluzzi *et al.*, 2003; Carleton *et al.*, 2003). In rodents, only 50% of the new neurons integrate and survive (Petreanu & Alvarez-Buylla, 2002; Winner *et al.*, 2002). Their death via apoptosis occurs during a critical period ranging from 14 to 28 days (Yamaguchi and Mori 2005), and is strongly influenced by sensory experience (Petreanu & Alvarez-Buylla, 2002; Rochefort *et al.*, 2002). Odour enrichment and odour learning promote the rate of survival and the integration of newborn neurons in the OB (Rochefort *et al.*, 2002; Miwa & Storm, 2005; Alonso *et al.*, 2006; Mouret *et al.*, 2008; Bovetti *et al.*, 2009; Moreno *et al.*, 2009; Veyrac *et al.*, 2009; Kermen *et al.*, 2010; Sultan *et al.*, 2010; Sultan *et al.*, 2011). Conversely, blocking odour signal transduction in

sensory neurons, by nostril occlusion or diazepam-enhanced inhibition decreases the survival of newly generated neurons (Corotto *et al.*, 1994; Petreanu & Alvarez-Buylla, 2002; Yamaguchi & Mori, 2005). Notably, the size of the OB does not change throughout life, even with the continuous arrival of newborn interneurons, suggesting that adult neurogenesis in the OB is a matter of replacement rather than addition (Biebl *et al.*, 2000; Petreanu & Alvarez-Buylla, 2002). To this end, it appears that the death of new neurons in the OB actually plays a permissive role in olfactory function. When a caspase inhibitor was used to locally prevent the elimination of newborn OB neurons, a significant number of new neurons were rescued from apoptosis, which led to a deficit in odour exploration and odour discrimination (Mouret *et al.*, 2008).

In order to study the function of adult neurogenesis, various approaches have been developed to abolish the neurogenic process, including anti-mitotic drugs, focal irradiation, and conditional transgenic ablation. Blockade of neurogenesis by infusion of an antimitotic drug impaired the ability of odour detection and short-term memory, suggesting that new neurons are involved in odour detection and odour memory processing. Electrophysiological recordings

revealed that ablation of adult born neurons impairs recurrent and lateral inhibition of OB neurons and reduces the frequency of gamma oscillations which leads to decreased OB sensitivity (Breton-Provencher *et al.*, 2009). In addition, gene deficient mice, which result in a decrease of new neurons in the OB, could not discriminate between dissimilar odours (Gheusi *et al.*, 2000; Bath *et al.*, 2008). Unfortunately, not all findings have supported this result. Mice treated with γ-ray irradiation to block neurogenesis showed normal OB sensitivity (Lazarini *et al.*, 2009), suggesting that odour discrimination was not affected. In another study, genetic ablation of newly born neurons in the OB impaired the structure and neural circuits in the OB (Imayoshi *et al.*, 2008; Sakamoto *et al.*, 2011). It was reported that newly generated GCs exhibit long term synaptic plasticity that is gradually lost during neuronal maturation, indicating that newly born GCs play a more important role in plasticity than mature GCs (Nissant *et al.*, 2009). While, Sultan et al. found newborn neurons to be responsible for processing learned odorants (Sultan *et al.*, 2011). SVZ NSCs also respond to injury, migrate to the site of damage and help with brain repair (Zhang *et al.*, 2004a; Zhang *et al.*, 2004b; Zhang *et al.*, 2014). Together, these findings suggest that neurogenesis has a role in olfaction, plasticity and regeneration in rodents. In addition to the cognitive functions discussed above, some studies have examined the role of adult olfactory neurogenesis in other contexts including parental behaviour, mate choice, and mate odour recognition. However, conflicting findings and non-specific ablation techniques have made it difficult to conclusively show a role of OB neurogenesis in these behaviours.

Dentate gyrus

Determining the role of adult born DG neurons in brain function has fuelled years of research. The first evidence of functional integration of adult born neurons in mammals was

provided by van Praag et al., when they showed that adult generated DG neurons become electrophysiologically functional in vivo and are integrated as granule cells (van Praag *et al.*, 2002). Soon after, electrophysiological characterization of individual newborn neurons showed that they become increasingly hyperpolarized, progress from low to high capacitance, and from receiving GABAergic input to glutamatergic input as they mature (Ambrogini *et al.*, 2004; Esposito *et al.*, 2005). Researchers have begun to unravel the functional role of new neurons on the existing neural circuitry and their contributions to brain function (Deng *et al.*, 2009). At present, there are multiple roles identified for adult neurogenesis including learning (Gould *et al.*, 1999), spatial memory and pattern separation (Shors *et al.*, 2001; Imayoshi *et al.*, 2008; Clelland *et al.*, 2009; Deng *et al.*, 2009; Kitamura *et al.*, 2009; Aimone *et al.*, 2011; Sahay *et al.*, 2011b). Consistent with this, running increases neurogenesis (van Praag *et al.*, 1999; Kobilo *et al.*, 2011; Gregoire *et al.*, 2014) and performance on pattern separation tasks (Creer *et al.*, 2010; Sahay *et al.*, 2011a), while suppression of adult neurogenesis impairs population coding of similar contexts (Niibori *et al.*, 2012). In addition, selective ablation using a tag and ablate strategy that selectively ablated a population of predominantly mature, adult-generated neurons either before or after learning, without affecting ongoing neurogenesis found that removal of these neurons before learning did not prevent the formation of new contextual fear or water maze memories. In contrast, removal of an equivalent population after learning degraded existing contextual fear and the spatial memory-dependent water maze memories, without affecting non-hippocampal memory (Arruda-Carvalho *et al.*, 2011). Interestingly, there is evidence that new DG neurons preferentially integrate into spatial memory networks (Kee *et al.*, 2007). Moreover, it appears that young DG neurons mediate pattern separation while old granule cells facilitate pattern completion (Aimone *et al.*, 2010; 2011; Nakashiba *et al.*, 2012).

Unfortunately, differences in spatial and cellular specificity provided by most ablation techniques have made it difficult to definitively establish whether the behavioural effects observed are always attributable to ablation of neurogenesis or other indirect impairments. Moreover, due to the diversity and complexity of behavioural tests, many discrepancies in the interpretation of the results have further complicated this issue.

I.1.5.2 Humans

Similarly to rodents, the adult human brain contains two main regions where continuous neurogenesis takes place, the SVZ (Sanai *et al.*, 2004; Quinones-Hinojosa *et al.*, 2006) and the subgranular zone in the hippocampal DG (Eriksson *et al.*, 1998; Roy *et al.*, 2000; Jessberger & Gage, 2014). Over the last two decades, creative strategies have been used to study neurogenesis in humans. The first studies, analysed hippocampal tissues from deceased cancer patients that had received injections of the thymidine analog BrdU before tumour-removing surgery and co-labelled these cells with neuronal markers such as DCX and neuronal nuclei (NeuN). These reports demonstrated that in vivo, large numbers of newly generated neurons are produced within the DG (Eriksson *et al.*, 1998; Knoth *et al.*, 2010). Kukekov and colleagues subsequently isolated multi-potent neurospheres from surgical biopsy specimens containing SVZ or hippocampus of adult human brains, suggesting the presence of NSCs in these regions (Kukekov *et al.*, 1999). The SVZ niche organization and cellular composition has also been studied. The organization of the human SVZ differs slightly from that of rodents, possessing a hypocellular gap between the ventricle-lining ependymal layer, but maintaining a sub-ependymal neurogenic niche containing neural precursors and neuroblasts (Sanai *et al.*, 2004; Quinones-Hinojosa *et al.*,

2006; Leonard *et al.*, 2009). Three distinct subtypes of astrocytes have been identified along the lateral wall of the lateral ventricles. These astrocytes are located at different locations along the anterior-posterior length of the ventricle vary in size, ultrastructure, and relationship to the ependymal zone (Quinones-Hinojosa *et al.*, 2006). A subpopulation of these astrocytes proliferate in vivo and behave as multi-potent precursor cells in vitro (Sanai *et al.*, 2004), implying that SVZ astrocytes of the adult human brain indeed are NSCs. Cells expressing neuronal markers TuJ1 and DCX have been observed in the SVZ and the majority of these cells have an elongated morphology suggesting they are in migration (Bernier *et al.*, 2000; Weickert *et al.*, 2000; Sanai *et al.*, 2004; Quinones-Hinojosa *et al.*, 2006; Ernst *et al.*, 2014).

In rodents, as mentioned previously, new neurons born in the SVZ migrate through the RMS and integrate into the OB. However, due to major morphological differences between the rodent and human, similar studies conducted in the RMS and OB have led to controversial conclusions. Curtis et al. found a stream of proliferating cell nuclear antigen (PCNA)+ proliferating cells along the under surface of the caudate nucleus (caudal to the genu of the corpus callosum and the frontal cortical white matter of the gyrus rectus) travel ventrally and rostrally to enter the anterior olfactory cortex. Within this pathway, cells expressing the neuronal marker bIII-Tubulin and migratory marker polysialylated-neural cell adhesion molecule (PSA-NCAM) and BrdU/NeuN-double labeled new neurons were demonstrated in the OB (Curtis *et al.*, 2007b). In addition, studies of the human OB have shown striking similarities to the rodent. For example, staining for DCX showing newly generated neuroblasts and Ki67+ and PCNA+ proliferating cells in the granular and glomerular layers that coexpressed markers of immature neurons, such as βIII-Tubulin, DCX, and neurogenic differentiation factor-1 (NeuroD) within the OB (Maresh *et al.*, 2008). Many of these neurons colabelled with various neuronal sub-type

markers including GABAergic and dopaminergic (Bedard & Parent, 2004). On the other hand, other studies have detected neuroblasts in the anterior ventral SVZ and RMS, but not in the OB. The Frisen group utilised the presence of atmospheric 14C during nuclear bomb testing to carbon date neurons and glial cells in human tissue samples. This technique showed substantial levels of neurogenesis in the human DG whereas no evidence of ongoing neurogenesis was detected in the human SVZ or OB (Bergmann *et al.*, 2012; Spalding *et al.*, 2013). Recently, the same group found neural precursors in the human SVZ making new neurons. However, these neurons generated a subset of striatal interneurons, a neurogenic route that is absent in the rodent brain (Ernst *et al.*, 2014).

Together, this work suggests that the generation of neuroblasts from neural stem and progenitor cells in the SVZ occurs in the adult human brain. Importantly, NSCs can still be isolated from the SVZ of elderly subjects, including those with severe neurodegeneration, such as Alzheimer's disease (Leonard *et al.*, 2009). This gives hope that when the precise regulation of NSCs is understood, endogenous regeneration will be feasible.

I.2 ALZHEIMER'S DISEASE

Alzheimer's disease (AD) is an aging-related degenerative neurological disease that leads to a premature deterioration of multiple cognitive modalities including, learning, memory, and personality. Brain degeneration and synaptic loss proceeds in a region-specific and temporally determined manner, beginning in the entorhinal cortex and advancing to the hippocampus and posterior temporal and parietal cortices (Braak & Braak, 1991b; a; 1995). Symptom onset is largely determined by genetic risk factors that separate AD into two forms: genetic/early-onset

familial (onset <60 years old) and sporadic/late-onset (onset >60 years old). Intriguingly, in both cases, patients display the same cognitive symptoms and pathological hallmarks. German pathologist Alois Alzheimer was the first to describe the neuropathology of AD, uncovering five neuropathologies including focal deposits (*amyloid plaques*), intraneuronal fibrils (*neurofibrillary tangles*), blood vessel abnormalities (*cerebrovascular amyloidoisis*), glial reactivity (*gliosis*) and lipoid deposits within non-neuronal cells (*lipid accumulations*) (Alzheimer, 1907). Importantly, over a hundred years later, these findings still drive the diagnostic criteria for AD, which largely relies on neuropathological detection of amyloid plaques and neurofibrillary tangles for a definitive AD diagnosis. In recent years, genetic and genome-wide association studies have solidified the importance of the five initial AD pathologies, showing clusters of genetic mutations related to amyloid processes and storage (PS1, PS2, APP, APOE, SORL1, CLU, CRI, PICALM, BIN1, ABCA7), immunity/inflammation (CLU, CRI, EPHA1, ABCA7, MS4A4A/MS4A6E, CD33, CD2AP) and lipid transport and metabolism (APOE, CLU, ABCA7, SORL1) (reviewed in (Tosto & Reitz, 2013; Karch *et al.*, 2014). However, while significant progress has been made towards understanding the metabolism and biological impact of AD-associated pathologies, AD remains the most prominent and costly neurodegenerative disease of our time, with no cures or disease modifying therapies.

I.2.1 Alzheimer's disease pathologies and neural stem cells

NSCs not only provide the potential for endogenous regenerative and preventative strategies to combat cognitive decline, but their activity is also deregulated in AD. NSC activity

decreases naturally during aging and is altered in models of neurodegenerative diseases, suggesting an involvement in aging- and disease-associated cognitive deficits (Demars *et al.*, 2010; Hamilton *et al.*, 2010; Lazarov & Marr, 2010; Lazarov *et al.*, 2010; Bouab *et al.*, 2011; Hamilton *et al.*, 2013). In fact, this decline in neurogenesis leads to deficits in olfactory function and hippocampal-dependent learning and memory, the main cognitive symptoms of AD (Bizon *et al.*, 2004; Enwere *et al.*, 2004; Dupret *et al.*, 2008). Thus, determining how AD-associated pathologies restrain neurogenesis could uncover new strategies for ameliorating brain function in AD.

I.2.1.1 Amyloid

Genetic linkage studies identified amyloid precursor protein (APP) and presenilins (PS) 1 and 2 as three early onset AD causing genes, over 20 years ago (reviewed in (Tanzi *et al.*, 1996; Tanzi, 2012). This enabled the development of numerous transgenic animal models and allowed for in depth work on the role of amyloid in AD. The initiating factor in AD is thought to come from genetic, age-related, and/or environmental factors that lead to an imbalance between the production, clearance and aggregation of the Aβ peptide causing it to accumulate within the brain (known as the amyloid cascade hypothesis) (Hardy & Higgins, 1992). Amyloid has been linked to a wide range of biological and pathological processes including, synaptic strength inflammation, mitochondrial dysfunction, autophagy and apoptosis (Selkoe, 1991; Rhein & Eckert, 2007; Sanz-Blasco *et al.*, 2008; Spires-Jones & Hyman, 2014). In addition, many studies have demonstrated roles for various amyloid species in the regulation of neural precursor behaviour.

APP is a transmembrane protein that can be metabolized by two distinct and mutually exclusive pathways: the secretory pathway (or non-amyloidogenic) and the amyloidogenic pathway. The non-amyloidogenic pathway involves proteolytic cleavage by α-secretase resulting in the generation of soluble N-terminal fragment (sAPP) α and a carboxyl terminal fragment 83 (CTF)-83 that is further cleaved by γ-secretase into P3 and amyloid intracellular domain (AICD). The cleavage of APP by α-secretase occurs within the sequence of amino acids of the amyloid beta (Aβ) peptide, and therefore precludes the formation of amyloid peptides (Haass & Selkoe, 1993). In the amyloidogenic pathway, APP is alternatively cleaved by β-secretase, releasing a smaller N-terminal fragment (sAPPβ) and a longer CTF99 that contains the full amyloidogenic sequence of amino acids. Further cleavage by γ-secretase at either position 40 or 42 of Aβ, yields $A\beta_{1\text{-}40}$ and $A\beta_{1\text{-}42}$ peptides (Aβ). AD-associated mutations affect the processing of APP, increasing the formation of $A\beta_{1\text{-}42}$ (Selkoe & Wolfe, 2000). Aβ species are released as monomers that progressively aggregate into dimers, trimers, oligomers, protofibrils and fibrils, to finally deposit and seed the amyloid plaques. The enzymatic actions of beta-site amyloid precursor protein cleaving enzyme 1 (BACE-1) comes from PS1 at its catalytic core (Vassar, 2004; Haass & Selkoe, 2007). Consistent with this, experiments have shown that increasing β-secretase leads to higher CTF99 and Aβ generation and a decrease of CTF83 and AICD, while increasing α-secretase activity increases AICD (Kume *et al.*, 2004). Importantly, γ-secretase is responsible for the intramembranous proteolysis of many other membrane proteins including Notch, a critical NSC regulator during development and adulthood (Gaiano & Fishell, 2002).

Amyloid and neural stem cells

The impact of APP fragments on adult SVZ neural precursors has been studied by increasing the concentration of specific amyloid species in 1) *in vitro* culture systems, 2) genetically mutated mice, or 3) by intracerebroventricularly (ICV) infusion.

In vitro

In vitro experiments on adult neural precursors have shown consistently that $A\beta_{1-42}$ upregulates neurosphere number and neurogenesis. When Heo and collegues treated neurospheres with three different forms of $A\beta_{1-42}$ they found that the oligomeric form increased the number of neurospheres, their size and neural differentiation capacity, while higher concentrations of monomeric and fibrillar $A\beta_{1-42}$ had the opposite effect on these measures (Heo *et al.*, 2007). A similar study by Sotthibundhu et al. treated neural precursors with oligomeric or fibrillar $A\beta_{1-42}$ and found a significant increase in the number of neurospheres and increased neurosphere size. When neurospheres were placed in differentiation conditions, $A\beta_{1-42}$ significantly increased the number of neurons per neurosphere compared with control conditions. Importantly, $A\beta_{1-16}$ and $A\beta_{1-40}$ had no effect on these parameters. Additionally, this study compared neurosphere formation in two Aβ-producing mouse models; C100 mice (overexpressing the human APP β-carboxyl-terminal 100 amino acid fragment) and $APP_{swe}/PS1_{DE9}$ (overexpressing human APP gene with the AD-linked Swedish mutation near the β-secretase cleavage site and the PS1 gene containing an exon-9 deleted variant). When SVZs from these mice were placed in culture they found an increase in the number of neurospheres at 5 months but not at 12 months (Sotthibundhu *et al.*, 2009). From these in vitro studies, it is clear that the APP fragments and Aβ aggregation status can regulate neural precursor activity.

Alzheimer's disease transgenic mice

Neurogenesis studies in AD mutant mice have mainly focused on hippocampal neurogenesis, however in the rare cases when the SVZ was studied in parallel, similar findings have been observed in the two regions. Generally, when one AD-associated mutation of APP and/or PS1 is expressed or in cases where only knock-in technology is used, an impairment of neurogenesis is detected. Conversely, in cases where APP mutations are combined (triple or quadruple mutations) increased proliferation and neurogenesis is observed (Chuang, 2010a; Crews *et al.*, 2010b; Lazarov & Marr, 2010; Lazarov *et al.*, 2010; Winner *et al.*, 2011; Zhou *et al.*, 2011).

APP mutant mice and neural stem cells

Jin and colleges are so far the only group to study both DG and SVZ neurogenesis in APP mutant mice. Using PDGF-$APP_{swe(K670N/M671L),ind(V717F)}$ (PDAPP) transgenic mice, they quantified neural precursor activity at a presymptomatic age (3 months), before amyloid depositions and neuronal loss is observed and after in 12 month-old mice. They found an increase in numbers of proliferating cells in both regions and at both ages (Jin *et al.*, 2004a). In addition, Becker et al. found a correlation between a reduction of amyloidosis and enhanced neurogenesis in APP mutant mice. They showed that anti-Aβ42 immunotherapy reduced amyloid deposition and enhanced the numbers of BrdU+ cells in the DG of $PDAPP_{ind}$ mice (Becker *et al.*, 2007). A second study placed APP_{swe} (APP23) mice in an enriched environment

that normally enhances neurogenesis and found that this reduced the ratio of Aβ42/Aβ40 and enhanced DG neurogenesis (Mirochnic *et al.*, 2009). These findings provided early links between amyloid deposition and altered neural precursor activity. However, mechanistic insights into how APP mutations increase neurogenesis have yet to be performed.

PSI mutant mice and neural stem cells

Unfortunately, studies on AD-associated PS1 mutations have not studied neurogenesis in the SVZ. However, PS1/γ-secretase processing of APP into AICD has been shown to regulate the expression of the EGF receptor, a critical determiner of NSC activation and proliferation (Repetto *et al.*, 2007).

APP/PS1 mutant mice and neural stem cells

A variety of mice expressing various combinations of APP and PS1 mutations have been created, however, SVZ neurogenesis has only been studied in the $APP_{swe}/PS1_{\Delta E9}$ mouse. Niidome and colleagues quantified the number of PCNA-positive proliferating cells in both the SVZ and DG and found no change. However, strangely the number of 1-day BrdU-positive proliferating cells was decreased in the DG, but not in the SVZ at 9 months of age (Niidome *et al.*, 2008). Demars et al., quantified the number of 1-day BrdU+ proliferating cells and newborn neurons in the SVZ and DG and found significant decrease in both regions that coincided with a drastic upregulation of tau hyper-phosphorylation already at 2 months of age. Moreover, when they grew neurospheres from the SVZ of $APP_{swe}/PS1_{\Delta E9}$ mice, they found that these spheres

exhibit impaired proliferation dynamics and aberrant tau hyper-phosphorylation as well (Demars *et al.*, 2010). Together, the work on APP and PS1 mutant mice, suggests that an additional consequence of aberrant APP processing in AD may be the dysregulation of NSCs. However, due to the multiple variables at play in transgenic mice and various mutations driven by various promoters, it is unclear how individual APP species alter neurogenesis.

Intracerebroventricular amyloid infusion and neural stem cells

Multiple studies have determined how specific APP fragments effect neurogenesis in vivo. Early studies showed reduced levels of the sAPPα fragment in AD patients (Van Nostrand *et al.*, 1992; Lannfelt *et al.*, 1995) and several AD-causing APP mutations lie in close proximity to the β-secretase cleavage site of APP, increasing sAPPβ production at the expense of sAPPα (Thinakaran *et al.*, 1996). Interestingly, ICV infusion of sAPPα increased synaptic density and improved memory retention (Meziane *et al.*, 1998). sAPPα has also been implicated in the enhancement of synaptogenesis, neurite outgrowth, cell survival, cell adhesion (Mattson, 1997; Gakhar-Koppole *et al.*, 2008). Interestingly, sAPPα binding sites have been detected on EGFR-expressing neural precursors and PSA-NCAM-expressing neuroblasts within the SVZ. sAPPα potentiates EGF-induced neurosphere growth *in vitro* and infusion of sAPPα into the lateral ventricle of mice led to an increase in proliferation. Conversely, blocking sAPPα secretion using an α-secretase inhibitor or downregulating APP synthesis by antisense oligonucleotide against APP decreased the proliferation of EGF responsive cells, which reduced the progenitor pool (Caille *et al.*, 2004). Recently, these findings have been confirmed and extended. Infusion of sAPPα into the lateral ventricle again increased proliferation and neural differentiation.

However, this led to a decrease in the number of GFAP+/Nestin+ neural precursors in both the SVZ and DG. Interestingly infusion of sAPPβ on the other hand, led to a significant decreased in these parameters, demonstrating that an imbalance of APP fragments can have significant effects on NSC regulation (Demars *et al.*, 2013). Infusion of other amyloid beta fragments, Aβ1-42 or Aβ25-35 into the lateral ventricle decreased cell proliferation in the SVZ (Haughey *et al.*, 2002b). Li and Zuo, ICV infused aggregated $A\beta_{25–35}$ and found inhibited neurogenesis and decreased numbers of 1 day BrdU-positive cells in the dentate gyrus, but no effect on the SVZ (Li & Zuo, 2005). These experiments suggest that select Aβ fragments can decrease neural precursor proliferation and differentiation. However, these findings are not unanimous, with a second study reporting that acute ICV injection of $A\beta_{1–42}$ stimulates neurosphere number and neurogenesis when neural precursors are subsequently placed *in vitro* (Sotthibundhu *et al.*, 2009). Collectively, infusion experiments have shed light into the possible consequences of various APP fragments within the adult neurogenic niche.

Taken together, transgenic mice and infusion experiments have demonstrated that APP metabolites, including sAPPα, sAPPβ, and Aβ fragments, can have unique roles that modulate neurogenesis differently. However, the combined effects of individual species and whether they are present under physiological conditions remain unknown.

I.2.1.2 Tau

Tau has been implicated in multiple forms of dementia including AD. In fact, the major component of neurofibrillary tangles is an abnormally hyper-phosphorylated and aggregated form of tau. Tau is a microtubule-associated protein found in most tissues and highly expressed

in the nervous system. In neurons, it is an important component of the cytoskeleton where it interacts with α- and β-tubulin to promote the assembly and stability of microtubules and vesicle transport (Lindwall & Cole, 1984; Kosik, 1993). The phosphorylation state of Tau is critical to stabilize the polymers of tubulin. Hyper-phosphorylated tau is insoluble, lacks affinity for microtubules, and self associates into paired helical filament structures. More than 30 mutations of Tau on chromosome 17 have been detected in frontotemporal dementia with Parkinsonism (Goedert & Jakes, 2005). In contrast, Tau mutations do not occur in Alzheimer's disease, and the extent of neuron loss is out of proportion with the number of neurofibrillary tangles (Gomez-Isla *et al.*, 1997). Nevertheless, increased levels of phosphorylated and total tau in the cerebrospinal fluid correlate with reductions in scores on cognitive examinations (Wallin *et al.*, 2006). Elevated levels of phosphorylated tau and total tau in the CSF have been used as biomarker test with good accuracy for predicting emergent Alzheimer's disease in patients with mild cognitive impairment (Mattsson *et al.*, 2009). Experimental models have demonstrated that Aβ accumulation precedes and drives tau aggregation (Gotz *et al.*, 2001; Oddo *et al.*, 2003a). Moreover, Aβ-induced degeneration of cultured neurons and cognitive deficits in mice with an Alzheimer's disease-like symptoms require the presence of endogenous tau (Rapoport *et al.*, 2002).

Tau transgenic AD-mice and neurogenesis

In order to study the impact of tau pathology in AD, Oddo et al., created the triple transgenic Alzheimer's disease mouse model (3xTg-AD) (Oddo *et al.*, 2003b). 3xTg-AD mice contain three mutations associated with familial Alzheimer's disease and dementia (APP_{swe},

$PS1_{M146V}$ and tau $_{P301L}$). Many of the neuropathologies initially described by Alois Alzheimer have been reported in these mice including amyloid deposition, neurofibrillary tangles, and gliosis each with distinct onset ages (Figure 5). Moreover, they show temporal and region-specific Aβ and tau pathology, which closely resembles that seen in the human AD brain. In addition, 3xTg-AD mice have clear functional and cognitive impairments, including reduced long-term potentiation, as well as deficient spatial, long-term and contextual memory (Oddo *et al.*, 2003a; Oddo *et al.*, 2003b). The spatial and temporal deposition of AD-associated pathology has been characterized in detail in 3xTg-AD mice. Intraneuronal Aβ accumulates within the cortex and hippocampus beginning at 3-4 months in female 3xTg-AD mice (Carroll *et al.*, 2007; Mastrangelo & Bowers, 2008), whereas the classical pathological changes start in the neocortex and expand towards the hippocampus from around 6 months for plaques and 12 months for NFTs (Oddo *et al.*, 2003a; Mastrangelo & Bowers, 2008). In addition, gliosis and microglial activation has been observed at 6-7 months of age (Janelsins *et al.*, 2005; Caruso *et al.*, 2013). The onset of cognitive deficits in these mice is between 4-6 months of age and correlates with the accumulation of intraneuronal Aβ (Billings *et al.*, 2005; Carroll *et al.*, 2007; McKee *et al.*, 2008). Moreover, cognitive deficits are closely followed by decreased long-term potentiation and impairment in basal synaptic transmission (Oddo *et al.*, 2003b).

Neurogenesis experiments in 3xTg-AD animals have been performed in both the SVZ and DG. Rodriguez et al. quantified phosphohistone-3 (PH3)+ proliferating cells within the SVZ and DG of 2, 3, 4, 6, 9, and 12 month old 3xTg-AD mice (Rodriguez *et al.*, 2008; Rodriguez *et al.*, 2009). In the DG, they compared male and female mice and found early deficits in proliferation starting at 4 months of age in the dorsal blade of the DG in female mice, while in

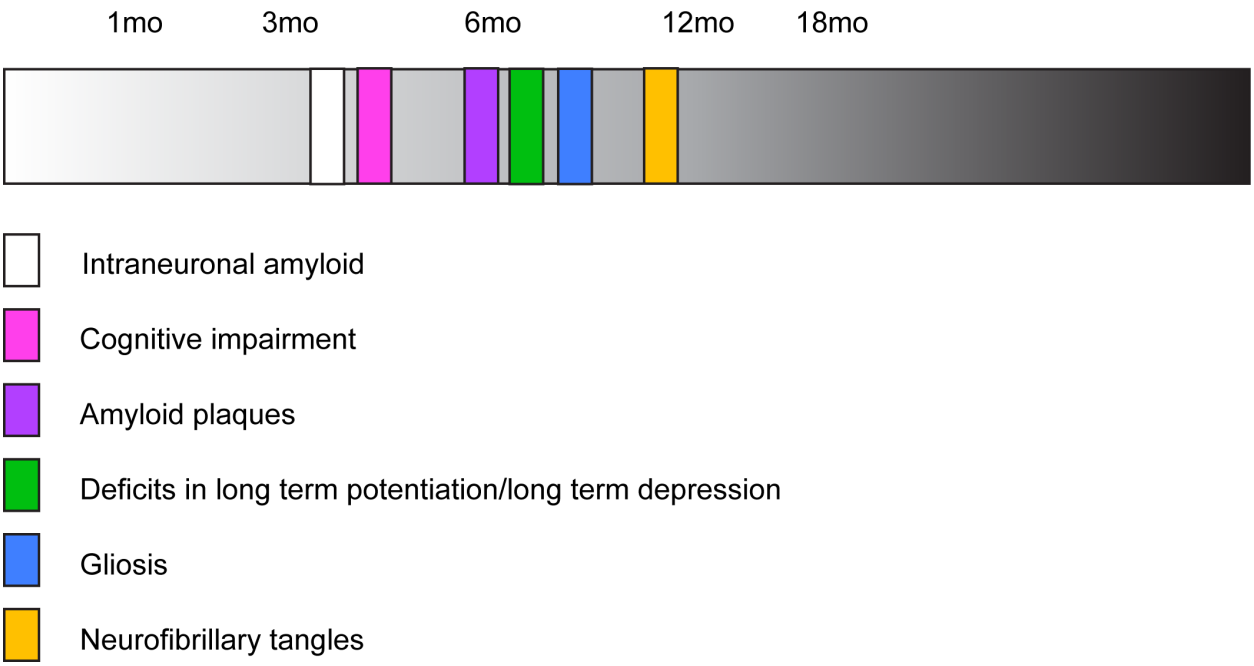

Figure 5. 3xTg-AD mouse model: onset of neuropathology and behavioural deficits.

The earliest neuropathogy observed in 3xTg-AD mice is intraneuronal amyloid beta deposition in the cortex and hippocampus at 3-4 months (Billings *et al.*, 2005). Amyloid plaque deposition has been reported as early as 6 months (Oddo *et al.*, 2003a; Billings *et al.*, 2005) but others have not observed plaques until much later, around 18 months of age (Mastrangelo & Bowers, 2008). Gliosis and microglial activation has been reported around 6-7 months of age (Janelsins *et al.*, 2005; Caruso *et al.*, 2013). Tau hyperphosphorylation has been observed at 11 months of age (Oddo *et al.*, 2003a; Mastrangelo & Bowers, 2008). Cognitive symptoms including deficits in long-term retention begin to appear at 4-5 months of age (Billings *et al.*, 2005; Carroll *et al.*, 2007; McKee *et al.*, 2008) and by 6 months there is a decrease in long-term potentiation and an impairment in basal synaptic transmission (Oddo *et al.*, 2003b). (Image generated by Laura Hamilton).

male mice, this decrease was delayed, only reaching significance at 9 months of age. Within the ventral blade, females showed significant deficits at 12 months, while males showed deficits at 6 months of age (Rodriguez *et al.*, 2008). In a follow-up study, the same group found impaired proliferation beginning at 3 months in the SVZ of male 3xTg-AD mice (Rodriguez *et al.*, 2009). This work was the first to study how an AD-like microenvironment containing both amyloid plaques and neurofibrillary tangles affects neurogenesis. These studies also took into account the age, sex, and both neurogenic niches, providing important clues into how neurogenesis is impacted as pathological hallmarks of AD progress. These findings suggested that early deficits in proliferation coincide with cognitive decline, however, the mechanisms underlying the deficits in neurogenesis were not investigated.

I.2.1.3 Cerebral amyloid angiopathy

Cerebral amyloid angiopathy (CAA) affects more than 90% of patients with Alzheimer's disease (Greenberg *et al.*, 2004) and results from the accumulation of amyloid beta in blood vessels, inducing vasoconstriction and occlusion of cerebral blood flow (Smith & Greenberg, 2009; Thal *et al.*, 2009). Aβ is also cytotoxic to endothelial (Xu *et al.*, 2001; Suhara *et al.*, 2003) and smooth-muscle cells (Van Nostrand *et al.*, 1998; Mok *et al.*, 2006), conferring a predisposition to cerebral hemorrhages (Suter *et al.*, 2002; Haglund *et al.*, 2006). Vascular injury and parenchymal inflammation has been suggested to perpetuate the cycle of protein aggregation and oxidation in the brain. The clearance of Aβ through diseased blood vessels and the blood-brain barrier is also impeded, perpetuating the deposition of amyloid throughout the brain (Shibata *et al.*, 2000; Weller *et al.*, 2008; Ito *et al.*, 2013). Although the role of amyloid

angiopathy in neurogenesis has not been directly explored, as mentioned previously, blood vessels are a critical component of the adult NSC niche, as they mediate the flow of molecules that regulate the proliferation of NSCs and progenitors. Moreover, recent parabiosis experiments have demonstrated a role of systemic factors in the suppression of neurogenesis during aging (Villeda *et al.*, 2011).

I.2.1.4 Gliosis/Inflammation

The presence of activated glial cells and the increase in inflammation-associated proteins in the AD brain has led to the consideration that chronic inflammation plays a role in the pathophysiology of AD (McGeer & McGeer, 1995). Astrocytes isolated from AD patients and reactive astrocytes from AD-transgenic mice have been shown to secrete TGFβ1 and IL10 (Apelt & Schliebs, 2001; Blasko *et al.*, 2004). Activated microglia and reactive astrocytes localize to amyloid plaques, and their biochemical markers are elevated in the brains of patients with AD (Wyss-Coray & Mucke, 2002). Another study showed that initially, microglia degrade Aβ but that chronically activated microglia release chemokines and a cascade of damaging cytokines including, IL-1, IL-6, and tumour necrosis factor α that damage cells (Akiyama *et al.*, 2000). Several mediators of inflammation such as IL-1β, IL-6, and tumour necrosis factor (TNF)-α have been extensively studied in the CSF of AD patients, but conflicting results have been observed (Teunissen *et al.*, 2002). Indeed, although the majority of studies report no difference (Lanzrein *et al.*, 1998; Galimberti *et al.*, 2008), others have seen an increase (Blum-Degen *et al.*, 1995; Tarkowski *et al.*, 1999) and even a decrease (Yamada *et al.*, 1995) in levels of these inflammatory markers in the CSF of AD patients compared with controls. Thus, it will be

interesting to see if there is a role for AD-associated inflammatory signals on neurogenesis and whether NSCs could also be contributing to the gliosis by over-producing new astrocytes during AD.

I.2.1.5 Lipoid accumulation

Lipids have wide-reaching functions in the body including, insulation, protection and energy production and storage. Moreover, lipids provide critical signals for the dynamic requirements of cellular behaviour by modulating gene expression, growth and survival pathways, and inflammatory and metabolic responses (Saltiel & Kahn, 2001; Hotamisligil, 2006). To execute these various tasks, the body absorbs, synthesizes and modifies all major classes of lipids including, fatty acids, glycerolipids (triglycerides, diglycerides, monoglycerides), glycerophospholipids (ex: phosphocholines. Lysophosphocholines, phosphatidylserines), sphingolipids, saccharolipides, polyketides, sterols (ex: cholesterol) and prenols (Fahy *et al.*, 2009). However, recent biochemical, genetic, and biomarker studies have provided compelling evidence linking aberrant lipid metabolism to neurodegeneration in AD (Fraser *et al.*, 2010; Astarita *et al.*, 2011; Podtelezhnikov *et al.*, 2011; Tanzi, 2012; Hussain *et al.*, 2013). Moreover, peripheral metabolic conditions such as insulin resistance, obesity, and dyslipidemia have been identified as major AD risk factors (reviewed in (Pasinetti & Eberstein, 2008)).

Neutral lipids in Alzheimer's disease

Neutral lipids comprising cholesterols, cholesterol-esters, fatty acids, and triglycerides are the main source of energy and membrane lipids in the body (reviewed by (Ruggles *et al.*, 2013)). In response to increased intracellular free fatty acid levels, fatty acids are preferentially converted into triglycerides and packaged into organelles called lipid droplets (Figure 6). Lipid droplets are made of a phospholipid monolayer that buds off the endoplasmic reticulum and surrounds the neutral lipid core (Martin & Parton, 2006; Ohsaki *et al.*, 2009; Digel *et al.*, 2010). The storage of lipids allows a cell to buffer the toxic impact of excess lipids and to survive periods of diminished nutrient availability. In times of lipid deficiency, lipases breakdown these stores to provides membrane building blocks, such as fatty acids or sterols, for cellular division and integrity (Martin & Parton, 2006). Beyond their role in lipid storage, lipid droplets participate in inflammatory responses through synthesis of eicosanoids and in metabolic disorders such as obesity, atherosclerosis, cancer, and neurodegeneration (Bozza & Viola, 2010; Greenberg & Coleman, 2011; Greenberg *et al.*, 2011).

Phospholipids

Phospholipids are composed of a hydrophilic glycerolphosphate head group and a hydrophobic diglyceride tail. In aqueous environments, phospholipids align to form mono or bi lipid membranes. Choline-containing phospholipids have been particularly implicated in the pathophysiology of AD. Phosphatidylcholine (PC) is the major phospholipid in cellular membranes and can be metabolized by phospholipases to yield second messengers including lysophospholipids and fatty acids (Klein, 2000; Tayebati & Amenta, 2013). Previous studies have found altered PC and lysophospholipid levels in plasma (Mulder *et al.*, 2003; Schaefer *et*

al., 2006) and CSF (Walter *et al.*, 2004) AD samples. Many studies have also demonstrated changes in phospholipid lipase activity in AD patients (Kanfer *et al.*, 1993; Ross *et al.*, 1998; Chalbot *et al.*, 2009) and made links between this activity and cognitive decline ((Gattaz *et al.*, 2004; Forlenza *et al.*, 2005) reviewed in (Schaeffer *et al.*, 2009)). A particularly interesting study discovered a set of ten phospholipids in plasma samples that predicted and distinguish cognitively normal participants who would progress to MCI or AD within 2–3 years from those destined to remain cognitively normal (Mapstone *et al.*, 2014), suggesting that changes in PCs play a predictive and/or causative role in AD pathogenesis.

Phospholipids and neural stem cells

The role of phospholipids has not generally been explored in the context of neurogenesis. However, one study knocked out the lysophosphatidic acid receptor to determine the impact on neurogenesis in the DG. These mice showed defects in 1-d BrdU+ proliferating cells, DCX+ neuroblasts and the survival of these cells in the adult DG (Matas-Rico *et al.*, 2008), suggesting that phospholipids are necessary for continued neurogenesis.

I.2.1.5 Cholesterol

Cholesterol is an essential component of cellular membranes where it regulates their fluidity. Within the body, cholesterol and triglycerides are shuttled by carrier proteins called apolipoproteins (Apo) that regulate their metabolism and distribution (Mahley *et al.*, 1996; Bu, 2009). There are 6 subtypes of Apos (A, B, C, D, E, H) each with affinity for different

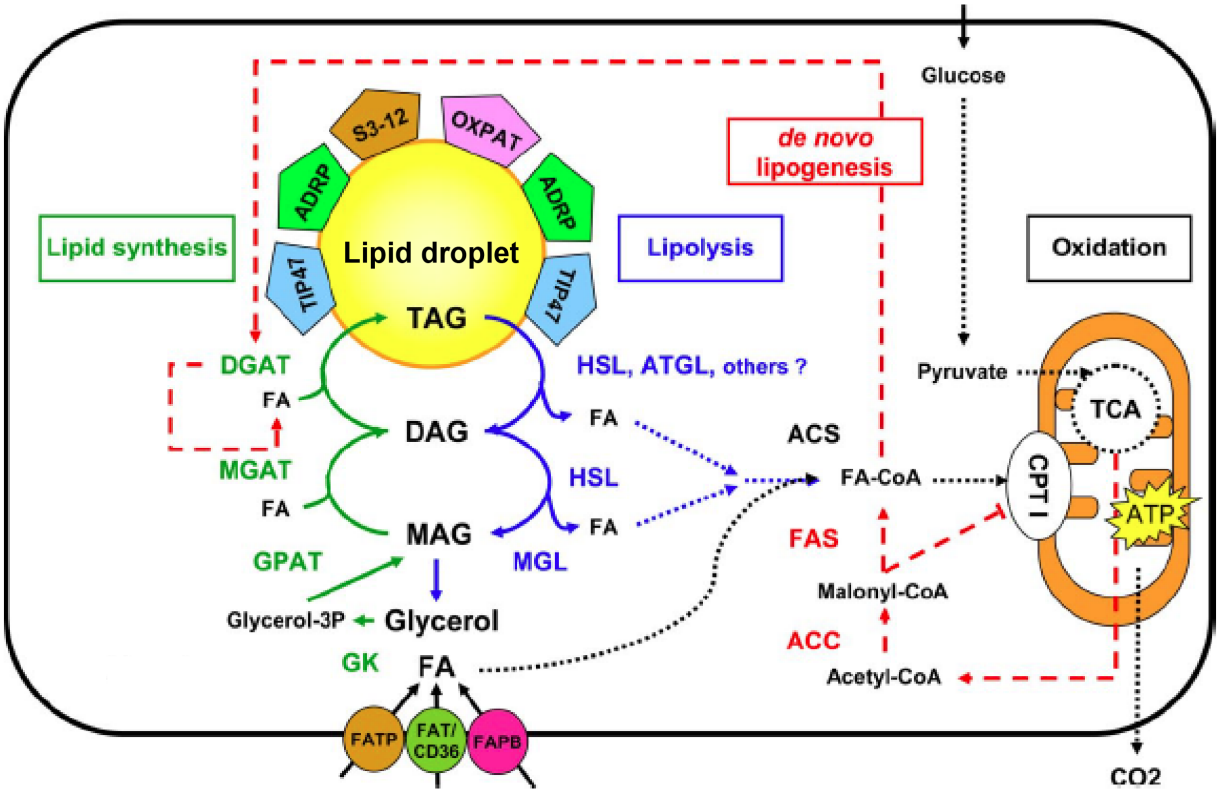

Figure 6. Biochemical pathway of triglyceride metabolism.

In response to excess lipid levels, fatty acids are preferentially converted into neutral lipids and packaged as lipid droplets (green). Sequential addition of fatty acids to glycerol forms monoacylglycerides (MAG), diacylglycerides (DAG), and triglycerides (TAG) via glycerol acyltransferase (GPAT), monoglycerol acyltransferase (MGAT), and diacylglycerol acyltransferase (DGAT) enzymes, respectively. The lipolysis (blue) of TAGs occurs via the sequential cleavage of fatty acids by adipose triglyceride lipase (ATGL), hormone sensitive lipase (HSL), and monoglycerol lipase (MGL) enzymes, respectively. Free fatty acids are then shuttled to the mitochondria for β-oxidation to produce ATP (red). Image adapted from (Moro et al., 2008, Am J Physiol Endochrinol Metab), reproduced with permission from the American Physiological Society © 2008.

lipoprotein particles. Astrocytes and microglia are the main source of ApoE in the brain (Xu *et al.*, 2006) where they deliver cholesterol and other essential lipids to neurons through members of the low-density lipoprotein receptor family (Herz & Bock, 2002; Herz & Chen, 2006; Lane-Donovan & Herz, 2014). In AD, the inheritance pattern of ApoE isoforms (ApoE2, ApoE3, or ApoE4) is a major determinant of the risk of late-onset Alzheimer's disease, where the inheritance of a single E4 allele increases the risk by a factor of 4, and two E4 alleles increase the risk by a factor of 19 (Corder *et al.*, 1993; Corder *et al.*, 1994; Strittmatter & Roses, 1996). ApoE isoforms likely impact the aggregation and deposition of AD pathologies. ApoE4 carriers have higher Aβ plaque load (Polvikoski *et al.*, 1995; Kok *et al.*, 2009; Reiman *et al.*, 2009) and tau phosphorylation (Leoni, 2011). Learning and memory is also impaired in ApoE4 knockin mice compared to ApoE3 knockin mice (Grootendorst *et al.*, 2005; Raber, 2008). The E4 allele is also a risk factor for atherosclerosis and other neurological disorders including CAA (Greenberg *et al.*, 1995), tauopathies and dementia with Lewy bodies (Josephs *et al.*, 2004), Parkinson's disease (Martinez *et al.*, 2005) and multiple sclerosis (Masterman & Hillert, 2004), suggesting a common link between lipid metabolism and aberrant protein aggregation. All together, deficient cholesterol metabolism provides an appealing hypothesis in the pathogenesis of AD because it ties together the ApoE genetic risk, amyloid production and aggregation, and vasculopathy.

I.2.1.5 APOE/cholesterol and neural stem cells

Unfortunately, work demonstrating a role for ApoE or cholesterol on neurogenesis has been rare. Levi and Michaelson counted the number of Ki67+ proliferating cells, DCX+ neuroblasts, and NeuN+ mature neurons in control, ApoE3 and ApoE4 mice and found no

difference in the SVZ and an increase in the DG of ApoE4 mice. When these mice were exposed to environmental enrichment, a well-known stimulator of DG neurogenesis (Mustroph *et al.*, 2012; Gregoire *et al.*, 2014), WT and ApoE3 mice showed a significant increase in proliferation and neurogenesis. Unexpectedly, environmental enrichment in apoE4 mice not only did not increase neurogenesis but instead, induced apoptosis (Levi & Michaelson, 2007). Li et al., studied ApoE knockout mice or mice with knockin alleles for human ApoE3 or ApoE4 and showed that neurogenesis is reduced in both ApoE-knockout and ApoE4-knockin mice (Li *et al.*, 2009). In the DG, ApoE-depletion in Nestin-reporter mice showed an acute increase in the proliferation of neural precursors followed by a premature depletion of GFAP+ and Nestin+ neural precursors. ApoE directly mediated this effect, as retroviral re-expression of ApoE rescued the phenotype (Yang *et al.*, 2011). These studies demonstrate a requirement for ApoE in neural precursor activity in the DG. Unfortunately, how ApoE regulates neurogenesis remains unknown.

I.2.1.5 Triglycerides-Fatty acids

Metabolites formed from the breakdown of triglycerides are used in signal transduction pathways, for membrane biosynthesis, and adenosine triphosphate (ATP) production through β-oxidation (Figure 6). The mobilization of triglycerides is carried out by triglyceride lipases, which sequentially cleave off fatty acids (Zechner *et al.*, 2012). Fatty acids are made up of a carbon-hydrogen backbone with a single carboxyl group. Three main criteria are used to classify fatty acids, their carbon chain length, the number of double bonds, and their position relative to

the carboxyl group (Figure 7). Briefly, fatty acid chains usually contain between 4-28 carbons and are either saturated (no double bonds) or unsaturated (one or more double bonds) with

Name	Abbreviation	Carbons: unsaturations	Omega
Saturated			
Palmitic acid	PA	16:0	
Stearic acid	SA	18:0	
Unsaturated			
monounsaturated			
Palmitoleic acid	POA	16:1	omega-7
Oleic acid	OA	18:1	omega-9
Eicosenoic acid	EA	20:1	omega-9
polyunsaturated			
Linoleic acid	LA	18:2	omega-6
Eicosadienoic acid	EDA	20:2	omega-6
Arachidonic acid	AA	20:4	omega-6
Eicosapentaenoic acid	EPA	20:5	omega-3
Docosapentaenoic acid	DPA	22:5	omega-3
Docosahexaenoic acid	DHA	22:6	omega-3

Figure 7. Fatty acid nomenclature and classification

hydrogens. The location of the first double bond relative to the carboxyl group determines the omega classification (i.e, when the first double bond is on the third carbon it is called an omega-3 fatty acid, on the sixth, an omega-6, and on the ninth, an omega-9) (Figure 7).

Several lines of evidence suggest that defects in fatty acid metabolism may initiate and/or accelerate the development of AD (reviewed in (Hussain *et al.*, 2013). Observational studies have associated low fish intake and low blood levels of omega-3 fatty acids to increased risk of dementia and AD (Gu *et al.*, 2010). On the other hand, high fat diets and increased free fatty acids can induce and exacerbate AD pathological hallmarks including, plaque and tangle formation (Patil & Chan, 2005; Julien *et al.*, 2010). Chronic administration of docosahaexanoic acid (DHA, 22:6), the main source of omega-3 in the brain, enhances long-term memory in young and aged rats (Gamoh *et al.*, 1999; Gamoh *et al.*, 2001), and dietary DHA has preventive and ameliorative effects on the impairment of spatial learning in Aβ-infused rats (Hashimoto *et al.*, 2005a; Hashimoto *et al.*, 2005b). This data indicates that alterations of fatty acid or their metabolites can lead to changes in brain function and that changes in the body's lipid profile can lead to AD-associated pathologies in the brain.

I.2.1.5 Fatty acids and neural stem cells

The effect of fatty acids on neurogenesis has only been studied in embryonic neurosphere cultures. DHA and omega-3 fatty acids have been studied most frequently because of their previously mentioned role in learning and memory. Neurospheres differentiated in the presence of DHA have fewer apoptotic cells, proliferate less, and produce significantly more neurons that are more developed when compared with the control (Kawakita *et al.*, 2006; Katakura *et al.*,

2009). Moreover, when compared to arachidonic acid (AA, 20:4), Sakayori and colleagues found that DHA increased the number of neurospheres, whereas AA had no effect. Under differentiation conditions, DHA treatment increased the number of neurons, while AA increased the number of astrocytes (Sakayori *et al.*, 2011). Building on their previous work, Katakura and colleagues simultaneously compared the effects of DHA, eicosapentaenoic acid (EPA, 20:5), and AA on gene expression and neurosphere differentiation. They showed that EPA and DHA but not AA treatment induced neuronal differentiation with a concomitant increase in NeuroD and Map2 mRNA levels. Interestingly, DHA but not EPA or AA inhibited mRNA levels of Hes1, an inhibitory factor of neuronal differentiation, while EPA but not DHA activated Hes6, an inhibitory factor of Hes1. EPA and DHA but not AA arrested the cell cycle of NSCs through increased p21cip1 and p27kip1 levels. These results indicate that omega-3 polyunsaturated fatty acids (DHA and EPA), but not AA, increase neuronal differentiation (Katakura *et al.*, 2013). In another study, the same group differentiated neural precursor with equivalent concentrations of DHA, AA, docosapentaenoic acid (DPA, 22:5), and Oleic acid (OA, 18:1). They again found that omega-3 fatty acids (DHA and DPA) increased neuronal fate choice using Tuj-1 and MAP2 markers, while OA and AA had no effect. In addition, they found no effect of any of these fatty acids on astrogliogenesis (Rashid *et al.*, 2013). Together these studies demonstrate that omega-3 fatty acids support survival and neuronal fate choice and differentiation of embryonic neural precursors. On the other hand, saturated fatty acids such as palmitic acid (PA, 16:0) have been negatively linked to AD (Patil & Chan, 2005). Treatment of neural precursors with PA dose-dependently increases caspase-mediated apoptosis altering bax and bcl-2 and leading cleavage of caspase-3. Moreover, the increase in apoptosis was partially dependent on MAPK signalling, as PA increased the phosphorylation of JNK in a dose-dependent manner and addition of a JNK

inhibitor could partially rescue caspase activation and the number of terminal deoxynucleotidyl transferase dUTP nick end labelling (TUNEL)+ cells (Yuan *et al.*, 2013; Wang *et al.*, 2014). In addition, non-toxic levels of PA were shown to increase astrogliogenesis and Stat3 signalling (Wang *et al.*, 2014). Thus, various fatty acids can impact neural precursor behaviour differently. The closest links between these results and adult neurogenesis are experiments with high fat diet paradigms. Post-natal AA- but not DHA-feeding increased the number of 1day BrdU+ proliferating cells in the DG (Maekawa *et al.*, 2009). Moreover, dietary administration of DHA in adult rats significantly increased the number of BrdU+/NeuN+ newborn neurons in the DG (Kawakita *et al.*, 2006).

Although the data linking lipids and adult neurogenesis is scarce, emerging studies on fatty acid binding and synthesis have yielding interesting results. Fatty acids are distributed in the brain via fatty acid binding proteins (FABPs) and loss of FABPs inhibits neurogenesis and cognitive function (reviewed in (Liu *et al.*, 2010)). FABPs are intracellular lipid trafficking proteins that play crucial roles in taking up fatty acids into the cytoplasm and transporting them to appropriate intracellular compartments (Owada, 2008; Storch & McDermott, 2009). Among various FABPs -3, -5 and -7 are expressed in the brain. FABP-3 is expressed in neurons of the mature brain, while FABP5 is expressed by both glia and neurons pre and post natally. During pre and perinatal stages FABP7 is mainly expressed in radial glia and immature astrocytes (Owada *et al.*, 1996). In adult rodent brains, immunohistochemistry showed that FABP5 and FABP7 are present in NSCs and their neuronal progenitors coexpressing GFAP, Nestin, Sox2 and DCX but not NeuN in the DG. A marked decrease in NSCs and neural progenitors was observed when FABP5, FABP7 or both were knocked out. Although 1-day BrdU+ proliferating cells were decreased in all knockout mice, the survival of these cells 28 days after injection was

increased in the FABP7/FABP5 double knockout mice compared to other three genotypes. Although this study does not directly study the role of fatty acids in neurogenesis it suggests that FABPs are required for DG neurogenesis (Matsumata *et al.*, 2012).

Although, many interesting links have been uncovered in the last decade, more work is needed to determine the role of lipids during physiological neurogenesis and whether changes in lipid species contribute to alterations in neurogenesis and under pathological conditions

I.2.2 Neurogenesis in humans with Alzheimer's disease

Studies on neurogenesis in human AD patients have led to variable results. The first study showed that protein expression of DCX, PSANCAM, TOAD-64/Ulip/CRMP (TUC-4), and NeuroD was increased in Western blots between controls and AD hippocampal samples. However, this study did not use age-matched controls, making it difficult to determine the meaning of these results (Jin *et al.*, 2004b). Other reports have indicated an increase in glial cell proliferation and vascular-associated changes in the presenile AD human hippocampus (Boekhoorn *et al.*, 2006a). Crews and colleagues performed cell counts and found a decrease in both Sox2- and DCX-positive cells in the hippocampus of AD patients (Crews *et al.*, 2010a). An important study by Perry and colleagues measured immunoreactivity of multiple stages of neurogenesis in the sub-granular layer and the granule cell layer of the DG and the SVZ at Braak stages 1-5. Musashi-1+ NSCs were significantly diminished in both SVZ and DG in AD patients and further decreased with increasing Braak stages. Conversely, immunoreactivities of Nestin and PSA-NCAM progenitors were significantly higher in AD and increased in later Braak stages

in the DG. In the SVZ, Nestin immunoreactivity was also significantly higher in AD and significantly increased in more advanced Braak stages, while no significant differences were seen for the other markers. In the DG, DCX was increased in the granule layer but not sub granule layer in AD, suggesting this may not be the result of normal neurogenesis (Perry *et al.*, 2012). In accord with the Perry study, Ziabreva et al., found a 9- fold decrease in Musashi + cells in the SVZ of AD patients (Ziabreva *et al.*, 2006). Together, these data although variable, suggest a dysregulation of neurogenesis in AD. This variability is likely due to the various ages and disease stages of AD compared and the differing markers used to study neurogenesis. More studies are needed to characterize how each step of the neurogenic process is altered and how they are temporally and spatially modulated with the respect to five AD-associated pathologies.

I.3 HYPOTHESIS, OBJECTIVES, AND EXPERIMENTAL RATIONAL

Problem: Alzheimer's disease leads to widespread degeneration and failing of many cognitive functions including learning and memory.

Hypothesis: AD-associated pathologies regulate neural stem cell activity in AD.

Objectives: the goal of this thesis was to uncover mechanisms regulating neural stem cell behaviour in Alzheimer's disease by:

1) Studying the onset of neurogenic defects in 3xTg-AD mice
2) Identifying novel and early suppressors of neurogenesis in 3xTg-AD mice and confirm their presence in human AD patients
3) Untangling the molecular mechanisms by which this/these suppressor(s) act to inhibit neurogenesis in 3xTg-AD mice.

Experimental rational:

We selected the 3xTg-AD mouse model for these studies for three main reasons: 1) their capacity to develop both amyloid plaques and neurofibrillary tangles 2) the fact that their pathology progression is slow, aggravated by age and deposits in a spatial pattern similar to what is observed in AD patients and 3) because they have age-related memory deficits.

We collaborated with Chemists to adapt novel techniques to localize and identify lipids in

the brain by lipid-imaging mass spectrometry (Martin Dufresne and Pierre Chaurand) and in the cerebral spinal fluid and plasma by lipidomic mass spectrometry (Alexandra Furtos).

We developed novel tools to study the role of lipids in the regulation of adult neural stem cells, including, intracerebroventricular infusion and acute injections of fatty acids and heavy fatty acids for metabolic tracing in the brain. We employed classic and modified neurosphere assays to assess neural stem cell activation and self-renewal and neural precursor expansion in vitro. Moreover, we utilized established ablation protocols to study neural stem cell behaviour in vivo.

This data obtained during my thesis has resulted in the following publications:

1. APPENDIX C: Hamilton LK , Truong MKV, Bednarczyk MR, Aumont A, Fernandes KJL. Cellular organization of the central canal ependymal zone, a niche of latent neural stem cells in the adult mammalian spinal cord. Neuroscience 164(3):1044–1056. Sep 2009.

2. CHAPTER 2: Hamilton LK, Aumont A, Julien C, Vadnais A, Calon F, Fernandes KJL. Widespread deficits in neurogenesis precede plaque and tangle formation in the 3xTg mouse model of Alzheimer's disease..Eur J Neurosci.2010 Sep;32(6):905-20.

3. Paliouras GN, Hamilton LK, Aumont A, Joppé SE, Barnabé-Heider F, Fernandes KJ. Mammalian target of rapamycin signalling is a key regulator of the transit amplifying progenitor pool in the adult and aging forebrain. J Neurosci. 2012 Oct 24;32(43):15012-26.

4. APPENDIX B: Hamilton LK, Joppe SE, Cochard LM, Fernandes KJLF. Aging and neurogenesis in the adult forebrain : what we have learned and where we should go from here. Eur J Neurosci. 2013 Jun;37(12):1978-86. doi: 10.1111/ejn.12207.

5. Lacroix S, Hamilton LK, Vaugeois A, Beaudoin S, Breault-Dugas C, Pineau I, Lévesque SA, Grégoire CA, Fernandes KJ. Central canal ependymal cells proliferate extensively in response to traumatic spinal cord injury but not demyelinating lesions. PLoS One. 2014 Jan 27;9(1):e85916.

6. CHAPTER 3: Hamilton LK, Dufresne M, Joppe SE, Petryszyn, Aumont, A., S Calon F, Parent M, Chaurand P, Fernandes KJL. Elevated oleic levels within the forebrain niche suppress neural stem cell activation in Alzheimer's disease. Submitted 2014.

7. Joppe SE, Hamilton LK, Cochard LM, Aumont A, Fernandes KJL. In preparation

CHAPTER 2

II. FIRST ARTICLE:

"WIDESPREAD DEFICITS IN ADULT NEUROGENESIS PRECEDE PLAQUE AND TANGLE FORMATION IN THE 3XTG MOUSE MODEL OF ALZHEIMER'S DISEASE"

Section: Molecular and Developmental Neuroscience

European Journal of Neuroscience

Widespread deficits in adult neurogenesis precede plaque and tangle formation in the 3xTg mouse model of Alzheimer's disease

Laura K. Hamilton[1,2,3], Anne Aumont[1,2,3], Carl Julien[4], Alexandra Vadnais[1], Frédéric Calon[4], and Karl J.L. Fernandes[1,2,3]

[1]Department of Pathology and Cell Biology, [2]Groupe de recherche sur le système nerveux central (GRSNC), [3]Center of Excellence in Neuromics of the Université de Montréal (CENUM), Université de Montréal, Montréal, Canada, and [4]Faculty of Pharmacy, Université de Laval, Centre Hospitalier de l'Université Laval Research Center, Quebec City, Canada

II.1 ABSTRACT

Alzheimer's Disease (AD) affects cognitive modalities that are known to be regulated by adult neurogenesis, such as hippocampal- and olfactory-dependent learning and memory. However, the relationship between AD-associated pathologies and alterations in adult neurogenesis has remained contentious. In the present study, we performed a detailed investigation of adult neurogenesis in the 3xTg mouse model of AD, a unique model that generates both amyloid plaques and neurofibrillary tangles, the hallmark pathologies of AD. In both neurogenic niches of the brain, the hippocampal dentate gyrus and the forebrain subventricular zone (SVZ), we found that 3xTg mice had decreased numbers of (i) proliferating cells, (ii) early lineage neural progenitors, and (iii) neuroblasts at middle-age (11-months-old) and old-age (18-months-old). These decreases correlated with major reductions in the addition of new neurons to the respective target areas, the dentate granule cell layer and the olfactory bulb. Within the SVZ niche, cytological alterations were observed that included a selective loss of sub-ependymal cells and the development of large lipid droplets within the ependyma of 3xTg mice, indicative of metabolic changes. Temporally, there was a marked acceleration of age-related decreases in 3xTg mice, which affected multiple stages of neurogenesis and was clearly apparent prior to the development of amyloid plaques or neurofibrillary tangles. Our findings indicate that AD-associated mutations suppress neurogenesis early during disease development. This suggests that deficits in adult neurogenesis may mediate premature cognitive decline in AD.
Keywords: stem cells, hippocampus, subventricular zone, amyloid precursor protein, tau

Keywords: stem cells, hippocampus, subventricular zone, amyloid precursor protein, tau

II.2 INTRODUCTION

There is increasing evidence that perturbations in adult neurogenesis may play a role in the cognitive dysfunction associated with aging and Alzheimer's Disease (AD). For example, many molecules linked to the development of AD, including Presenilins, Amyloid Precursor Protein (APP), tau, and ApoE4, have recently been shown to be potential regulators of adult neurogenesis (Caille *et al.*, 2004; Chuang, 2010b; Lazarov & Marr, 2010). Moreover, when adult neurogenesis is experimentally ablated, changes reminiscent of those seen during aging and in AD are observed (Rosen *et al.*, 1984; Bacon *et al.*, 1998; Lazarov & Marr, 2010), such as defects in hippocampus-dependent learning and memory, olfactory deficits, and olfactory bulb atrophy (Mak *et al.*, 2007; Imayoshi *et al.*, 2008; Breton-Provencher *et al.*, 2009; Clelland *et al.*, 2009; Deng *et al.*, 2009; Kitamura *et al.*, 2009). Since aging is associated with a significant drop in neurogenesis and is also the primary risk factor for AD (Kuhn *et al.*, 1996; Kempermann *et al.*, 1998; Cameron & McKay, 1999; Knoth *et al.*, 2010), decreases in adult neurogenesis may be involved in mediating aging- or AD-related cognitive decline.

Surprisingly, contradictory conclusions have emerged from previous studies that have attempted to link AD to changes in neurogenesis, with both increases and decreases in neurogenesis having been reported (Chuang, 2010b; Elder *et al.*, 2010). These differing conclusions may reflect variability in key study conditions, including age, types of AD genetic mutations, and the stage of development of the amyloid and/or tau pathologies. Specifically, since adult neurogenesis is tightly regulated by the neurogenic microenvironment (i.e., adjacent cells, extracellular matrix, diffusible factors and circulating signals) (Fuchs *et al.*, 2004; Morrison & Spradling, 2008; Walker *et al.*, 2009), experimental models having different types,

levels, or localizations of AD-induced pathologies are likely to have diverse effects on neural precursor survival, proliferation, migration and/or differentiation.

In the present study, we used the 3xTg model of AD (Oddo *et al.*, 2003b) to investigate the influence of the AD-associated microenvironment on adult neurogenesis. 3xTg mice carry the $PS1_{M146V}$, APP_{swe} and tau_{P301L} human mutations, and provide the closest recapitulation of the cellular microenvironment in AD as they progressively develop both classical pathologies, amyloid plaques and neurofibrillary tangles (Oddo *et al.*, 2003a; Mastrangelo & Bowers, 2008). To systematically evaluate AD-induced changes in neurogenesis, we examined key stages of the neurogenic process in both neurogenic regions of the adult brain, the hippocampal dentate gyrus (DG) and the forebrain subventricular zone (SVZ) while simultaneously assessing amyloid and tau pathology progression. Our findings suggest that the AD microenvironment can suppress adult neurogenesis early during disease development and independently of plaque and tangle deposition.

II.3 MATERIALS AND METHODS

II.3.1 Animals

Experiments were conducted in accordance with the guidelines of the Canadian Council of Animal Care and were approved by the institutional animal care committee. The generation of the 3xTg-AD mice has been described previously (Oddo *et al.*, 2003b). Briefly, 3xTg-AD mice were originally derived by co-microinjecting two independent transgenes encoding human APP_{Swe} and the human tau_{P301L} (both under control of the neuron-specific mouse Thy1.2 regulatory element) into single-cell embryos harvested from homozygous mutant $PS1_{M146V}$ knock-in (PS1-KI) mice. The non-transgenic wildtype (WT) mice used are littermates from the

original PS1-KI mice and are on the same background as the 3xTg mice (C57BL6/129SVJ). All mice were kept in identical housing conditions and given free access to a standard rodent diet (#2018, Harlan Teklad, Madison, USA) and water.

For the present experiments, a total of 17 female WT and 17 female 3xTg mice were used. All 34 mice received injections of 5-bromo-2-deoxyuridine (BrdU): twenty-one days prior to sacrifice, they were administered three 100 µl intraperitoneal injections of BrdU (1.5 mg/injection, Sigma, Oakville, Canada) at three-hour intervals.

II.3.2 Tissue processing and collection for immunohistochemical experiments

Mice received a lethal dose of chloral hydrate (7%) and were then perfused trans-cardially with 25 ml of phosphate-buffered saline (PBS) followed by 40 ml of 4% formaldehyde, freshly prepared from paraformaldehyde pH 7.4. Perfusion-fixed brains were removed and post-fixed in 4% formaldehyde for an additional 4 h, and then kept in PBS at 4°C until sectioning. Using a mouse brain mold (1mm mouse coronal Alto brain matrice, Harvard Apparatus Canada, St Laurent, Canada), each brain was divided into three blocks prior to vibratome sectioning: an anterior 3 mm block containing the olfactory bulbs, an intermediate 6 mm block containing the forebrain lateral ventricles and hippocampus, and a 4 mm posterior block containing the cerebellum and brainstem. Both the anterior and intermediate blocks were sectioned in the coronal plane, from rostral to caudal, at 40 µm thickness using a vibrating microtome (Leica VT1000S, Leica Microsystems, Richmond Hill, ON, Canada). For the anterior block, the olfactory bulbs were serially sectioned into 6 wells of a 6-well plate, such that each well contained a series of sections that were 240 µm apart. For the intermediate block, SVZ sections were collected beginning when the genu of the corpus callosum became continuous (approximate

coordinates Bregma +1.15), and the subsequent 48 sections (=1.92 mm) were collected into a 24-well plate. The entire hippocampus was then serially sectioned into 6 wells of a 6-well plate, such that each well contained a series of 10 sections that were 240 μm apart. Tissue sections were collected into an anti-freeze solution (glycerol:ethylene glycol:PBS 1X, 3:3:4) and stored at -20°C.

II.3.3 Immunohistochemistry

Basic immunohistochemical procedures were performed as detailed previously (Bednarczyk *et al.*, 2009). The primary antibodies used were: mouse anti-human Ki67 (1:200, BD Biosciences, Mississauga, Canada), rat anti-BrdU (1:200, AbD Serotec, Raleigh, USA), goat anti-human DCX (1:1000, Santa Cruz Biotechnology, Santa Cruz, USA), mouse anti-rat Mash-1 (1:100, BD Biosciences), mouse anti-mouse NeuN (1:200, Millipore, Billerica, USA), mouse anti-human Tau (HT7) (1:200, Pierce Biotechnology, Rockford, USA), rabbit anti-human Amyloid Precursor Protein (Y188) (1:750, Abcam, Cambridge, USA), mouse anti-human PHF-Tau (AT8) (1:100, Pierce Biotechnology), mouse anti-human PHF-Tau (AT180) (1:20, Pierce Biotechnology), mouse anti-human PHF-1 (1:20, courtesy of Dr. Peter Davies, Albert Einstein College of Medicine, Bronx, USA). For brightfield immunohistochemistry, primary antibodies were detected using species-appropriate biotinylated secondary antibodies (Jackson ImmunoResearch, West Grove, USA), the signal was amplified using the avidin-biotin-peroxidase system (VectaStain ABC Kit, Vector Laboratories, Burlington, Canada), and revealed using a 3,3-diaminobenzidine (DAB)-containing solution (Sigma). For fluorescence immunohistochemistry, primary antibodies were detected using species-appropriate secondary antibodies that were conjugated to either Alexa 555 (1:1000, Invitrogen, Burlington, Canada),

Alexa 488 (1:1000, Invitrogen) or Alexa 647 (1:1000, Invitrogen). Fluorescent nuclear counterstaining was performed with 0.2 μM Hoechst 33342 (Sigma). Microscopy was performed using a motorized Olympus IX81 microscope and/or a Leica SP1 laser-scanning confocal microscope.

The HT7, Y188, AT8, AT180 and PHF-1 antibodies strongly labeled sub-populations of neurons on sections from 3xTg mice, and did not produce any staining patterns above background on sections from WT mice. The Y188 antibody yielded some diffuse and low level staining in WT mice, presumably due to cross-reactivity with endogenous mouse APP. On Western blots, the HT7 and Y188 antibodies detected bands only at the appropriate respective sizes.

II.3.4 Resin-embedded semi-thin sections

Some sections processed for brightfield immunohistochemistry with Ki67 were further sectioned to 1 μm thickness to improve resolution of the signal. Following application of the DAB solution, sections were rinsed in phosphate buffer, fixed with 1% osmic acid (Electron Microscopy Science, Hatfield, USA) for 30 minutes, dehydrated in a graded series of ethanols and propylene oxide (Fisher Scientific) and then embedded in electron microscopy grade Resin (Durcupan ACM, Sigma). Resin-embedded sections were cut at 1 micron thickness on an Ultracut E, Reichert Jung ultramicrotome (Leica, Richmond Hill, Canada), counterstained with 0.5-1% toluidine blue (Fisher Scientific) and mounted on slides. They were then coverslipped using Permount (Fisher Scientific), and photographed using a 100X objective.

II.3.5 Oil Red O staining

40 μm coronal sections through the SVZ were mounted on slides, washed with 60% isopropanol in distilled H_2O (Fisher Scientific) and incubated in 0.3% Oil Red O solution in 60% isopropanol (Allied Chemical, Morristown, USA) for 10 minutes. Slides were washed once with 60% isopropanol and three times with distilled H_2O. They were then coverslipped with 75% glycerol (Fisher Scientific) in distilled H_2O.

II.3.6 Estimates of cell numbers

In order to estimate changes in the relative numbers of immunohistochemically defined cell types, WT and 3xTg sections from the olfactory bulb, SVZ and hippocampus were chosen from within pre-determined stereotaxic windows and then precisely matched to equal levels using specific tissue landmarks. All cell counting was performed on coded slides by a blinded experimenter.

Hippocampus. For each marker analyzed, quantifications were performed on 5 sections at 240 μm intervals through the hippocampus from stereotaxic levels -1.3 to -2.3 mm Bregma (for BrdU and DCX) or -2.3 to -3.3 mm Bregma (for Ki67). To match the section levels, landmarks were used that included size of the hippocampus, shape of the dentate granule layer, thickness of the corpus callosum and size of the lateral ventricles. Counts were limited to positive cells within the subgranular zone and granular zone of the dentate gyrus. Averages per section were obtained by averaging the counts from left and right hemispheres.

Olfactory bulbs. Relative changes in the number of BrdU(+) cells in the olfactory bulbs were measured by using 6 sections at 240 μm intervals from +5.30 to +4.10 mm Bregma. To match

the section levels, landmarks including the size and shape of the main olfactory bulb, size and shape of the subependymal zone, and the absence of the accessory olfactory bulb were used.

SVZ. For quantification of markers expressed by SVZ cell populations, 5 sections at 320 μm intervals were quantified from +1.15 to -0.15 mm Bregma. To match the section levels, landmarks were used that included the genu of the corpus callosum, corpus callosum thickness, size of the lateral ventricles, location/size of the anterior and posterior commissures and the connection of the lateral ventricles with the dorsal third ventricle. Counts were limited to the SVZ and both the left and right hemispheres were included. Averages per section were obtained by averaging the counts from left and right hemispheres.

Quantifications are shown as uncorrected cell counts per section. In control experiments, we found that there was no detectable difference in the size of the objects counted, as nuclear profiles had an identical size distribution between WT and Tg mice at 11 months (7.734 ± 0.4539 vs. 7.205 ± 0.6278 μm), and at 18 months (7.167 ± 0.1211, vs. 6.951 ± 0.2409 μm) (data not shown). There were also no apparent differences in the sizes of the brain structures that were analyzed, as all of the tissue landmarks indicated above appeared at the same time in all mice, regardless of whether they were WT or 3xTg mice, and 11 or 18 months of age. Based on these two criteria, the uncorrected cell counts are expected to provide an approximation of relative changes in cell numbers between groups.

*Quantification from semi-thin sections.*1 μm serial sections through the lateral ventricles at 0.86mm Bregma were photographed using a 100X objective. Digital images were used to reconstruct the walls of the lateral ventricle into one complete ventricle for each animal. Counting of ependymal cells which are stained light blue and are in contact with the ventricle, sub-ependymal cells which are stained dark blue, proliferating Ki67(+) cells which are stained

black, and lipid droplets was achieved using the striatal side of each ventricle (see Fig. 5a) and manually tagging each cell type.

II.3.7 Protein isolation and fractionation

For biochemical analyses, mice were deeply anaesthetised with 100µl/g of a ketamine (30mg/ml, Bioniche Animal Health, Belleville, Canada) and xylazine (2mg/ml, Bimeda-MTC, Cambridge, Canada) solution, and then perfused intracardially with Phosphate Buffered Saline (PBS) pH 7.4 containing protease inhibitors (1 tablet/200ml PBS, Sigma Fast kit containing 12 inhibitors) and phosphatase inhibitors (1mM pyrophosphate and 50mM sodium fluoride, Sigma). For each mouse, the brain was rapidly dissected out and divided into cortex, hippocampus, striatum and olfactory bulb. The tissues were immediately flash frozen on dry ice and weighed to determine dilution volumes of lysing buffer for each sample. Each brain region was then lysed and sequentially separated into soluble, membranous and insoluble protein fractions, as follows. Frozen tissues were incubated in Tris Buffered Saline (TBS) (0.05M Tris base, Wisent, St-Bruno, Canada; 0.138M NaCl, EMD; 2.7mM KCl, EMD, Gibbstown, USA) supplemented with protease inhibitors (Complete cocktail tablet, Roche Diagnostic, Laval, Canada) and phosphatase inhibitors (10µg/ml Pepstatin, Sigma; 20 µg/ml Fenvalevate, Sigma; 9.8 µg/ml Canthavidin, Sigma; 446.10 µg/ml Sodium pyrophosphate, Sigma; 50 mM Sodium fluoride, Sigma). Each sample was then homogenized, sonicated for 3X5 seconds at 15 second intervals, and centrifuged for 20 minutes at 4ºC at 100 000g. The supernatant containing the soluble fraction was then collected and kept at -80ºC. To obtain the membranous protein fraction, the pellet was resuspended in buffer (150mM NaCl , EMD; 10mM NaH2PO4, Amresco, Solon, USA; 0.5% Deoxycholate, EMD; 1% Triton-X 100, Fisher Scientific; 5% SDS, J.T. Baker, Philipsburg,

USA) supplemented with the same protease and phosphatase inhibitors as above. Each sample was then homogenized, sonicated 3X5 seconds at 15 second intervals on ice, and centrifuged for 20 minutes at 4ºC at 100 000g. The supernatant containing the membrane fraction was then collected and kept at -80ºC. The remaining pellet was resuspended in 90% formic acid (J.T. Baker), homogenized, sonicated 3X5 seconds at 15 second intervals, and centrifuged for 20 minutes at 4ºC at 100 000g. The supernatant containing the insoluble fraction was collected and kept at -80ºC. Formic acid fractions were evaporated using a Savant Speed Vac plus SC110A (Thermo Scientific, Waltham, USA) with Savant refrigerated vapour trap RVT 400 (Thermo Scientific) for 2-5 hours to remove the formic acid. The proteins were then resuspended in TBS. The protein concentration of all fractions was determined using the bicinchoninic acid assay (Pierce Biotechnology).

II.3.8 Western blotting

35-60µg of protein from each sample was boiled in sample buffer containing 0.5M Tris-HCl, pH6.8 (Fisher Scientific), 15% glycerol (Fisher Scientific), 10% SDS (Fisher Scientific), bromophenol blue (Fisher Scientific), and β-Mercaptoethanol (Bishop, Burlington, Canada), separated using SDS-PAGE (10% Acrylamide, Bio Rad, Mississauga, Canada), and transferred onto a nitrocellulose membrane (0.45µm, Bio Rad). Membranes were immersed in Ponceau Red (0.2% Ponceau S, Fisher Scientific, in 11% trichloroacetic acid, Fisher Scientific) to visualize the proteins, washed in Tris-buffered saline containing 0.2% Tween (Fisher Scientific) (TBS-T) and blocked in 5% skim milk powder (Carnation, Markham, Canada). They were then incubated overnight at 4°C with primary antibody. The following antibodies were used: mouse anti-human Tau (HT7) (1:1000, Pierce Biotechnology), rabbit anti-human APP (Y188) (1:1000, Abcam),

mouse anti-human PHF-Tau (AT8) (1:50, Pierce Biotechnology), mouse anti-human PHF-Tau (AT180) (1:100, Pierce Biotechnology) and mouse anti-Xenopus β-actin (1:10 000, Abcam).

HRP-conjugated secondary antibodies, diluted in blocking solution, were used as follows: anti-mouse IgG (1:5000, Bio Rad) or anti-rabbit IgG (1:5000, Millipore). Secondary antibodies were detected using the ECL chemiluminescence reagent kit (GE Health Care, Baie d'Urfé, Canada) and X-Omat Blue film (Kodak). Membranes were subsequently stripped with Re-Blot Plus Mild (Millipore), re-blocked and re-probed as described above. Quantitative density of bands was performed using NIH ImageJ software. Reported values are calculated as measured absorbance divided by β-actin absorbance. When reporting fold changes in absorbance between WT and 3xTg, the β-actin normalized 3xTg absorbance was divided by the β-actin normalized WT absorbance.

II.3.9 Dot Blots

20μg of protein from each sample was applied to a nitrocellulose membrane (0.45μm, Bio Rad) using the Schleicher & Schuell (S&S) Minifold-I Dot-Blot System (Keene, USA). When the wells were dry, the membrane was removed and dried on filter paper for 15 minutes. The membrane was then blocked in 5% milk in TBS-T for 30 minutes and incubated with the mouse anti-human β-amyloid 1-42 (12F4) (1:500, Covance, Emeryville, USA) primary antibody for 1 hour. Membranes were washed in TBS-T and incubated with anti-mouse IgG (1:5000, Bio Rad) for 30 min at room temperature. Secondary antibodies were detected using the ECL chemiluminescence reagent kit (GE Health Care) and X-Omat Blue film (Kodak).

II.3.10 Statistical Analyses

For each animal, the average number of cells per section was first calculated (5-6 sections/animal), and then the statistical analyses were performed using the average number of cells/section/animal (generally 4 animals/group). Unpaired t-tests were performed to compare the means between pairs of groups, and were two-tailed unless otherwise indicated. A probability value of $p \leq 0.05$ was considered to be statistically significant. All statistical analyses were achieved using GraphPad Prism, Version 5.02 (GraphPad Software, Inc, La Jolla, CA, USA). In the Results, data are expressed as mean ±standard error of the mean (SEM). For illustrative purposes, cell counts obtained from all tissue sections of all animals are presented in the figures using vertical scatterplots, with the group means shown as horizontal lines.

II.4 RESULTS

II.4.1 Region-specific expression of tau/APP human transgenes

The 3xTg mice were generated by injection of neuron-specific Thy1.2 promoter-driven APP_{swe} and tau_{P301L} transgenes into $PS1_{M146V}$ single cell embryos (Oddo *et al.*, 2003b). We began by assessing the temporal and spatial expression patterns of the APP and tau transgenes, as well as their proximity to the hippocampal and SVZ stem cell niches.

We first confirmed biochemically that APP and tau transgenes were overexpressed in our 3xTg mice. Protein lysates were prepared from the cortex, hippocampus, striatum (including the striatal SVZ), and olfactory bulbs of 11-month-old WT and 3xTg mice, and each lysate was sequentially separated into soluble, membranous and insoluble protein fractions as previously described (Calon *et al.*, 2004; Tremblay *et al.*, 2007; Julien *et al.*, 2008; Phivilay *et al.*, 2009) (see Materials and Methods). When the soluble fractions were probed with HT7 (a

phosphorylation-independent antibody against human tau) and the membrane fraction was probed with Y188 (an antibody against human APP) (Fig. 1), 3xTg mice were found to have significantly higher levels of both tau (Fig. 1A) and APP (Fig. 1B) than their age-matched WT controls. Both antibodies also showed some cross-reactivity against the respective WT mouse proteins. Densitometry measurements for tau and APP, normalized against β-actin, confirmed overexpression of these proteins in the cortex (tau 1.3x, APP 1.5x), hippocampus (tau 4.6x, APP 1.6x), striatum (tau 1.9x, APP 1.5x) and olfactory bulbs (tau 2.8x, APP 1.4x) relative to WT controls.

Transgene expression in each of these brain regions was visualized using multi-label fluorescence immunohistochemistry. Brain sections from both middle-aged (11-month-old) and old-aged (18-month-old) 3xTg mice displayed strong and specific immunoreactivity for HT7 and APP. In the hippocampus, CA1 pyramidal neurons that were HT7(+), APP(+), or HT7(+)/APP(+) were clearly apparent, increasing in number and intensity from 11 to 18 months of age (Fig. 1C). There were no HT7(+) or APP(+) cells observed within the neurogenic DG, but some HT7(+) fibers were present within the hilus (data not shown). In the striatum, HT7(+) fibers were abundant and could be observed extending to the edge of the striatal SVZ at both 11 and 18 months, while APP was not detectable (Fig. 1D). Neither APP nor HT7 was detectable within the SVZ itself. In the olfactory bulb, APP(+) neurons were observed in the mitral cell layer, and HT7 immunoreactivity was not detected (Fig. 1E). Finally, in the cortex, sub-populations of cortical neurons were observed that were HT7(+), APP(+), or HT7(+)/APP(+); these cells increased in number and expression from middle-aged to old-aged 3xTg mice, and were observed both on caudal brain sections at the level of the hippocampus (Fig.1F) and rostral sections at the level of the striatum.

Collectively, these results demonstrate that the APP and hTau transgenes are strongly expressed in AD-relevant brain areas, and that they are not directly expressed by the neurogenic cells within the SVZ or DG.

II.4.2 Alterations in adult neurogenesis in the 3xTg hippocampus

In order to study hippocampal neurogenesis in the 3xTg mice, we divided the multi-step neurogenic process into two main stages: (1) a *proliferative* stage, in which activated neural stem cells produce rapidly dividing progenitors and neuroblasts, and (2) a *post-mitotic* stage, in which proliferating neuroblasts stop dividing, mature, and can functionally integrate into hippocampal circuitry.

Immunohistochemistry for Ki67, a marker of cell proliferation, revealed a significant decrease in the proliferative phase of hippocampal neurogenesis in 3xTg mice. Ki67 quantifications showed that cell proliferation was decreased by more than 80% in 11-month-old 3xTg mice compared to WT controls (8.68 ± 1.44 vs. 1.62 ± 0.43 cells/section, p= 0.0033; n=4/group) (Fig. 2A-C). Proliferation decreased further with age in both groups, and by 18 months was too low to accurately quantify (data not shown).

A concurrent decrease in the 3xTg hippocampal neuroblast population was likewise observed. Fluorescence immunohistochemistry for Doublecortin (DCX), a marker for the proliferative and post-mitotic neuroblast population, revealed highly significant reductions in DCX expression at both 11 and 18 months of age (Fig. 2D-F). In 11-month-old 3xTg mice, DCX expression was decreased by 89% compared to age-matched WT mice (29.19 ± 5.02 vs. 2.97 ± 0.65 cells/section, p= 0.0020; n=4/group). In 18-month-old mice, an age-related decrease in DCX(+) cells was observed in both WT and 3xTg mice, and the number of DCX(+) cells

remained 85% lower in 3xTg mice (8.60 ± 3.40 vs. 1.28 ± 0.45 cells/section, p=0.0770; n=4/group) (Fig. 2F). Strikingly, there was no significant difference between the 11-month 3xTg mice and 18-month WT mice (Fig. 2F).

To determine whether the above deficits in the 3xTg mice ultimately led to the addition of fewer new cells to the dentate granule cell layer, mice were injected with BrdU 21 days before sacrifice and the number of BrdU-retaining granule cells was quantified. Compared to WT mice, 11-month-old 3xTg mice were found to have a 64% reduction in the number of BrdU-retaining cells within the subgranular zone and granule cell layer of the dentate gyrus (2.17 ± 0.40 vs. 0.80 ± 0.35 cells/section, p= 0.0343; n=6 (WT), n=5 (3xTg)) (Fig. 2G-I). At 18 months of age, the number of BrdU (+) cells was too low to assess in both WT and 3xTg groups (data not shown).

Thus, both the proliferative and post-mitotic stages of hippocampal neurogenesis are highly decreased in 3xTg mice.

II.4.3 Reduced neurogenesis in the 3xTg forebrain SVZ and olfactory bulb

Cells produced in the forebrain SVZ stem cell niche contribute to the plasticity of the forebrain and play an essential role in olfaction. To assess SVZ neurogenesis in 3xTg mice, we sub-divided the SVZ/olfactory bulb (OB) neurogenic process into two main stages: (1) a *proliferative* stage comprised of activated stem cells, rapidly dividing progenitor cells and migratory neuroblasts, and (2) a *post-mitotic* stage in which neuroblasts have migrated to the olfactory bulb and differentiated into olfactory bulb neurons.

Expression of multiple markers revealed a generalized decrease in cells in the proliferative stage of neurogenesis in 3xTg mice. First, immunohistochemistry for Ki67 at 11 months of age showed that the total proliferating cell population in 3xTg mice was reduced by

45% compared to WT mice (557.2 ± 39.50 vs. 299.60 ± 34.07 cells/section, p=0.0026; n=4/group) (Fig. 3A-D,G). At 18 months, both WT and 3xTg mice had undergone an aging-dependent reduction in Ki67, but the difference had increased to 60% (369.4 ± 72.24 vs. 147.3 ± 10.82 cells/section, p=0.0228; n=4/group) (Fig. 3E-G). Interestingly, there was no statistical difference in SVZ proliferation between 11-month-old 3xTg mice and 18-month-old WT mice (Fig. 3G). Next, to confirm that the reduction in SVZ cell proliferation involved a decrease in progenitor and intermediate neuroblast populations, we performed immunohistochemistry for Mash-1, a marker of neuronal progenitors and neuroblasts (Fig. 3H-L). Quantification showed that 3xTg mice had a 35% decrease in Mash-1(+) cells at 11 months of age (317.3 ± 24.23 vs. 204.6 ± 33.19 cells/section, p=0.0369; n=4 (WT), n=3 (3xTg)) (Fig. 3 H,I,L). At 18 months, 3xTg mice still had 30% fewer Mash-1(+) cells (195.1 ± 13.83 vs. 136.0 ± 13.49 cells/section, p=0.0222; n=4/group) (Fig. 3 J-L). Immunoreactivity for the neuroblast marker, DCX, was also visibly decreased in 3xTg mice relative to age-matched controls at both 11 and 18 months of age (data not shown).

We next assessed the longer term fate of dividing SVZ cells. In the SVZ, stem cells divide approximately every 28 days, progenitors divide approximately every 15 hours, and neuroblasts migrate to the olfactory bulb within 14 days of being produced (Morshead *et al.*, 1994). Using the 21 day BrdU-retaining paradigm described earlier, we quantified the number of BrdU-retaining cells in the SVZ (a measure of how many stem cells divided during the BrdU pulse) and in the olfactory bulb (a measure of SVZ-derived neurons added to the bulb). In the SVZ, there was a 41% decrease in the number of BrdU(+) cells in 11-month-old 3xTg mice (20.60 ± 5.03 vs. 12.10 ± 3.49 cells/section; p=0.0529; n=4/group) (Fig. 4A-C). There remained a 38% difference at 18 months (p=0.1196; data not shown and Fig. 4C). In the olfactory bulb,

there was a 30% decrease in BrdU(+) cells in 11 month old 3xTg mice (146.40 ± 11.56 vs. 102.13 ± 14.62 cells/section; p= 0.0063; n=4/group) (Fig. 4D-F), and no significant difference by 18 months of age (data not shown and Fig. 4F).

Together, the above results reveal deficits at all stages of SVZ/OB neurogenesis in 3xTg mice, and that these changes are already apparent by middle-age.

II.4.4 Structural changes within the SVZ of 3xTg mice

To determine the effects of the previous findings on the cellular organization of the SVZ, we used semi-thin sections to examine the structural characteristics of the 3xTg SVZ at higher resolution. Pre-embedding immunohistochemistry was performed for the proliferative marker Ki67, sections were counterstained with toludine blue, and the walls of the lateral ventricles were reconstructed from photomicrographs of the 1 µm serial sections as described in the Materials and Methods.

Quantification of the reconstructed ventricles revealed that i) the overall number of Ki67(+) cells decreased significantly in the 3xTg mice (26.67 ± 0.67 vs. 13.00 ± 4.51 cells/1µm section, p= 0.0400; 1 ventricle/animal, n=3/group) (Fig. 5B,E,F); ii) there was a significant decrease in the number of subependymal cells in the 3xTg mice (146.7 ± 8.57 vs. 96.67 ± 14.44 cells/1µm section, p= 0.0408; 1ventricle/animal, n=3/group) (Fig. 5C,E,F); and iii) there was no change in the number of ependymal cells lining the ventricle (93.33 ± 1.86 vs. 101.0 ± 34.51 cells/1µm section, p= 0.8353; 1ventricle/animal, n=3/group) (Fig. 5E,F). Intriguingly, 3xTg ependymal cells contained large, cytoplasmic deposits reminiscent of lipid droplets (0.33 ± 0.33 vs. 28.00 ± 5.13 lipid droplets/1µm section, p=0.0058; 1 ventricle/animal, n=3/group) (Fig.5D-F). These droplets measured from 2-6 µm, were almost exclusively found in the 3xTg mice, and

were most abundant in the ventral region of the ventricle. Staining of 40 μm SVZ sections with Oil Red O, a lipid-specific stain, confirmed that these structure were lipid droplets (Fig. 5G). Thus, 3xTg mice possess marked changes in the SVZ niche that include losses of proliferating cells and sub-ependymal cells, as well as metabolic abnormalities in ependymal cells.

II.4.5 Status of AD-associated amyloid and tau pathologies

Previous studies have shown that 3xTg mice exhibit a progressive and age-dependent formation of AD-associated amyloid plaques and neurofibrillary tangles (Oddo *et al.*, 2003a; Oddo *et al.*, 2003b; Mastrangelo & Bowers, 2008). Development of these pathologies occurs through a multi-stage process that is sensitive to modulation by a variety of physiological parameters, such as housing conditions and diet (Lazarov *et al.*, 2005; Lim *et al.*, 2005; Halagappa *et al.*, 2007; Hu *et al.*, 2010). We therefore investigated the stage and localization of amyloid and tau pathologies in our own 11-month-old 3xTg mice.

To evaluate the development of amyloid pathology (Fig. 6A), we first assessed accumulation of the soluble $A\beta_{1-42}$ metabolite of APP, an early step in the formation of amyloid plaques. Dot blots of the soluble protein fractions of brain lysates from 11-month-old 3xTg and WT mice were probed with the 12F4 antibody against $A\beta_{1-42}$; this revealed an accumulation of $A\beta_{1-42}$ in lysates of the cortex, hippocampus, striatum and olfactory bulbs that was specific to 3xTg mice (Fig. 6B). To determine whether soluble $A\beta_{1-42}$ had yet formed insoluble oligomers or plaques, we also probed the insoluble fractions of our protein lysates, but no $A\beta_{1-42}$ was detected in these fractions (not shown). Importantly, these same insoluble protein fractions did contain aggregates of tau (Fig. 6F). Two additional lines of evidence indicated that $A\beta_{1-42}$ had not yet been deposited as insoluble extracellular plaques in our 11-month-old 3xTg mice. First, when

3xTg tissue sections were processed for immunohistochemistry using the 12F4 antibody, which is selective for extracellular $A\beta_{1-42}$ on tissue sections (Mastrangelo & Bowers, 2008), no $A\beta_{1-42}$ immunoreactivity was detected (data not shown). Second, thioflavin-S staining, which readily detects plaque-associated β-pleated sheets, did not reveal any extracellular aggregations (data not shown). Together, these data indicate that amyloid pathologies are at a relatively early stage of progression in the 11-month-old 3xTg mice used in this study.

We also assessed the stage of development of tau pathologies. In AD, tau accumulates in hyperphosphorylated states within the somato-dendritic compartment of neurons. Formation of neurofibrillary pre-tangles and tangles is associated with a temporal sequence of phosphorylation events that can be identified using specific antibodies, including AT8 (serine 202 and threonine 205 phosphorylation), AT180 (threonine 231 and serine 235 phosphorylation), and PHF-1 (serine 396 and 404 phosphorylation). These epitopes delineate early, intermediate, and late pathology states, respectively (Deters *et al.*, 2008) (Fig. 6C). In 11-month-old 3xTg mice, biochemical analyses revealed prominent increases in AT8-immunoreactive bands at approximately 50KDa in the soluble fractions from the hippocampus (6.4x), striatum (2.7x) and olfactory bulbs (3.6x) relative to age-matched controls (Fig.6D). The same analysis for AT180 likewise identified increases in the hippocampus (2.7x), striatum (1.3x) and olfactory bulbs (2.0x) (Fig. 6E). In both cases, these changes were strongest in the hippocampus, and in neither case was tau hyperphosphorylation detected in the cortical samples. Interestingly, samples blotted with the AT8 antibody also yielded a 3xTg-specific band at approximately 17KDa in all brain regions, which may correspond to a previously identified 17 KDa neurotoxic fragment of tau (Park & Ferreira, 2005). Finally, we probed our insoluble protein fractions with hTau; this

revealed the appearance of a prominent hTau-reactive band below 50KDa that was specific to the hippocampus of 3xTg mice (Fig. 6F), indicating that tau had become filamentous and insoluble.

To further localize the progression of tau pathology, we performed immunohistochemistry for AT8, AT180 and PHF-1 (a marker of tangle-associated tau paired helical filaments) (Fig.6G-K). In 11-month-old 3xTg mice, there were large numbers of AT8-immunoreactive neurons in the hippocampal CA1 region (Fig. 6G) and relatively fewer AT180(+) neurons (Fig. 6H). These neurons had pronounced immunoreactivity in their cell bodies and basal dendritic processes. By 18 months of age, the number of AT8(+) neurons had decreased (Fig. 6G) while AT180(+) cells had increased (Fig. 6H), consistent with progression to an intermediate stage of tau hyperphosphorylation. Moreover, immunohistochemistry for PHF-1 revealed the appearance of small numbers of PHF-1(+) CA1 neurons at 18 months (Fig. 6I). Within the dentate gyrus stem cell niche, AT8(+) neurons were observed scattered in the hilus of 11-month 3xTg mice (Fig. 6J). AT180(+) neurons were also found in the hilus of 11- month 3xTg mice and in rare upper dentate granule neurons of 18-month-old 3xTg mice (Fig. 6K). Outside the hippocampus, small numbers of neurons labelled with these markers of tau hyperphosphorylation were present in the amygdala and cortex, but no immunoreactivity was observed in the striatum, striatal SVZ, or olfactory bulbs (data not shown).

Together, these results show that amyloid plaque and neurofibrillary tangle development are at early-to-intermediate stages of development in our 11-month-old 3xTg mice.

II.5 DISCUSSION

In this study, we investigated neural precursor populations in the brains of middle-aged and old 3xTg mice. We demonstrate a major reduction in adult neurogenesis in 3xTg mice that is

widespread and already present by middle-age, prior to plaque and tangle formation. Our principal findings are that (i) in both neurogenic niches of the adult brain, the hippocampus and forebrain SVZ, 3xTg mice have fewer proliferating cells, neural progenitors and neuroblasts, resulting in decreased numbers of adult-born cells being added to the dentate granule cell layer and the olfactory bulbs; (ii) levels of neurogenesis in middle-aged 3xTg mice are similar to those in old wildtype mice, indicating a marked acceleration of aging-related changes in neural stem cell activity; (iii) in the forebrain SVZ, there is a selective loss of sub-ependymal cells and a pronounced accumulation of large lipid droplets within ependymal cells, suggestive of significant organizational and metabolic changes within this stem cell niche; and (iv) disturbances of adult neurogenesis are clearly evident at early stages of amyloid and tau pathology progression, before the appearance of the hallmark Aβ plaques and tangles. Given the important roles of the hippocampal and forebrain stem cell systems in learning and memory and overall brain plasticity, these findings suggest that early disturbance in the adult brain's neurogenic regions may be a contributing factor to AD-induced premature cognitive decline.

II.5.1 Age-related decreases in adult neurogenesis are accelerated prior to plaque and tangle formation in 3xTg mice

As mammals age, both the SVZ and hippocampal neurogenic niches undergo significant structural changes and reductions in their rates of neurogenesis (Kuhn *et al.*, 1996; Eriksson *et al.*, 1998; Kempermann *et al.*, 1998; Cameron & McKay, 1999; Luo *et al.*, 2006; Knoth *et al.*, 2010). Since stem cells are, by definition, long-lived and exposed to the noxious effects of both extrinsic and intrinsic effectors of damage (Van Zant & Liang, 2003), they are likely to have a selective vulnerability to aging-related changes and aging-related neurodegenerative diseases

such as AD. Moreover, stem cells may not only be the victims of aging-related changes, but also an important contributing factor to the tissue aging process when they are damaged or deregulated.

Our analyses revealed that middle-aged 3xTg mice have prominent reductions in both early proliferating progenitor populations and later post-mitotic stages of DG and SVZ neurogenesis. Furthermore, in both these stem cell niches, the neurogenic parameters examined in middle-aged 3xTg mice were found to be reduced, highlighting a significant and widespread acceleration of aging-dependent decreases. Within the SVZ of 11-month-old 3xTg mice, there was a 41% reduction in the number of 21-day BrdU-retaining cells, consistent with either depletion or increased quiescence of the SVZ stem cell population. Previous examination of cell proliferation in 3xTg mice had identified a reduced expression of the mitotic marker, phosphohistone-3, in both the DG and the SVZ (Rodriguez *et al.*, 2008; Rodriguez *et al.*, 2009); however, these earlier studies did not further characterize the phosphohistone-3 (+) cells or any other aspects of the neurogenic pathways, thus the overall impact of the 3xTg model on neurogenesis remained to be determined (Chuang, 2010b).

More detailed analysis of the 3xTg SVZ revealed a selective depletion of cells within the subependymal compartment, where stem cells, transit-amplifying progenitor cells, neuroblasts, oligodendrocyte progenitors and astrocytes are normally located (Doetsch *et al.*, 1997). We also identified a highly significant increase in the number of large lipid droplets observed within the cytoplasm of SVZ ependymal cells. This may be significant because ependymal cells are a crucial element of the SVZ niche, and are actively involved in the secretion, transport and absorption of molecules into and from the cerebrospinal fluid. Lipid droplets are cellular stores of neutral lipids such as triglycerides and steryl esters (Goodman, 2008), and their appearance is

indicative of significant metabolic/energetic changes within the SVZ niche. Since the cellular organization of the human SVZ appears to differ somewhat from that of the mouse (Sanai *et al.*, 2004; Curtis *et al.*, 2007a), it will be important to determine if similar changes in cellular organization and metabolism occur in the SVZ of AD patients.

The accelerated age-related deficits in neurogenesis occurred prior to the overt formation of AD-associated neuropathologies. We found that $A\beta_{1-42}$ had accumulated within the soluble fraction of our lysates, but had not yet been deposited as insoluble extracellular plaques. For tau, phosphorylation-specific antibodies showed that early and intermediate stages of hyper-phosphorylation were present at 11 months, and only at 18 months did we begin to detect late-stage PHF-1 staining of fibrillar tau. The timing of amyloid and tau pathologies measured in our mice is significantly delayed in comparison to the original description of the 3xTg mouse model (Oddo *et al.*, 2003b), however our analysis of these pathologies is highly consistent with a very thorough and more recent testing of pathology development in these mice (Mastrangelo & Bowers, 2008). This later onset of pathologies has been attributed to sex differences, neuroinflammatory factors, and "drift" of transgenic characteristics (Mastrangelo & Bowers, 2008), and is likely further complicated by the sensitivity of pathology development to housing conditions such as environmental enrichment and diet (Lazarov *et al.*, 2005; Lim *et al.*, 2005; Halagappa *et al.*, 2007). Our finding that widespread decreases in adult neurogenesis occur prior to plaque formation is in line with other identified plaque-independent effects of β-amyloid, such as perturbations of synaptic transmission (Hartley *et al.*, 1999; Hsia *et al.*, 1999). A greater understanding of the reasons and consequences of these changes may provide important clues to understanding how neural precursor activity is altered in AD.

II.5.2 Potential mechanisms of neural precursor regulation in the 3xTg model

The mechanisms by which adult neurogenesis may be dys-regulated in AD have yet to be fully understood. Previous studies have examined neurogenesis in transgenic AD mouse models carrying single mutations used to generate the 3xTg model. A study on $PS1_{M146V}$-KI mice showed reduced DG neurogenesis, reporting a 25% reduction in proliferation by BrdU and a 35% reduction in new mature neurons by BrdU/NeuN at 3 months of age (Wang *et al.*, 2004; Chuang, 2010b). Another study in female Thy-1-APP_{swe} mutant mice showed no difference in proliferation by BrdU or new mature neurons by BrdU/NeuN, but a decrease of almost half of the newly born neurons by DCX at 5 months of age. However, at 25 months they reported a 3-fold increase in proliferation, a 6-fold increase in new mature neurons, and a 3-fold increase in newly born neurons in the DG (Ermini *et al.*, 2008; Chuang, 2010b). A studying looking at neurogenesis in the DG of 8- to 10-week-old male tau-P301L transgenic mice found no change in Ki67, 28day BrdU or DCX (Boekhoorn *et al.*, 2006b). None of these studies examined the SVZ of their mice. Thus it is possible that the PS1 mutation dominates over the APP and tau mutations in the 3xTg model. Interestingly, the PS1/γ-secretase complex is also an essential regulator of the Notch signalling pathway (De Strooper *et al.*, 1999; Struhl & Greenwald, 1999), which is required for maintenance of adult neural stem cell populations (Alexson *et al.*, 2006).

There are also numerous possibilities through which the stem cell niche, or regulatory microenvironment, could be impacted by AD mutations or mutant proteins. APP is cleaved to generate soluble APP (sAPP) and soluble $A\beta_{1-42}$. $A\beta_{1-42}$ administration has been shown to affect neural precursor proliferation and differentiation in culture and in vivo (Haughey *et al.*, 2002a; Haughey *et al.*, 2002b; Lopez-Toledano & Shelanski, 2004), and could gain access to neural stem cell niches by axonal transport and synaptic release (Lazarov *et al.*, 2005; Szodorai *et al.*,

2009) or by accumulation in the CSF (Lue *et al.*, 1999; McLean *et al.*, 1999). sAPP is released extracellularly from APP-expressing cells and has been shown to preferentially bind to neural precursors and potentially regulate neural precursor proliferation (Caille *et al.*, 2004). Besides metabolites of APP, there is also recent evidence that PS1 mutations can alter hippocampal neurogenesis through non-cell autonomous mechanisms involving changes in microglial-secreted factors (Choi *et al.*, 2008). Furthermore, AD is associated with reductions in cholinergic neurotransmission, which is an important positive regulator of hippocampal neurogenesis (Itou *et al.*, 2010) and has yet to be studied in 3xTg mice.

We identified three additional noteworthy and novel alterations occurring within the vicinity of the DG and/or SVZ stem cell niches in 3xTg mice. First, we observed accumulations of large lipid droplets within the SVZ ependymal layer, indicative of significant metabolic alterations within the SVZ niche. This is a particularly intriguing finding given that ApoE4, the strongest genetic risk factor known for sporadic AD, is likewise involved in lipid transport. Second, 3xTg mice possessed tau-overexpressing fibers in the striatum, directly adjacent to the SVZ (Fig. 1D); neurotransmitters, such as dopamine, released from these fibers normally contribute to the regulation of SVZ neural precursor activity (Kippin *et al.*, 2005). Third, we identified neurons in the hilus of the dentate gyrus that were immunoreactive for hyper-phosporylated tau (Fig. 6J,K); hilar neurons normally form synapses onto newly born hippocampal neurons and regulate their maturation through GABAergic mechanisms (Tozuka *et al.*, 2005; Ge *et al.*, 2006; Liu *et al.*, 2006; Ge *et al.*, 2007). More detailed examination of the possible impact of these alterations is warranted.

II.5.3 Impact of deficits in neurogenesis on cognitive impairments in AD

Our findings add to the growing body of evidence that important biological changes occur prior to the development of hallmark pathological features of AD. The number of plaques and levels of secreted Aβ do not correlate well with the clinical onset of AD (Arriagada *et al.*, 1992; Samuel *et al.*, 1994). Similarly, the number of tangles is only slightly more predictive of overall cognitive dysfunction in human AD (McKee *et al.*, 1991; Arriagada *et al.*, 1992). Interestingly, in our study, the changes in neurogenesis in 3xTg mice were already well established prior to the deposition of amyloid plaques and neurofibrillary tangles. A previous study in 3xTg mice reported cognitive impairments as early as 4 months of age, prior to plaque and tangle formation, and in the absence of any reported cell death (Billings *et al.*, 2005; Gimenez-Llort *et al.*, 2007). Instead, they showed that these deficits correlated with the levels of intraneuronal $A\beta_{42}$. This suggests that cognitive impairments are an early symptom in the 3xTg and cell death has not been reported in this model. Thus the causes of early cognitive impairment remain elusive, but could possibly involve deficits in neurogenesis.

When considering how the deficits in neurogenesis observed in the 3xTg mice might relate to the symptomology of AD, it is also important to recognize the distinction between genetically determined lifespan and actual lifespan. The gap between the two varies considerably between species, as many factors contribute or alter the lifespan of an animal. For example, humans have the ability to control their environment by changing their diet, physical activity, education, stress, and medical attention, all of which have been shown to impact on lifespan (Christensen & Vaupel, 1996; Faragher *et al.*, 2009; Fontana *et al.*, 2010; Kenyon, 2010; Rockenfeller & Madeo, 2010). It is possible that, with the increased knowledge of these factors,

humans have pushed the limits of their genetically determined lifespan beyond its programmed capability. This could explain why AD is a disease only naturally found in humans.

II.5.4 Conclusions

Alzheimer's Disease is often regarded as a form of accelerated aging. Here, using the 3xTg model of AD, we found an acceleration of aging-related changes in both the mitotic and post-mitotic stages of adult neurogenesis. These changes occurred before development of the pathological hallmarks of the disease (Fig. 7). Although neurogenic activity was found to be diminished in 3xTg mice, recent studies have shown that environmental enrichment can promote hippocampal neurogenesis in at least some AD mouse models (Hu *et al.*, 2010; Lazarov & Marr, 2010). Given the important contribution of adult neurogenesis to learning, memory, and overall brain plasticity, it will be important to determine whether preventing or reversing age-related declines in the production of new neurons can functionally compensate for AD-associated deficits.

II.6 FIGURES AND FIGURE LEGENDS

Figure 1

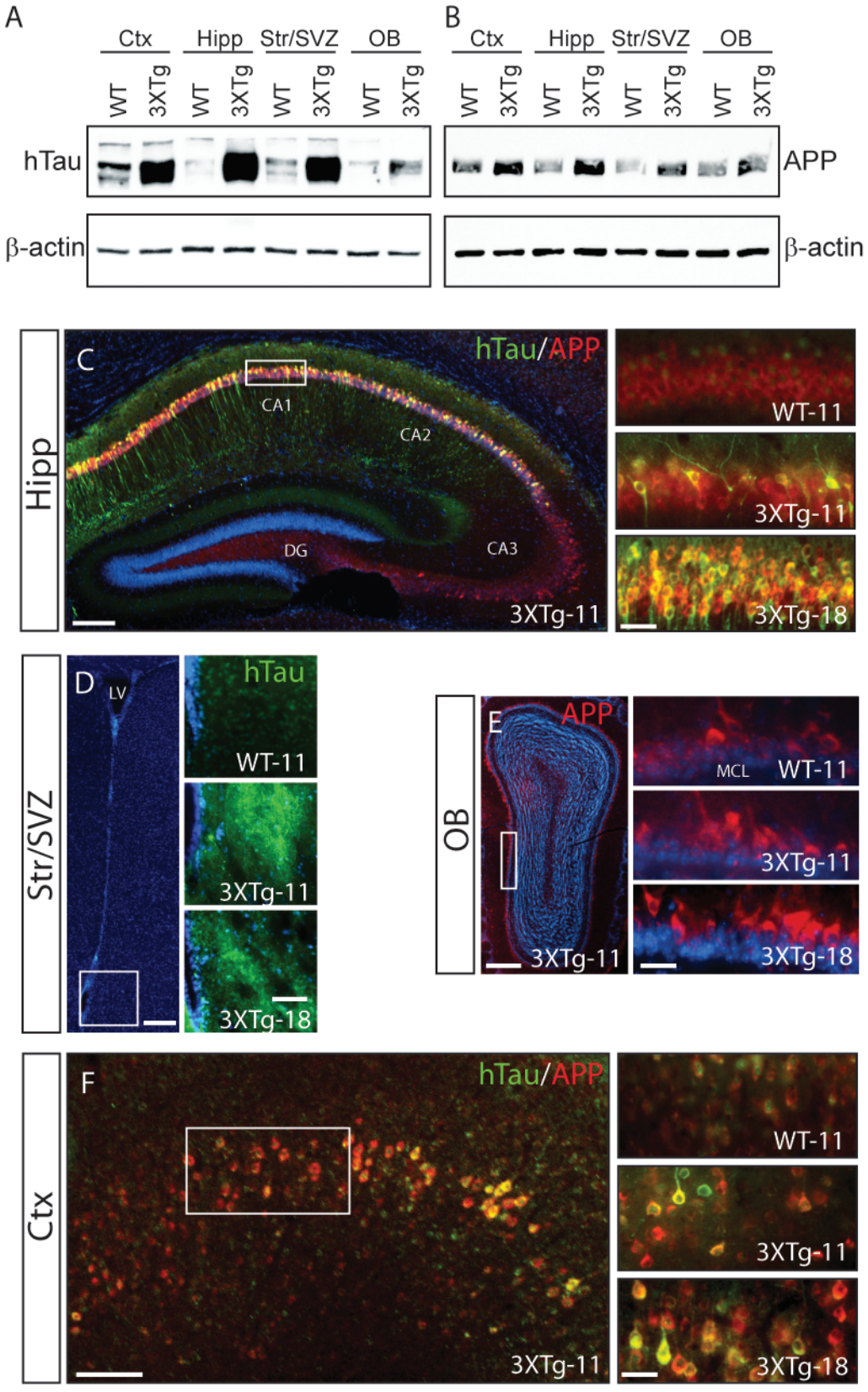
A
Ctx
Hipp
Str/SVZ
OB
WT
3XTg
hTau
β-actin
B
APP
C
hTau/APP
CA1
CA2
DG
CA3
3XTg-11
WT-11
3XTg-18
Hipp
D
LV
hTau
Str/SVZ
E
APP
MCL
OB
F
Ctx

Figure 1. APPswe and tau P301L transgene expression in the brains of 11-and 18- month-old 3xTg mice

(A,B) Western blot analysis of protein levels in the cortex (Ctx), hippocampus (Hipp), striatum (Str/SVZ), and olfactory bulbs (OB) of 11-month-old wildtype (WT) and 3xTg mice, probed for either **A,** hTau in the soluble fraction using the HT7 antibody, or **B,** APP in the membrane fraction using the 12F4 antibody. **(C-F)** Immunofluorescence labelling for hTau and APP in **C,** hippocampus, **D,** striatum/SVZ, **E,** olfactory bulb, and **F,** cortex of 11-month-old wildtype (WT-11), 11-month-old 3xTg (3XTg-11), and 18-month-old 3xTg (3XTg-18) mice. For each panel, images on the right are high magnification micrographs of a region corresponding to the boxed area. Scales bars; in C,F = 200μm (inset = 40 μm), in D = 300 μm (inset = 60 μm), in E= 350 μm (inset = 40 μm). Abbreviations: SVZ (subventricular zone), DG (dentate gyrus), MCL (mitral cell layer).

Figure 2

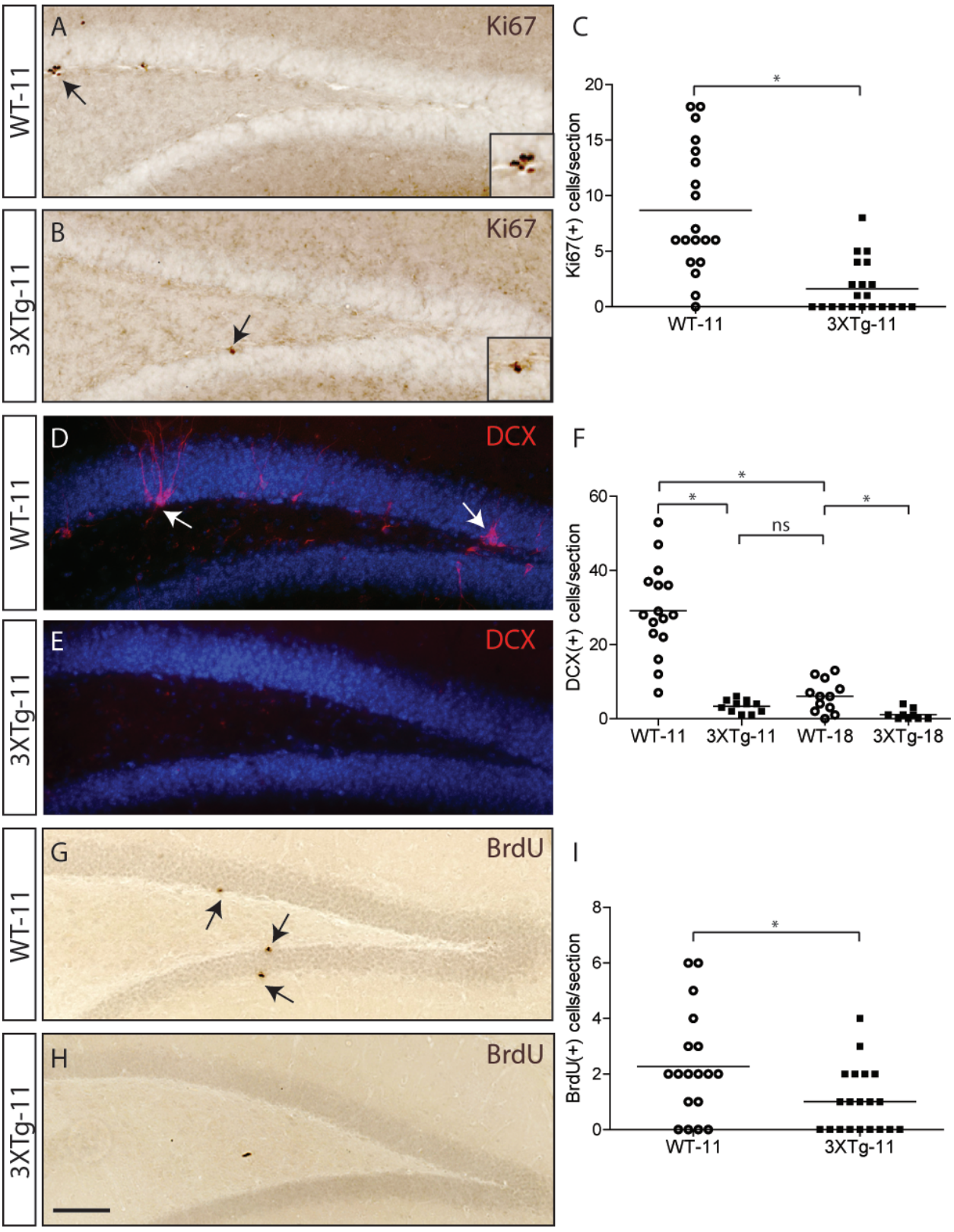
WT-11
A
Ki67
3XTg-11
B
Ki67
C
Ki67(+) cells/section
20
15
10
5
0
*
WT-11
3XTg-11
WT-11
D
DCX
3XTg-11
E
DCX
F
DCX(+) cells/section
60
40
20
0
*
*
*
ns
WT-11
3XTg-11
WT-18
3XTg-18
WT-11
G
BrdU
3XTg-11
H
BrdU
I
BrdU(+) cells/section
8
6
4
2
0
*
WT-11
3XTg-11

Figure 2. Proliferation, neurogenesis and survival of newly born cells are all reduced in the dentate gyrus of the 3xTg hippocampus.

(A-C) Immunoreactivity for the proliferative marker Ki67 in 11-month-old **A,** wildtype (WT-11) and **B,** 3xTg (3XTg-11) mice. Insets show higher magnification of cells indicated with arrows. **C,** Number of Ki67(+) cells/section of the hippocampus quantified from each group. **(D-F)** Fluorescence immunohistochemistry for the neuroblast marker DCX in 11-month-old **D,** wildtype (WT-11) and **E,** 3xTg (3XTg-11) mice. Nuclei are counterstained with Hoechst 33342. **F,** Number of DCX(+) cells/section of dentate gyrus quantified from each 11-month-old and 18-month-old group. **(G-I)** Immunoreactivity for 21 day BrdU-retaining cells in 11-month-old **G,** wildtype (WT-11) and **H,** 3xTg (3XTg-11) mice. **I,** Number of Ki67(+) cells quantified from each section. In all panels, arrows indicate positive cells. Statistical analysis was performed on the average number of cells/section/animal for each group. *$p \leq 0.05$ (*)*, *$p \leq 0.01$ (**)*, not significant *(ns)*. Scale bar; in H = 60μm (for A-H).

Figure 3

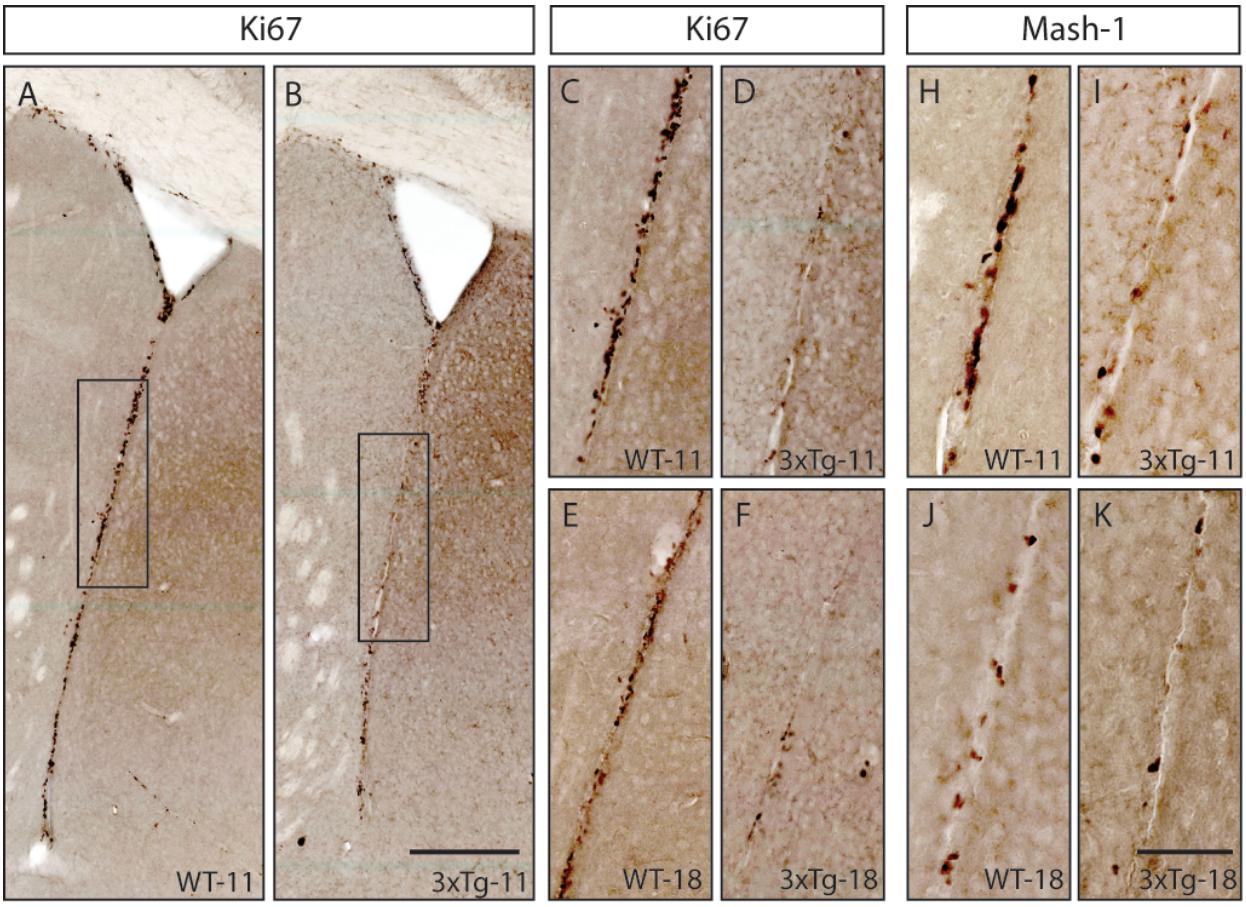
Ki67
Ki67
Mash-1
A
B
C
D
H
I
E
F
J
K
WT-11
3xTg-11
WT-11
3xTg-11
WT-11
3xTg-11
WT-18
3xTg-18
WT-18
3xTg-18

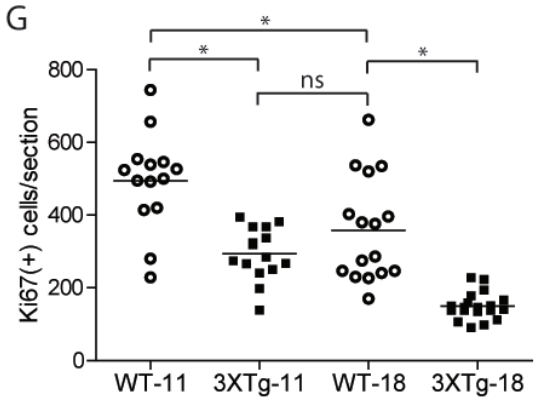
G
Ki67(+) cells/section
800
600
400
200
0
ns
*
*
*
WT-11
3XTg-11
WT-18
3XTg-18

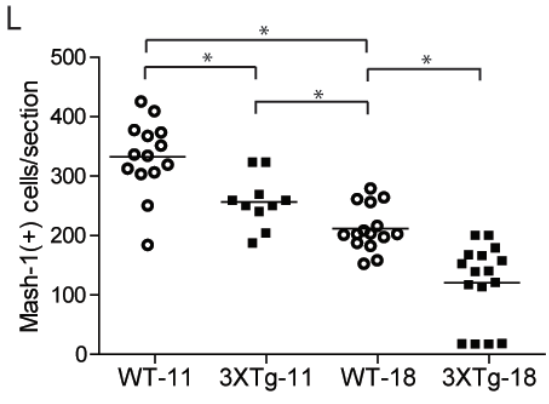
L
Mash-1(+) cells/section
500
400
300
200
100
0
*
*
*
*
WT-11
3XTg-11
WT-18
3XTg-18

Figure 3. Cell proliferation and neural progenitors are decreased in the 3xTg SVZ.

(**A-G**) Immunoreactivity for the proliferative marker Ki67 and (**H-L**) the progenitor cell marker Mash-1 in the SVZ. **A,** Low magnifications of Ki67 in 11-month-old wildtype (WT-11) **B,** 11-month-old 3xTg (3XTg-11). (**C-F**) High magnifications of Ki67 in boxed area. (**H-K**) High magnifications of Mash-1 in boxed area. Note the reduced numbers of both Ki67(+) and Mash-1(+) nuclei in the 3xTg mice at each age. **G,** Number of Ki67(+) cells quantified from each section. **L,** Number of Mash-1(+) cells quantified from each section. Statistical analysis was performed on the average number of cells/section/animal for each group. *p≤0.05 (*)*, *p≤0.01 (**)*, not significant *(ns)*. Scale bars; in B = 350 μm (for A,B), in K = 100μm (for C-F, H-K).

Figure 4

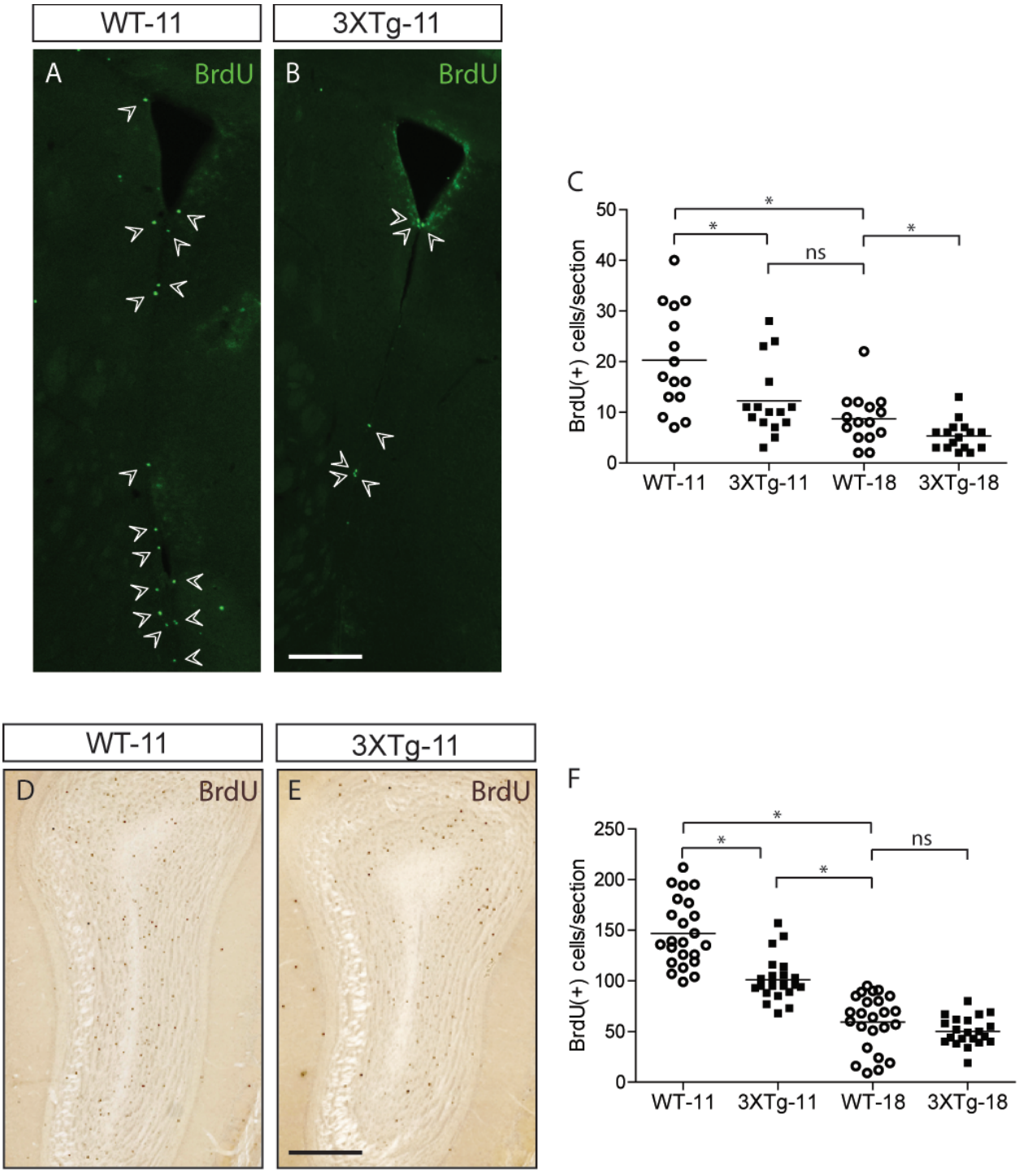
WT-11
3XTg-11
A
BrdU
B
BrdU
C
BrdU(+) cells/section
50
40
30
20
10
0
*
*
ns
*
WT-11
3XTg-11
WT-18
3XTg-18
WT-11
3XTg-11
D
BrdU
E
BrdU
F
BrdU(+) cells/section
250
200
150
100
50
0
*
*
*
ns
WT-11
3XTg-11
WT-18
3XTg-18

Figure 4. Decreased numbers of 21 day BrdU-retaining cells in the SVZ and olfactory bulbs of 3xTg mice.

(A-C) Fluorescence immunohistochemistry for 21-day BrdU-retaining cells in the SVZ of **A,** 11-month-old wildtype (WT-11) and **B,** 11-month-old 3xTg (3XTg-11) mice. Arrowheads identify all BrdU-immunoreactive nuclei. **C,** Quantification of the number of BrdU(+) cells/section in 11- and 18- month old WT and 3xTg mice. **(D-F)** Immunohistochemistry for BrdU in the olfactory bulbs of **D,** WT-11 and **E,** 3xTg-11 mice, showing BrdU-immunoreactive nuclei distributed mainly within the internal granule cell layer. **F,** Quantification of the number of BrdU(+) cells/section of the olfactory bulb, showing a significant decrease in 11-months 3xTg mice compared to age-matched WT mice. Statistical analysis was performed on the average number of cells/section/animal for each group *p≤0.05 (*)*, *p≤0.01 (**)*, not significant *(ns)*. Scale bars; in B = 350 μm (for A, B), in E = 350 μm (for D, E).

Figure 5

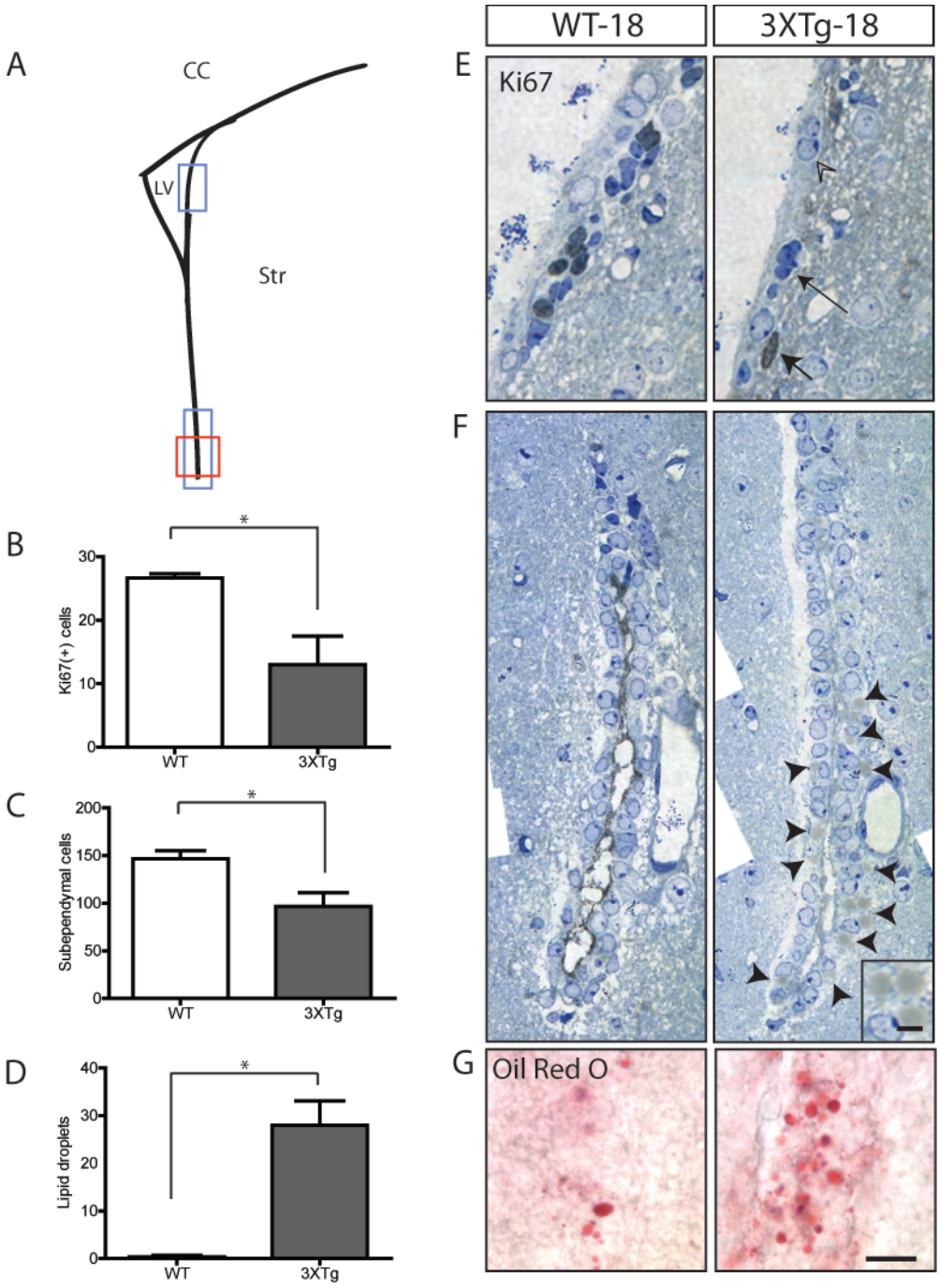
A
CC
LV
Str
B
Ki67(+) cells
30
20
10
0
WT
3XTg
*
C
Subependymal cells
200
150
100
50
0
WT
3XTg
*
D
Lipid droplets
40
30
20
10
0
WT
3XTg
*
WT-18
3XTg-18
E
Ki67
F
G
Oil Red O

Figure 5. Cytological alterations in the SVZ of 3xTg mice.

Montages of the walls of the lateral ventricles were reconstructed from micrographs of 1 μm semi-thin sections from 18-month-old WT and 3xTg mice, as described in Materials and Methods. **A,** Schematic of the lateral ventricle with blue boxes representing where **E** and **F** are located and red box where **G** is located. The number of **B,** Ki67(+) cells, **C,** subependymal cells, and **D,** lipid droplets were quantified. (E-F) Note that 18-month-old 3xTg mice have significant reductions in the number of Ki67(+) cells and subependymal cells compared to age-matched controls. Also, while the number of ependymal cells is unchanged (not shown), there is a major increase in the appearance of large lipid droplets within the cytoplasm of ependymal cells. **G**, Oil Red O staining of lipid droplets on 40μm sections of SVZ. In E, open arrowhead identifies a representative ependymal cell, long arrow identifies a representative subependymal cell and short arrow identifies a representative Ki67(+) cell. Arrowheads in F indicate lipid droplets. Statistical analysis was performed on the average number of cells/ventricle/animal for each group. *$P \leq 0.05$ (*).* Scale bar; in G = 25μm (for E-G), inset in F = 5μm. Abbreviations: CC (corpus callosum), Str (Striatum), LV (lateral ventricle).

Figure 6

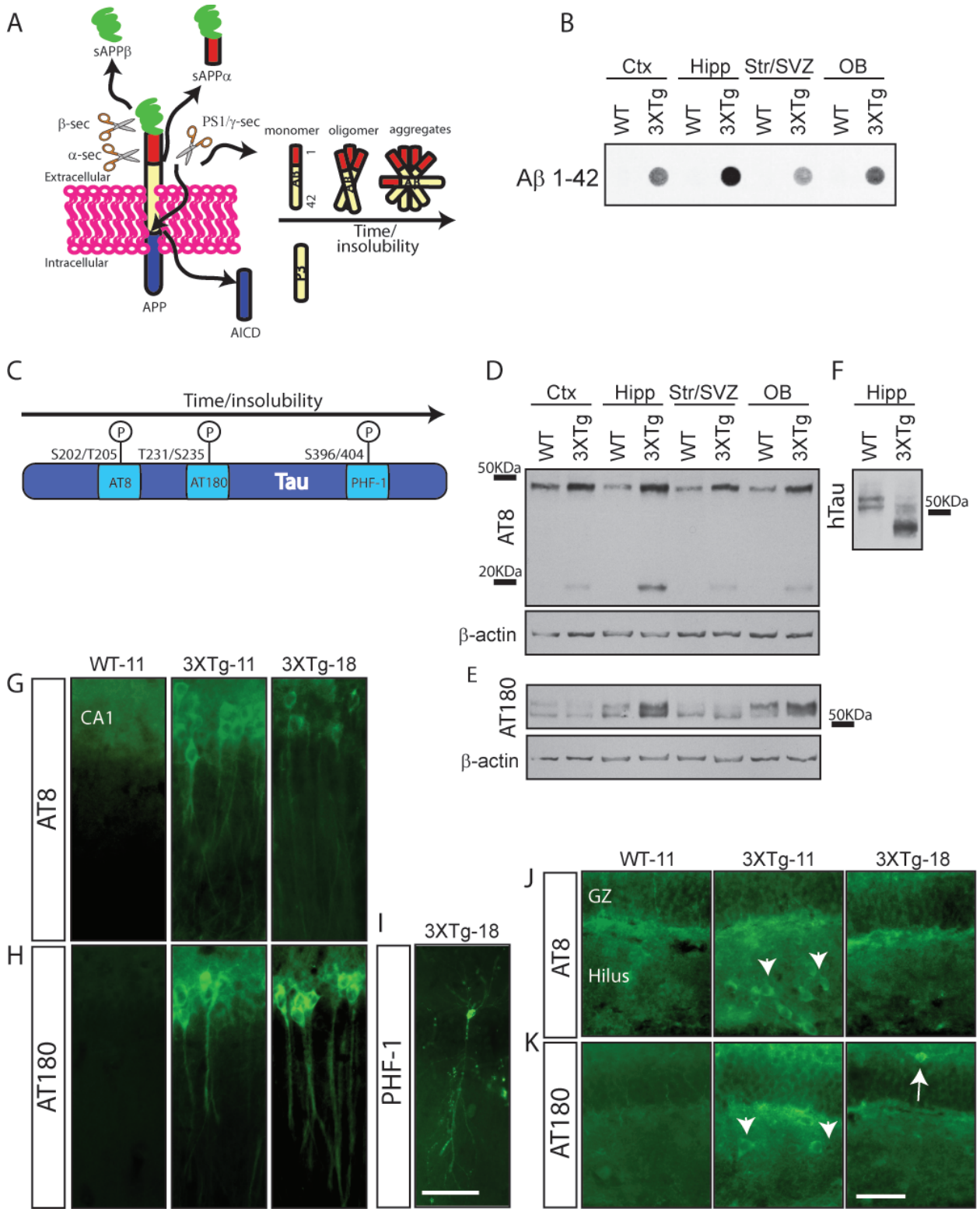
A
sAPPβ
sAPPα
β-sec
α-sec
PS1/γ-sec
Extracellular
Intracellular
APP
AICD
monomer
oligomer
aggregates
Time/
insolubility
B
Ctx
Hipp
Str/SVZ
OB
WT
3XTg
Aβ 1-42
C
Time/insolubility
S202/T205
T231/S235
S396/404
AT8
AT180
Tau
PHF-1
D
50KDa
20KDa
AT8
β-actin
E
AT180
50KDa
β-actin
F
Hipp
hTau
50KDa
G
WT-11
3XTg-11
3XTg-18
CA1
AT8
H
AT180
I
3XTg-18
PHF-1
J
WT-11
3XTg-11
3XTg-18
GZ
Hilus
AT8
K
AT180

Figure 6. Temporal and spatial localization of AD-associated neuropathologies.

A, Schematic representation of APP cleavage and development of Aβ plaques. APP cleavage generates multiple intracellular and extracellular metabolites (AICD, P3, sAPP, Aβ). Under normal physiological conditions, APP is cleaved mainly by α-sec and γ-sec to generate sAPPα and P3 fragments. Under pathological conditions, APP is cleaved mainly by β-sec leading to the generation of sAPPβ, and PS1/γ-sec cleavage is upregulated which results in increased production of the soluble Aβ1-42 metabolite. With increasing time and concentration, Aβ1-42 oligomerizes and eventually forms insoluble aggregates, resulting in amyloid plaque deposition. **B,** Biochemical detection of Aβ1-42 peptide by dot blot. Accumulation of Aβ1-42 is detected in the soluble protein fractions from the cortex (Ctx), hippocampus (Hipp), striatum (Str/SVZ) and olfactory bulbs (OB) of 11-month-old 3xTg mice but not WT mice. **C,** Schematic of time/pathology-associated tau hyperphosphorylation during development of neurofibrillary tangles. AT8, AT180 and PHF-1 antibodies recognize phosphorylation-specific sites associated with early, intermediate and late stages of hyperphosphorylation, respectively. (**D-F),** Biochemical detection of tau hyperphosphorylation status by Western blotting. The soluble fractions from the cortex, hippocampus, striatum and olfactory bulbs of 11-month-old wildtype (WT) and 3xTg mice were probed with **D,** AT8 and **E,** AT180 antibodies. Note that AT8 gave an expected band at approximately 50 KDa as well as an approximately 17 KDa fragment. AT180 yielded bands at approximately 55 and 60 KDa. Both AT8 and AT180 were increased most strongly in the hippocampus. Densitometry quantifications are reported in Results. **F,** The insoluble fraction of hippocampal protein lysates were probed with the phosphorylation-independent tau antibody, HT7. Note the appearance of a strong, 3xTg-specific band just below 50 KDa. **(G-K)** Detection of tau hyperphosphorylation in the hippocampus by fluorescence

immunohistochemistry. In the CA1 layer of the hippocampus of 11- and 18-month-old mice, immunoreactivity specific to 3xTg mice was detected for **G,** AT8 and **H,** AT180. Note that somatodendritic accumulation of AT8 was highest at 11 months, while AT180 was highest at 18 months. **I,** Rare CA1 cells immunoreactive for PHF-1 were observed solely in the 18-month 3xTg mice. **(J-K)** In the dentate gyrus of the hippocampus, neurons immunoreactive for **J,** AT8 and **K,** AT180 were present in the hilus of 11-month-old 3xTg mice (arrowheads). At 18 months, occasional AT180(+) neurons in the outer granule cell layer were also observed (arrow). Scale bars; in I,K = 60μm (for G-I), and (J,K) respectively. Abbreviations: AICD (APP intracellular domain), sAPP (soluble amyloid precursor protein), sec (secretase), GZ (granular zone).

Figure 7

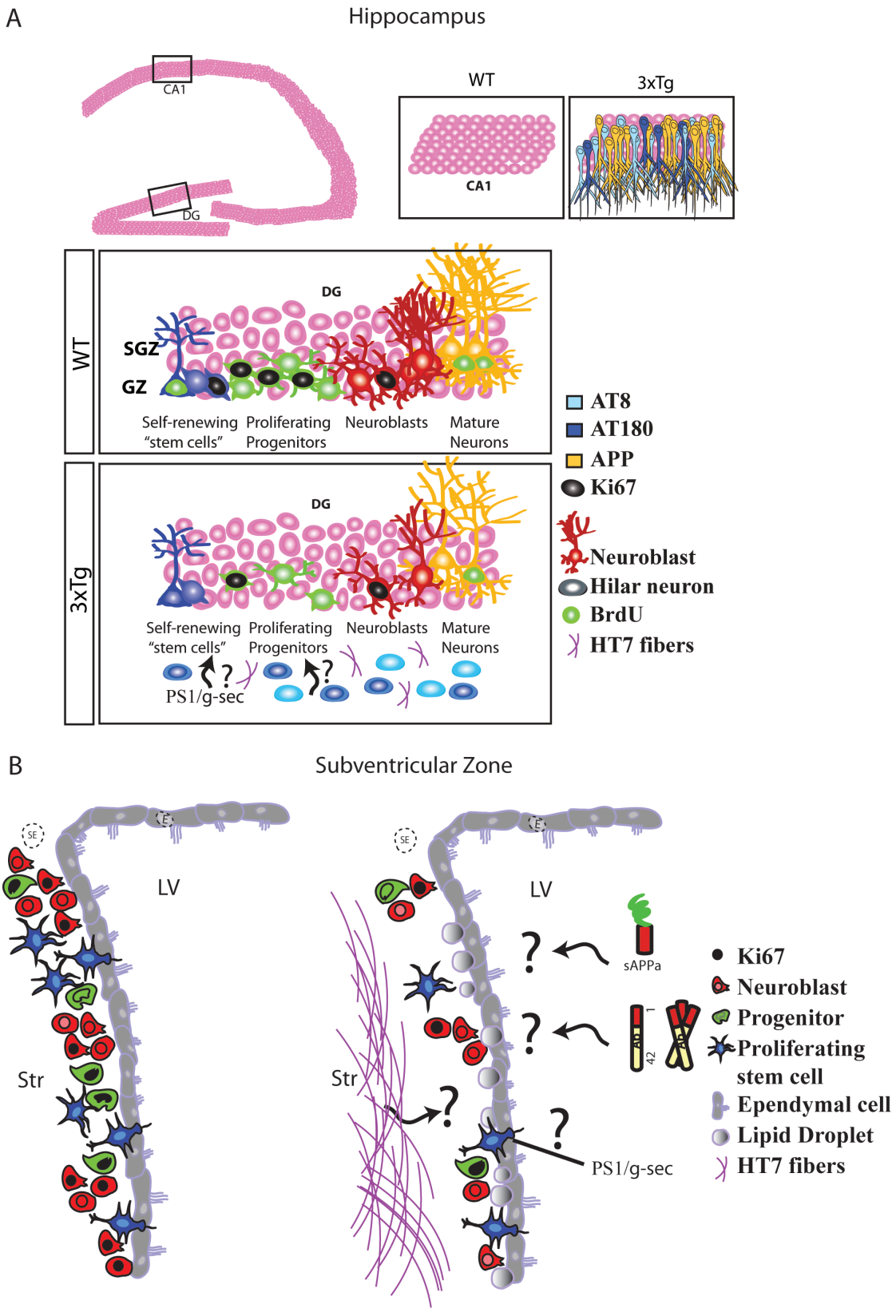
A
Hippocampus
CA1
DG
WT
3xTg
CA1
WT
DG
SGZ
GZ
Self-renewing "stem cells"
Proliferating Progenitors
Neuroblasts
Mature Neurons
3xTg
DG
Self-renewing "stem cells"
Proliferating Progenitors
Neuroblasts
Mature Neurons
PS1/g-sec
AT8
AT180
APP
Ki67
Neuroblast
Hilar neuron
BrdU
HT7 fibers
B
Subventricular Zone
LV
Str
LV
Str
sAPPa
Aβ 1
42
PS1/g-sec
Ki67
Neuroblast
Progenitor
Proliferating stem cell
Ependymal cell
Lipid Droplet
HT7 fibers

Figure 7. Summary of observations in the middle-aged 3xTg hippocampus and SVZ.

Schematic representation of our findings in the hippocampus (**A**) and SVZ (**B**) of 11-month-old wildtype (WT-11) and 3xTg (3XTg-11) mice. **A,** In the CA1 layer of the hippocampus, there is abundant expression of the APP (yellow) and tau (HT7) transgenes in 3xTg pyramidal neurons including sub-populations of AT8(+) (light blue) and AT180(+) (dark blue), indicating they are at early to intermediate stages of tau pathology. In the DG, there are HT7(+) fibers and AT8(+) and AT180(+) cell bodies in the hilus of 3xTg mice. These pathological events in the CA1 and hilus are correlated with decreased numbers of proliferating cells (black nucleus/Ki67), neuroblasts (DCX) and 21-day label-retaining cells (green nucleus/BrdU) within the SGZ neurogenic niche when compared to 11-month-old controls. **B,** In the SVZ, 3xTg mice possess fewer total numbers of subependymal cells, including fewer total proliferating cells (black nucleus/Ki67), neuroblasts (DCX), neural progenitors (Mash-1) and activated/proliferative stem cells (label-retaining BrdU) when compared to the controls. The number of ependymal cells is unchanged, however in 3xTg mice they frequently contain large cytoplasmic lipid droplets (grey circles). No APP or tau transgene expression is present within the SVZ itself, but HT7(+) fibers are abundantly present in the parenchyma of the immediately adjacent striatum (purple fibers). Question marks indicate some potential routes through which AD-associated mutations and pathologies might affect the DG or SVZ neurogenic niches (see Discussion). Abbreviations: DG (dentate gyrus), SGZ (subgranular zone), GZ (granular zone), LV (lateral ventricle), Str (striatum), SE (subependyma), E (ependyma).

II.7 ACKNOWLEDGEMENTS

This work was supported by funds from the Canadian Institutes of Health Research, Grant number 86600, the Scottish Rite Charitable Foundation of Canada, Grant number 07114, the Alzheimer Societies of Canada and Saskatchewan, New Investigator Grant, and the Stranahan Foundation and American Alzheimer Association, Grant number NIRG-07-60174. The authors are grateful to Dr. Nicole Leclerc and to members of the Fernandes lab for helpful discussions and advice.

CHAPTER 3

III. SECOND ARTICLE

"ELEVATED OLEIC ACID LEVELS WITHIN THE FOREBRAIN NICHE SUPPRESS NEURAL STEM CELL ACTIVATION IN ALZHEIMER'S DISEASE"

Manuscript in revision for re-submission

Elevated oleic acid levels within the forebrain niche suppress neural stem cell activation in Alzheimer's disease

Laura K. Hamilton[1], Martin Dufresne[2], Sandra E. Joppé[1], Sarah Petryszyn[3], Anne Aumont[1], Frédéric Calon[4], Alexandra Furtos[2], Martin Parent[3], Pierre Chaurand[2], and Karl J. L. Fernandes[1]

[1]Research Center of the University of Montreal Hospital (CRCHUM), CNS Research Group (GRSNC), and Department of Neurosciences, Faculty of Medicine, Université de Montréal, Montreal, QC, Canada. [2]Faculty of Arts and Sciences, Department of Chemistry, Université de Montréal, Montreal, QC, Canada. [3]Department of Psychiatry and Neuroscience, Faculty of Medicine, Université Laval, Quebec City, QC, Canada. [4]Faculty of Pharmacy, Université Laval and CHU-Q Research Center, Quebec City, QC, Canada

III.1 ABSTRACT

Lipid metabolism is fundamental for brain development and function, but its roles in normal and pathological neural stem cell (NSC) regulation remain largely unexplored. Here, we uncover a novel fatty acid-mediated mechanism suppressing endogenous NSC activity in Alzheimer's disease (AD). We found that postmortem AD brains and 3xTg-AD mice accumulate neutral lipids within ependymal cells, the main support cell of the forebrain NSC niche. Mass spectrometry and microarray analyses identified these lipids as oleic acid-enriched triglycerides that originate from niche-derived rather than peripheral lipid metabolism defects. In wild-type mice, locally increasing oleic acid was sufficient to recapitulate the AD-associated ependymal triglyceride phenotype, rapidly de-regulate the Akt-FoxO3 NSC preservation pathway, and inhibit NSC-mediated regenerative capacity. These studies support a novel pathogenic mechanism in which AD-induced perturbation of fatty acid metabolism within niche ependymal cells suppresses the homeostatic and regenerative functions of adult NSCs.

Keywords: Alzheimer's disease, stem cell, lipids, fatty acid, ependymal.

III.2 INTRODUCTION

Preservation of stem cell activity within adult tissues is essential for maintaining tissue structure and function. In the brain, experimental inhibition of neural stem cell (NSC) activity leads to deficits in learning and memory, mood and stress regulation (Snyder *et al.*, 2001; Imayoshi *et al.*, 2008; Sakamoto *et al.*, 2011; Sakamoto *et al.*, 2014). In addition, following neural damage, NSC-derived progeny are re-directed to areas of degeneration, where they are involved in wound-healing and cell replacement, and can serve as a target for therapeutic manipulations (Kolb *et al.*, 2007; de Chevigny *et al.*, 2008; Erlandsson *et al.*, 2011). NSC activity decreases naturally during aging and is dysregulated in models of neurodegenerative diseases, suggesting an involvement in aging- and disease-associated cognitive deficits (Demars *et al.*, 2010; Hamilton *et al.*, 2010; Lazarov & Marr, 2010; Lazarov *et al.*, 2010; Bouab *et al.*, 2011; Hamilton *et al.*, 2013). Thus, dissecting the mechanisms involved in NSC dysregulation could provide new opportunities for preventive and regenerative therapeutic strategies for neurodegeneration.

Within the lateral ventricle subventricular zone, NSCs are ideally positioned to be regulated by environmental signals. Systemic signals reach NSCs via their contacts with the cerebrospinal fluid (CSF) and SVZ blood vessels (Mirzadeh *et al.*, 2008; Tavazoie *et al.*, 2008; Codega *et al.*, 2014). A major source of local signals are the adjacent ependymal cells, which constitute approximately 25% of cells within this NSC niche (Doetsch *et al.*, 1997) and surround NSCs in pinwheel structures within the walls of the lateral ventricles (Mirzadeh *et al.*, 2008). Ependymal cells provide a critical barrier mediating the exchange of ions, macromolecules and immune cells between the brain and the circulating CSF, secrete a variety of molecules that regulate NSC activity, and have recently been identified as a site of lipid synthesis and storage

(Hamilton *et al.*, 2010; Bouab *et al.*, 2011; Etschmaier *et al.*, 2011). Recently, lipids have gained attention in the regulation of NSC behavior. Lipid metabolism genes were shown to be among the major classes of transcriptional differences between quiescent and activated NSCs (Codega *et al.*, 2014). Moreover, brain fatty acid metabolism is required for hippocampal neurogenesis (Matsumata *et al.*, 2012; Chorna *et al.*, 2013; Knobloch *et al.*, 2013) and exercise-induced cognitive enhancement (Chorna *et al.*, 2013).

Interestingly, Alzheimer's disease (AD) is associated with declines in both neurogenesis-regulated cognitive processes and aberrations in lipid metabolism. Indeed, lipid accumulations were one of the five original AD-associated tissue pathologies first reported by Alois Alzheimer himself (Alzheimer, 1907). More recently, links have strengthened between aberrant lipid metabolism and neurodegeneration in AD (Fraser *et al.*, 2010; Astarita *et al.*, 2011; Podtelezhnikov *et al.*, 2011; Tanzi, 2012; Hussain *et al.*, 2013), while epidemiological studies have demonstrated that AD risk factors include peripheral metabolic conditions such as insulin resistance, obesity and dyslipidemia (reviewed in (Pasinetti & Eberstein, 2008)). However, deeper mechanistic insights into the role of abnormal lipid metabolism in AD have been hindered by the technical complexity involved with localizing, identifying, and determining the biological functions of individual lipid species in the brain.

In the present study, we developed novel methodologies to overcome these limitations, allowing us to uncover a new pathological mechanism in AD. Our results reveal that lipid metabolism defects originating within a major neurogenic niche can disrupt NSC-mediated regeneration and plasticity.

III.3 MATERIAL AND METHODS

III.3.1 Human specimens

Tissue samples were obtained from the human brain bank of the Centre de recherche de l'Institut universitaire en santé mentale de Québec, which required informed consent before donation. Experiments were conducted in accordance with the Ethics Committee at the Institut universitaire en santé mentale de Québec.

III.3.2 Mice

Experiments were conducted in accordance with the guidelines of the Canadian Council of Animal Care and were approved by the institutional animal care committee of the University of Montreal and the CRCHUM. Experiments were performed using either male C57BL6 mice (Charles River) or female 3xTg-AD mice and strain controls (below).

3xTg-AD mice and strain controls. The generation of the 3xTg-AD mice has been described previously (Oddo *et al.*, 2003a). Briefly, 3xTg-AD mice were originally derived by co-microinjecting two independent transgenes encoding human APP_{Swe} and the human tau_{P301L} (both under control of the neuron-specific mouse Thy1.2 regulatory element) into single-cell embryos harvested from homozygous mutant $PS1_{M146V}$ knock in (PS1-KI) mice. Wildtype mice are the PS1-knock-in mice background strain, a product of a cross between C57BL/6J females (B6) and 129S1/SvImJ males (129S). Ages are specified in figure legends. All mice were kept in identical housing conditions and given free access to a standard rodent diet (#2018, Harlan Teklad) and water.

III.3.3 Tissue fixation and processing

Mouse

Mice received a lethal dose of ketamine (Bimeda-MTC)/xylazine (Bayer Healthcare)/acepromazine (Boehringer Ingelheim Canada Ltd) and were then perfused transcardially with phosphate-buffered saline (PBS) followed by 4% paraformaldehyde pH 7.4. The brains were removed and postfixed in 4% paraformaldehyde for 24 h. The entire forebrain and hippocampus of each animal was cut into 40 μm coronal sections using a vibrating microtome (Leica VT1000S) and the tissue sections were stored at -20°C in an antifreeze solution (glycerol:ethylene glycol:PBS, 3:3:4) until use.

Human

Human brains were sliced into 0.5 cm-thick slabs that were fixed by immersion with 4% PFA in 0.1 M PB (pH 7.4) for 48 h. The slabs containing the striatum were stored at 4°C in 0.1 M PBS (pH 7.4) with 15% sucrose and 0.1% sodium azide. They were then cut into 50 μm-thick coronal sections using a freezing microtome and the tissue sections were stored at -20°C in an antifreeze solution (glycerol:ethylene glycol:PB, 3:3:4) until use.

III.3.4 SVZ microdissections

Microdissected SVZs were obtained from freshly dissected adult mouse brains as follows. A 2-mm-thick coronal section through the forebrain (corresponding to the region between 3 and 5 mm posterior to the anterior edge of the olfactory bulbs) was cut in a coronal mouse brain mold. Using a dissecting microscope, a fine-tipped tungsten needle was used to dissect out a block of SVZ tissue, by first making lateral cuts through the corpus callosum

(dorsally) and above the anterior commissures (ventrally), and then tracing the gray-white boundaries at the SVZ/ striatum and SVZ/septum borders. A block of striatal tissue of similar size was cut from the center of the adjacent striatum for biochemical comparison and to provide a control for SVZ microdissection purity.

III.3.5 In vivo surgical procedures

Intracerebroventricular osmotic pumps. For intracerebroventricular infusions, mice were locally injected with buprivacaine (Hospira) and operated under isoflurane anesthesia (Baxter). Cannulae attached to 7 day Alzet osmotic pumps (0.5 µl/h infusion rate, model 1007D; Durect), were stereotaxically implanted at 0.0mm anteroposterior and 0.9mm lateral to Bregma according to manufacturer`s instructions. Pumps contained either Vehicle (fatty acid-free bovine serum albumin, as above), 10 mM ^{12}C-oleic acid conjugated to Vehicle, or 10mM ^{13}C-oleic acid conjugated to Vehicle (the latter for metabolic labeling studies).

SVZ regeneration assay. Assay was performed based on Doetsch et al. (Doetsch *et al.*, 1999b). 2% Cytosine b-D-arabinofuranoside hydrochloride (AraC) (Sigma) was dissolved in either vehicle (FAF BSA) or 500µM Oleic acid conjugated to FAF-BSA (as above) and was infused using 7 day osmotic pumps (as above). Pumps were excised from the mice 6 days after implantation and the mice were perfused for tissue analysis 24 hours later.

Acute intracerebroventricular injections. A 10 µl Hamilton syringe (26s/2"/2) (Hamilton Company) was used to perform stereotaxic injections into the lateral ventricle of C57BL6 mice (0.0mm anteroposterior and 0.9mm lateral to Bregma with a depth of -1.5mm

below the skull). 2µl of Vehicle or 500µM oleic acid was slowly injected (1µl/min) into the lateral ventricle. With an approximate CSF volume of 8µl, the effective oleic acid concentration is thus estimated at 100 µM, matching the *in vitro* conditions. Mice were sacrificed 4 hours post-injection, ipsilateral and contralateral SVZs and their respectively striata were microdissected, lysed and then run for Western blotting (as below).

Extraction of cerebrospinal fluid and plasma. 7-month wild-type and 3xTg-AD mice were used for isolation of both cerebrospinal fluid (CSF) and blood plasma. CSF was extracted from the cisterna magna of anaesthetized mice using a pulled glass capillary tube. Approximately 5-7 microliters were obtained from each mouse. Blood samples were collected from the posterior *vena cava*. Interval between anaethesia injection and blood collection was approximately 5 minutes. Blood samples were transferred to a microtainer containing K_2EDTA (BD Biosciences) inverted 20 times, and the plasma extracted after centrifuging at 1000 g for 15 minutes at 4°C. All samples were stored at −80°C until lipid extraction.

III.3.6 Oil Red O staining

40 µm (mice) and 50 µm (human) coronal floating sections were washed with 60% 2-propanol (Fisher), incubated in 0.3% Oil Red O (Allied Chemical) for 10 minutes, then rinsed in 60% 2-propanol followed by once with distilled H_2O.

III.3.7 Electron microscopy

40 µm coronal sections through the SVZ from WT and 3xTg-AD mice (n=3/group) were rinsed in phosphate buffer, fixed with 1% osmic acid (Electron Microscopy Science) for 30

minutes, dehydrated in a graded series of ethanols and propylene oxide (Fisher) and then embedded in electron microscopy grade Resin (Durcupan ACM, Sigma). Resin-embedded sections were mounted on the tip of a resin block for sectioning. Ultrathin sections were cut with an ultramicrotome (Reichert Ultracut S; Leica Canada), collected on bare square-meshed copper grids, stained with uranyl acetate and lead citrate, and examined with an electron microscope (Philips CM100; FEI)

Quantification of lipid droplet containing SVZ cells. At least 50 ependymal (cells contacting the ventricle with a very light nucleus, and possessing cilia) and 50 non-ependymal cells (cells under the ependymal cells, absence of cilia) were evaluated from each mouse (n=3/condition). The quantifications were done directly on the electron microscope, for the presence of lipid droplet within the cells. Electron micrographs were obtained using an AMT digital camera.

III.3.8 Laser desorption-ionization imaging mass spectrometry (IMS)

Tissue coating. Silver and gold were deposited over the tissues sections following previously published protocols with the following changes (Thomas *et al.*, 2012; Dufresne *et al.*, 2013). For silver deposition, tissue sections were mounted on a silver pre-coated microscope slide (50 nm thick silver layer) and subsequently received a 14±2 nm thick silver layer by sputtering. For gold deposition, tissue sections were mounted on an Indium-Tin-Oxide microscope slide (Delta Technologies, Stillwater, MN) and coated with a 28±3 nm thick layer of gold deposited by sputtering. Matrix deposition was carried out in a sublimation apparatus (Chemglass Life Science, Vineland, NJ) as previously described (Chaurand *et al.*, 2011). For

DAN, sublimation protocol was optimized for a fixed vacuum of 5×10^{-2} Torr monitoring temperature, time of application, and matrix deposited amounts measured with a high-precision balance to ensure the best MALDI IMS efficiency (Thomas *et al.*, 2012).

Mass spectrometry. IMS, MS and MS/MS spectra acquisition were performed on either a MALDI TOF/TOF Ultraflextreme mass spectrometer or a SolariX XR 7T FT-ICR mass spectrometer both equipped with SmartBeam II Nd:YAG/355 nm laser (Bruker Daltonics, Billerica, MA). For TOF MS analyses: profiling MS data were acquired by summing 10 times 250 laser shots from the selected tissue sections. IMS data were acquired under delayed extraction conditions and in reflectron geometry using 250 shots per pixel at 10 μm lateral resolution with a spectral resolution of 15,000 at *m/z* 881. For LDI analysis, the laser energy was set in the same range as for conventional MALDI experiments providing a few micro joules of energy on target. Acceleration voltage was set to 25 kV and all other instrumental parameters were optimized for maximum signal to noise ratio. Lipid characterization was performed by comparing accurate mass measurements (less than 10 ppm) with the LIPID MAPS prediction tool (http://www.lipidmaps.org/.html) and confirmed by MS/MS measurements acquired in LIFT-TOF/TOF. MS and MS/MS data were processed using flexAnalysis v3.4 software. IMS data were recalibrated after acquisition with flexAnalysis Batch Process v3.4 software using the silver/gold clusters as internal mass standards. IMS data were reconstructed and visualized using flexImaging v4.0 software.

For FT-ICR analyses: profiling MS data were acquired by summing 10 times 100 laser shots from the selected tissue sections with a spectral resolution of 500,000 at m/z 881. IMS data were acquired using 100 shots per pixel using a 10 μm lateral resolution and with a spectral resolution of 50,000 at *m/z* 881. Lipid characterization was performed by comparing accurate

mass measurements (less than 1 ppm) with the LIPID MAPS prediction tool (http://www.lipidmaps.org/.html) and confirmed by MS/MS using CID fragmentation mode according to previously described methods (Cheng *et al.*, 1998). All the data MS and MS/MS data were processed using DataAnalysis v3.4 software. IMS data were reconstructed and visualized with flexImaging v4.0 software.

III.3.9 Liquid chromatography-mass spectrometry (LC-MS)

Methyl-tert-butyl ether Lipid extraction. Plasma and cerebrospinal fluid lipid extraction was performed according to (Matyash *et al.*, 2008). Briefly, 200 µl of MS-grade methanol containing internal standards IS 2, 3, 4, 5, used to follow each class of lipid through the lipid extraction protocol (Figure S2B), was added to a 20 µl plasma or 5µl CSF aliquots, placed into glass tubes with Teflon-lined caps, and vortexed. One ml of Methyl *tert*-butyl ether (MTBE, Fisher) was added and the mixture was incubated for 1 h at room temperature in a shaker. Phase separation was induced by adding 250 µl of MS-grade water (Fisher). After 10 min of incubation at room temperature, the sample was centrifuged at 1,000 g for 10 min, the upper (organic) phase was collected, and the lower phase was re-extracted with 2 ml of the solvent mixture (MTBE/methanol/water 10:3:2.5, v/v/v). Combined organic phases were dried under a nitrogen stream. Extracted lipids were re-solubilized in 300 µl (plasma) or 100µl (CSF) of MS-grade 2-propanol (Fisher) containing IS1.

LC-MS. LC-MS separations were carried out on a Synapt G2-S instrument coupled to an Acquity UPLC Class I system (both from Waters). Elution was performed at 550 µL/min on a CSH C18, 1.7 um, 2.1 x 75 mm chromatographic column maintained at 65^{o}C. The eluents

consisted of 10 mM Ammonium Formate, 0.1% formic acid and 40 % acetonitrile in water (eluent A) and 10 mM Ammonium Formate, 0.1% formic acid, 10% acetonitrile and 90% 2-propanol (eluent B). The initial mobile phase contained 15% B and was maintained for 0.2 min in the beginning of the run. The following gradient elution was then applied: 15 to 30% B from 0.2 to 2 min; 30 to 50% B from 2 to 2.5 min; 50 to 80% B from 2.5 to 11 min; 80 to 99% B from 11 to 11.5 min; hold at 99% B for 0.9 min. Eluent B was then decreased from 99 to 15% in 0.1 min and held constant for up to 16 min to permit column equilibration. The auto-sampler was maintained at 10^{o}C to avoid sample degradation. The injection volume of the plasma extracts was 1 µL and 2 µL for analyses in positive and negative mode respectively. Aliquots of 5 µL were injected from CSF extracts for positive mode analysis and 6 µL of pooled triplicate extractions that were 3-fold concentrated were injected for negative mode. Injections were randomized in order to diminish potential instrument bias during the acquisition. The electrospray interface was operated either in positive or negative ion mode. Mass spectra were acquired in MS^{e} mode from m/z 100 to 1200 with a scan time of 0.3 s. Collision energy ramps of 20 to 35 V and 20 to 45 V were applied in the trap and transfer cells respectively. Leucine encephalin was used in the lock-spray every 10 s for accurate mass correction. MassLynx was used for instrument control and data acquisition while TargetLynx and MetaboLynx were used for data processing. Injection list was as described in Figure S2A. Quality control Internal standard (1) was used to ensure the reproducibility of sample injections in the MS (Figure S2). Graphs of normalized peak area were achieved by normalizing the extracted ion counts for each m/z peak area to the volume of sample injected and then multiplying by initial sample dilution ratio.

III.3.10 Microarray

RNA was isolated from snap-frozen SVZ microdissections using the RNeasy mini microarray kit as per manufacturer's instructions (Qiagen). For each sample, 5µg of RNA was reverse transcribed using Superscript II reverse transcriptase. The cDNA was purified using Qiagen PCR purification column as per the manufacturer's protocol. Following purification, 1 µg of purified cDNA (in a total volume of 40 µl) was mixed with 40 µl of 5' Cy3 labeled random nonamers (Trilink Biotechnology) and heated at 95°C for 10 minutes and snap cooled in ice/water slurry for 10 minutes. The samples were then mixed with 10 µl of 10mM dNTP mix, 8 µl of water and 2 µl of Klenow fragment (3'to 5' exo^-) (NEB) and incubated at 37ºC for 2 hours. The labeling reaction was stopped by adding 10 µl 0.5M EDTA and then isopropanol precipitated with the addition of 11 µl 5M NaCl. The labeled DNA was resuspended in 40 µL water and quantified using a Nanodrop. Following quantification, 4 µg of labeled material was dried by Speedvac and resuspended in a total of 3.3 µl of tracking control solution. Hybridizations were carried out using the SurePrint G3 Mouse GE 8x60K Microarray (Agilent Technologies) containing probes targeting 39,430 Entre Gene RNAs and 16,251 lincRNAs. Arrays were scanned at 5µm resolution using a GenePix4000B scanner (Molecular Devices). Data from scanned images were extracted using GenePix 6.1 (Axon). Chip annotations file was updated to a more recent version (20130207). Expression data was analyzed using Bioconductor packages (http://www.bioconductor.org/) and R statistical language (www.r-project.org). Bioconductor *limma (Smyth et al., 2005)* package was used to background correct, log2-transform, aggregate and quantile-normalize the median probe intensities. Probe intensities were averaged when more than one probe was associated with a given probe identifier. The resulting matrix showing 55,681 probes as rows and 8 samples as columns was filtered to

exclude lincRNA entries and probes in intensities below background in more than half of the samples. 32,684 probes were used as input for linear modeling using the method available in *limma* which uses a moderated t-statistic to assess significance. A 3xTg-AD vs WT in 7 months was evaluated and probes presenting a p-value lower than 0.005 and a fold-change greater than 1.4 or lower than –1.4 were considered for further analysis. Enrichment analysis was performed using the Database for Annotation, Visualization and Integrated Discovery (DAVID, http://david.abcc.ncifcrf.gov/) (Huang da *et al.*, 2009a; Huang da *et al.*, 2009b) and through the use of Ingenuity Pathways Analysis (IPA) (Ingenuity Systems, www.ingenuity.com). High-level and low-level categories resulting from the IPA Functional Analysis were manually curated. In addition to manual curation of the gene lists, IPA results and manufacturer Gene Ontology annotations, the Bioconductor R package GO.db 2.9 (20130302) (Carlson) were used to retrieve genes involved in lipid-related activities.

III.3.11 Neurosphere assays

Neurospheres were generated according to a procedure modified from Reynolds and Weiss (Reynolds & Weiss, 1992). 2 month-old C57BL6 mice were euthanized using ketamine/xylazine/acepromazine. Both SVZs, including their associated striata were dissected into ice cold HBSS (Wisent), dissociated to single cells using papain (Worthington), diluted to 30 ml in DMEM/F-12 (3:1; both from Invitrogen) supplemented with 2% B27 (Invitrogen), 1µg/ml fungizone (Invitrogen), 1% penicillin/streptomycin (Wisent) and 20 ng/ml EGF (Sigma) and seeded in 75cm^2 flasks to generate primary neurospheres. To generate secondary neurospheres, primary neurospheres were mechanically dissociated and re-seeded at 1.5cells/µl in 24 well plates in the same media as above.

Preparation and treatment with oleic acid-albumin complexes. Fatty acid-free bovine serum albumin (FAF-BSA) (Bioshop) was dissolved in 0.1M Tris-HCl pH 8.0. Oleic acid (OA) (Sigma) was conjugated to FAF-BSA at a molar ratio of 5:1. A 10mM stock solution was sterilized by filtration and used for subsequent working dilutions. OA was added to newly dissociated primary neurospheres at the concentrations indicated and with a final dilution volume of < 0.01%. Concentration range was selected based on dose responses analyses. Fatty acid-free BSA was used as the vehicle control at equal final volumes. To test the effect on neurosphere initiation, OA was added on the day of plating. To test the effect on neurosphere growth OA was added four days post-plating. Neurosphere number and diameter were quantified after 10-13 d *in vitro*.

Self-renewal assay. Dissociated primary neurospheres were grown into secondary neurospheres in the presence of Vehicle, 50μM or 100μM oleic acid for 10-14 days (as above) (n=6 experiments). 60 secondary neurospheres (diameter approximately 200 μm) were then handpicked from each condition using a micropipette and in inverted microscope (4X total magnification) and transferred to a 1.5 mL tube, dissociated for 5 minutes, the cell density determined by using a hemocytometer, and the cells re-plated at 1.5 cells/μl in regular proliferation media (as above). After 7 days tertiary neurospheres were counted and measured. Self-renewal capacity was determined by normalizing the neurosphere number to the neurosphere cell density. To estimate the number of neural stem cells within each neurosphere, the normalized number was divided by the number of cells (12 000) and the neurospheres (60) plated.

TUNEL and proliferation assay. To assess proliferation and cell death, dissociated neurospheres were plated in proliferation media (as above with addition of 1% Fetal bovine serum) containing either Vehicle, 50μM or 100μM of oleic acid onto poly-L-lysine coated chamber slides at a density of 25 000cells/cm^2 for 2 days. Standard immunocytochemistry was performed for Ki67 (as above). The TUNEL assay for cell death was performed following the secondary antibody step and according to manufacturer's instructions (Roche) with omission of the dUTP enzyme as a negative control and addition of DNAse (Sigma) as a positive control.

Carboxyfluorescein Diacetate, Succinimidyl Ester (CFSE) cell division assay. To assess proliferation, dissociated neurospheres were treated with 1μM CSFE (Life technology) at 1 million cells/ml for 8 minutes at 37°C. The reaction was quenched with 100% FBS and washed with PBS and DMEM/F-12 (3:1; both from Invitrogen). Labeled cells were subsequently plated onto poly-L-lysine coated dishes at a density of 12 500cells/cm^2 in proliferation media (as above with addition of 1% Fetal bovine serum) containing either Vehicle, 50μM or 100μM of oleic acid or differentiation media (as above with omission of EGF) for 3 days. The cells were then harvested, washed and run on an LSRII cytometer (BD Biosciences), and data analysis was performed using FlowJo v7.6.5 (Tree Star).

III.3.12 Immunohistochemistry

Immunohistochemical procedures were performed as detailed previously (Gregoire *et al.*, 2014). Mouse anti-human Ki67 was used at 1:100 (BD Biosciences). For brightfield immunohistochemistry, primary antibodies were detected using species-appropriate biotinylated secondary antibodies (Jackson ImmunoResearch), the signal was amplified using the avidin-

biotin-peroxidase system (VectaStain ABC Kit, Vector Laboratories), and revealed using a 3,3-diaminobenzidine (DAB)-containing solution (Sigma). Microscopy was performed using a motorized Olympus IX81 microscope.

Quantifications of immunohistochemistry. All quantifications were performed on coded slides by a blinded experimenter. For quantification of markers expressed by SVZ and dentate gyrus cell populations, 4-6 ventricles from sections at 120 μm intervals through the striatal SVZ or dentate gyrus were quantified. Counts were limited to the subventricular zone and subgranular zone respectively and both the left and right hemispheres were included.

III.3.13 Western blotting

Western blotting was performed as previously described (Hamilton *et al.*, 2010). The following antibodies were used: phospho-AKT (Ser473) (1:1000, Cell Signaling), phospho-FoxO1(Thr24)/3a (Thr32)/4 (Thr28)(1:1000, Cell Signaling), phosphoFoxO3a (Ser318/321)(1:1000, Cell Signaling), beta-actin (1:20 000, Abcam). HRP-conjugated secondary antibodies, were used at following dilutions: anti-mouse IgG (1:5000, Bio Rad) or anti-rabbit IgG (1:5000, Millipore). Secondary antibodies were detected using the Clarity (Bio-Rad) and ChemiDoc (Bio-Rad). Quantitative densitometry of bands was performed using Image Lab version 4.1 (Bio-Rad).

III.3.14 Statistical Analyses

All statistical analyses were achieved using GraphPad Prism, Version 5.02 (GraphPad Software, Inc). Statistical analysis used a two-tailed unpaired or paired Student's *t*-test and as

indicated in figure legends. Error bars represent mean ± standard error of the mean (SEM). Significance level was set at $p \leq 0.05$.

III.4 RESULTS

III.4.1 AD-associated suppression of neurogenesis coincides spatially and temporally with aberrant triglyceride accumulations within ependymal cells of the subventricular zone NSC niche

The triple-transgenic AD (3xTg-AD) mouse is a unique AD model that undergoes an age-related accumulation of both amyloid plaques and neurofibrillary tangle pathologies, closely resembling the AD microenvironment (Oddo *et al.*, 2003a). We have previously shown that NSC-derived neurogenesis is suppressed in 3xTg-AD mice at both 11- and 18-months of age, and that this suppression occurs prior to appearance of the amyloid plaques and neurofibrillary tangles, suggesting that other mechanisms are involved (Hamilton *et al.*, 2010). By examining younger ages, we found that 5-month old 3xTg-AD mice already have a significant suppression of Ki67-positive proliferating cells in the subventricular zone (SVZ) (Figure 1A,C) and dentate gyrus (Figure 1D) NSC niches. Notably, we discovered that this suppression occurred concomitant to a specific accumulation of Oil Red O (ORO)-positive neutral lipid droplets along the brain-CSF barrier, including the forebrain subventricular zone (SVZ) NSC niche (Figure 1B). Electron microscopy of the SVZ niche revealed that lipid droplets were found uniquely in ependymal cells of the brain-CSF barrier and did not accumulate in the sub-ependymal populations of neural precursors themselves (Figure 1E,F). ORO-positive lipid droplets continued increasing with age in ventricular zones along the entire anterior-posterior axis of 3xTg-AD mice; however, even at 11 months of age, they were never detected outside of the ventricular zone in control or 3xTg-AD mice (Figure 1G,H), identifying the brain-CSF barrier as a novel and selective site of aberrant lipid metabolism.

We tested whether aberrant lipid accumulations are also found in human AD brain samples (Figure 1I,J). Remarkably, we found similar lipid accumulations along the lateral ventricles in post-mortem brain tissues from 9 AD patients (78.0 ± 2.89 years old) and 5 age-matched cognitively normal individuals (79.6 ± 5.88 years old) (Figure 1I,J, Figure S1A,B and Table S1 for patient information). Four of the five controls presented sparse ORO staining of the ependymal layer along the majority of the ventricular wall (Figure 1I). In contrast, the majority of AD brains showed dense accumulations of ORO at the basal surface of the ependyma (Figure 1J), with four of the nine presenting a mixture of dense and sparse areas (Figure S1A,B). Although it is not currently possible to prospectively identify AD patients during early adulthood, collectively, these mouse and human data suggest that AD-induced lipid accumulations are an early event in the disease.

We next developed a novel Imaging Mass Spectrometry (IMS)-based lipidomics strategy that would allow us to identify the species of lipids accumulating within the SVZ niche. IMS is a unique form of mass spectrometry that employs laser desorption-ionization to collect mass spectra data at high-resolution intervals across a tissue section, thereby revealing the spatial distribution of individual biomolecules within the unperturbed tissue architecture. IMS revealed that lipid accumulations in the SVZ niche are selectively enriched in triglycerides. Twelve distinct triglycerides were found to be increased by 2- to 27- fold in the SVZ niche of 3xTg-AD mice compared to strain controls (Figure 1K). The four largest increases occurred in triglycerides having structures of 50:1, 52:2, 54:2, 54:3 (total carbons:unsaturations) (Figure 1L), and IMS ion density maps illustrated a specific enrichment of these triglycerides along the ventricular borders. (Figure 1M and Figure S1C).

Together, these data reveal a selective accumulation of triglycerides within the forebrain NSC niche in postmortem human AD brains and 3xTg-AD mice, and at least in 3xTg-AD mice, this accumulation coincides with impaired adult neurogenesis during early adulthood.

III.4.2 AD-associated triglycerides accumulating in the SVZ niche are enriched in oleic acid and can be recapitulated in wild-type mice by intracerebroventricular oleic acid infusion

Fatty acids can have varying effects on energy metabolism, intracellular and cell-cell signaling, gene expression and membrane properties. We therefore identified the constituent fatty acids of the accumulating ependymal triglycerides using tandem mass spectrometry. Sequential ionization of the three most increased triglycerides yielded predictions of oleic acid (18:1), palmitic acid (16:0), stearic acid (18:0), palmitoleic acid (16:1), eicosenoic acid (20:1) and eicosadienoic acid (20:2) side-chains in an approximately 7:5:3:1:1:1 ratio (Figure 2A). Interestingly, these fatty acids are closely related within a common fatty acid biosynthetic pathway (Figure 2B).

Since oleic acid (OA) was the major fatty acid accumulating in the SVZ niche, we investigated the consequences of increasing local OA levels in the SVZ of wild-type mice. Remarkably, OA administration to wild-type mice for 7 days by direct intracerebroventricular (ICV) infusion resulted in formation of ORO-positive ependymal lipid droplets that closely resembled those of 3xTg-AD mice and human AD patients (Figure 2C,D). Moreover, IMS showed a concomitant increase in AD-associated triglycerides (Figure 2E). We therefore directly traced the incorporation of the infused OA by performing a more sensitive *in vivo* metabolic

labeling procedure that uses OA comprised entirely of heavy ^{13}C ("^{13}C OA")(Figure 2F-H). Comparison of IMS spectra between ^{13}C OA and regular ^{12}C OA showed that OA infusion into wild-type mice is sufficient to generate virtually all the AD-associated triglycerides. For example, ^{13}C OA shifted the triglyceride 50:1 by exactly 18.060 atomic units (incorporation of 1 OA side-chain), the triglyceride 52:2 by 18.060 and 36.120 atomic units (incorporation of up to 2 OA side-chains) (Figure 2F,G), the triglyceride 54:2 by 18.060 and 36.120 atomic units (incorporation of up to 2 OA side-chains) and the species 54:3 by 18.060, 36.120 and 54.180 atomic units (incorporation of up to 3 OA side chains). Uptake of ^{13}C OA into each of the 12 AD-associated triglycerides is summarized in Figure 2H and shows that 11 of the 12 AD-associated triglycerides are replicated in wild-type mice by ICV infusion of OA. These metabolic labeling experiments also demonstrated that OA at the brain-CSF barrier can be metabolized locally to generate longer chain and polyunsaturated fatty acids, as some AD-associated triglycerides contained ^{13}C OA that had been elongated (56:4, 56:5), reduced (52:2, 52:3), saturated (52:2, 54:2) and/or desaturated (54:4, 56:4, 56:5). Thus, these *in vivo* metabolic labeling experiments reveal that elevation of a single fatty acid, OA, is sufficient to induce ependymal lipid droplet accumulation, and that locally increased OA can be metabolically processed to replicate the AD-associated triglyceride phenotype.

III.4.3 AD-associated triglycerides and their component fatty acids originate from local rather than systemic sources

As accumulating ependymal lipids may originate from multiple sources, we studied the plasma and CSF of 3xTg-AD mice using a liquid chromatography mass spectrometry (LC-MS)-

based lipidomic approach (See Methods and Figure S2). Unexpectedly, concentrations of the 12 AD-associated triglycerides and their associated free fatty acids were unchanged between 3xTg-AD mice and their strain controls in both these circulating fluids (Figure 3A,B). Conversely, cholesterol was increased in the plasma (Figure S3E) but not within the SVZ (Figure S1D) of 3xTg-AD mice, showing that central and peripheral lipid profiles are distinct. We therefore explored whether lipid metabolism was altered within the SVZ niche itself.

Gene expression in the SVZ of 3xTg-AD versus control mice was compared using a 55,681-probe genome-wide microarray, and revealed 993 significantly up- or down-regulated genes (fold change ≥ 1.4 and $p \leq 0.005$) (Figure 3C). Functional analysis of this dataset identified Cellular Metabolism (comprised of carbohydrate, nucleic acid, amino acid and lipid metabolism) as one of the top five significantly altered categories, along with neurogenesis-related categories such as Cognitive Function, Cell Cycle and Proliferation and Cellular Differentiation (Figure 3D and Table S2). Manual and database-mediated extraction of lipid-related genes revealed that 142 of the 993 significantly modulated changes (= 14.3%) were lipid-related (Figure 3E, and Table S3), including genes implicated in various aspects of fatty acid metabolism (i.e., PLA2, SCD1, ELOVL7, FABP5, LIPIN2 and NPC1).

Together, these data show that AD-associated triglycerides accumulating in SVZ ependymal cells are unlikely to originate in the periphery, and identify the SVZ niche itself as a novel site of AD-associated alterations in lipid metabolism gene expression.

III.4.4 Elevated oleic acid levels suppress NSC activation and the AKT-FoxO3a NSC preservation pathway in vitro and in vivo

Although fatty acid synthesis is essential for maintaining high levels of NSC activity (Knobloch *et al.*, 2013), little is known about the roles played by specific fatty acids in NSC regulation. We therefore investigated the biological impact that AD-associated increases in oleic acid within the SVZ niche have on NSC function.

We found that OA concentration is a critical determinant of NSC colony formation in *in vitro* neurosphere assays. Specifically, doubling the OA concentration was sufficient to convert it from a positive to a negative regulator of neurosphere number (Figure 4A-F and Figure S4A-D). Neural precursors exposed to elevated OA at the time of initial plating (when neurosphere growth requires NSC activation) generated 50% fewer neurosphere colonies (Figure 4A,B), while neural precursors exposed to the same OA concentration after 4 days in vitro (when neurosphere growth is driven by proliferation of progenitors) were unaffected (Figure 4C,D). Consistent with this data, neurosphere self-renewal assays showed that when OA and vehicle-treated spheres of equal sizes were dissociated and re-plated under identical neurosphere-forming conditions, there were 20% fewer neurosphere-initiating NSCs in OA-treated neurospheres (Figure 4E,F). Flow cytometry and immunocytochemistry confirmed that 100μM OA inhibits division of a sub-population of neural precursors but does not have a generalized impact on either proliferation or cell death (Figure S4E-G). Thus, in vitro, OA selectively inhibits expansion of the NSC pool.

We then used a well-characterized SVZ regeneration model in order to evaluate whether excess OA can suppress NSC activation within the more complex *in vivo* environment. In this model, cytosine arabinoside (AraC) is used to eliminate the constitutively proliferating progenitor cells, leaving behind only NSCs that selectively repopulate the SVZ niche (Doetsch *et al.*, 1999b). When OA was co-infused during AraC-induced depletion of proliferating SVZ cells, it significantly inhibited the NSC-mediated recovery of SVZ cell proliferation (Figure 4G-I). Interestingly, recovery of neural precursor proliferation also tended towards a decrease in the dentate gyrus, a NSC niche not in direct contact with ependymal cells, suggesting that lipid alterations at the brain-CSF barrier can penetrate deeper into the brain (Figure 4I). Thus, increased OA at the brain-CSF barrier can suppress NSC activation, adversely impacting their ability to maintain CNS homeostasis.

Building on our microarray analysis, we performed an Ingenuity Pathway Analysis (IPA) to uncover critical stem cell regulatory pathways that are altered in 3xTg-AD mice. This highlighted multiple members of the FoxO family of transcription factors (FoxO4, FoxO1, FoxO3a) (Supplemental Table 3), which has been previously shown to control NSC self-renewal (Paik *et al.*, 2009; Ro *et al.*, 2013). Since FoxO3a in particular is necessary and sufficient for NSC preservation (Renault *et al.*, 2009; Schmidt-Strassburger *et al.*, 2012), we evaluated whether it is directly regulated by OA. *In vitro,* neural precursors treated with OA showed a rapid increase in phosphorylation of FoxO3a and its upstream kinase, AKT, within 2-4 hours (Figure 4J-L). Remarkably, a single ICV injection of OA into wild-type mice also induced rapid phosphorylation of the AKT-FoxO3a pathway within the ipsilateral SVZ, (Figure 4M-P)

corroborating the *in vitro* observations. Thus, locally increasing a single fatty acid, OA, is sufficient to dysregulate NSC signaling and activity.

III.5 DISCUSSION

We identified lipid metabolism abnormalities within the adult NSC niche of AD mice and patients and used recently developed methodologies to dissect their impact on NSC activity. Our data reveal a novel mechanism of stem cell dysregulation in which adult NSC activity is suppressed via disease-induced perturbations of niche fatty acid metabolism.

Previous studies have shown that brain fatty acid synthesis is required for hippocampal neurogenesis (Knobloch *et al.*, 2013) and for exercise-induced neurogenesis and cognitive enhancement (Chorna *et al.*, 2013). Conversely, alterations in lipid metabolism are associated with many cognitive disorders, including Huntington's, Parkinson's, Niemann-Pick's and Alzheimer's diseases (Sharon *et al.*, 2003; Adibhatla & Hatcher, 2008; Martinez-Vicente *et al.*, 2010; Merlo *et al.*, 2010; Guschina *et al.*, 2011; de la Monte & Tong, 2014). However, the complexity of brain lipid identification and localization has presented a major obstacle to deciphering the role of specific brain lipids under normal and pathological conditions. Using novel imaging techniques, we identified a selective accumulation of 12 triglycerides enriched with oleic acid side chains in ependymal cells at the brain-CSF barrier. Oleic acid elevation was sufficient to not only recapitulate the AD-associated triglyceride profile, but also to selectively suppress NSC expansion in vitro, diminish NSC regenerative capacity in vivo, and disrupt the critical AKT-FoxO3 signaling pathway involved in long-term NSC preservation. Thus, like many other niche signals, specific fatty acids can influence NSC maintenance via regulation of NSC activation and quiescence.

A key mechanistic feature of our findings is that AD-associated lipid metabolism disturbances are particularly prominent in the ependymal niche cells that surround NSCs. Brain ependymal cells possess the structural and enzymatic characteristics necessary for protecting and processing a wide variety of molecules in the CSF, thus forming an important barrier at the brain-CSF interface. Interestingly, however, the aberrant accumulation of oleic acid-enriched triglycerides at the brain-CSF interface occurred in the absence of changes in circulating triglycerides or fatty acids and correlated with extensive changes in local lipid metabolism gene expression, suggesting that AD is, in part, a metabolic disease of the brain.

Our data also raise a number of important questions. First, since aberrant ependymal lipid metabolism is observed in both AD patients and a genetic mouse model carrying three early onset dementia-causing genes, it will be important to determine how these genes regulate lipid metabolism within ependymal cells. It also remains to be determined whether peripheral lipid metabolism disturbances associated with insulin resistance, obesity and dyslipidemia (AD risk factors) can exacerbate local fatty acid-mediated mechanisms of NSC dysregulation. Interestingly, our data from the 3xTg-AD mouse model leads to a clear prediction that AD is associated with early onset lipid metabolism changes that suppress adult neurogenesis beginning in early adulthood; testing this prediction in humans awaits the development of diagnostic and imaging tools that can allow identification of pre-AD individuals and measurement of their *in vivo* neurogenesis and ependymal fatty acid levels.

Collectively, this work shows that excessive levels of OA at the ependymal surface of the brain result in the deterioration of neurogenic niches in AD. Future work focused on fatty acid

metabolism at the brain-CSF barrier may lead to new therapeutic approaches to prevent cognitive decline and improve stem cell-mediated brain repair during AD.

III.6 FIGURES AND LEGENDS

Figure 1

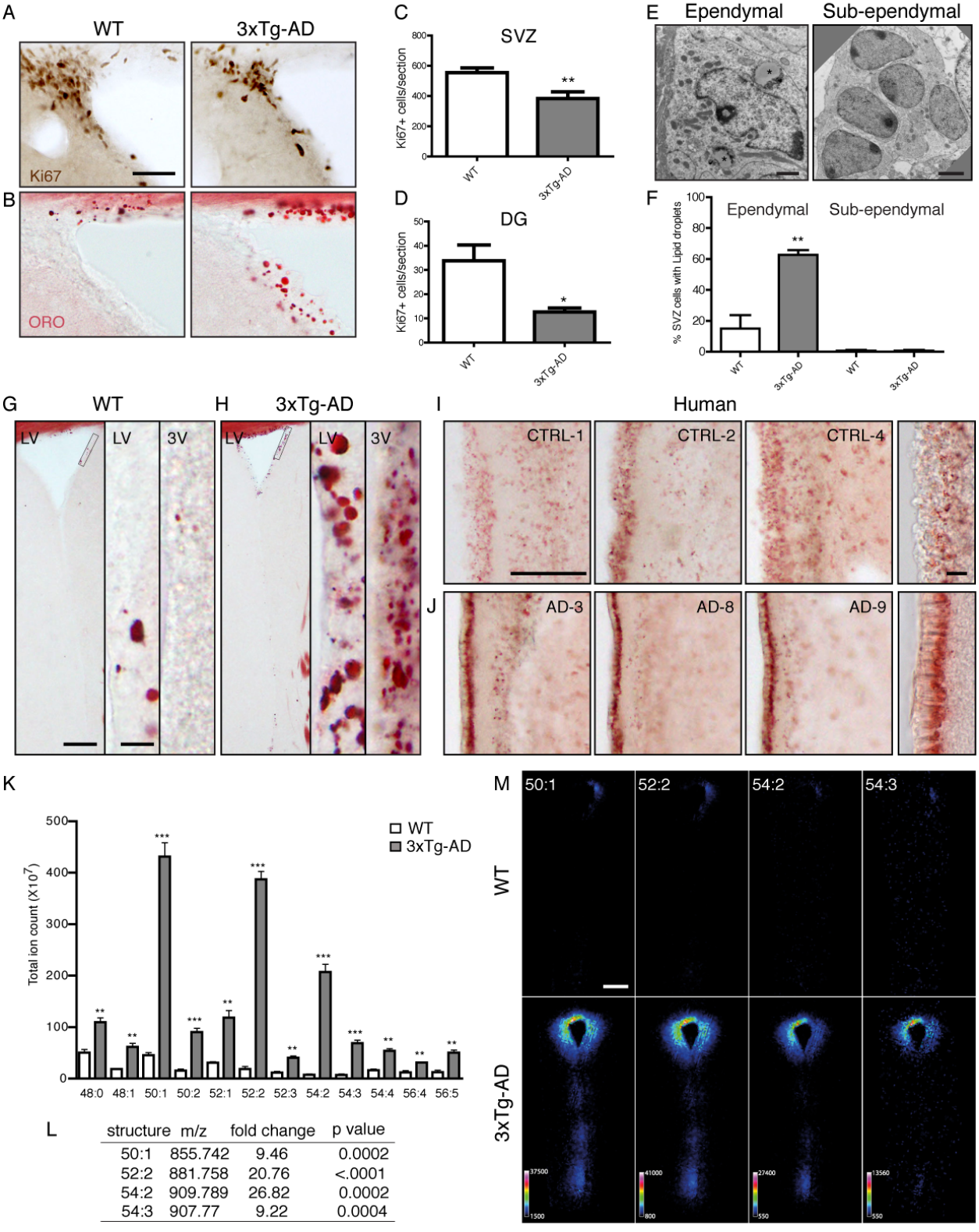

L

structure	m/z	fold change	p value
50:1	855.742	9.46	0.0002
52:2	881.758	20.76	<.0001
54:2	909.789	26.82	0.0002
54:3	907.77	9.22	0.0004

Figure 1: Reduced neurogenesis in 3xTg-AD mice correlates with aberrant triglyceride accumulations within ependymal niche cells in the SVZ of AD mice and patients

(A-B) Ki67+ proliferating cells (A) and Oil Red O staining (B) in the SVZ niche of 5-month old wild-type (WT) and 3xTg-AD mice. (C-D) Quantification of Ki67+ cells in the SVZ (C) and dentate gyrus (D) of WT (n=4) and 3xTg-AD (n=4) mice. (E-F) Representative electron micrographs (E) and quantifications (F) of lipid droplets in 3xTg-AD ependymal cells versus sub-ependymal cells (n=3 mice). (G-J) Oil red O staining of coronal sections containing the lateral (LV) and third ventricle (3V) of 11-month WT (G) and 3xTg-AD (H) mice, or (I-J) of transverse sections containing the lateral ventricle and the SVZ of normal individuals (CTRL) (I) and Alzheimer disease (AD) patients (J). Panels at right show representative higher magnification images. (K-M) Imaging mass spectrometry showing selective triglyceride accumulation surrounding the lateral ventricle of 5-month old 3xTg-AD mice. Structures (total carbons:unsaturations) of the 12 enriched triglycerides with their associated total ion counts (K). Table of mass/charge (m/z) ratios and fold changes of the four most enriched triglycerides (50:1, 52:2, 54:2, 54:3) (L) along with representative ion density maps (M). Scale bars in A, 100μm, in F, 1 μm and 2 μm respectively, in G (for G,H) and I (for I,J) 100μm and 10 μm respectively, in M 200μm. Error bars = mean±sem. Unpaired t-test * $p \leq 0.05$, ** $p \leq 0.005$, *** $p \leq 0.0005$.

Figure 2

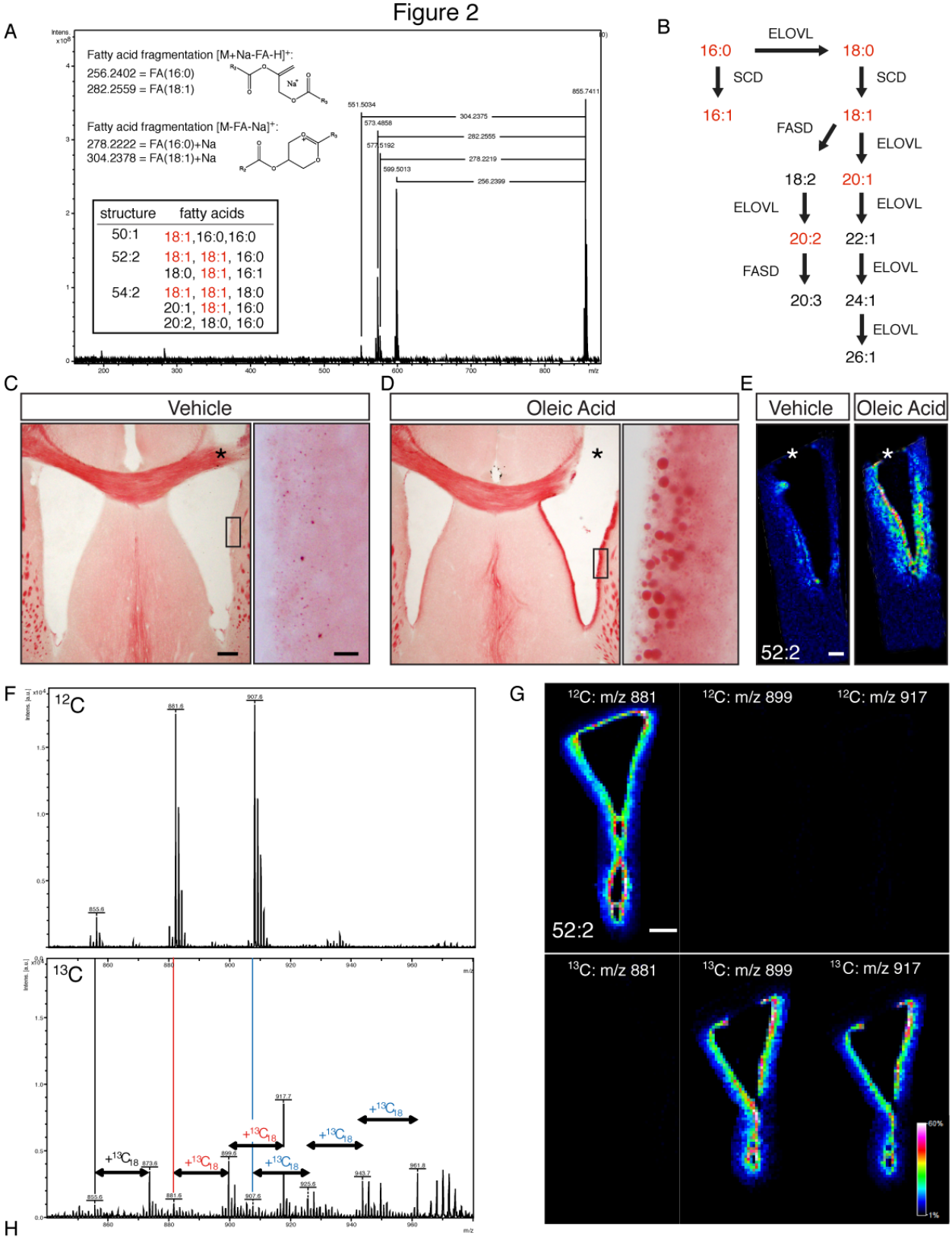

Structure	48:0	48:1	50:1	50:2	52:1	52:2	52:3	54:2	54:3	54:4	56:4	56:5
Number of ^{13}C-OA	0	1	1	2	1	2	2	2	3	3	3	3

Figure 2: Intracerebroventricular oleic acid infusion is sufficient to recapitulate the AD-associated triglyceride phenotype in wild-type mice

(A) Tandem mass spectrometry of the three major triglycerides (50:1, 52:2, 54:2) to identify their fatty acid side-chains. Shown is the fractionation pattern from the sodium-adducted triglyceride 50:1. Inset table summarizes the combined fractionation patterns of the three major triglycerides, showing a predominant enrichment of oleic acid (red). (B) Fatty acid biosynthesis pathway involved in the production and subsequent processing of oleic acid (18:1). Fatty acids identified as enriched in the 3xTg-AD SVZ are shown in red. Enzymes involved at each step are shown, and include the SCD, ELOVL and FASD gene families. (C-E) Intracerebroventricular (ICV) infusion of vehicle (C) or oleic acid (D) for 7 days, with boxed areas magnified at right. (E) Representative imaging mass spectrometry ion density maps following vehicle or oleic acid (OA) infusion, showing an AD-associated triglyceride that is induced by OA infusion. (F-H) Imaging mass spectrometry following metabolic labeling with ^{12}C OA versus ^{13}C OA (F), with sample ion density maps of 52:2 (G). Table summarizing the number of ^{13}C OA chains incorporated into each AD-associated triglyceride (H). Scale bars in C (for C,D) 200μm and 10μm respectively and in E and G 200μm. Error bars = mean ±sem. (*) in C-E denotes ipsilateral injection side.

Figure 3

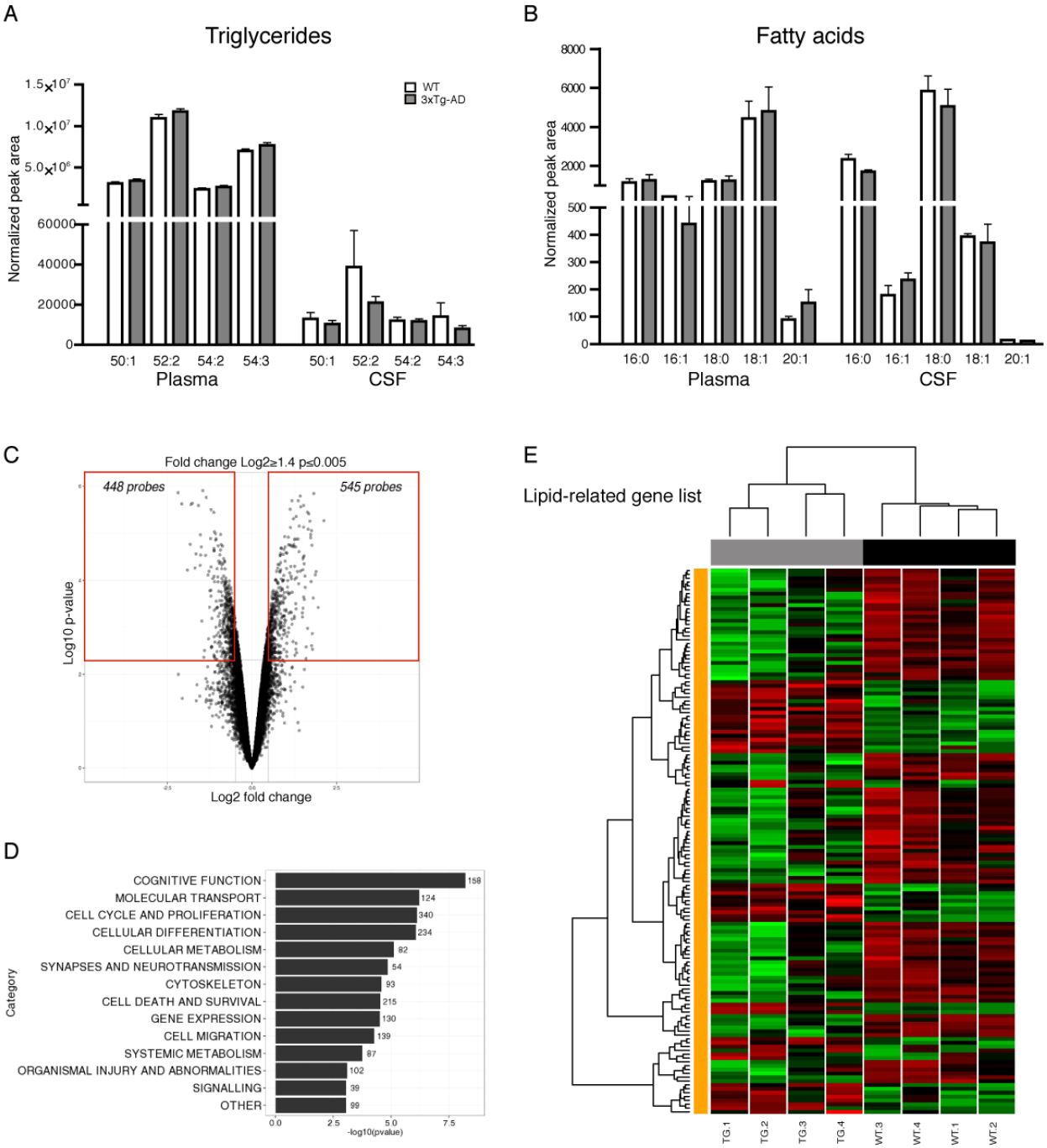
A
Triglycerides
WT
3xTg-AD
Normalized peak area
50:1
52:2
54:2
54:3
Plasma
CSF
B
Fatty acids
16:0
16:1
18:0
18:1
20:1
C
Fold change Log2≥1.4 p≤0.005
448 probes
545 probes
Log10 p-value
Log2 fold change
D
COGNITIVE FUNCTION
MOLECULAR TRANSPORT
CELL CYCLE AND PROLIFERATION
CELLULAR DIFFERENTIATION
CELLULAR METABOLISM
SYNAPSES AND NEUROTRANSMISSION
CYTOSKELETON
CELL DEATH AND SURVIVAL
GENE EXPRESSION
CELL MIGRATION
SYSTEMIC METABOLISM
ORGANISMAL INJURY AND ABNORMALITIES
SIGNALLING
OTHER
Category
-log10(pvalue)
E
Lipid-related gene list
TG.1
TG.2
TG.3
TG.4
WT.3
WT.4
WT.1
WT.2

Figure 3: Lipid metabolism is altered within the SVZ of 3xTg mice

(A-B) LC-MS analysis of lipid species within plasma and CSF of WT (n=4) and 3xTg-AD (n=4) mice. Normalized peak area for the four major AD-associated triglycerides (A) and their associated fatty acids (B) showing no significant differences. (C-E) Microarray of microdissected SVZs of 7-month old mice wild-type (n=4) and 3xTg-AD (n=4). Volcano plot (C). Ingenuity Pathway Analysis of differentially regulated categories, hand-curated into thematic categories (D). Heatmap of differentially regulated lipid-related genes, grouped hierarchically. Lipid-related genes were extracted from the list of 993 modulated genes manually and by cross-referencing with the Gene Ontology terms "lipid", "lipoprotein", "triglyceride" and "fatty acid" (E). Error bars = mean±sem.

Figure 4

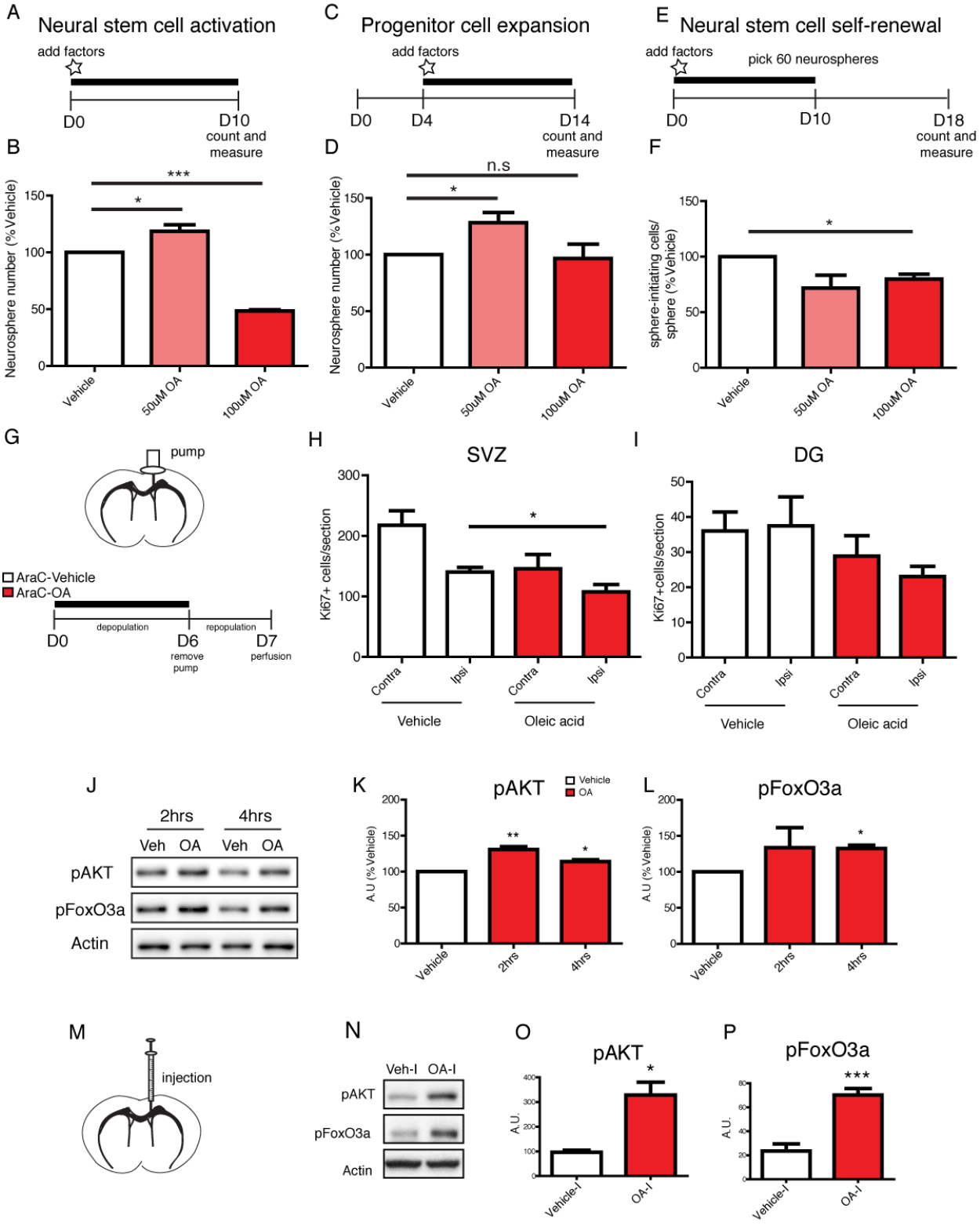
A
Neural stem cell activation
add factors
D0
D10
count and measure
B
Neurosphere number (% Vehicle)
***
*
Vehicle
50uM OA
100uM OA
C
Progenitor cell expansion
add factors
D0
D4
D14
count and measure
D
Neurosphere number (% Vehicle)
n.s
*
Vehicle
50uM OA
100uM OA
E
Neural stem cell self-renewal
add factors
pick 60 neurospheres
D0
D10
D18
count and measure
F
sphere-initiating cells/ sphere (% Vehicle)
*
Vehicle
50uM OA
100uM OA
G
pump
AraC-Vehicle
AraC-OA
depopulation
repopulation
D0
D6
remove pump
D7
perfusion
H
SVZ
Ki67+ cells/section
*
Contra
Ipsi
Contra
Ipsi
Vehicle
Oleic acid
I
DG
Ki67+cells/section
Contra
Ipsi
Contra
Ipsi
Vehicle
Oleic acid
J
2hrs
4hrs
Veh
OA
Veh
OA
pAKT
pFoxO3a
Actin
K
pAKT
Vehicle
OA
A.U (% Vehicle)
**
*
Vehicle
2hrs
4hrs
L
pFoxO3a
A.U (% Vehicle)
*
Vehicle
2hrs
4hrs
M
injection
N
Veh-I
OA-I
pAKT
pFoxO3a
Actin
O
pAKT
A.U.
*
Vehicle-I
OA-I
P
pFoxO3a
A.U.
***
Vehicle-I
OA-I

Figure 4: Oleic acid inhibits neural stem cell activation *in vitro* and *in vivo*

(A-D) Primary neurospheres from C57BL6 mice were dissociated and re-plated under neurosphere-forming conditions, and treated with either vehicle or oleic acid (50 or 100 μM) on the day of plating (D0, neural stem cell activation) (A,B), or four days later (D4, progenitor expansion) (C,D). (E,F) Neural stem cell self-renewal was assessed in dissociated secondary neurospheres plated in identical conditions after 10 days of continuous treatment with OA or Vehicle. Timeline is shown in **(**E**),** and neural stem cell number is quantified in (F). (G-I) Intracerebroventricular (ICV) infusion of oleic acid *in vivo*. Schematic of AraC SVZ regeneration assay (G) with quantification of Ki67+ proliferating cells in the SVZ (H) and dentate gyrus (DG)(I). (J-P) Acute regulation of the AKT-FoxO3a pathway by oleic acid *in vitro* (J-L) and *in vivo* (M-P). Dissociated primary neurospheres from C57BL6 mice were plated and grown in the presence of EGF for two days, acutely treated for 2 or 4 hours with either Vehicle or 100μM Oleic acid, and analyzed by Western Blotting. Shown is a representative western blot from one experiment (J), and densitometric quantifications for signals for phosphorylated AKT (pAKT) (K) and phosphorylated FoxO3a (pFoxO3a) (L). Schematic of ICV injection of oleic acid (M). Western blotting for pAKT and pFoxO3a in lysates of ipsilateral SVZ microdissections 4 hours following a single ICV injection of Vehicle or Oleic acid (N), quantified in (O, P). Error bars = mean ±sem. Unpaired t-test H, I, O, P or paired t-test B, D, F, K, L * $p \leq 0.05$, ** $p \leq 0.005$, *** $p \leq 0.0005$.

III.7 SUPPLEMENTAL FIGURES AND LEGENDS

Supplementary Figure 1

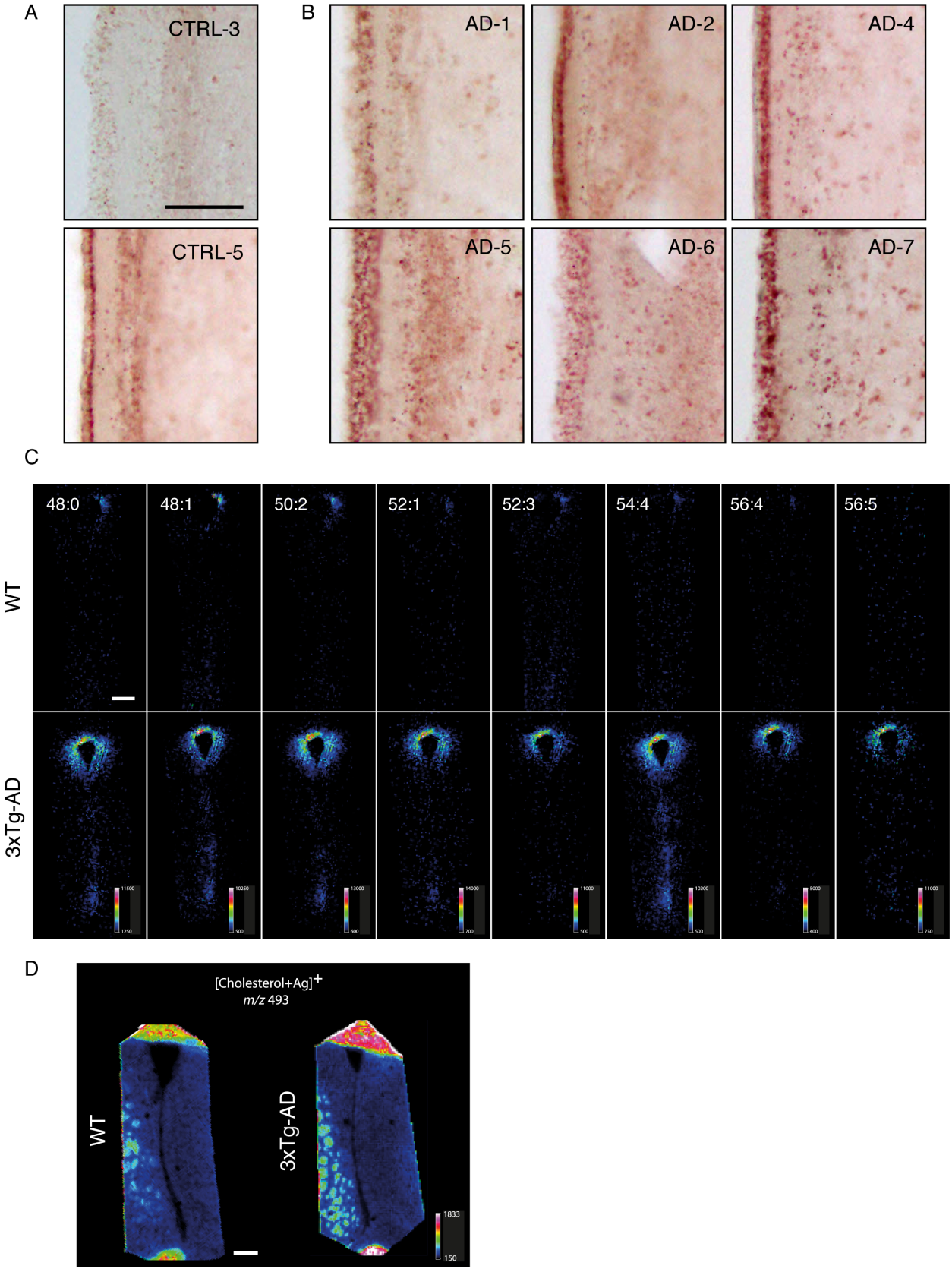

Supplemental Figure 1: Oil Red O-stained sections from remaining human brains and ion density maps of 8 additional AD-associated triglycerides.

Oil Red O staining of sections from the remaining 2 control (CTRL) (A) and 6 Alzheimer's disease (AD) (B) brains. Representative ion density maps from imaging mass spectrometry of the eight additional triglycerides accumulating surrounding the lateral ventricle of 3xTg-AD mice (C). Ion density map for cholesterol (D). Structures represent (total carbons:unsaturations). Scale bars in A (for A, B) represent 100μm and in C and D represent 200μm.

Supplementary Figure 2

A

Injection List

IPA
IPA
QC1
QC2
QC3
Sample
Sample
Sample
Sample
Sample
Sample
Sample
Sample
QC1
Sample
Sample
Sample
Sample
Sample
Sample
Sample
Sample
QC1
Sample
Sample
Sample
Sample
Sample
Sample
Sample
Sample
Sample
QC1
IPA

B

	Internal Standard	Company	Concentration
1	1,2-ditridecanoyl-sn-glycero-3-phosphocholine	Avanti polar lipids	2uM
2	1,2-diheptadecanoyl-sn-glycero-3-phosphocholine	Avanti polar lipids	1 uM
3	Hexadecanoic-2,2-d2 Acid	CDN Isotopes	20uM
4	1,3-diheptadecanoyl glycerol	Avanti polar lipids	5uM
5	1,3-dihexadecanoyl-2octadecanoyl-sn-glycerol	Avanti polar lipids	1uM

C

Plasma

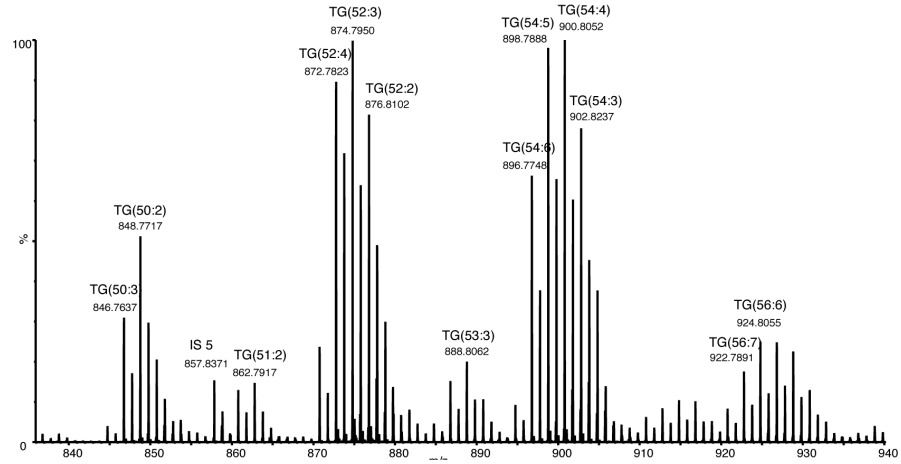

D

Cerebrospinal fluid

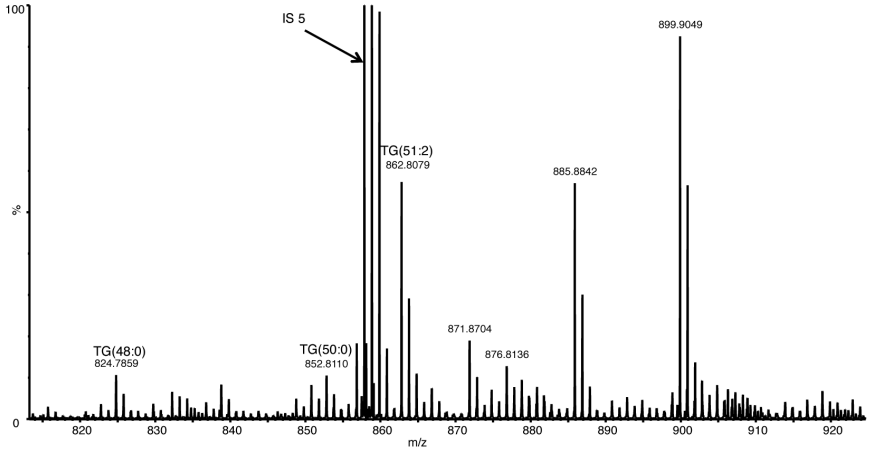

Supplemental Figure 2: Liquid chromatography mass spectrometry (LC-MS) sample list and internal standards.

(A) Schematic of LC-MS sample injection list. The column was washed with 2-propanol (IPA) three times, followed by three quality controls (QC1, QC2, QC3 (human plasma mixtures)), followed by triplicates of each WT and 3xTg-AD plasma or cerebrospinal fluid sample, loaded in random order. (B) Table of internal standards used either during (2-5) or after (1) the plasma and CSF lipid extractions. (C-D) Representative mass spectra of mass/charge 800-1000 showing the triglyceride elution range with internal standard 5 at 857.8371 in plasma (C) and CSF (D).

Supplementary Figure 3

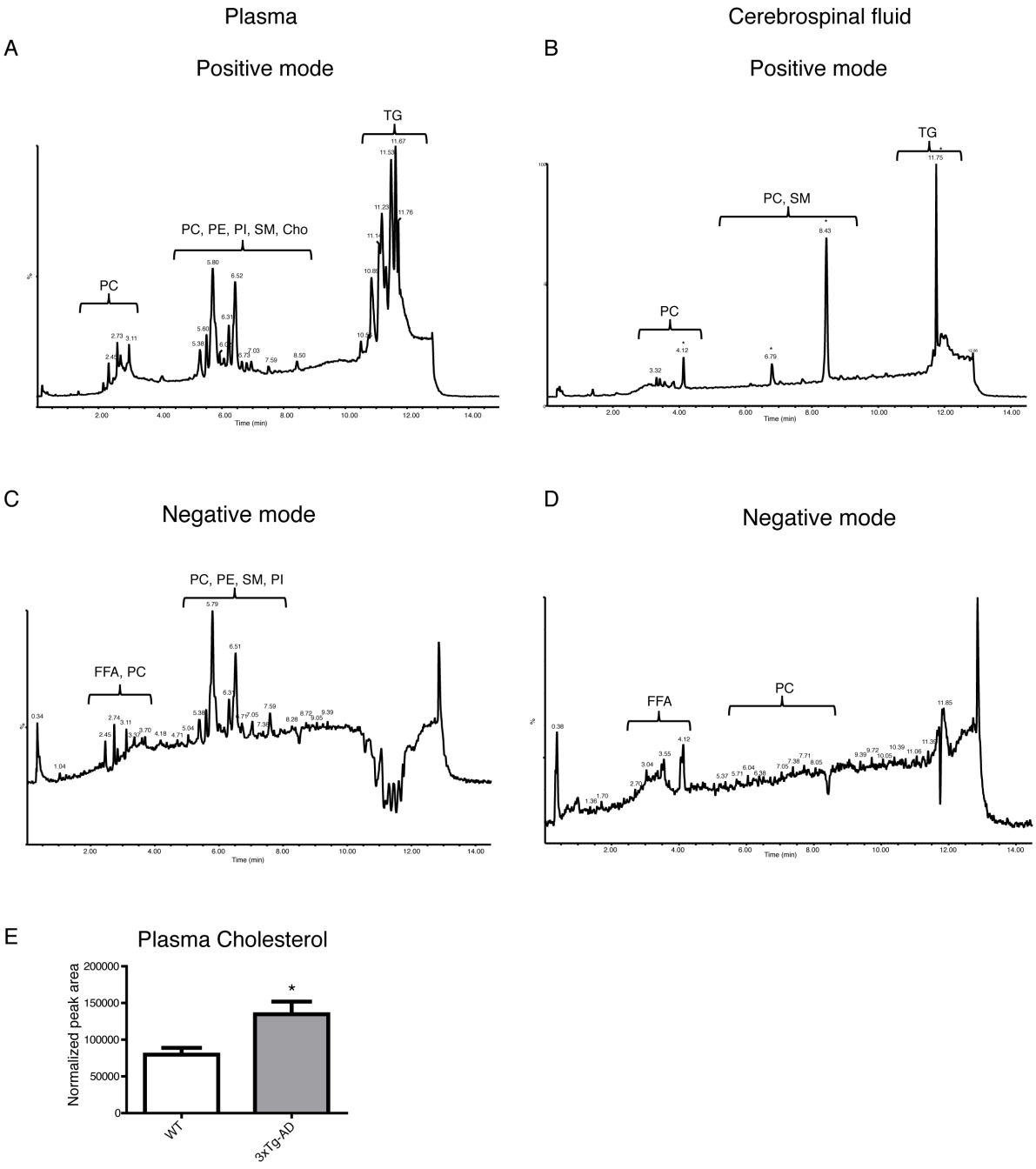

Supplemental Figure 3: LC-MS detects all major lipid classes in both plasma and CSF samples.

Representative chromatographs of plasma (A, C) and CSF (B, D). Positive mode showing the elution of lipid species phosphocholines (PC), phosphoethanolamines (PE), (phosphoinositols (PI), sphingomyelin (SM), cholesterol (Cho) and triglycerides (TG). Negative mode showing elution of free fatty acids (FFA), phosphocholines (PC), phosphoethanolamines (PE), (phosphoinositols (PI), sphingomyelin (SM). Cholesterol was only detected in plasma samples, and was increased in 3xTg mice (E). Error bars = mean ± sem. Unpaired t-test * $p \leq 0.05$.

Supplementary Figure 4

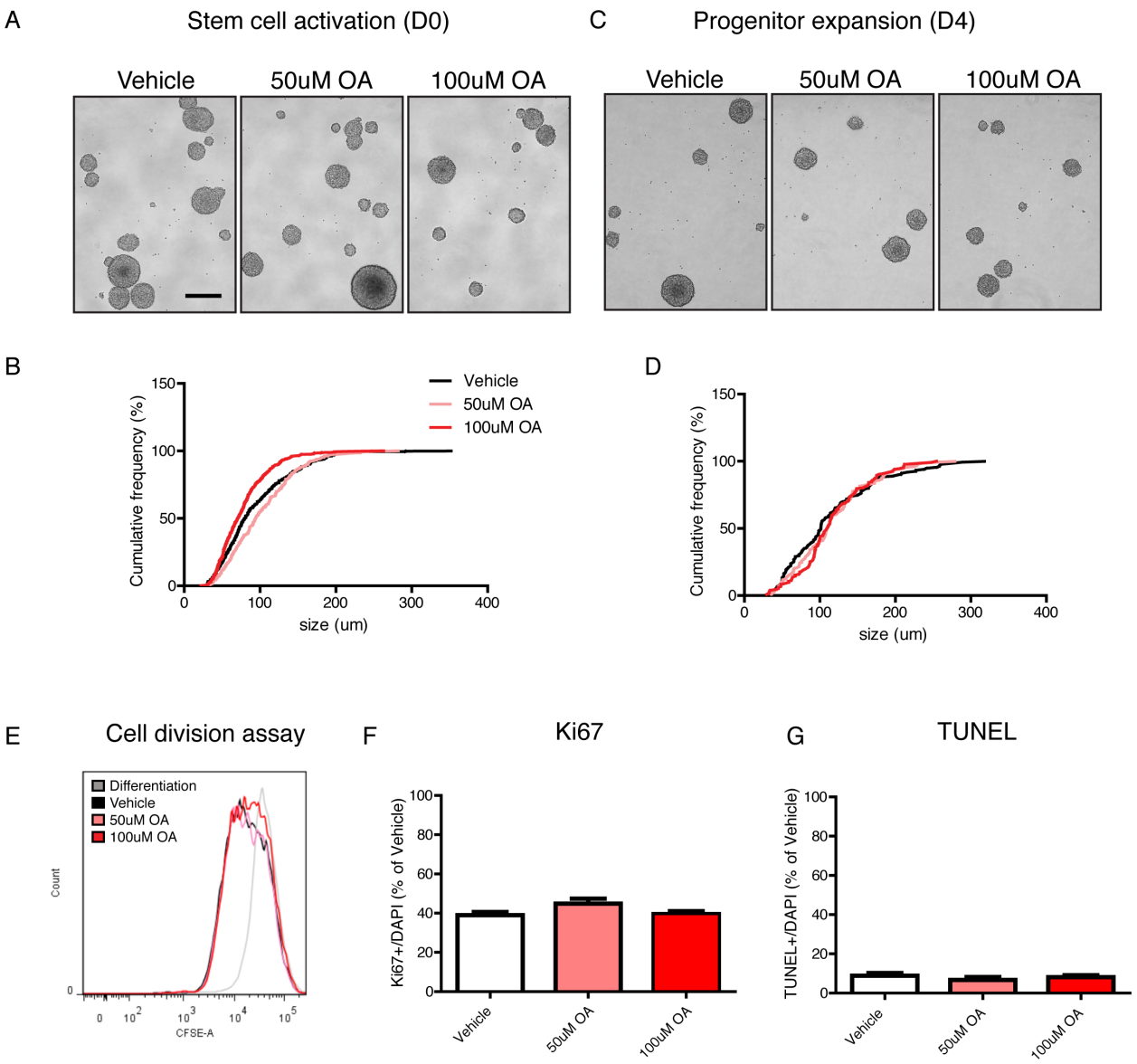

Supplemental Figure 4: Neural precursors treated with oleic acid

(A-D) Primary neurospheres from C57BL6 mice were dissociated and re-plated under neurosphere-forming conditions, and either treated with on the day of plating (D0, neural stem cell activation) (A, B) or four days later (D4, progenitor expansion) (C, D). Cells were treated with Vehicle (fatty acid-free bovine serum albumin) or 50μM or 100μM oleic acid conjugated to the Vehicle. Representative micrographs of neurospheres treated on D0 (A) and their sizes (B) and treated on D4 (C) and their sizes (D). (E-G) Dissociated primary neurospheres from C57BL6 mice plated in the presence of EGF and treated on the day of plating with Vehicle (fatty acid-free bovine serum albumin) or 50μM or 100μM oleic acid conjugated to the Vehicle for 2-3 days. Quantification by flow cytometry of Carboxyfluorescein Diacetate, Succinimidyl Ester (CFSE), a cell division assay (E), shows a 7-9% increase in CFSE retention in response to 100 μM oleic acid, indicating that OA does not have a generalized effect on neural precursor division, but inhibits the proliferation of a small sub-population (representative example from 3 independent experiments). As a positive control, cells were differentiated without EGF. Quantification of immunocytochemistry experiments for Ki67 (proliferation) (F) and TUNEL (cell death) (G), expressed as percentage of Hoechst-positive nuclei, showing that there is no significant change in the overall number of cycling or dying cells. Scale bar in A) (for A,B) represents 200um. Data from 3 independent experiments.

Supplementary Table 1

Patient	Age (yrs)	Sex	Braak stage	Cause of death	Post-mortem delay (hrs)
CTRL-1	71	F	N/A	pulmonary embolism	5
CTRL-2	89	F	N/A	acute pulmonary edema	6
CTRL-3	76	F	N/A	suicide by firearm	4
CTRL-4	97	F	N/A	cerebellar hemorrhage	4
CTRL-5	65	M	N/A	cardiac infarction	10
AD-1	81	F	V/VI	unknown	6
AD-2	83	F	V/VI	respiratory failure	7
AD-3	79	F	V/VI	bronchopneumonia	9
AD-4	84	M	V/VI	cardiogenic shock	13
AD-5	86	F	V/VI	pneumonia	20
AD-6	59	M	N/D	cardiac failure	4
AD-7	84	F	V/VI	cardio-respiratory arrest	37
AD-8	70	M	N/D	respiration failure	26
AD-9	76	M	V/VI	aspiration pneumonia	24

Supplementary Table 1: Patient information for human brains.

Table of patient and pathology data (A). Braak staging refers to methods used to classify the degree of pathology in diagnosed AD patients. N/D: not determined, N/A: not available.

III.8 ACKNOWLEDGMENTS

We thank members of the Fernandes laboratory for discussion and critiques; Dr. S. Lacroix and N. Fortin for CSF and plasma extractions; Bruker Daltonics for access to the FT-ICR and K. Kellersberger for assistance with all FT-ICR related data acquisition; the Genomics platform at The Institute for Research on Immunology and Cancer (IRIC) for microarray and bio-informatics analyses; and D. Gauchat at the CRCHUM cytometry core facility for assistance with flow cytometry. L.H. is funded by studentships from the Alzheimer Society of Canada and the Fonds de recherche de Québec en Santé (FRQS). K.F. holds a Canada Research Chair in Neural Stem Cell Biology. This work has been supported by the Canadian Institutes of Health Research (CIHR). The authors declare no competing interests.

III.9 AUTHOR CONTRIBUTIONS

L.H developed the concept, carried out experiments, analysed data and co-wrote the paper. M.D and P.C. developed and carried out IMS experiments and analysed data. S.J. helped with neurogenesis experiments and flow cytometry. S.P. and M.P. carried out the human studies. A.A helped with neurogenesis experiments. A.F. performed the LC-MS experiments and analysed data. F.C. provided the 3xTg-AD mice. K.F. developed the concept, analysed data and wrote the paper. All authors revised the manuscript.

CHAPTER 4

IV. GENERAL DISCUSSION

IV.1 NEUROGENESIS IN ALZHEIMER'S DISEASE

The aim of this thesis work was to uncover mechanisms regulating NSC behaviour in AD. While studies were emerging on neurogenesis in AD mouse models, conflicting findings led us to study how the various steps of neurogenesis change as a result of aging, neuropathology development, and neurogenic niches. In my first paper (Chapter 2), we demonstrated that APP and human Tau transgenes are strongly expressed in AD-relevant brain areas, and that the neurogenic cells within the SVZ and DG do not directly express them. Characterization of the proliferation, differentiation, and survival of neural precursors in the hippocampal DG and SVZ/OB, showed that all steps of neurogenesis were greatly impaired in 11- and 18-month-old female 3xTg-AD mice. Within the SVZ, we found a 30-45% loss in the total numbers of cells expressing Ki67, MASH1, BrdU between WT and 3xTg mice. Consistent with this, quantification of the total cell numbers in the SVZ was also 35% less. Within the SVZ, post-mitotic cells make up approximately 28% of the niche cells, while the remaining cells are comprised of approximately 33% neuroblasts, 22% NSCs and niche astrocytes and 10% progenitors (Doetsch *et al*., 1997). Therefore, it appears that 3xTg-AD mice have a proportional loss of neural precursors and total SVZ cells at 11 and 18 months of age. However, since we have yet to pinpoint a time point when one population is lost prior to the other we cannot say which precedes the other. When it comes to stem cell number and newborn neuron survival, unfortunately in our first study we did not double label BrdU+ cells with markers of NSCs (GFAP/Sox2 or Nestin/Sox2) or mature neurons (NeuN) or glia (GFAP). The label-retaining BrdU paradigm used is based on the principle that all dividing cells will incorporate BrdU upon DNA synthesis in S-phase. However, following a post-chase period of 21 days, the vast majority

of labeled cells including rapidly dividing cells including the neural progenitors and neuroblasts will have diluted out the label, while quiescent or slowly dividing NSCs and cells that incorporated the label prior to their last division (newborn mature neurons or glia) will maintain the label and can be detected by immunohistochemistry. Thus, we cannot conclude that the cells we have quantified are definitive NSCs or mature neurons. What we can say is that under normal circumstances, neuroblasts born in the SVZ migrate to the OB and make up approximately 90% of the LRC-BrdU+ cells in the OB ((Bouab *et al*., 2011) Figure 4p). Therefore, the number of BrdU+ cells in the SVZ would represent the number of quiescent or slowly dividing cells and those in the OB should give a pretty good estimate of the number of new neurons in the OB. Since the adult born mature neurons in the dentate gyrus remain in the dentate gyrus the label-retaining population should include both NSCs and mature neurons. In addition, a major caveat of this technique to keep in mind is that many cellular processes can result in synthesis of new DNA without the cell going through mitosis. However, the most commonly used BrdU paradigm and thus the one employed in this study (50 mg/kg) does not detect DNA repair and apoptosis, two processes that potentially involve DNA synthesis (Cooper-Kuhn & Kuhn, 2002).

An interestingly point that comes from this first study is that the DG had an 80% loss in Ki67 positive cells between WT and 3xTg mice at 11 months while the SVZ only showed a 45% loss. There are many possible reasons for why DG cells are inhibited prior to the SVZ. One explanation could be that in AD and in the 3xTg-AD mouse model, amyloid and tau pathology deposit in a stereotypical manner, beginning in more caudal regions including the entorhinal cortex and hippocampus and progresses to more rostral regions including the forebrain with age and disease progression. This could make DG cells susceptible at earlier time points to further inhibitory signals. In addition, the DG is in general a much more quiescent niche than the SVZ

and could therefore be more vulnerable to depletion, while the SVZ could resist for a longer period of time.

In order to begin untangling the possible mechanisms inhibiting neurogenesis, we next characterized the phosphorylation status of tau and the deposition of amyloid beta (Aβ). Interestingly, we found that the deficits in neurogenesis occurred prior to the development of neurofibrillary tangles and Aβ plaques and instead, correlated with aberrant lipid accumulations within the SVZ niche. This work suggested that deficits in neurogenesis are a prominent feature in this AD model and that frank Aβ plaques and neurofibrillary tangles do not correlate with these deficits. Our project was in progress when two papers by Rodriguez et al., came out, demonstrating sex differences in the onset of neurogenic deficits in the 3xTg-AD model. In the DG, they compared male and female mice and found early deficits in proliferation starting at 4 months of age in the dorsal blade of the DG in female mice, while in male mice, this decrease was delayed, only reaching significance at 9 months of age. Within the ventral blade, females showed significant deficits at 12 months, while males showed deficits at 6 months of age (Rodriguez *et al.*, 2008). In the SVZ, they only studied male mice and showed that proliferation was inhibited beginning at 3 month of age (Rodriguez *et al.*, 2009). Together, this work provided clear evidence that neurogenesis was inhibited in both the SVZ and DG of a mouse model that recapitulates the major AD-associated pathologies and cognitive symptoms (Chapter 1, Figure 5).

IV.2 IDENTIFICATION AND QUANTIFICATION OF LIPID ACCUMULATION IN ALZHEIMER'S DISEASE

In my second paper (Chapter 3), we took a multidisciplinary approach to study the mechanisms underlying defective neurogenesis in the 3xTg-AD mice. To determine if deficits in neurogenesis could be contributing to the cognitive deficits in AD, we first set out to determine if the onset of cognitive decline in 3xTg-AD mice correlated with deficits in neurogenesis in female 3xTg-AD mice. We found that at 5 months, 3xTg-AD mice had fewer proliferating neural precursors in both the DG and SVZ. Further analysis has shown that 2-month old 3xTg-AD mice already present deficits in proliferation and neurogenesis in both the DG and SVZ (data not shown). However, we have yet to perform an in depth time course of ages prior to 2 months of age. Intriguingly, at both 2 (data not shown) and 5 months of age we found a gross accumulation of neutral lipids within ependymal cells along the entire ventricular axis.

To determine if this lipid accumulation was a phenotype present in AD patients, we used the same neutral lipid stain on the lateral ventricle of human AD patients and age-matched controls. Remarkably, we found a similar accumulation of neutral lipids within AD ependymal cells. The role of lipids in regulating neural precursor function had not been extensively studied, however, this struck us as an emerging and interesting field. After reviewing the literature we found many circumstantial links between neurodegeneration and aberrant lipid metabolism (reviewed in (Hussain *et al.*, 2013)). Observational studies associated low fish intake and low blood levels of omega-3 fatty acids to increased risk of dementia and AD (Gu *et al.*, 2010). On the other hand, high fat diets and increased free fatty acids can induce and exacerbate AD pathological hallmarks including, plaque and tangle formation (Patil & Chan, 2005; Julien *et al.*,

2010) and gliosis and inflammation (Gupta *et al.*, 2012). Diets rich in polyunsaturated fatty acids improve mouse cognitive decline in aging and AD mutant mice (Fernandez-Fernandez *et al.*, 2012). However, technical hurdles in the identification and localization of lipids in the brain needed to be overcome in order to dissect their contribution to NSC regulation. To address this, we began a collaboration with the laboratory of Dr. Pierre Chaurand, a leader in the technique of laser desorption ionization, a method used to detect and measure proteins and lipids within the intact tissue architecture. The development of optimal conditions for lipid identification by the Chaurand lab, allowed us to identify, localize and quantitate the precise lipid species accumulating within the ependymal zone. After measuring major lipid classes, we found 12 specific triglycerides increased between 2-27 fold in 3xTg-AD mice. Triglycerides are stored in response to excess fatty acid levels, thus we used tandem mass spectrometry to fractionate the side chains of each of the top 3 triglycerides to determine the component fatty acid chains. This analysis yielded 6 fatty acids of oleic acid (OA, 18:1), palmitic acid (PA, 16:0), stearic acid (SA, 18:0), palmitoleic acid (POA, 16:1), eicosenoic acid (EA, 20:1) and eicosadienoic acid (EDA, 20:2) side-chains in an approximately 7:5:3:1:1:1 ratio. Interestingly, the three human studies that looked at fatty acid levels in AD brains found increases in the levels of OA (reviewed in Hussain et al. 2013). Fraser, Astarita, and Cunnane, measured fatty acid levels in multiple brain regions of AD patients and age-matched controls. Fraser et al., found an increase in PA and OA and a decrease in SA in the frontal and temporal lobe of AD patients (Fraser *et al.*, 2010). While Astarita et al., showed an elevation of POA and OA in the mid-frontal cortex and hippocampus of AD patients (Astarita *et al.*, 2011). Moreover, Cunnane et al., found a 10-20% increase in OA isomers and a 12-14% decrease in DHA composition in AD brains (Cunnane *et al.*, 2012). ICV infusion of OA into WT mice led to neutral lipid accumulation resembling that seen in the 3xTg-

AD mice, implying that an elevation of free OA levels may be the initiating factor for the observed triglyceride accumulation. Importantly, ICV infusion of heavy-labelled C13-OA in WT mice recapitulated the 11 of the 12 triglycerides seen in the 3xTg-AD mice, suggesting that the SVZ possesses the enzymes necessary for the elongation, reduction, saturation, and desaturation of fatty acids. This was an interesting observation, as it is the first demonstration that ependymal cells actively metabolize lipids. This data led us to hypothesize that elevated OA levels in the SVZ niche were contributing to the deficits in neurogenesis seen in the 3xTg-AD mice.

IV.3 SOURCES OF ABERRANT BRAIN LIPID ACCUMULATION IN ALZHEIMER'S DISEASE

To further understand why the brain accumulates lipids in AD, we considered the possibility of local and peripheral sources. Indeed, mounting evidence suggested that the brain fatty acid profile is altered in AD and may depend on that of the periphery. Cunnane et al., measured and identified plasma and brain lipids altered between non-cognitively impaired (NCI), mild-cognitively impaired (MCI), and AD patients. The main differences they found were in the levels of plasma free OA and OA isomers, being 80% lower in AD and 70% lower in MCI compared to NCI. Free linoleic acid (18:2) and the sum of free omega-6 fatty acids were 50-80% lower in AD and MCI than in NCI. Compared to the NCI group, neither free DHA nor the sum of free omega-3 fatty acids was significantly changed in MCI or AD. After looking at multiple brain regions, they found that AD brains had 12-14% lower DHA composition specifically in phosphatidylserines of the mid-frontal and superior temporal cortex. Moreover, in the superior temporal and midfrontal cortex, OA isomers were 10-20% higher in AD. Therefore the only

correlation between brain and serum fatty acid levels was in total DHA% in phosphotidylserine of the mid-frontal cortex and superior temporal cortex in AD compared to NCI (Cunnane *et al.*, 2012). In our study, we measured lipid levels in plasma and CSF extracts from WT and 3xTg-AD mice, paying particular attention to the triglycerides and component fatty acids observed in the 3xTg-AD lipid inclusions. Interestingly, we found no changes in any of the 12 triglycerides or their component fatty acid chains, again suggesting that aberrant OA-accumulation in the SVZ arises from local SVZ metabolism defects and not the periphery. Indeed, microarray analysis on microdissected SVZs from WT and 3xTg-AD mice, showed differential gene profiles of over a hundred genes related to lipid metabolism including an up regulation of SCD-1, the rate-limiting enzyme in the synthesis of OA from SA. Intriguingly, during brain development, OA is synthesized in the periventricular zone coinciding with a spike in SCD-1 activity (Polo-Hernandez *et al.*, 2010; Polo-Hernandez *et al.*, 2014). In humans, it has been demonstrated that AD patients have an increase in the ratio of OA/SA and concomitant elevation of mRNA levels of SCD-1 (Astarita *et al.*, 2011). Compellingly, previously work has shown that macrophages treated with Aβ become activated and selectively increase SCD-1 activity (Uryu *et al.*, 2003). Thus, it will be interesting to determine if reducing Aβ levels decreases OA in AD. Another way OA could accumulate is by defective triglyceride lipolysis. Along these lines, adipose triglyceride lipase (ATGL) is the rate-limiting enzyme the lipolysis of triacylglycerol to diacylglycerol (Chapter 1, Figure 6) and ATGL-knockout mice selectively accumulate neutral lipids within ependymal barriers (Etschmaier *et al.*, 2011). Thus, an activation of OA synthesis and/or an inhibition of lipolysis enzymes could lead to the storage of triglycerides within ependymal cells in AD. Our data collectively supports a model in which a trigger, possibly Aβ, up regulates SCD-1 activity, this in turn increases the levels of circulating OA in the brain and

causes it to be deposited in lipid droplets in the SVZ.

IV.4 REGULATION OF NEURAL STEM CELLS BY FATTY ACIDS

After establishing that elevated local OA levels were likely the signal leading to triglyceride accumulation, we wondered whether altered OA levels could be a factor contributing to the inhibition of neural precursor behaviour in AD. We took advantage of the in vitro neurosphere assay to first assess the impact of various concentrations of OA. A dose-response of 0.001uM-1000uM of OA showed that at low concentrations (0.001-50uM) OA either had no effect or slightly increased neurosphere numbers, while at concentrations higher than 50uM an inhibition of neurosphere number was observed (unpublished data and Chapter 3). We chose 50 and 100 uM for our further studies as this was the range used in most fatty acid studies and because one induced a positive effect and the other a negative affect on neurosphere growth in our hands. Concurrently, a few groups began treating neural precursors with fatty acids. Sakayori and colleagues grew embryonically derived neurospheres in the presence of DHA and AA and showed that DHA increased neurosphere number while AA had no effect (Sakayori *et al.*, 2011). While others differentiated embryonic neurospheres in the presence of DHA, AA, EPA, DPA, PA or OA (Sakayori *et al.*, 2011; Katakura *et al.*, 2013; Rashid *et al.*, 2013; Yuan *et al.*, 2013; Wang *et al.*, 2014). Overall, these studies found that DHA in particular, repeatedly enhanced neuronal fate choice and differentiation and other polyunsaturated omega-3 fatty acids such as EPA and DPA have similar effects (Kawakita *et al.*, 2006; Katakura *et al.*, 2009; Sakayori *et al.*, 2011; Katakura *et al.*, 2013; Rashid *et al.*, 2013). AA, an omega-6 fatty acid has shown conflicting results (Sakayori *et al.*, 2011; Rashid *et al.*, 2013). OA, an omega-9 fatty acid had no effect on neural precursor differentiation in vitro (Rashid *et al.*, 2013) but enhanced neuronal

differentiation in explants and slice cultures (Polo-Hernandez *et al.*, 2014). Lastly, PA a saturated fatty acid promoted astrogliogenesis at low doses and apoptosis at high doses (Yuan *et al.*, 2013; Wang *et al.*, 2014).

To gain insight into whether OA was modulating NSC or progenitor behaviour, we divided the neurosphere assay into two phases, NSC activation and progenitor cell expansion. We found that 100uM OA inhibited neurosphere number only when treated during NSC activation. This suggested that high OA selectively inhibits NSC activation. To make sure that the decrease in neurosphere number was not due to changes in cell death or generalized proliferative defects, we performed a TUNEL apoptosis assay in combination with immunocytochemistry for Ki67 and observed no differences. To determine if OA was modulating NSC self-renewal, we developed a technique that would allow us to assess the number of stem cells per neurosphere. This method demonstrated that OA treated spheres contained fewer NSCs. Together, our in vitro data showed that increased OA levels could selectively inhibit the activation of adult NSCs. Thus, a more detailed map of how fatty acids impact NSC proliferation and differentiation will provide important information on how changes in lipid levels can modulate brain activity and function.

We next wanted to determine if OA inhibited NSC activation in vivo. To do this, we employed a well-established AraC regeneration assay in which AraC is ICV infused for 6 days to eliminate all the constitutively proliferating progenitors and neuroblasts leaving only quiescent NSCs (Doetsch *et al.*, 1999b). Doetsch et al., performed a detailed characterization of the dynamics of SVZ depletion and regeneration following AraC treatment (Doetsch *et al*., 1999b). Using the same paradigm employed in our study, Doetsch and colleagues found that after 6 days of AraC, only ependymal cells, tanycytes, and type B cells remained. To identify which cells

divided at different survivals after AraC treatment, [3H] thymidine or BrdU was injected 1 hr. before sacrifice and mice were sacrificed 0, 0.5, 1, 2, and 3 days after pump removal and the labeled cells were characterized by electron microscopy. At 0 days, no 3H-thymidine-labeled cells were encountered, At 0.5 day and 1 day, 99% dividing cells were identified at the EM in the injected hemisphere: 97% corresponded to type B cells and two to microglia (Fig. 4A and Table 1). None corresponded to ependymal cells or tanycytes. In our study we co-infused 500uM of OA or vehicle during the 6 days of SVZ depopulation (Doetsch *et al*., 1999b). We sacrificed one group of mice at 0 or 1 day after pump removal. At 0 days we counted the number of Ki67+ proliferating cells and found no significant difference between vehicle and OA treated, suggesting that the depopulation of SVZ cells occurred at the same level in both groups (data not shown). However, at the 1 day time point we found a decrease in the number of Ki67+ in the OA treated group. The fact that SVZ depopulation was the same strongly suggests that OA selectively inhibited the regeneration capacity of type B NSCs. Interestingly, the DG also showed inhibited proliferation, however it did not reach statistical significance. Together, these experiments uncovered a novel mechanism by which increased OA could inhibit NSC and neurogenesis in AD.

An interestingly finding from this study is that DG proliferation is inhibited in the 3xTg-AD mouse model and following anti-mitotic AraC treatment even though no ependymal cells are present in the DG. This suggests that it is not necessarily the lipid-laden ependymal cells that directly inhibit neurogenesis. They may simply be the consequence of excess accumulation of lipids in the environment not dissimilar to amyloid plaques that appear to be the mere consequence of elevated amyloid levels. This hypothesis should be tested in two ways. First, identifying the exact mechanisms that lead to excess OA-enriched triglycerides in ependymal

cells. It has been previously shown that SCD-1 the main enzyme responsible for OA synthesis is expressed within the periventricular regions of the SVZ (Polo-Hernandez *et al*., 2014) and our microarray data found an increase in the transcription of this gene within microdissected 3xTg-AD SVZs. Determining if elevated SCD-1 expression in ependymal cells is sufficient to cause the AD-associated triglyceride profile and if inhibiting this activation can reverse the neurogenic deficits are part of the revisions for the publication of this paper and will provide insight into the role of ependymal cells in the inhibition of neurogenesis in AD. Second, LDI-MS on hippocampal brain sections can be performed and to reveal if excess lipids are reaching the DG.

More work is needed to prove which cell types specially produce OA under normal and pathological conditions. New data has shown that fatty acid synthase, the key enzyme of de novo lipogenesis is active in adult neural precursors and that conditional deletion of fatty acid synthase in Nestin+ neural precursors impairs adult DG neurogenesis and the increase in proliferation seen after exercise (Chorna *et al.*, 2013; Knobloch *et al.*, 2013). Therefore, uncovering how fatty acids and lipids in general are produced and metabolized within the brain is an important novel field of study that will surely provide much needed information in the future. Another point we have not addressed is how OA gets transmitted to NSCs. It is likely that fatty acid binding proteins (FABP)s that are involved in shuttling fatty acids between cells play a role in this process. FABP5 and FABP7 are present in NSCs and their neuronal progenitors coexpressing GFAP, Nestin, Sox2 and DCX but not NeuN in the DG. Importantly, a marked decrease in NSCs and neural progenitors is observed when FABP5, FABP7 or both are knocked out. Intriguingly, FABP7 but not FABP5 levels are increased in the serum of multiple dementia-related diseases including AD and Parkinson's disease (Teunissen *et al.*, 2011) and FABP3 levels are decreased in the brains of AD and down syndrome patients (Cheon *et al.*, 2003).

IV.5 OLEIC ACID AND THE AKT-FOXO3 NEURAL STEM CELL PRESERVATION PATHWAY

To begin to unravel the molecular mechanism of how OA inhibits NSC activation we looked back into our microarray analysis to find genetic links between lipids and neural stem cell regulation. The FoxO transcription factor family particularly stood out, as it had been previously linked to metabolism and adult NSC preservation (Paik *et al.*, 2009; Renault *et al.*, 2009; Schmidt-Strassburger *et al.*, 2012; Ro *et al.*, 2013; Yeo *et al.*, 2013). We performed an acute stimulation experiment where neural precursors were treated with OA for various periods of time and measured the response of the AKT-FoxO signalling. Remarkably, we found that OA could acutely induce AKT phosphorylation and the phosphorylation of its downstream FoxO3 *in vitro*. To mimic this experiment *in vivo*, we performed a single OA ICV injection and sacrificed the mice at various time-points and similarly found a robust activation of the AKT-FoxO3 pathway. To determine if the hyper-activation of the AKT-pathway by OA is a necessary component of the inhibition of NSC activation we have since performing two experiments (Annex). *In vitro*, we treated neurospheres with vehicle or OA alone or in combination with a PI3K-inhibitor (LY2094002). As previously, OA inhibited neurosphere number when compared to vehicle alone. However, when combined with LY, OA lost its negative effect, instead producing the same number of neurospheres as vehicle treated with LY. This data provides evidence that the effects of OA require modulation of P13K-AKT-signalling. Due to the continued difficulty in labeling and targeting NSCs in vivo, we used a novel approach to target ventricle contacting GFAP-expressing NSCs using electroporation or electropermeabilization, a molecular biology

technique in which an electrical field is applied to cells in order to increase the permeability of the cell membrane, allowing chemicals, drugs, or DNA to be introduced into the cell (Barnabe-Heider *et al*., 2008). In this study, we electroporated GFAP-cre in R26-flox-stop-flox-EYFP mice to induce the excision of the flox sites and allows for the expression of YFP in GFAP+ cells and their progeny. To test the effects of OA on ventricle-contacting GFAP-expressing NSCs we placed 7-day osmotic pumps containing vehicle or OA immediately following electroporation. After 7 days, we sacrificed the mice and quantified the number of YFP+ cells per ventricle. This analysis revealed an inhibition of the number of YFP+ NSCs in the OA treated group, however it did not reach statistical significance $p = 0.08$. To determine if this reduction required modulation of AKT-signalling we performed a second experiment where GFAP-cre and AKT-kinase dead were co-electroporated prior to pump placement. In this experiment, we found the number of YFP+ NSCs to be more similar between vehicle and OA p = 0.2. Together, these experiments provide in vitro and in vivo evidence that the negative effects of OA required the activation of AKT-signalling. In the future, we plan to perform similar experiments using mutant FOXO3a plasmids to determine if it is indeed the downstream target of AKT in this context.

These experiments show that lipid-sensing signalling occurs in NSCs and that changes in lipid levels can regulate the quiescence or activation status of NSCs through these pathways. Fitting with this, Codega et al. performed a microarray on purified quiescent vs. active SVZ NSCs and found lipid metabolism genes to be one of the main differentiating gene classes between the two, suggesting a role for lipids in NSC regulation (Codega *et al.*, 2014). Together, this work suggests that in AD, chronically elevated OA levels dysregulate the AKT-FoxO3 pathway and NSC behaviour possibly by promoting early over proliferation leading to premature

NSC exhaustion or by directly inhibiting NSC activation.

IV.6 GENERAL CONCLUSIONS

Identifying novel, effective therapeutics for AD is one of the major unmet medical needs of our time. Although billions of dollars have been invested into AD research and clinical trials, it remains the most prevalent and costly neurodegenerative disease with no cure or disease modifying therapies. Amyloid beta has kept the AD field fixated for the last hundred years and although these studies have provided important insight, the etiology and pathophysiology underlying AD remains a mystery. Novel therapies will require a fresh way of thinking about AD research. New techniques and technologies from multiple fields can be harnessed to enact a multidisciplinary systems approach. Current techniques are available from cell biology and regenerative medicine fields including exogenous implantation of new cells or endogenous stimulation of existing cells. These methods could allow for enhanced or sustained levels of neurogenesis throughout life and are useful for a wide-range of neurological disorders. In AD, the main target would be to prevent or restore the neuronal dysfunction and loss. There are, however, many hurdles to the application of these therapies for AD, including getting the cells to survive in a less than ideal environment and to integrate into an already existing complex brain. With this in mind, enhancing endogenous neurogenesis would be more amenable to widespread implementation in patients as delivery of exogenous implantation therapies requires invasive procedures. Thus, understanding the factors regulating neurogenesis under normal and pathological conditions will bring us closer to determining the elements needed to enhance and sustain appropriate levels of neurogenesis throughout life and following damage or degeneration.

Indeed, uncovering AD-associated factors that impinge on neurogenesis gives us clues as to why neurodegeneration may be happening and provides targets for regeneration.

My thesis work has demonstrated that neurogenesis is impeded in the 3xTg-AD mouse model of AD. Therefore, not only is the brain microenvironment toxic to existing cells, it may also be inhibiting its only source of regenerative potential. Our data implicates fatty acids as novel regulators of adult neurogenesis. We localized and identified deficient lipid metabolism as a novel player in AD and provided important new links between AD-associated brain lipid metabolism defects and how they can impact a neurogenic niche and its activity.

An important prediction from these studies is that one or all of the three mutations found in the 3xTg-AD mouse triggers abnormal lipid metabolism. At present the only upstream link between these mutations and lipid metabolism come from the study that shows that Aβ can trigger SCD-1 expression (Uryu *et al*., 2003). It would thus be interesting to study lipid accumulation in APP (Swedish), PS1 (M146V), and tau (P301L) single mutant mice to gain insight into which mutation triggers aberrant lipid metabolism.

Although we have only scratched the surface of how lipid metabolism can impinge on neurogenesis and neurodegeneration, we are hopeful that in the future, these findings will have therapeutic value.

GENERAL REFERENCES

Adachi, K., Mirzadeh, Z., Sakaguchi, M., Yamashita, T., Nikolcheva, T., Gotoh, Y., Peltz, G., Gong, L., Kawase, T., Alvarez-Buylla, A., Okano, H. & Sawamoto, K. (2007) Beta-catenin signaling promotes proliferation of progenitor cells in the adult mouse subventricular zone. *Stem Cells*, **25**, 2827-2836.

Adibhatla, R.M. & Hatcher, J.F. (2008) Altered lipid metabolism in brain injury and disorders. *Sub-cellular biochemistry*, **49**, 241-268.

Aguirre, A. & Gallo, V. (2007) Reduced EGFR signaling in progenitor cells of the adult subventricular zone attenuates oligodendrogenesis after demyelination. *Neuron glia biology*, **3**, 209-220.

Aguirre, A., Rizvi, T.A., Ratner, N. & Gallo, V. (2005) Overexpression of the epidermal growth factor receptor confers migratory properties to nonmigratory postnatal neural progenitors. *The Journal of neuroscience : the official journal of the Society for Neuroscience*, **25**, 11092-11106.

Aguirre, A., Rubio, M.E. & Gallo, V. (2010) Notch and EGFR pathway interaction regulates neural stem cell number and self-renewal. *Nature*, **467**, 323-327.

Ahn, S. & Joyner, A.L. (2005) In vivo analysis of quiescent adult neural stem cells responding to Sonic hedgehog. *Nature*, **437**, 894-897.

Aimone, J.B., Deng, W. & Gage, F.H. (2010) Adult neurogenesis: integrating theories and separating functions. *Trends in cognitive sciences*, **14**, 325-337.

Aimone, J.B., Deng, W. & Gage, F.H. (2011) Resolving new memories: a critical look at the dentate gyrus, adult neurogenesis, and pattern separation. *Neuron*, **70**, 589-596.

Aimone, J.B., Li, Y., Lee, S.W., Clemenson, G.D., Deng, W. & Gage, F.H. (2014) Regulation and function of adult neurogenesis: from genes to cognition. *Physiological reviews*, **94**, 991-1026.

Akiyama, H., Arai, T., Kondo, H., Tanno, E., Haga, C. & Ikeda, K. (2000) Cell mediators of inflammation in the Alzheimer disease brain. *Alzheimer disease and associated disorders*, **14 Suppl 1**, S47-53.

Alexson, T.O., Hitoshi, S., Coles, B.L., Bernstein, A. & van der Kooy, D. (2006) Notch signaling is required to maintain all neural stem cell populations--irrespective of spatial or temporal niche. *Developmental neuroscience*, **28**, 34-48.

Alonso, M., Viollet, C., Gabellec, M.M., Meas-Yedid, V., Olivo-Marin, J.C. & Lledo, P.M. (2006) Olfactory discrimination learning increases the survival of adult-born neurons in

the olfactory bulb. *The Journal of neuroscience : the official journal of the Society for Neuroscience*, **26**, 10508-10513.

Altman, J. & Das, G.D. (1965) Autoradiographic and histological evidence of postnatal hippocampal neurogenesis in rats. *The Journal of comparative neurology*, **124**, 319-335.

Alvarez-Buylla, A., Garcia-Verdugo, J.M. & Tramontin, A.D. (2001) A unified hypothesis on the lineage of neural stem cells. *Nature reviews. Neuroscience*, **2**, 287-293.

Alvarez-Buylla, A. & Ihrie, R.A. (2014) Sonic hedgehog signaling in the postnatal brain. *Seminars in cell & developmental biology*, **33**, 105-111.

Alvarez-Buylla, A. & Lim, D.A. (2004) For the long run: maintaining germinal niches in the adult brain. *Neuron*, **41**, 683-686.

Alzheimer, A. (1907) Über eine eigenartige Erkrankung der Hirnrinde. *Allgemeine Zeitschrift für Psychiatrie und psychisch-gerichtliche Medizin*, **64** pp. 146–148.

Ambrogini, P., Lattanzi, D., Ciuffoli, S., Agostini, D., Bertini, L., Stocchi, V., Santi, S. & Cuppini, R. (2004) Morpho-functional characterization of neuronal cells at different stages of maturation in granule cell layer of adult rat dentate gyrus. *Brain research*, **1017**, 21-31.

Andreu-Agullo, C., Morante-Redolat, J.M., Delgado, A.C. & Farinas, I. (2009) Vascular niche factor PEDF modulates Notch-dependent stemness in the adult subependymal zone. *Nature neuroscience*, **12**, 1514-1523.

Apelt, J. & Schliebs, R. (2001) Beta-amyloid-induced glial expression of both pro- and anti-inflammatory cytokines in cerebral cortex of aged transgenic Tg2576 mice with Alzheimer plaque pathology. *Brain research*, **894**, 21-30.

Arriagada, P.V., Growdon, J.H., Hedley-Whyte, E.T. & Hyman, B.T. (1992) Neurofibrillary tangles but not senile plaques parallel duration and severity of Alzheimer's disease. *Neurology*, **42**, 631-639.

Arruda-Carvalho, M., Sakaguchi, M., Akers, K.G., Josselyn, S.A. & Frankland, P.W. (2011) Posttraining ablation of adult-generated neurons degrades previously acquired memories. *The Journal of neuroscience : the official journal of the Society for Neuroscience*, **31**, 15113-15127.

Astarita, G., Jung, K.M., Vasilevko, V., Dipatrizio, N.V., Martin, S.K., Cribbs, D.H., Head, E., Cotman, C.W. & Piomelli, D. (2011) Elevated stearoyl-CoA desaturase in brains of patients with Alzheimer's disease. *PloS one*, **6**, e24777.

Bacon, A.W., Bondi, M.W., Salmon, D.P. & Murphy, C. (1998) Very early changes in olfactory functioning due to Alzheimer's disease and the role of apolipoprotein E in olfaction. *Annals of the New York Academy of Sciences*, **855**, 723-731.

Balordi, F. & Fishell, G. (2007a) Hedgehog signaling in the subventricular zone is required for both the maintenance of stem cells and the migration of newborn neurons. *The Journal of neuroscience : the official journal of the Society for Neuroscience*, **27**, 5936-5947.

Balordi, F. & Fishell, G. (2007b) Mosaic removal of hedgehog signaling in the adult SVZ reveals that the residual wild-type stem cells have a limited capacity for self-renewal. *The Journal of neuroscience : the official journal of the Society for Neuroscience*, **27**, 14248-14259.

Barkho, B.Z., Song, H., Aimone, J.B., Smrt, R.D., Kuwabara, T., Nakashima, K., Gage, F.H. & Zhao, X. (2006) Identification of astrocyte-expressed factors that modulate neural stem/progenitor cell differentiation. *Stem cells and development*, **15**, 407-421.

Barnabe-Heider, F., Meletis, K., Eriksson, M., Bergmann, O., Sabelstrom, H., Harvey, M.A., Mikkers, H. & Frisen, J. (2008) Genetic manipulation of adult mouse neurogenic niches by in vivo electroporation. *Nature methods*, **5**, 189-196.

Barres, B.A. (2008) The mystery and magic of glia: a perspective on their roles in health and disease. *Neuron*, **60**, 430-440.

Basak, O., Giachino, C., Fiorini, E., Macdonald, H.R. & Taylor, V. (2012) Neurogenic subventricular zone stem/progenitor cells are Notch1-dependent in their active but not quiescent state. *The Journal of neuroscience : the official journal of the Society for Neuroscience*, **32**, 5654-5666.

Basak, O. & Taylor, V. (2009) Stem cells of the adult mammalian brain and their niche. *Cellular and molecular life sciences : CMLS*, **66**, 1057-1072.

Bath, K.G., Mandairon, N., Jing, D., Rajagopal, R., Kapoor, R., Chen, Z.Y., Khan, T., Proenca, C.C., Kraemer, R., Cleland, T.A., Hempstead, B.L., Chao, M.V. & Lee, F.S. (2008) Variant brain-derived neurotrophic factor (Val66Met) alters adult olfactory bulb neurogenesis and spontaneous olfactory discrimination. *The Journal of neuroscience : the official journal of the Society for Neuroscience*, **28**, 2383-2393.

Becker, M., Lavie, V. & Solomon, B. (2007) Stimulation of endogenous neurogenesis by anti-EFRH immunization in a transgenic mouse model of Alzheimer's disease. *Proceedings of the National Academy of Sciences of the United States of America*, **104**, 1691-1696.

Bedard, A. & Parent, A. (2004) Evidence of newly generated neurons in the human olfactory bulb. *Brain research. Developmental brain research*, **151**, 159-168.

Bednarczyk, M.R., Aumont, A., Decary, S., Bergeron, R. & Fernandes, K.J. (2009) Prolonged voluntary wheel-running stimulates neural precursors in the hippocampus and forebrain of adult CD1 mice. *Hippocampus*, **19**, 913-927.

Belluzzi, O., Benedusi, M., Ackman, J. & LoTurco, J.J. (2003) Electrophysiological differentiation of new neurons in the olfactory bulb. *The Journal of neuroscience : the official journal of the Society for Neuroscience*, **23**, 10411-10418.

Bergmann, O., Liebl, J., Bernard, S., Alkass, K., Yeung, M.S., Steier, P., Kutschera, W., Johnson, L., Landen, M., Druid, H., Spalding, K.L. & Frisen, J. (2012) The age of olfactory bulb neurons in humans. *Neuron*, **74**, 634-639.

Bernier, P.J., Vinet, J., Cossette, M. & Parent, A. (2000) Characterization of the subventricular zone of the adult human brain: evidence for the involvement of Bcl-2. *Neuroscience research*, **37**, 67-78.

Biebl, M., Cooper, C.M., Winkler, J. & Kuhn, H.G. (2000) Analysis of neurogenesis and programmed cell death reveals a self-renewing capacity in the adult rat brain. *Neuroscience letters*, **291**, 17-20.

Billings, L.M., Oddo, S., Green, K.N., McGaugh, J.L. & LaFerla, F.M. (2005) Intraneuronal Abeta causes the onset of early Alzheimer's disease-related cognitive deficits in transgenic mice. *Neuron*, **45**, 675-688.

Bizon, J.L., Lee, H.J. & Gallagher, M. (2004) Neurogenesis in a rat model of age-related cognitive decline. *Aging cell*, **3**, 227-234.

Blasko, I., Stampfer-Kountchev, M., Robatscher, P., Veerhuis, R., Eikelenboom, P. & Grubeck-Loebenstein, B. (2004) How chronic inflammation can affect the brain and support the development of Alzheimer's disease in old age: the role of microglia and astrocytes. *Aging cell*, **3**, 169-176.

Blum-Degen, D., Muller, T., Kuhn, W., Gerlach, M., Przuntek, H. & Riederer, P. (1995) Interleukin-1 beta and interleukin-6 are elevated in the cerebrospinal fluid of Alzheimer's and de novo Parkinson's disease patients. *Neuroscience letters*, **202**, 17-20.

Boekhoorn, K., Joels, M. & Lucassen, P.J. (2006a) Increased proliferation reflects glial and vascular-associated changes, but not neurogenesis in the presenile Alzheimer hippocampus. *Neurobiology of disease*, **24**, 1-14.

Boekhoorn, K., Terwel, D., Biemans, B., Borghgraef, P., Wiegert, O., Ramakers, G.J., de Vos, K., Krugers, H., Tomiyama, T., Mori, H., Joels, M., van Leuven, F. & Lucassen, P.J. (2006b) Improved long-term potentiation and memory in young tau-P301L transgenic mice before onset of hyperphosphorylation and tauopathy. *J Neurosci*, **26**, 3514-3523.

Bonaguidi, M.A., Peng, C.Y., McGuire, T., Falciglia, G., Gobeske, K.T., Czeisler, C. & Kessler, J.A. (2008) Noggin expands neural stem cells in the adult hippocampus. *The Journal of neuroscience : the official journal of the Society for Neuroscience*, **28**, 9194-9204.

Bonaguidi, M.A., Wheeler, M.A., Shapiro, J.S., Stadel, R.P., Sun, G.J., Ming, G.L. & Song, H. (2011) In vivo clonal analysis reveals self-renewing and multipotent adult neural stem cell characteristics. *Cell*, **145**, 1142-1155.

Bond, A.M., Bhalala, O.G. & Kessler, J.A. (2012) The dynamic role of bone morphogenetic proteins in neural stem cell fate and maturation. *Developmental neurobiology*, **72**, 1068-1084.

Bouab, M., Paliouras, G.N., Aumont, A., Forest-Berard, K. & Fernandes, K.J. (2011) Aging of the subventricular zone neural stem cell niche: evidence for quiescence-associated changes between early and mid-adulthood. *Neuroscience*, **173**, 135-149.

Bovetti, S., Veyrac, A., Peretto, P., Fasolo, A. & De Marchis, S. (2009) Olfactory enrichment influences adult neurogenesis modulating GAD67 and plasticity-related molecules expression in newborn cells of the olfactory bulb. *PloS one*, **4**, e6359.

Bozza, P.T. & Viola, J.P. (2010) Lipid droplets in inflammation and cancer. *Prostaglandins, leukotrienes, and essential fatty acids*, **82**, 243-250.

Braak, H. & Braak, E. (1991a) Demonstration of amyloid deposits and neurofibrillary changes in whole brain sections. *Brain Pathol*, **1**, 213-216.

Braak, H. & Braak, E. (1991b) Neuropathological stageing of Alzheimer-related changes. *Acta neuropathologica*, **82**, 239-259.

Braak, H. & Braak, E. (1995) Staging of Alzheimer's disease-related neurofibrillary changes. *Neurobiology of aging*, **16**, 271-278; discussion 278-284.

Breton-Provencher, V., Lemasson, M., Peralta, M.R., 3rd & Saghatelyan, A. (2009) Interneurons produced in adulthood are required for the normal functioning of the olfactory bulb network and for the execution of selected olfactory behaviors. *The Journal of neuroscience : the official journal of the Society for Neuroscience*, **29**, 15245-15257.

Brezun, J.M. & Daszuta, A. (1999) Depletion in serotonin decreases neurogenesis in the dentate gyrus and the subventricular zone of adult rats. *Neuroscience*, **89**, 999-1002.

Brezun, J.M. & Daszuta, A. (2000) Serotonin may stimulate granule cell proliferation in the adult hippocampus, as observed in rats grafted with foetal raphe neurons. *The European journal of neuroscience*, **12**, 391-396.

Brill, M.S., Ninkovic, J., Winpenny, E., Hodge, R.D., Ozen, I., Yang, R., Lepier, A., Gascon, S., Erdelyi, F., Szabo, G., Parras, C., Guillemot, F., Frotscher, M., Berninger, B., Hevner,

R.F., Raineteau, O. & Gotz, M. (2009) Adult generation of glutamatergic olfactory bulb interneurons. *Nature neuroscience*, **12**, 1524-1533.

Bu, G. (2009) Apolipoprotein E and its receptors in Alzheimer's disease: pathways, pathogenesis and therapy. *Nature reviews. Neuroscience*, **10**, 333-344.

Butovsky, O., Ziv, Y., Schwartz, A., Landa, G., Talpalar, A.E., Pluchino, S., Martino, G. & Schwartz, M. (2006) Microglia activated by IL-4 or IFN-gamma differentially induce neurogenesis and oligodendrogenesis from adult stem/progenitor cells. *Molecular and cellular neurosciences*, **31**, 149-160.

Caille, I., Allinquant, B., Dupont, E., Bouillot, C., Langer, A., Muller, U. & Prochiantz, A. (2004) Soluble form of amyloid precursor protein regulates proliferation of progenitors in the adult subventricular zone. *Development*, **131**, 2173-2181.

Calon, F., Lim, G.P., Yang, F., Morihara, T., Teter, B., Ubeda, O., Rostaing, P., Triller, A., Salem, N., Jr., Ashe, K.H., Frautschy, S.A. & Cole, G.M. (2004) Docosahexaenoic acid protects from dendritic pathology in an Alzheimer's disease mouse model. *Neuron*, **43**, 633-645.

Cameron, H.A., McEwen, B.S. & Gould, E. (1995) Regulation of adult neurogenesis by excitatory input and NMDA receptor activation in the dentate gyrus. *The Journal of neuroscience : the official journal of the Society for Neuroscience*, **15**, 4687-4692.

Cameron, H.A. & McKay, R.D. (1999) Restoring production of hippocampal neurons in old age. *Nature neuroscience*, **2**, 894-897.

Cao, X., Li, L.P., Qin, X.H., Li, S.J., Zhang, M., Wang, Q., Hu, H.H., Fang, Y.Y., Gao, Y.B., Li, X.W., Sun, L.R., Xiong, W.C., Gao, T.M. & Zhu, X.H. (2013a) Astrocytic adenosine 5'-triphosphate release regulates the proliferation of neural stem cells in the adult hippocampus. *Stem Cells*, **31**, 1633-1643.

Cao, X., Li, L.P., Wang, Q., Wu, Q., Hu, H.H., Zhang, M., Fang, Y.Y., Zhang, J., Li, S.J., Xiong, W.C., Yan, H.C., Gao, Y.B., Liu, J.H., Li, X.W., Sun, L.R., Zeng, Y.N., Zhu, X.H. & Gao, T.M. (2013b) Astrocyte-derived ATP modulates depressive-like behaviors. *Nature medicine*, **19**, 773-777.

Capela, A. & Temple, S. (2002) LeX/ssea-1 is expressed by adult mouse CNS stem cells, identifying them as nonependymal. *Neuron*, **35**, 865-875.

Carleton, A., Petreanu, L.T., Lansford, R., Alvarez-Buylla, A. & Lledo, P.M. (2003) Becoming a new neuron in the adult olfactory bulb. *Nature neuroscience*, **6**, 507-518.

Carlson, M. GO db: A set of annotation maps describing the entire Gene Ontology.

Carroll, J.C., Rosario, E.R., Chang, L., Stanczyk, F.Z., Oddo, S., LaFerla, F.M. & Pike, C.J. (2007) Progesterone and estrogen regulate Alzheimer-like neuropathology in female 3xTg-AD mice. *The Journal of neuroscience : the official journal of the Society for Neuroscience*, **27**, 13357-13365.

Caruso, D., Barron, A.M., Brown, M.A., Abbiati, F., Carrero, P., Pike, C.J., Garcia-Segura, L.M. & Melcangi, R.C. (2013) Age-related changes in neuroactive steroid levels in 3xTg-AD mice. *Neurobiology of aging*, **34**, 1080-1089.

Chalbot, S., Zetterberg, H., Blennow, K., Fladby, T., Grundke-Iqbal, I. & Iqbal, K. (2009) Cerebrospinal fluid secretory Ca2+-dependent phospholipase A2 activity is increased in Alzheimer disease. *Clinical chemistry*, **55**, 2171-2179.

Chaurand, P., Cornett, D.S., Angel, P.M. & Caprioli, R.M. (2011) From whole-body sections down to cellular level, multiscale imaging of phospholipids by MALDI mass spectrometry. *Molecular & cellular proteomics : MCP*, **10**, O110 004259.

Cheng, C., Gross, M.L. & Pittenauer, E. (1998) Complete structural elucidation of triacylglycerols by tandem sector mass spectrometry. *Analytical chemistry*, **70**, 4417-4426.

Cheon, M.S., Kim, S.H., Fountoulakis, M. & Lubec, G. (2003) Heart type fatty acid binding protein (H-FABP) is decreased in brains of patients with Down syndrome and Alzheimer's disease. *Journal of neural transmission. Supplementum*, 225-234.

Choi, S.H., Veeraraghavalu, K., Lazarov, O., Marler, S., Ransohoff, R.M., Ramirez, J.M. & Sisodia, S.S. (2008) Non-cell-autonomous effects of presenilin 1 variants on enrichment-mediated hippocampal progenitor cell proliferation and differentiation. *Neuron*, **59**, 568-580.

Chorna, N.E., Santos-Soto, I.J., Carballeira, N.M., Morales, J.L., de la Nuez, J., Catala-Valentin, A., Chornyy, A.P., Vazquez-Montes, A. & De Ortiz, S.P. (2013) Fatty acid synthase as a factor required for exercise-induced cognitive enhancement and dentate gyrus cellular proliferation. *PloS one*, **8**, e77845.

Christensen, K. & Vaupel, J.W. (1996) Determinants of longevity: genetic, environmental and medical factors. *J Intern Med*, **240**, 333-341.

Chuang, T.T. (2010a) Neurogenesis in mouse models of Alzheimer's disease. *Biochimica et biophysica acta*, **1802**, 872-880.

Chuang, T.T. (2010b) Neurogenesis in mouse models of Alzheimer's disease. *Biochim Biophys Acta*.

Clelland, C.D., Choi, M., Romberg, C., Clemenson, G.D., Jr., Fragniere, A., Tyers, P., Jessberger, S., Saksida, L.M., Barker, R.A., Gage, F.H. & Bussey, T.J. (2009) A

functional role for adult hippocampal neurogenesis in spatial pattern separation. *Science*, **325**, 210-213.

Codega, P., Silva-Vargas, V., Paul, A., Maldonado-Soto, A.R., Deleo, A.M., Pastrana, E. & Doetsch, F. (2014) Prospective identification and purification of quiescent adult neural stem cells from their in vivo niche. *Neuron*, **82**, 545-559.

Colak, D., Mori, T., Brill, M.S., Pfeifer, A., Falk, S., Deng, C., Monteiro, R., Mummery, C., Sommer, L. & Gotz, M. (2008) Adult neurogenesis requires Smad4-mediated bone morphogenic protein signaling in stem cells. *The Journal of neuroscience : the official journal of the Society for Neuroscience*, **28**, 434-446.

Conover, J.C., Doetsch, F., Garcia-Verdugo, J.M., Gale, N.W., Yancopoulos, G.D. & Alvarez-Buylla, A. (2000) Disruption of Eph/ephrin signaling affects migration and proliferation in the adult subventricular zone. *Nature neuroscience*, **3**, 1091-1097.

Cooper-Kuhn, C.M. & Kuhn, H.G. (2002) Is it all DNA repair? Methodological considerations for detecting neurogenesis in the adult brain. *Brain research. Developmental brain research*, **134**, 13-21.

Corbit, K.C., Aanstad, P., Singla, V., Norman, A.R., Stainier, D.Y. & Reiter, J.F. (2005) Vertebrate Smoothened functions at the primary cilium. *Nature*, **437**, 1018-1021.

Corbit, K.C., Shyer, A.E., Dowdle, W.E., Gaulden, J., Singla, V., Chen, M.H., Chuang, P.T. & Reiter, J.F. (2008) Kif3a constrains beta-catenin-dependent Wnt signalling through dual ciliary and non-ciliary mechanisms. *Nature cell biology*, **10**, 70-76.

Corder, E.H., Saunders, A.M., Risch, N.J., Strittmatter, W.J., Schmechel, D.E., Gaskell, P.C., Jr., Rimmler, J.B., Locke, P.A., Conneally, P.M., Schmader, K.E. & et al. (1994) Protective effect of apolipoprotein E type 2 allele for late onset Alzheimer disease. *Nature genetics*, **7**, 180-184.

Corder, E.H., Saunders, A.M., Strittmatter, W.J., Schmechel, D.E., Gaskell, P.C., Small, G.W., Roses, A.D., Haines, J.L. & Pericak-Vance, M.A. (1993) Gene dose of apolipoprotein E type 4 allele and the risk of Alzheimer's disease in late onset families. *Science*, **261**, 921-923.

Corotto, F.S., Henegar, J.R. & Maruniak, J.A. (1994) Odor deprivation leads to reduced neurogenesis and reduced neuronal survival in the olfactory bulb of the adult mouse. *Neuroscience*, **61**, 739-744.

Corti, S., Nizzardo, M., Nardini, M., Donadoni, C., Locatelli, F., Papadimitriou, D., Salani, S., Del Bo, R., Ghezzi, S., Strazzer, S., Bresolin, N. & Comi, G.P. (2007) Isolation and characterization of murine neural stem/progenitor cells based on Prominin-1 expression. *Experimental neurology*, **205**, 547-562.

Craig, C.G., Tropepe, V., Morshead, C.M., Reynolds, B.A., Weiss, S. & van der Kooy, D. (1996) In vivo growth factor expansion of endogenous subependymal neural precursor cell populations in the adult mouse brain. *The Journal of neuroscience : the official journal of the Society for Neuroscience*, **16**, 2649-2658.

Creer, D.J., Romberg, C., Saksida, L.M., van Praag, H. & Bussey, T.J. (2010) Running enhances spatial pattern separation in mice. *Proceedings of the National Academy of Sciences of the United States of America*, **107**, 2367-2372.

Crews, L., Adame, A., Patrick, C., Delaney, A., Pham, E., Rockenstein, E., Hansen, L. & Masliah, E. (2010a) Increased BMP6 levels in the brains of Alzheimer's disease patients and APP transgenic mice are accompanied by impaired neurogenesis. *The Journal of neuroscience : the official journal of the Society for Neuroscience*, **30**, 12252-12262.

Crews, L., Rockenstein, E. & Masliah, E. (2010b) APP transgenic modeling of Alzheimer's disease: mechanisms of neurodegeneration and aberrant neurogenesis. *Brain Struct Funct*, **214**, 111-126.

Cunnane, S.C., Schneider, J.A., Tangney, C., Tremblay-Mercier, J., Fortier, M., Bennett, D.A. & Morris, M.C. (2012) Plasma and brain fatty acid profiles in mild cognitive impairment and Alzheimer's disease. *Journal of Alzheimer's disease : JAD*, **29**, 691-697.

Curtis, M.A., Eriksson, P.S. & Faull, R.L. (2007a) Progenitor cells and adult neurogenesis in neurodegenerative diseases and injuries of the basal ganglia. *Clinical and experimental pharmacology & physiology*, **34**, 528-532.

Curtis, M.A., Kam, M., Nannmark, U., Anderson, M.F., Axell, M.Z., Wikkelso, C., Holtas, S., van Roon-Mom, W.M., Bjork-Eriksson, T., Nordborg, C., Frisen, J., Dragunow, M., Faull, R.L. & Eriksson, P.S. (2007b) Human neuroblasts migrate to the olfactory bulb via a lateral ventricular extension. *Science*, **315**, 1243-1249.

de Chevigny, A., Cooper, O., Vinuela, A., Reske-Nielsen, C., Lagace, D.C., Eisch, A.J. & Isacson, O. (2008) Fate mapping and lineage analyses demonstrate the production of a large number of striatal neuroblasts after transforming growth factor alpha and noggin striatal infusions into the dopamine-depleted striatum. *Stem Cells*, **26**, 2349-2360.

de la Monte, S.M. & Tong, M. (2014) Brain metabolic dysfunction at the core of Alzheimer's disease. *Biochemical pharmacology*, **88**, 548-559.

De Strooper, B., Annaert, W., Cupers, P., Saftig, P., Craessaerts, K., Mumm, J.S., Schroeter, E.H., Schrijvers, V., Wolfe, M.S., Ray, W.J., Goate, A. & Kopan, R. (1999) A presenilin-1-dependent gamma-secretase-like protease mediates release of Notch intracellular domain. *Nature*, **398**, 518-522.

DeCarolis, N.A., Mechanic, M., Petrik, D., Carlton, A., Ables, J.L., Malhotra, S., Bachoo, R., Gotz, M., Lagace, D.C. & Eisch, A.J. (2013) In vivo contribution of nestin- and GLAST-lineage cells to adult hippocampal neurogenesis. *Hippocampus*, **23**, 708-719.

Demars, M., Hu, Y.S., Gadadhar, A. & Lazarov, O. (2010) Impaired neurogenesis is an early event in the etiology of familial Alzheimer's disease in transgenic mice. *Journal of neuroscience research*, **88**, 2103-2117.

Demars, M.P., Hollands, C., Zhao Kda, T. & Lazarov, O. (2013) Soluble amyloid precursor protein-alpha rescues age-linked decline in neural progenitor cell proliferation. *Neurobiology of aging*, **34**, 2431-2440.

Deng, W., Saxe, M.D., Gallina, I.S. & Gage, F.H. (2009) Adult-born hippocampal dentate granule cells undergoing maturation modulate learning and memory in the brain. *The Journal of neuroscience : the official journal of the Society for Neuroscience*, **29**, 13532-13542.

Deters, N., Ittner, L.M. & Gotz, J. (2008) Divergent phosphorylation pattern of tau in P301L tau transgenic mice. *The European journal of neuroscience*, **28**, 137-147.

Digel, M., Ehehalt, R. & Fullekrug, J. (2010) Lipid droplets lighting up: insights from live microscopy. *FEBS letters*, **584**, 2168-2175.

Doetsch, F., Caille, I., Lim, D.A., Garcia-Verdugo, J.M. & Alvarez-Buylla, A. (1999a) Subventricular zone astrocytes are neural stem cells in the adult mammalian brain. *Cell*, **97**, 703-716.

Doetsch, F., Garcia-Verdugo, J.M. & Alvarez-Buylla, A. (1997) Cellular composition and three-dimensional organization of the subventricular germinal zone in the adult mammalian brain. *The Journal of neuroscience : the official journal of the Society for Neuroscience*, **17**, 5046-5061.

Doetsch, F., Garcia-Verdugo, J.M. & Alvarez-Buylla, A. (1999b) Regeneration of a germinal layer in the adult mammalian brain. *Proceedings of the National Academy of Sciences of the United States of America*, **96**, 11619-11624.

Doetsch, F., Petreanu, L., Caille, I., Garcia-Verdugo, J.M. & Alvarez-Buylla, A. (2002) EGF converts transit-amplifying neurogenic precursors in the adult brain into multipotent stem cells. *Neuron*, **36**, 1021-1034.

Dranovsky, A., Picchini, A.M., Moadel, T., Sisti, A.C., Yamada, A., Kimura, S., Leonardo, E.D. & Hen, R. (2011) Experience dictates stem cell fate in the adult hippocampus. *Neuron*, **70**, 908-923.

Dufresne, M., Thomas, A., Breault-Turcot, J., Masson, J.F. & Chaurand, P. (2013) Silver-assisted laser desorption ionization for high spatial resolution imaging mass spectrometry of olefins from thin tissue sections. *Analytical chemistry*, **85**, 3318-3324.

Dupret, D., Revest, J.M., Koehl, M., Ichas, F., De Giorgi, F., Costet, P., Abrous, D.N. & Piazza, P.V. (2008) Spatial relational memory requires hippocampal adult neurogenesis. *PloS one*, **3**, e1959.

Elder, G.A., Gama Sosa, M.A., De Gasperi, R., Dickstein, D.L. & Hof, P.R. (2010) Presenilin transgenic mice as models of Alzheimer's disease. *Brain Struct Funct*, **214**, 127-143.

Encinas, J.M., Michurina, T.V., Peunova, N., Park, J.H., Tordo, J., Peterson, D.A., Fishell, G., Koulakov, A. & Enikolopov, G. (2011) Division-coupled astrocytic differentiation and age-related depletion of neural stem cells in the adult hippocampus. *Cell stem cell*, **8**, 566-579.

Enwere, E., Shingo, T., Gregg, C., Fujikawa, H., Ohta, S. & Weiss, S. (2004) Aging results in reduced epidermal growth factor receptor signaling, diminished olfactory neurogenesis, and deficits in fine olfactory discrimination. *The Journal of neuroscience : the official journal of the Society for Neuroscience*, **24**, 8354-8365.

Eriksson, P.S., Perfilieva, E., Bjork-Eriksson, T., Alborn, A.M., Nordborg, C., Peterson, D.A. & Gage, F.H. (1998) Neurogenesis in the adult human hippocampus. *Nature medicine*, **4**, 1313-1317.

Erlandsson, A., Lin, C.H., Yu, F. & Morshead, C.M. (2011) Immunosuppression promotes endogenous neural stem and progenitor cell migration and tissue regeneration after ischemic injury. *Experimental neurology*, **230**, 48-57.

Ermini, F.V., Grathwohl, S., Radde, R., Yamaguchi, M., Staufenbiel, M., Palmer, T.D. & Jucker, M. (2008) Neurogenesis and alterations of neural stem cells in mouse models of cerebral amyloidosis. *Am J Pathol*, **172**, 1520-1528.

Ernst, A., Alkass, K., Bernard, S., Salehpour, M., Perl, S., Tisdale, J., Possnert, G., Druid, H. & Frisen, J. (2014) Neurogenesis in the striatum of the adult human brain. *Cell*, **156**, 1072-1083.

Esposito, M.S., Piatti, V.C., Laplagne, D.A., Morgenstern, N.A., Ferrari, C.C., Pitossi, F.J. & Schinder, A.F. (2005) Neuronal differentiation in the adult hippocampus recapitulates embryonic development. *The Journal of neuroscience : the official journal of the Society for Neuroscience*, **25**, 10074-10086.

Etschmaier, K., Becker, T., Eichmann, T.O., Schweinzer, C., Scholler, M., Tam-Amersdorfer, C., Poeckl, M., Schuligoi, R., Kober, A., Chirackal Manavalan, A.P., Rechberger, G.N., Streith, I.E., Zechner, R., Zimmermann, R. & Panzenboeck, U. (2011) Adipose

triglyceride lipase affects triacylglycerol metabolism at brain barriers. *Journal of neurochemistry*, **119**, 1016-1028.

Fahy, E., Subramaniam, S., Murphy, R.C., Nishijima, M., Raetz, C.R., Shimizu, T., Spener, F., van Meer, G., Wakelam, M.J. & Dennis, E.A. (2009) Update of the LIPID MAPS comprehensive classification system for lipids. *Journal of lipid research*, **50 Suppl**, S9-14.

Faragher, R.G., Sheerin, A.N. & Ostler, E.L. (2009) Can we intervene in human ageing? *Expert Rev Mol Med*, **11**, e27.

Fernandez-Fernandez, L., Comes, G., Bolea, I., Valente, T., Ruiz, J., Murtra, P., Ramirez, B., Angles, N., Reguant, J., Morello, J.R., Boada, M., Hidalgo, J., Escorihuela, R.M. & Unzeta, M. (2012) LMN diet, rich in polyphenols and polyunsaturated fatty acids, improves mouse cognitive decline associated with aging and Alzheimer's disease. *Behavioural brain research*, **228**, 261-271.

Fontana, L., Klein, S. & Holloszy, J.O. (2010) Effects of long-term calorie restriction and endurance exercise on glucose tolerance, insulin action, and adipokine production. *Age (Dordr)*, **32**, 97-108.

Forlenza, O.V., Wacker, P., Nunes, P.V., Yacubian, J., Castro, C.C., Otaduy, M.C. & Gattaz, W.F. (2005) Reduced phospholipid breakdown in Alzheimer's brains: a 31P spectroscopy study. *Psychopharmacology*, **180**, 359-365.

Franch-Marro, X., Wendler, F., Griffith, J., Maurice, M.M. & Vincent, J.P. (2008) In vivo role of lipid adducts on Wingless. *Journal of cell science*, **121**, 1587-1592.

Fraser, T., Tayler, H. & Love, S. (2010) Fatty acid composition of frontal, temporal and parietal neocortex in the normal human brain and in Alzheimer's disease. *Neurochemical research*, **35**, 503-513.

Fuchs, E., Tumbar, T. & Guasch, G. (2004) Socializing with the neighbors: stem cells and their niche. *Cell*, **116**, 769-778.

Gaiano, N. & Fishell, G. (2002) The role of notch in promoting glial and neural stem cell fates. *Annual review of neuroscience*, **25**, 471-490.

Gakhar-Koppole, N., Hundeshagen, P., Mandl, C., Weyer, S.W., Allinquant, B., Muller, U. & Ciccolini, F. (2008) Activity requires soluble amyloid precursor protein alpha to promote neurite outgrowth in neural stem cell-derived neurons via activation of the MAPK pathway. *The European journal of neuroscience*, **28**, 871-882.

Galimberti, D., Fenoglio, C. & Scarpini, E. (2008) Inflammation in neurodegenerative disorders: friend or foe? *Current aging science*, **1**, 30-41.

Gamoh, S., Hashimoto, M., Hossain, S. & Masumura, S. (2001) Chronic administration of docosahexaenoic acid improves the performance of radial arm maze task in aged rats. *Clinical and experimental pharmacology & physiology*, **28**, 266-270.

Gamoh, S., Hashimoto, M., Sugioka, K., Shahdat Hossain, M., Hata, N., Misawa, Y. & Masumura, S. (1999) Chronic administration of docosahexaenoic acid improves reference memory-related learning ability in young rats. *Neuroscience*, **93**, 237-241.

Gao, Z., Ure, K., Ables, J.L., Lagace, D.C., Nave, K.A., Goebbels, S., Eisch, A.J. & Hsieh, J. (2009) Neurod1 is essential for the survival and maturation of adult-born neurons. *Nature neuroscience*, **12**, 1090-1092.

Garcia, A.D., Doan, N.B., Imura, T., Bush, T.G. & Sofroniew, M.V. (2004) GFAP-expressing progenitors are the principal source of constitutive neurogenesis in adult mouse forebrain. *Nature neuroscience*, **7**, 1233-1241.

Gattaz, W.F., Forlenza, O.V., Talib, L.L., Barbosa, N.R. & Bottino, C.M. (2004) Platelet phospholipase A(2) activity in Alzheimer's disease and mild cognitive impairment. *J Neural Transm*, **111**, 591-601.

Ge, S., Goh, E.L., Sailor, K.A., Kitabatake, Y., Ming, G.L. & Song, H. (2006) GABA regulates synaptic integration of newly generated neurons in the adult brain. *Nature*, **439**, 589-593.

Ge, S., Pradhan, D.A., Ming, G.L. & Song, H. (2007) GABA sets the tempo for activity-dependent adult neurogenesis. *Trends in neurosciences*, **30**, 1-8.

Ge, S., Sailor, K.A., Ming, G.L. & Song, H. (2008) Synaptic integration and plasticity of new neurons in the adult hippocampus. *The Journal of physiology*, **586**, 3759-3765.

Genander, M. & Frisen, J. (2010) Ephrins and Eph receptors in stem cells and cancer. *Current opinion in cell biology*, **22**, 611-616.

Gheusi, G., Cremer, H., McLean, H., Chazal, G., Vincent, J.D. & Lledo, P.M. (2000) Importance of newly generated neurons in the adult olfactory bulb for odor discrimination. *Proceedings of the National Academy of Sciences of the United States of America*, **97**, 1823-1828.

Gheusi, G., Lepousez, G. & Lledo, P.M. (2013) Adult-born neurons in the olfactory bulb: integration and functional consequences. *Current topics in behavioral neurosciences*, **15**, 49-72.

Giachino, C., Basak, O., Lugert, S., Knuckles, P., Obernier, K., Fiorelli, R., Frank, S., Raineteau, O., Alvarez-Buylla, A. & Taylor, V. (2014) Molecular diversity subdivides the adult forebrain neural stem cell population. *Stem Cells*, **32**, 70-84.

Gimenez-Llort, L., Blazquez, G., Canete, T., Johansson, B., Oddo, S., Tobena, A., LaFerla, F.M. & Fernandez-Teruel, A. (2007) Modeling behavioral and neuronal symptoms of Alzheimer's disease in mice: a role for intraneuronal amyloid. *Neuroscience and biobehavioral reviews*, **31**, 125-147.

Givogri, M.I., de Planell, M., Galbiati, F., Superchi, D., Gritti, A., Vescovi, A., de Vellis, J. & Bongarzone, E.R. (2006) Notch signaling in astrocytes and neuroblasts of the adult subventricular zone in health and after cortical injury. *Developmental neuroscience*, **28**, 81-91.

Goedert, M. & Jakes, R. (2005) Mutations causing neurodegenerative tauopathies. *Biochimica et biophysica acta*, **1739**, 240-250.

Gomez-Isla, T., Hollister, R., West, H., Mui, S., Growdon, J.H., Petersen, R.C., Parisi, J.E. & Hyman, B.T. (1997) Neuronal loss correlates with but exceeds neurofibrillary tangles in Alzheimer's disease. *Annals of neurology*, **41**, 17-24.

Gonzalez-Perez, O., Romero-Rodriguez, R., Soriano-Navarro, M., Garcia-Verdugo, J.M. & Alvarez-Buylla, A. (2009) Epidermal growth factor induces the progeny of subventricular zone type B cells to migrate and differentiate into oligodendrocytes. *Stem Cells*, **27**, 2032-2043.

Goodman, J.M. (2008) The gregarious lipid droplet. *The Journal of biological chemistry*, **283**, 28005-28009.

Gotz, J., Chen, F., van Dorpe, J. & Nitsch, R.M. (2001) Formation of neurofibrillary tangles in P301l tau transgenic mice induced by Abeta 42 fibrils. *Science*, **293**, 1491-1495.

Gould, E., Reeves, A.J., Fallah, M., Tanapat, P., Gross, C.G. & Fuchs, E. (1999) Hippocampal neurogenesis in adult Old World primates. *Proceedings of the National Academy of Sciences of the United States of America*, **96**, 5263-5267.

Greenberg, A.S. & Coleman, R.A. (2011) Expanding roles for lipid droplets. *Trends in endocrinology and metabolism: TEM*, **22**, 195-196.

Greenberg, A.S., Coleman, R.A., Kraemer, F.B., McManaman, J.L., Obin, M.S., Puri, V., Yan, Q.W., Miyoshi, H. & Mashek, D.G. (2011) The role of lipid droplets in metabolic disease in rodents and humans. *The Journal of clinical investigation*, **121**, 2102-2110.

Greenberg, S.M., Gurol, M.E., Rosand, J. & Smith, E.E. (2004) Amyloid angiopathy-related vascular cognitive impairment. *Stroke; a journal of cerebral circulation*, **35**, 2616-2619.

Greenberg, S.M., Rebeck, G.W., Vonsattel, J.P., Gomez-Isla, T. & Hyman, B.T. (1995) Apolipoprotein E epsilon 4 and cerebral hemorrhage associated with amyloid angiopathy. *Annals of neurology*, **38**, 254-259.

Gregoire, C.A., Bonenfant, D., Le Nguyen, A., Aumont, A. & Fernandes, K.J. (2014) Untangling the influences of voluntary running, environmental complexity, social housing and stress on adult hippocampal neurogenesis. *PloS one*, **9**, e86237.

Gritti, A., Frolichsthal-Schoeller, P., Galli, R., Parati, E.A., Cova, L., Pagano, S.F., Bjornson, C.R. & Vescovi, A.L. (1999) Epidermal and fibroblast growth factors behave as mitogenic regulators for a single multipotent stem cell-like population from the subventricular region of the adult mouse forebrain. *The Journal of neuroscience : the official journal of the Society for Neuroscience*, **19**, 3287-3297.

Gritti, A., Parati, E.A., Cova, L., Frolichsthal, P., Galli, R., Wanke, E., Faravelli, L., Morassutti, D.J., Roisen, F., Nickel, D.D. & Vescovi, A.L. (1996) Multipotential stem cells from the adult mouse brain proliferate and self-renew in response to basic fibroblast growth factor. *The Journal of neuroscience : the official journal of the Society for Neuroscience*, **16**, 1091-1100.

Grootendorst, J., Bour, A., Vogel, E., Kelche, C., Sullivan, P.M., Dodart, J.C., Bales, K. & Mathis, C. (2005) Human apoE targeted replacement mouse lines: h-apoE4 and h-apoE3 mice differ on spatial memory performance and avoidance behavior. *Behavioural brain research*, **159**, 1-14.

Gu, Y., Nieves, J.W., Stern, Y., Luchsinger, J.A. & Scarmeas, N. (2010) Food combination and Alzheimer disease risk: a protective diet. *Archives of neurology*, **67**, 699-706.

Gupta, S., Knight, A.G., Gupta, S., Keller, J.N. & Bruce-Keller, A.J. (2012) Saturated long-chain fatty acids activate inflammatory signaling in astrocytes. *Journal of neurochemistry*, **120**, 1060-1071.

Guschina, I., Millership, S., O'Donnell, V., Ninkina, N., Harwood, J. & Buchman, V. (2011) Lipid classes and fatty acid patterns are altered in the brain of gamma-synuclein null mutant mice. *Lipids*, **46**, 121-130.

Haass, C. & Selkoe, D.J. (1993) Cellular processing of beta-amyloid precursor protein and the genesis of amyloid beta-peptide. *Cell*, **75**, 1039-1042.

Haass, C. & Selkoe, D.J. (2007) Soluble protein oligomers in neurodegeneration: lessons from the Alzheimer's amyloid beta-peptide. *Nature reviews. Molecular cell biology*, **8**, 101-112.

Haglund, M., Passant, U., Sjobeck, M., Ghebremedhin, E. & Englund, E. (2006) Cerebral amyloid angiopathy and cortical microinfarcts as putative substrates of vascular dementia. *International journal of geriatric psychiatry*, **21**, 681-687.

Halagappa, V.K., Guo, Z., Pearson, M., Matsuoka, Y., Cutler, R.G., Laferla, F.M. & Mattson, M.P. (2007) Intermittent fasting and caloric restriction ameliorate age-related behavioral

deficits in the triple-transgenic mouse model of Alzheimer's disease. *Neurobiology of disease*, **26**, 212-220.

Hamilton, L.K., Aumont, A., Julien, C., Vadnais, A., Calon, F. & Fernandes, K.J. (2010) Widespread deficits in adult neurogenesis precede plaque and tangle formation in the 3xTg mouse model of Alzheimer's disease. *The European journal of neuroscience*, **32**, 905-920.

Hamilton, L.K., Joppe, S.E., L, M.C. & Fernandes, K.J. (2013) Aging and neurogenesis in the adult forebrain: what we have learned and where we should go from here. *The European journal of neuroscience*, **37**, 1978-1986.

Han, Y.G., Spassky, N., Romaguera-Ros, M., Garcia-Verdugo, J.M., Aguilar, A., Schneider-Maunoury, S. & Alvarez-Buylla, A. (2008) Hedgehog signaling and primary cilia are required for the formation of adult neural stem cells. *Nature neuroscience*, **11**, 277-284.

Hansen, D.V., Lui, J.H., Parker, P.R. & Kriegstein, A.R. (2010) Neurogenic radial glia in the outer subventricular zone of human neocortex. *Nature*, **464**, 554-561.

Hardy, J.A. & Higgins, G.A. (1992) Alzheimer's disease: the amyloid cascade hypothesis. *Science*, **256**, 184-185.

Hartley, D.M., Walsh, D.M., Ye, C.P., Diehl, T., Vasquez, S., Vassilev, P.M., Teplow, D.B. & Selkoe, D.J. (1999) Protofibrillar intermediates of amyloid beta-protein induce acute electrophysiological changes and progressive neurotoxicity in cortical neurons. *The Journal of neuroscience : the official journal of the Society for Neuroscience*, **19**, 8876-8884.

Hashimoto, M., Hossain, S., Agdul, H. & Shido, O. (2005a) Docosahexaenoic acid-induced amelioration on impairment of memory learning in amyloid beta-infused rats relates to the decreases of amyloid beta and cholesterol levels in detergent-insoluble membrane fractions. *Biochimica et biophysica acta*, **1738**, 91-98.

Hashimoto, M., Tanabe, Y., Fujii, Y., Kikuta, T., Shibata, H. & Shido, O. (2005b) Chronic administration of docosahexaenoic acid ameliorates the impairment of spatial cognition learning ability in amyloid beta-infused rats. *The Journal of nutrition*, **135**, 549-555.

Haughey, N.J., Liu, D., Nath, A., Borchard, A.C. & Mattson, M.P. (2002a) Disruption of neurogenesis in the subventricular zone of adult mice, and in human cortical neuronal precursor cells in culture, by amyloid beta-peptide: implications for the pathogenesis of Alzheimer's disease. *Neuromolecular Med*, **1**, 125-135.

Haughey, N.J., Nath, A., Chan, S.L., Borchard, A.C., Rao, M.S. & Mattson, M.P. (2002b) Disruption of neurogenesis by amyloid beta-peptide, and perturbed neural progenitor cell homeostasis, in models of Alzheimer's disease. *Journal of neurochemistry*, **83**, 1509-1524.

Heo, C., Chang, K.A., Choi, H.S., Kim, H.S., Kim, S., Liew, H., Kim, J.A., Yu, E., Ma, J. & Suh, Y.H. (2007) Effects of the monomeric, oligomeric, and fibrillar Abeta42 peptides on the proliferation and differentiation of adult neural stem cells from subventricular zone. *Journal of neurochemistry*, **102**, 493-500.

Herz, J. & Bock, H.H. (2002) Lipoprotein receptors in the nervous system. *Annual review of biochemistry*, **71**, 405-434.

Herz, J. & Chen, Y. (2006) Reelin, lipoprotein receptors and synaptic plasticity. *Nature reviews. Neuroscience*, **7**, 850-859.

High, F.A., Lu, M.M., Pear, W.S., Loomes, K.M., Kaestner, K.H. & Epstein, J.A. (2008) Endothelial expression of the Notch ligand Jagged1 is required for vascular smooth muscle development. *Proceedings of the National Academy of Sciences of the United States of America*, **105**, 1955-1959.

Hoglinger, G.U., Rizk, P., Muriel, M.P., Duyckaerts, C., Oertel, W.H., Caille, I. & Hirsch, E.C. (2004) Dopamine depletion impairs precursor cell proliferation in Parkinson disease. *Nature neuroscience*, **7**, 726-735.

Holland, E.C. & Varmus, H.E. (1998) Basic fibroblast growth factor induces cell migration and proliferation after glia-specific gene transfer in mice. *Proceedings of the National Academy of Sciences of the United States of America*, **95**, 1218-1223.

Holmberg, J., Armulik, A., Senti, K.A., Edoff, K., Spalding, K., Momma, S., Cassidy, R., Flanagan, J.G. & Frisen, J. (2005) Ephrin-A2 reverse signaling negatively regulates neural progenitor proliferation and neurogenesis. *Genes & development*, **19**, 462-471.

Hotamisligil, G.S. (2006) Inflammation and metabolic disorders. *Nature*, **444**, 860-867.

Hsia, A.Y., Masliah, E., McConlogue, L., Yu, G.Q., Tatsuno, G., Hu, K., Kholodenko, D., Malenka, R.C., Nicoll, R.A. & Mucke, L. (1999) Plaque-independent disruption of neural circuits in Alzheimer's disease mouse models. *Proceedings of the National Academy of Sciences of the United States of America*, **96**, 3228-3233.

Hsieh, J. (2012) Orchestrating transcriptional control of adult neurogenesis. *Genes & development*, **26**, 1010-1021.

Hu, Y.S., Xu, P., Pigino, G., Brady, S.T., Larson, J. & Lazarov, O. (2010) Complex environment experience rescues impaired neurogenesis, enhances synaptic plasticity, and attenuates neuropathology in familial Alzheimer's disease-linked APPswe/PS1DeltaE9 mice. *FASEB J*, **24**, 1667-1681.

Huang da, W., Sherman, B.T. & Lempicki, R.A. (2009a) Systematic and integrative analysis of large gene lists using DAVID bioinformatics resources. *Nature protocols*, **4**, 44-57.

Huang da, W., Sherman, B.T., Zheng, X., Yang, J., Imamichi, T., Stephens, R. & Lempicki, R.A. (2009b) Extracting biological meaning from large gene lists with DAVID. *Current protocols in bioinformatics / editoral board, Andreas D. Baxevanis ... [et al.]*, **Chapter 13**, Unit 13 11.

Hussain, G., Schmitt, F., Loeffler, J.P. & Gonzalez de Aguilar, J.L. (2013) Fatting the brain: a brief of recent research. *Frontiers in cellular neuroscience*, **7**, 144.

Ihrie, R.A., Shah, J.K., Harwell, C.C., Levine, J.H., Guinto, C.D., Lezameta, M., Kriegstein, A.R. & Alvarez-Buylla, A. (2011) Persistent sonic hedgehog signaling in adult brain determines neural stem cell positional identity. *Neuron*, **71**, 250-262.

Imayoshi, I., Sakamoto, M., Ohtsuka, T., Takao, K., Miyakawa, T., Yamaguchi, M., Mori, K., Ikeda, T., Itohara, S. & Kageyama, R. (2008) Roles of continuous neurogenesis in the structural and functional integrity of the adult forebrain. *Nature neuroscience*, **11**, 1153-1161.

Imayoshi, I., Sakamoto, M., Yamaguchi, M., Mori, K. & Kageyama, R. (2010) Essential roles of Notch signaling in maintenance of neural stem cells in developing and adult brains. *The Journal of neuroscience : the official journal of the Society for Neuroscience*, **30**, 3489-3498.

Imura, T., Kornblum, H.I. & Sofroniew, M.V. (2003) The predominant neural stem cell isolated from postnatal and adult forebrain but not early embryonic forebrain expresses GFAP. *The Journal of neuroscience : the official journal of the Society for Neuroscience*, **23**, 2824-2832.

Ito, S., Matsumiya, K., Ohtsuki, S., Kamiie, J. & Terasaki, T. (2013) Contributions of degradation and brain-to-blood elimination across the blood-brain barrier to cerebral clearance of human amyloid-beta peptide(1-40) in mouse brain. *Journal of cerebral blood flow and metabolism : official journal of the International Society of Cerebral Blood Flow and Metabolism*, **33**, 1770-1777.

Itou, Y., Nochi, R., Kuribayashi, H., Saito, Y. & Hisatsune, T. (2010) Cholinergic activation of hippocampal neural stem cells in aged dentate gyrus. *Hippocampus*.

Jackson, E.L., Garcia-Verdugo, J.M., Gil-Perotin, S., Roy, M., Quinones-Hinojosa, A., VandenBerg, S. & Alvarez-Buylla, A. (2006) PDGFR alpha-positive B cells are neural stem cells in the adult SVZ that form glioma-like growths in response to increased PDGF signaling. *Neuron*, **51**, 187-199.

Janelsins, M.C., Mastrangelo, M.A., Oddo, S., LaFerla, F.M., Federoff, H.J. & Bowers, W.J. (2005) Early correlation of microglial activation with enhanced tumor necrosis factor-alpha and monocyte chemoattractant protein-1 expression specifically within the

entorhinal cortex of triple transgenic Alzheimer's disease mice. *Journal of neuroinflammation*, **2**, 23.

Jankovski, A. & Sotelo, C. (1996) Subventricular zone-olfactory bulb migratory pathway in the adult mouse: cellular composition and specificity as determined by heterochronic and heterotopic transplantation. *The Journal of comparative neurology*, **371**, 376-396.

Jessberger, S. & Gage, F.H. (2014) Adult neurogenesis: bridging the gap between mice and humans. *Trends in cell biology*, **24**, 558-563.

Jiao, J. & Chen, D.F. (2008) Induction of neurogenesis in nonconventional neurogenic regions of the adult central nervous system by niche astrocyte-produced signals. *Stem Cells*, **26**, 1221-1230.

Jin, K., Galvan, V., Xie, L., Mao, X.O., Gorostiza, O.F., Bredesen, D.E. & Greenberg, D.A. (2004a) Enhanced neurogenesis in Alzheimer's disease transgenic (PDGF-APPSw,Ind) mice. *Proceedings of the National Academy of Sciences of the United States of America*, **101**, 13363-13367.

Jin, K., Peel, A.L., Mao, X.O., Xie, L., Cottrell, B.A., Henshall, D.C. & Greenberg, D.A. (2004b) Increased hippocampal neurogenesis in Alzheimer's disease. *Proceedings of the National Academy of Sciences of the United States of America*, **101**, 343-347.

Johe, K.K., Hazel, T.G., Muller, T., Dugich-Djordjevic, M.M. & McKay, R.D. (1996) Single factors direct the differentiation of stem cells from the fetal and adult central nervous system. *Genes & development*, **10**, 3129-3140.

Josephs, K.A., Tsuboi, Y., Cookson, N., Watt, H. & Dickson, D.W. (2004) Apolipoprotein E epsilon 4 is a determinant for Alzheimer-type pathologic features in tauopathies, synucleinopathies, and frontotemporal degeneration. *Archives of neurology*, **61**, 1579-1584.

Julien, C., Tremblay, C., Bendjelloul, F., Phivilay, A., Coulombe, M.A., Emond, V. & Calon, F. (2008) Decreased drebrin mRNA expression in Alzheimer disease: correlation with tau pathology. *Journal of neuroscience research*, **86**, 2292-2302.

Julien, C., Tremblay, C., Phivilay, A., Berthiaume, L., Emond, V., Julien, P. & Calon, F. (2010) High-fat diet aggravates amyloid-beta and tau pathologies in the 3xTg-AD mouse model. *Neurobiology of aging*, **31**, 1516-1531.

Kaneko, N., Marin, O., Koike, M., Hirota, Y., Uchiyama, Y., Wu, J.Y., Lu, Q., Tessier-Lavigne, M., Alvarez-Buylla, A., Okano, H., Rubenstein, J.L. & Sawamoto, K. (2010) New neurons clear the path of astrocytic processes for their rapid migration in the adult brain. *Neuron*, **67**, 213-223.

Kanfer, J.N., Pettegrew, J.W., Moossy, J. & McCartney, D.G. (1993) Alterations of selected enzymes of phospholipid metabolism in Alzheimer's disease brain tissue as compared to non-Alzheimer's demented controls. *Neurochemical research*, **18**, 331-334.

Karalay, O., Doberauer, K., Vadodaria, K.C., Knobloch, M., Berti, L., Miquelajauregui, A., Schwark, M., Jagasia, R., Taketo, M.M., Tarabykin, V., Lie, D.C. & Jessberger, S. (2011) Prospero-related homeobox 1 gene (Prox1) is regulated by canonical Wnt signaling and has a stage-specific role in adult hippocampal neurogenesis. *Proceedings of the National Academy of Sciences of the United States of America*, **108**, 5807-5812.

Karch, C.M., Cruchaga, C. & Goate, A.M. (2014) Alzheimer's disease genetics: from the bench to the clinic. *Neuron*, **83**, 11-26.

Katakura, M., Hashimoto, M., Okui, T., Shahdat, H.M., Matsuzaki, K. & Shido, O. (2013) Omega-3 polyunsaturated Fatty acids enhance neuronal differentiation in cultured rat neural stem cells. *Stem cells international*, **2013**, 490476.

Katakura, M., Hashimoto, M., Shahdat, H.M., Gamoh, S., Okui, T., Matsuzaki, K. & Shido, O. (2009) Docosahexaenoic acid promotes neuronal differentiation by regulating basic helix-loop-helix transcription factors and cell cycle in neural stem cells. *Neuroscience*, **160**, 651-660.

Kawakita, E., Hashimoto, M. & Shido, O. (2006) Docosahexaenoic acid promotes neurogenesis in vitro and in vivo. *Neuroscience*, **139**, 991-997.

Kee, N., Teixeira, C.M., Wang, A.H. & Frankland, P.W. (2007) Imaging activation of adult-generated granule cells in spatial memory. *Nature protocols*, **2**, 3033-3044.

Kempermann, G., Kuhn, H.G. & Gage, F.H. (1998) Experience-induced neurogenesis in the senescent dentate gyrus. *The Journal of neuroscience : the official journal of the Society for Neuroscience*, **18**, 3206-3212.

Kempermann, G. & Neumann, H. (2003) Neuroscience. Microglia: the enemy within? *Science*, **302**, 1689-1690.

Kenyon, C.J. (2010) The genetics of ageing. *Nature*, **464**, 504-512.

Kermen, F., Sultan, S., Sacquet, J., Mandairon, N. & Didier, A. (2010) Consolidation of an olfactory memory trace in the olfactory bulb is required for learning-induced survival of adult-born neurons and long-term memory. *PloS one*, **5**, e12118.

Kippin, T.E., Kapur, S. & van der Kooy, D. (2005) Dopamine specifically inhibits forebrain neural stem cell proliferation, suggesting a novel effect of antipsychotic drugs. *The Journal of neuroscience : the official journal of the Society for Neuroscience*, **25**, 5815-5823.

Kitamura, T., Saitoh, Y., Takashima, N., Murayama, A., Niibori, Y., Ageta, H., Sekiguchi, M., Sugiyama, H. & Inokuchi, K. (2009) Adult neurogenesis modulates the hippocampus-dependent period of associative fear memory. *Cell*, **139**, 814-827.

Klein, J. (2000) Membrane breakdown in acute and chronic neurodegeneration: focus on choline-containing phospholipids. *J Neural Transm*, **107**, 1027-1063.

Knobloch, M., Braun, S.M., Zurkirchen, L., von Schoultz, C., Zamboni, N., Arauzo-Bravo, M.J., Kovacs, W.J., Karalay, O., Suter, U., Machado, R.A., Roccio, M., Lutolf, M.P., Semenkovich, C.F. & Jessberger, S. (2013) Metabolic control of adult neural stem cell activity by Fasn-dependent lipogenesis. *Nature*, **493**, 226-230.

Knoth, R., Singec, I., Ditter, M., Pantazis, G., Capetian, P., Meyer, R.P., Horvat, V., Volk, B. & Kempermann, G. (2010) Murine features of neurogenesis in the human hippocampus across the lifespan from 0 to 100 years. *PloS one*, **5**, e8809.

Kobilo, T., Yuan, C. & van Praag, H. (2011) Endurance factors improve hippocampal neurogenesis and spatial memory in mice. *Learn Mem*, **18**, 103-107.

Kok, E., Haikonen, S., Luoto, T., Huhtala, H., Goebeler, S., Haapasalo, H. & Karhunen, P.J. (2009) Apolipoprotein E-dependent accumulation of Alzheimer disease-related lesions begins in middle age. *Annals of neurology*, **65**, 650-657.

Kokovay, E., Wang, Y., Kusek, G., Wurster, R., Lederman, P., Lowry, N., Shen, Q. & Temple, S. (2012) VCAM1 is essential to maintain the structure of the SVZ niche and acts as an environmental sensor to regulate SVZ lineage progression. *Cell stem cell*, **11**, 220-230.

Kolb, B., Morshead, C., Gonzalez, C., Kim, M., Gregg, C., Shingo, T. & Weiss, S. (2007) Growth factor-stimulated generation of new cortical tissue and functional recovery after stroke damage to the motor cortex of rats. *Journal of cerebral blood flow and metabolism : official journal of the International Society of Cerebral Blood Flow and Metabolism*, **27**, 983-997.

Komekado, H., Yamamoto, H., Chiba, T. & Kikuchi, A. (2007) Glycosylation and palmitoylation of Wnt-3a are coupled to produce an active form of Wnt-3a. *Genes to cells : devoted to molecular & cellular mechanisms*, **12**, 521-534.

Kornack, D.R. & Rakic, P. (1999) Continuation of neurogenesis in the hippocampus of the adult macaque monkey. *Proceedings of the National Academy of Sciences of the United States of America*, **96**, 5768-5773.

Kosik, K.S. (1993) The molecular and cellular biology of tau. *Brain Pathol*, **3**, 39-43.

Kriegstein, A. & Alvarez-Buylla, A. (2009) The glial nature of embryonic and adult neural stem cells. *Annual review of neuroscience*, **32**, 149-184.

Kuhn, H.G., Dickinson-Anson, H. & Gage, F.H. (1996) Neurogenesis in the dentate gyrus of the adult rat: age-related decrease of neuronal progenitor proliferation. *The Journal of neuroscience : the official journal of the Society for Neuroscience*, **16**, 2027-2033.

Kuhn, H.G., Winkler, J., Kempermann, G., Thal, L.J. & Gage, F.H. (1997) Epidermal growth factor and fibroblast growth factor-2 have different effects on neural progenitors in the adult rat brain. *The Journal of neuroscience : the official journal of the Society for Neuroscience*, **17**, 5820-5829.

Kukekov, V.G., Laywell, E.D., Suslov, O., Davies, K., Scheffler, B., Thomas, L.B., O'Brien, T.F., Kusakabe, M. & Steindler, D.A. (1999) Multipotent stem/progenitor cells with similar properties arise from two neurogenic regions of adult human brain. *Experimental neurology*, **156**, 333-344.

Kume, H., Maruyama, K. & Kametani, F. (2004) Intracellular domain generation of amyloid precursor protein by epsilon-cleavage depends on C-terminal fragment by alpha-secretase cleavage. *International journal of molecular medicine*, **13**, 121-125.

Kurayoshi, M., Yamamoto, H., Izumi, S. & Kikuchi, A. (2007) Post-translational palmitoylation and glycosylation of Wnt-5a are necessary for its signalling. *The Biochemical journal*, **402**, 515-523.

Lagace, D.C., Noonan, M.A. & Eisch, A.J. (2007) Hippocampal neurogenesis: a matter of survival. *Am J Psychiatry*, **164**, 205.

Lai, K., Kaspar, B.K., Gage, F.H. & Schaffer, D.V. (2003) Sonic hedgehog regulates adult neural progenitor proliferation in vitro and in vivo. *Nature neuroscience*, **6**, 21-27.

Lane-Donovan, C. & Herz, J. (2014) Is apolipoprotein e required for cognitive function in humans?: implications for Alzheimer drug development. *JAMA neurology*, **71**, 1213-1215.

Lannfelt, L., Basun, H., Wahlund, L.O., Rowe, B.A. & Wagner, S.L. (1995) Decreased alpha-secretase-cleaved amyloid precursor protein as a diagnostic marker for Alzheimer's disease. *Nature medicine*, **1**, 829-832.

Lanzrein, A.S., Johnston, C.M., Perry, V.H., Jobst, K.A., King, E.M. & Smith, A.D. (1998) Longitudinal study of inflammatory factors in serum, cerebrospinal fluid, and brain tissue in Alzheimer disease: interleukin-1beta, interleukin-6, interleukin-1 receptor antagonist, tumor necrosis factor-alpha, the soluble tumor necrosis factor receptors I and II, and alpha1-antichymotrypsin. *Alzheimer disease and associated disorders*, **12**, 215-227.

Lazarini, F., Mouthon, M.A., Gheusi, G., de Chaumont, F., Olivo-Marin, J.C., Lamarque, S., Abrous, D.N., Boussin, F.D. & Lledo, P.M. (2009) Cellular and behavioral effects of cranial irradiation of the subventricular zone in adult mice. *PloS one*, **4**, e7017.

Lazarov, O. & Marr, R.A. (2010) Neurogenesis and Alzheimer's disease: at the crossroads. *Experimental neurology*, **223**, 267-281.

Lazarov, O., Mattson, M.P., Peterson, D.A., Pimplikar, S.W. & van Praag, H. (2010) When neurogenesis encounters aging and disease. *Trends in neurosciences*, **33**, 569-579.

Lazarov, O., Robinson, J., Tang, Y.P., Hairston, I.S., Korade-Mirnics, Z., Lee, V.M., Hersh, L.B., Sapolsky, R.M., Mirnics, K. & Sisodia, S.S. (2005) Environmental enrichment reduces Abeta levels and amyloid deposition in transgenic mice. *Cell*, **120**, 701-713.

Lee, C., Hu, J., Ralls, S., Kitamura, T., Loh, Y.P., Yang, Y., Mukouyama, Y.S. & Ahn, S. (2012) The molecular profiles of neural stem cell niche in the adult subventricular zone. *PloS one*, **7**, e50501.

Lehtinen, M.K., Zappaterra, M.W., Chen, X., Yang, Y.J., Hill, A.D., Lun, M., Maynard, T., Gonzalez, D., Kim, S., Ye, P., D'Ercole, A.J., Wong, E.T., LaMantia, A.S. & Walsh, C.A. (2011) The cerebrospinal fluid provides a proliferative niche for neural progenitor cells. *Neuron*, **69**, 893-905.

Leonard, B.W., Mastroeni, D., Grover, A., Liu, Q., Yang, K., Gao, M., Wu, J., Pootrakul, D., van den Berge, S.A., Hol, E.M. & Rogers, J. (2009) Subventricular zone neural progenitors from rapid brain autopsies of elderly subjects with and without neurodegenerative disease. *The Journal of comparative neurology*, **515**, 269-294.

Leoni, V. (2011) The effect of apolipoprotein E (ApoE) genotype on biomarkers of amyloidogenesis, tau pathology and neurodegeneration in Alzheimer's disease. *Clinical chemistry and laboratory medicine : CCLM / FESCC*, **49**, 375-383.

Leranth, C. & Hajszan, T. (2007) Extrinsic afferent systems to the dentate gyrus. *Progress in brain research*, **163**, 63-84.

Levi, O. & Michaelson, D.M. (2007) Environmental enrichment stimulates neurogenesis in apolipoprotein E3 and neuronal apoptosis in apolipoprotein E4 transgenic mice. *Journal of neurochemistry*, **100**, 202-210.

Lewis, P.M., Dunn, M.P., McMahon, J.A., Logan, M., Martin, J.F., St-Jacques, B. & McMahon, A.P. (2001) Cholesterol modification of sonic hedgehog is required for long-range signaling activity and effective modulation of signaling by Ptc1. *Cell*, **105**, 599-612.

Li, G., Bien-Ly, N., Andrews-Zwilling, Y., Xu, Q., Bernardo, A., Ring, K., Halabisky, B., Deng, C., Mahley, R.W. & Huang, Y. (2009) GABAergic interneuron dysfunction impairs hippocampal neurogenesis in adult apolipoprotein E4 knockin mice. *Cell stem cell*, **5**, 634-645.

Li, X. & Zuo, P. (2005) Effects of Abeta25-35 on neurogenesis in the adult mouse subventricular zone and dentate gyrus. *Neurological research*, **27**, 218-222.

Lie, D.C., Colamarino, S.A., Song, H.J., Desire, L., Mira, H., Consiglio, A., Lein, E.S., Jessberger, S., Lansford, H., Dearie, A.R. & Gage, F.H. (2005) Wnt signalling regulates adult hippocampal neurogenesis. *Nature*, **437**, 1370-1375.

Lim, D.A. & Alvarez-Buylla, A. (1999) Interaction between astrocytes and adult subventricular zone precursors stimulates neurogenesis. *Proceedings of the National Academy of Sciences of the United States of America*, **96**, 7526-7531.

Lim, D.A., Tramontin, A.D., Trevejo, J.M., Herrera, D.G., Garcia-Verdugo, J.M. & Alvarez-Buylla, A. (2000) Noggin antagonizes BMP signaling to create a niche for adult neurogenesis. *Neuron*, **28**, 713-726.

Lim, G.P., Calon, F., Morihara, T., Yang, F., Teter, B., Ubeda, O., Salem, N., Jr., Frautschy, S.A. & Cole, G.M. (2005) A diet enriched with the omega-3 fatty acid docosahexaenoic acid reduces amyloid burden in an aged Alzheimer mouse model. *The Journal of neuroscience : the official journal of the Society for Neuroscience*, **25**, 3032-3040.

Lindwall, G. & Cole, R.D. (1984) Phosphorylation affects the ability of tau protein to promote microtubule assembly. *The Journal of biological chemistry*, **259**, 5301-5305.

Liu, R.Z., Mita, R., Beaulieu, M., Gao, Z. & Godbout, R. (2010) Fatty acid binding proteins in brain development and disease. *The International journal of developmental biology*, **54**, 1229-1239.

Liu, Z., Neff, R.A. & Berg, D.K. (2006) Sequential interplay of nicotinic and GABAergic signaling guides neuronal development. *Science*, **314**, 1610-1613.

Lois, C. & Alvarez-Buylla, A. (1994) Long-distance neuronal migration in the adult mammalian brain. *Science*, **264**, 1145-1148.

Lopez-Toledano, M.A. & Shelanski, M.L. (2004) Neurogenic effect of beta-amyloid peptide in the development of neural stem cells. *The Journal of neuroscience : the official journal of the Society for Neuroscience*, **24**, 5439-5444.

Lue, L.F., Kuo, Y.M., Roher, A.E., Brachova, L., Shen, Y., Sue, L., Beach, T., Kurth, J.H., Rydel, R.E. & Rogers, J. (1999) Soluble amyloid beta peptide concentration as a predictor of synaptic change in Alzheimer's disease. *The American journal of pathology*, **155**, 853-862.

Luo, J., Daniels, S.B., Lennington, J.B., Notti, R.Q. & Conover, J.C. (2006) The aging neurogenic subventricular zone. *Aging cell*, **5**, 139-152.

Ma, D.K., Ming, G.L. & Song, H. (2005) Glial influences on neural stem cell development: cellular niches for adult neurogenesis. *Current opinion in neurobiology*, **15**, 514-520.

Maekawa, M., Takashima, N., Matsumata, M., Ikegami, S., Kontani, M., Hara, Y., Kawashima, H., Owada, Y., Kiso, Y., Yoshikawa, T., Inokuchi, K. & Osumi, N. (2009) Arachidonic acid drives postnatal neurogenesis and elicits a beneficial effect on prepulse inhibition, a biological trait of psychiatric illnesses. *PloS one*, **4**, e5085.

Mahley, R.W., Nathan, B.P. & Pitas, R.E. (1996) Apolipoprotein E. Structure, function, and possible roles in Alzheimer's disease. *Annals of the New York Academy of Sciences*, **777**, 139-145.

Mak, G.K., Enwere, E.K., Gregg, C., Pakarainen, T., Poutanen, M., Huhtaniemi, I. & Weiss, S. (2007) Male pheromone-stimulated neurogenesis in the adult female brain: possible role in mating behavior. *Nature neuroscience*, **10**, 1003-1011.

Mamber, C., Kozareva, D.A., Kamphuis, W. & Hol, E.M. (2013) Shades of gray: The delineation of marker expression within the adult rodent subventricular zone. *Progress in neurobiology*, **111**, 1-16.

Mapstone, M., Cheema, A.K., Fiandaca, M.S., Zhong, X., Mhyre, T.R., MacArthur, L.H., Hall, W.J., Fisher, S.G., Peterson, D.R., Haley, J.M., Nazar, M.D., Rich, S.A., Berlau, D.J., Peltz, C.B., Tan, M.T., Kawas, C.H. & Federoff, H.J. (2014) Plasma phospholipids identify antecedent memory impairment in older adults. *Nature medicine*, **20**, 415-418.

Maresh, A., Rodriguez Gil, D., Whitman, M.C. & Greer, C.A. (2008) Principles of glomerular organization in the human olfactory bulb--implications for odor processing. *PloS one*, **3**, e2640.

Martin, S. & Parton, R.G. (2006) Lipid droplets: a unified view of a dynamic organelle. *Nature reviews. Molecular cell biology*, **7**, 373-378.

Martinez, M., Brice, A., Vaughan, J.R., Zimprich, A., Breteler, M.M., Meco, G., Filla, A., Farrer, M.J., Betard, C., Singleton, A., Hardy, J., De Michele, G., Bonifati, V., Oostra, B.A., Gasser, T., Wood, N.W. & Durr, A. (2005) Apolipoprotein E4 is probably responsible for the chromosome 19 linkage peak for Parkinson's disease. *American journal of medical genetics. Part B, Neuropsychiatric genetics : the official publication of the International Society of Psychiatric Genetics*, **136B**, 72-74.

Martinez-Vicente, M., Talloczy, Z., Wong, E., Tang, G., Koga, H., Kaushik, S., de Vries, R., Arias, E., Harris, S., Sulzer, D. & Cuervo, A.M. (2010) Cargo recognition failure is responsible for inefficient autophagy in Huntington's disease. *Nature neuroscience*, **13**, 567-576.

Masterman, T. & Hillert, J. (2004) The telltale scan: APOE epsilon4 in multiple sclerosis. *The Lancet. Neurology*, **3**, 331.

Mastrangelo, M.A. & Bowers, W.J. (2008) Detailed immunohistochemical characterization of temporal and spatial progression of Alzheimer's disease-related pathologies in male triple-transgenic mice. *BMC neuroscience*, **9**, 81.

Matas-Rico, E., Garcia-Diaz, B., Llebrez-Zayas, P., Lopez-Barroso, D., Santin, L., Pedraza, C., Smith-Fernandez, A., Fernandez-Llebrez, P., Tellez, T., Redondo, M., Chun, J., De Fonseca, F.R. & Estivill-Torrus, G. (2008) Deletion of lysophosphatidic acid receptor LPA1 reduces neurogenesis in the mouse dentate gyrus. *Molecular and cellular neurosciences*, **39**, 342-355.

Matsumata, M., Sakayori, N., Maekawa, M., Owada, Y., Yoshikawa, T. & Osumi, N. (2012) The effects of Fabp7 and Fabp5 on postnatal hippocampal neurogenesis in the mouse. *Stem Cells*, **30**, 1532-1543.

Mattson, M.P. (1997) Cellular actions of beta-amyloid precursor protein and its soluble and fibrillogenic derivatives. *Physiological reviews*, **77**, 1081-1132.

Mattsson, N., Zetterberg, H., Hansson, O., Andreasen, N., Parnetti, L., Jonsson, M., Herukka, S.K., van der Flier, W.M., Blankenstein, M.A., Ewers, M., Rich, K., Kaiser, E., Verbeek, M., Tsolaki, M., Mulugeta, E., Rosen, E., Aarsland, D., Visser, P.J., Schroder, J., Marcusson, J., de Leon, M., Hampel, H., Scheltens, P., Pirttila, T., Wallin, A., Jonhagen, M.E., Minthon, L., Winblad, B. & Blennow, K. (2009) CSF biomarkers and incipient Alzheimer disease in patients with mild cognitive impairment. *Jama*, **302**, 385-393.

Matyash, V., Liebisch, G., Kurzchalia, T.V., Shevchenko, A. & Schwudke, D. (2008) Lipid extraction by methyl-tert-butyl ether for high-throughput lipidomics. *Journal of lipid research*, **49**, 1137-1146.

McGeer, P.L. & McGeer, E.G. (1995) The inflammatory response system of brain: implications for therapy of Alzheimer and other neurodegenerative diseases. *Brain research. Brain research reviews*, **21**, 195-218.

McKee, A.C., Carreras, I., Hossain, L., Ryu, H., Klein, W.L., Oddo, S., LaFerla, F.M., Jenkins, B.G., Kowall, N.W. & Dedeoglu, A. (2008) Ibuprofen reduces Abeta, hyperphosphorylated tau and memory deficits in Alzheimer mice. *Brain research*, **1207**, 225-236.

McKee, A.C., Kosik, K.S. & Kowall, N.W. (1991) Neuritic pathology and dementia in Alzheimer's disease. *Ann Neurol*, **30**, 156-165.

McLean, C.A., Cherny, R.A., Fraser, F.W., Fuller, S.J., Smith, M.J., Beyreuther, K., Bush, A.I. & Masters, C.L. (1999) Soluble pool of Abeta amyloid as a determinant of severity of neurodegeneration in Alzheimer's disease. *Annals of neurology*, **46**, 860-866.

Menn, B., Garcia-Verdugo, J.M., Yaschine, C., Gonzalez-Perez, O., Rowitch, D. & Alvarez-Buylla, A. (2006) Origin of oligodendrocytes in the subventricular zone of the adult

brain. *The Journal of neuroscience : the official journal of the Society for Neuroscience*, **26**, 7907-7918.

Merkle, F.T., Mirzadeh, Z. & Alvarez-Buylla, A. (2007) Mosaic organization of neural stem cells in the adult brain. *Science*, **317**, 381-384.

Merkle, F.T., Tramontin, A.D., Garcia-Verdugo, J.M. & Alvarez-Buylla, A. (2004) Radial glia give rise to adult neural stem cells in the subventricular zone. *Proceedings of the National Academy of Sciences of the United States of America*, **101**, 17528-17532.

Merlo, S., Spampinato, S., Canonico, P.L., Copani, A. & Sortino, M.A. (2010) Alzheimer's disease: brain expression of a metabolic disorder? *Trends in endocrinology and metabolism: TEM*, **21**, 537-544.

Meziane, H., Dodart, J.C., Mathis, C., Little, S., Clemens, J., Paul, S.M. & Ungerer, A. (1998) Memory-enhancing effects of secreted forms of the beta-amyloid precursor protein in normal and amnestic mice. *Proceedings of the National Academy of Sciences of the United States of America*, **95**, 12683-12688.

Mira, H., Andreu, Z., Suh, H., Lie, D.C., Jessberger, S., Consiglio, A., San Emeterio, J., Hortiguela, R., Marques-Torrejon, M.A., Nakashima, K., Colak, D., Gotz, M., Farinas, I. & Gage, F.H. (2010) Signaling through BMPR-IA regulates quiescence and long-term activity of neural stem cells in the adult hippocampus. *Cell stem cell*, **7**, 78-89.

Mirochnic, S., Wolf, S., Staufenbiel, M. & Kempermann, G. (2009) Age effects on the regulation of adult hippocampal neurogenesis by physical activity and environmental enrichment in the APP23 mouse model of Alzheimer disease. *Hippocampus*, **19**, 1008-1018.

Mirzadeh, Z., Merkle, F.T., Soriano-Navarro, M., Garcia-Verdugo, J.M. & Alvarez-Buylla, A. (2008) Neural stem cells confer unique pinwheel architecture to the ventricular surface in neurogenic regions of the adult brain. *Cell stem cell*, **3**, 265-278.

Miwa, N. & Storm, D.R. (2005) Odorant-induced activation of extracellular signal-regulated kinase/mitogen-activated protein kinase in the olfactory bulb promotes survival of newly formed granule cells. *The Journal of neuroscience : the official journal of the Society for Neuroscience*, **25**, 5404-5412.

Mok, S.S., Losic, D., Barrow, C.J., Turner, B.J., Masters, C.L., Martin, L.L. & Small, D.H. (2006) The beta-amyloid peptide of Alzheimer's disease decreases adhesion of vascular smooth muscle cells to the basement membrane. *Journal of neurochemistry*, **96**, 53-64.

Monje, M.L., Toda, H. & Palmer, T.D. (2003) Inflammatory blockade restores adult hippocampal neurogenesis. *Science*, **302**, 1760-1765.

Moreno, M.M., Linster, C., Escanilla, O., Sacquet, J., Didier, A. & Mandairon, N. (2009) Olfactory perceptual learning requires adult neurogenesis. *Proceedings of the National Academy of Sciences of the United States of America*, **106**, 17980-17985.

Morrison, S.J. & Spradling, A.C. (2008) Stem cells and niches: mechanisms that promote stem cell maintenance throughout life. *Cell*, **132**, 598-611.

Morshead, C.M., Craig, C.G. & van der Kooy, D. (1998) In vivo clonal analyses reveal the properties of endogenous neural stem cell proliferation in the adult mammalian forebrain. *Development*, **125**, 2251-2261.

Morshead, C.M., Garcia, A.D., Sofroniew, M.V. & van Der Kooy, D. (2003) The ablation of glial fibrillary acidic protein-positive cells from the adult central nervous system results in the loss of forebrain neural stem cells but not retinal stem cells. *The European journal of neuroscience*, **18**, 76-84.

Morshead, C.M., Reynolds, B.A., Craig, C.G., McBurney, M.W., Staines, W.A., Morassutti, D., Weiss, S. & van der Kooy, D. (1994) Neural stem cells in the adult mammalian forebrain: a relatively quiescent subpopulation of subependymal cells. *Neuron*, **13**, 1071-1082.

Mouret, A., Gheusi, G., Gabellec, M.M., de Chaumont, F., Olivo-Marin, J.C. & Lledo, P.M. (2008) Learning and survival of newly generated neurons: when time matters. *The Journal of neuroscience : the official journal of the Society for Neuroscience*, **28**, 11511-11516.

Mulder, C., Wahlund, L.O., Teerlink, T., Blomberg, M., Veerhuis, R., van Kamp, G.J., Scheltens, P. & Scheffer, P.G. (2003) Decreased lysophosphatidylcholine/phosphatidylcholine ratio in cerebrospinal fluid in Alzheimer's disease. *J Neural Transm*, **110**, 949-955.

Mustroph, M.L., Chen, S., Desai, S.C., Cay, E.B., DeYoung, E.K. & Rhodes, J.S. (2012) Aerobic exercise is the critical variable in an enriched environment that increases hippocampal neurogenesis and water maze learning in male C57BL/6J mice. *Neuroscience*, **219**, 62-71.

Nakashiba, T., Cushman, J.D., Pelkey, K.A., Renaudineau, S., Buhl, D.L., McHugh, T.J., Rodriguez Barrera, V., Chittajallu, R., Iwamoto, K.S., McBain, C.J., Fanselow, M.S. & Tonegawa, S. (2012) Young dentate granule cells mediate pattern separation, whereas old granule cells facilitate pattern completion. *Cell*, **149**, 188-201.

Nedergaard, M., Ransom, B. & Goldman, S.A. (2003) New roles for astrocytes: redefining the functional architecture of the brain. *Trends in neurosciences*, **26**, 523-530.

Nguyen-Ba-Charvet, K.T., Picard-Riera, N., Tessier-Lavigne, M., Baron-Van Evercooren, A., Sotelo, C. & Chedotal, A. (2004) Multiple roles for slits in the control of cell migration in

the rostral migratory stream. *The Journal of neuroscience : the official journal of the Society for Neuroscience*, **24**, 1497-1506.

Niibori, Y., Yu, T.S., Epp, J.R., Akers, K.G., Josselyn, S.A. & Frankland, P.W. (2012) Suppression of adult neurogenesis impairs population coding of similar contexts in hippocampal CA3 region. *Nature communications*, **3**, 1253.

Niidome, T., Taniuchi, N., Akaike, A., Kihara, T. & Sugimoto, H. (2008) Differential regulation of neurogenesis in two neurogenic regions of APPswe/PS1dE9 transgenic mice. *Neuroreport*, **19**, 1361-1364.

Nissant, A., Bardy, C., Katagiri, H., Murray, K. & Lledo, P.M. (2009) Adult neurogenesis promotes synaptic plasticity in the olfactory bulb. *Nature neuroscience*, **12**, 728-730.

Noctor, S.C., Martinez-Cerdeno, V., Ivic, L. & Kriegstein, A.R. (2004) Cortical neurons arise in symmetric and asymmetric division zones and migrate through specific phases. *Nature neuroscience*, **7**, 136-144.

Nomura, T., Goritz, C., Catchpole, T., Henkemeyer, M. & Frisen, J. (2010) EphB signaling controls lineage plasticity of adult neural stem cell niche cells. *Cell stem cell*, **7**, 730-743.

Nusslein-Volhard, C. & Wieschaus, E. (1980) Mutations affecting segment number and polarity in Drosophila. *Nature*, **287**, 795-801.

Nyfeler, Y., Kirch, R.D., Mantei, N., Leone, D.P., Radtke, F., Suter, U. & Taylor, V. (2005) Jagged1 signals in the postnatal subventricular zone are required for neural stem cell self-renewal. *The EMBO journal*, **24**, 3504-3515.

Obermair, F.J., Fiorelli, R., Schroeter, A., Beyeler, S., Blatti, C., Zoerner, B. & Thallmair, M. (2010) A novel classification of quiescent and transit amplifying adult neural stem cells by surface and metabolic markers permits a defined simultaneous isolation. *Stem cell research*, **5**, 131-143.

Oddo, S., Caccamo, A., Kitazawa, M., Tseng, B.P. & LaFerla, F.M. (2003a) Amyloid deposition precedes tangle formation in a triple transgenic model of Alzheimer's disease. *Neurobiology of aging*, **24**, 1063-1070.

Oddo, S., Caccamo, A., Shepherd, J.D., Murphy, M.P., Golde, T.E., Kayed, R., Metherate, R., Mattson, M.P., Akbari, Y. & LaFerla, F.M. (2003b) Triple-transgenic model of Alzheimer's disease with plaques and tangles: intracellular Abeta and synaptic dysfunction. *Neuron*, **39**, 409-421.

Ohsaki, Y., Cheng, J., Suzuki, M., Shinohara, Y., Fujita, A. & Fujimoto, T. (2009) Biogenesis of cytoplasmic lipid droplets: from the lipid ester globule in the membrane to the visible structure. *Biochimica et biophysica acta*, **1791**, 399-407.

Ortega, F., Gascon, S., Masserdotti, G., Deshpande, A., Simon, C., Fischer, J., Dimou, L., Chichung Lie, D., Schroeder, T. & Berninger, B. (2013) Oligodendrogliogenic and neurogenic adult subependymal zone neural stem cells constitute distinct lineages and exhibit differential responsiveness to Wnt signalling. *Nature cell biology*, **15**, 602-613.

Owada, Y. (2008) Fatty acid binding protein: localization and functional significance in the brain. *The Tohoku journal of experimental medicine*, **214**, 213-220.

Owada, Y., Yoshimoto, T. & Kondo, H. (1996) Spatio-temporally differential expression of genes for three members of fatty acid binding proteins in developing and mature rat brains. *Journal of chemical neuroanatomy*, **12**, 113-122.

Paik, J.H., Ding, Z., Narurkar, R., Ramkissoon, S., Muller, F., Kamoun, W.S., Chae, S.S., Zheng, H., Ying, H., Mahoney, J., Hiller, D., Jiang, S., Protopopov, A., Wong, W.H., Chin, L., Ligon, K.L. & DePinho, R.A. (2009) FoxOs cooperatively regulate diverse pathways governing neural stem cell homeostasis. *Cell stem cell*, **5**, 540-553.

Paliouras, G.N., Hamilton, L.K., Aumont, A., Joppe, S.E., Barnabe-Heider, F. & Fernandes, K.J. (2012) Mammalian target of rapamycin signaling is a key regulator of the transit-amplifying progenitor pool in the adult and aging forebrain. *The Journal of neuroscience : the official journal of the Society for Neuroscience*, **32**, 15012-15026.

Palma, V., Lim, D.A., Dahmane, N., Sanchez, P., Brionne, T.C., Herzberg, C.D., Gitton, Y., Carleton, A., Alvarez-Buylla, A. & Ruiz i Altaba, A. (2005) Sonic hedgehog controls stem cell behavior in the postnatal and adult brain. *Development*, **132**, 335-344.

Park, S.Y. & Ferreira, A. (2005) The generation of a 17 kDa neurotoxic fragment: an alternative mechanism by which tau mediates beta-amyloid-induced neurodegeneration. *The Journal of neuroscience : the official journal of the Society for Neuroscience*, **25**, 5365-5375.

Pasinetti, G.M. & Eberstein, J.A. (2008) Metabolic syndrome and the role of dietary lifestyles in Alzheimer's disease. *Journal of neurochemistry*, **106**, 1503-1514.

Pastrana, E., Cheng, L.C. & Doetsch, F. (2009) Simultaneous prospective purification of adult subventricular zone neural stem cells and their progeny. *Proceedings of the National Academy of Sciences of the United States of America*, **106**, 6387-6392.

Patil, S. & Chan, C. (2005) Palmitic and stearic fatty acids induce Alzheimer-like hyperphosphorylation of tau in primary rat cortical neurons. *Neuroscience letters*, **384**, 288-293.

Peretto, P., Dati, C., De Marchis, S., Kim, H.H., Ukhanova, M., Fasolo, A. & Margolis, F.L. (2004) Expression of the secreted factors noggin and bone morphogenetic proteins in the subependymal layer and olfactory bulb of the adult mouse brain. *Neuroscience*, **128**, 685-696.

Perry, E.K., Johnson, M., Ekonomou, A., Perry, R.H., Ballard, C. & Attems, J. (2012) Neurogenic abnormalities in Alzheimer's disease differ between stages of neurogenesis and are partly related to cholinergic pathology. *Neurobiology of disease*, **47**, 155-162.

Petreanu, L. & Alvarez-Buylla, A. (2002) Maturation and death of adult-born olfactory bulb granule neurons: role of olfaction. *The Journal of neuroscience : the official journal of the Society for Neuroscience*, **22**, 6106-6113.

Petrova, R., Garcia, A.D. & Joyner, A.L. (2013) Titration of GLI3 repressor activity by sonic hedgehog signaling is critical for maintaining multiple adult neural stem cell and astrocyte functions. *The Journal of neuroscience : the official journal of the Society for Neuroscience*, **33**, 17490-17505.

Phivilay, A., Julien, C., Tremblay, C., Berthiaume, L., Julien, P., Giguere, Y. & Calon, F. (2009) High dietary consumption of trans fatty acids decreases brain docosahexaenoic acid but does not alter amyloid-beta and tau pathologies in the 3xTg-AD model of Alzheimer's disease. *Neuroscience*, **159**, 296-307.

Piccin, D. & Morshead, C.M. (2011) Wnt signaling regulates symmetry of division of neural stem cells in the adult brain and in response to injury. *Stem Cells*, **29**, 528-538.

Piccin, D., Yu, F. & Morshead, C.M. (2013) Notch signaling imparts and preserves neural stem characteristics in the adult brain. *Stem cells and development*, **22**, 1541-1550.

Pierfelice, T., Alberi, L. & Gaiano, N. (2011) Notch in the vertebrate nervous system: an old dog with new tricks. *Neuron*, **69**, 840-855.

Platel, J.C., Dave, K.A., Gordon, V., Lacar, B., Rubio, M.E. & Bordey, A. (2010) NMDA receptors activated by subventricular zone astrocytic glutamate are critical for neuroblast survival prior to entering a synaptic network. *Neuron*, **65**, 859-872.

Podtelezhnikov, A.A., Tanis, K.Q., Nebozhyn, M., Ray, W.J., Stone, D.J. & Loboda, A.P. (2011) Molecular insights into the pathogenesis of Alzheimer's disease and its relationship to normal aging. *PloS one*, **6**, e29610.

Polo-Hernandez, E., De Castro, F., Garcia-Garcia, A.G., Tabernero, A. & Medina, J.M. (2010) Oleic acid synthesized in the periventricular zone promotes axonogenesis in the striatum during brain development. *Journal of neurochemistry*, **114**, 1756-1766.

Polo-Hernandez, E., Tello, V., Arroyo, A.A., Dominguez-Prieto, M., de Castro, F., Tabernero, A. & Medina, J.M. (2014) Oleic acid synthesized by stearoyl-CoA desaturase (SCD-1) in the lateral periventricular zone of the developing rat brain mediates neuronal growth, migration and the arrangement of prospective synapses. *Brain research*, **1570**, 13-25.

Polvikoski, T., Sulkava, R., Haltia, M., Kainulainen, K., Vuorio, A., Verkkoniemi, A., Niinisto, L., Halonen, P. & Kontula, K. (1995) Apolipoprotein E, dementia, and cortical deposition of beta-amyloid protein. *The New England journal of medicine*, **333**, 1242-1247.

Ponti, G., Obernier, K. & Alvarez-Buylla, A. (2013) Lineage progression from stem cells to new neurons in the adult brain ventricular-subventricular zone. *Cell Cycle*, **12**, 1649-1650.

Quinones-Hinojosa, A., Sanai, N., Soriano-Navarro, M., Gonzalez-Perez, O., Mirzadeh, Z., Gil-Perotin, S., Romero-Rodriguez, R., Berger, M.S., Garcia-Verdugo, J.M. & Alvarez-Buylla, A. (2006) Cellular composition and cytoarchitecture of the adult human subventricular zone: a niche of neural stem cells. *The Journal of comparative neurology*, **494**, 415-434.

Raber, J. (2008) AR, apoE, and cognitive function. *Hormones and behavior*, **53**, 706-715.

Radley, J.J. & Jacobs, B.L. (2002) 5-HT1A receptor antagonist administration decreases cell proliferation in the dentate gyrus. *Brain research*, **955**, 264-267.

Rapoport, M., Dawson, H.N., Binder, L.I., Vitek, M.P. & Ferreira, A. (2002) Tau is essential to beta -amyloid-induced neurotoxicity. *Proceedings of the National Academy of Sciences of the United States of America*, **99**, 6364-6369.

Rashid, M.A., Katakura, M., Kharebava, G., Kevala, K. & Kim, H.Y. (2013) N-Docosahexaenoylethanolamine is a potent neurogenic factor for neural stem cell differentiation. *Journal of neurochemistry*, **125**, 869-884.

Reiman, E.M., Chen, K., Liu, X., Bandy, D., Yu, M., Lee, W., Ayutyanont, N., Keppler, J., Reeder, S.A., Langbaum, J.B., Alexander, G.E., Klunk, W.E., Mathis, C.A., Price, J.C., Aizenstein, H.J., DeKosky, S.T. & Caselli, R.J. (2009) Fibrillar amyloid-beta burden in cognitively normal people at 3 levels of genetic risk for Alzheimer's disease. *Proceedings of the National Academy of Sciences of the United States of America*, **106**, 6820-6825.

Renault, V.M., Rafalski, V.A., Morgan, A.A., Salih, D.A., Brett, J.O., Webb, A.E., Villeda, S.A., Thekkat, P.U., Guillerey, C., Denko, N.C., Palmer, T.D., Butte, A.J. & Brunet, A. (2009) FoxO3 regulates neural stem cell homeostasis. *Cell stem cell*, **5**, 527-539.

Repetto, E., Yoon, I.S., Zheng, H. & Kang, D.E. (2007) Presenilin 1 regulates epidermal growth factor receptor turnover and signaling in the endosomal-lysosomal pathway. *The Journal of biological chemistry*, **282**, 31504-31516.

Reynolds, B.A., Tetzlaff, W. & Weiss, S. (1992) A multipotent EGF-responsive striatal embryonic progenitor cell produces neurons and astrocytes. *The Journal of neuroscience : the official journal of the Society for Neuroscience*, **12**, 4565-4574.

Reynolds, B.A. & Weiss, S. (1992) Generation of neurons and astrocytes from isolated cells of the adult mammalian central nervous system. *Science*, **255**, 1707-1710.

Reynolds, B.A. & Weiss, S. (1996) Clonal and population analyses demonstrate that an EGF-responsive mammalian embryonic CNS precursor is a stem cell. *Developmental biology*, **175**, 1-13.

Rhein, V. & Eckert, A. (2007) Effects of Alzheimer's amyloid-beta and tau protein on mitochondrial function -- role of glucose metabolism and insulin signalling. *Archives of physiology and biochemistry*, **113**, 131-141.

Ribak, C.E., Shapiro, L.A., Perez, Z.D. & Spigelman, I. (2009) Microglia-associated granule cell death in the normal adult dentate gyrus. *Brain Struct Funct*, **214**, 25-35.

Ricard, J., Salinas, J., Garcia, L. & Liebl, D.J. (2006) EphrinB3 regulates cell proliferation and survival in adult neurogenesis. *Molecular and cellular neurosciences*, **31**, 713-722.

Richards, L.J., Kilpatrick, T.J. & Bartlett, P.F. (1992) De novo generation of neuronal cells from the adult mouse brain. *Proceedings of the National Academy of Sciences of the United States of America*, **89**, 8591-8595.

Rietze, R.L., Valcanis, H., Brooker, G.F., Thomas, T., Voss, A.K. & Bartlett, P.F. (2001) Purification of a pluripotent neural stem cell from the adult mouse brain. *Nature*, **412**, 736-739.

Ro, S.H., Liu, D., Yeo, H. & Paik, J.H. (2013) FoxOs in neural stem cell fate decision. *Archives of biochemistry and biophysics*, **534**, 55-63.

Rochefort, C., Gheusi, G., Vincent, J.D. & Lledo, P.M. (2002) Enriched odor exposure increases the number of newborn neurons in the adult olfactory bulb and improves odor memory. *The Journal of neuroscience : the official journal of the Society for Neuroscience*, **22**, 2679-2689.

Rockenfeller, P. & Madeo, F. (2010) Ageing and eating. *Biochim Biophys Acta*, **1803**, 499-506.

Rodriguez, J.J., Jones, V.C., Tabuchi, M., Allan, S.M., Knight, E.M., LaFerla, F.M., Oddo, S. & Verkhratsky, A. (2008) Impaired adult neurogenesis in the dentate gyrus of a triple transgenic mouse model of Alzheimer's disease. *PloS one*, **3**, e2935.

Rodriguez, J.J., Jones, V.C. & Verkhratsky, A. (2009) Impaired cell proliferation in the subventricular zone in an Alzheimer's disease model. *Neuroreport*, **20**, 907-912.

Rohatgi, R., Milenkovic, L. & Scott, M.P. (2007) Patched1 regulates hedgehog signaling at the primary cilium. *Science*, **317**, 372-376.

Rosen, W.G., Mohs, R.C. & Davis, K.L. (1984) A new rating scale for Alzheimer's disease. *Am J Psychiatry*, **141**, 1356-1364.

Ross, B.M., Moszczynska, A., Erlich, J. & Kish, S.J. (1998) Phospholipid-metabolizing enzymes in Alzheimer's disease: increased lysophospholipid acyltransferase activity and decreased phospholipase A2 activity. *Journal of neurochemistry*, **70**, 786-793.

Roy, N.S., Wang, S., Jiang, L., Kang, J., Benraiss, A., Harrison-Restelli, C., Fraser, R.A., Couldwell, W.T., Kawaguchi, A., Okano, H., Nedergaard, M. & Goldman, S.A. (2000) In vitro neurogenesis by progenitor cells isolated from the adult human hippocampus. *Nature medicine*, **6**, 271-277.

Ruggles, K.V., Turkish, A. & Sturley, S.L. (2013) Making, baking, and breaking: the synthesis, storage, and hydrolysis of neutral lipids. *Annual review of nutrition*, **33**, 413-451.

Sachewsky, N., Leeder, R., Xu, W., Rose, K.L., Yu, F., van der Kooy, D. & Morshead, C.M. (2014) Primitive neural stem cells in the adult mammalian brain give rise to GFAP-expressing neural stem cells. *Stem cell reports*, **2**, 810-824.

Sahay, A., Scobie, K.N., Hill, A.S., O'Carroll, C.M., Kheirbek, M.A., Burghardt, N.S., Fenton, A.A., Dranovsky, A. & Hen, R. (2011a) Increasing adult hippocampal neurogenesis is sufficient to improve pattern separation. *Nature*, **472**, 466-470.

Sahay, A., Wilson, D.A. & Hen, R. (2011b) Pattern separation: a common function for new neurons in hippocampus and olfactory bulb. *Neuron*, **70**, 582-588.

Sakamoto, M., Ieki, N., Miyoshi, G., Mochimaru, D., Miyachi, H., Imura, T., Yamaguchi, M., Fishell, G., Mori, K., Kageyama, R. & Imayoshi, I. (2014) Continuous postnatal neurogenesis contributes to formation of the olfactory bulb neural circuits and flexible olfactory associative learning. *The Journal of neuroscience : the official journal of the Society for Neuroscience*, **34**, 5788-5799.

Sakamoto, M., Imayoshi, I., Ohtsuka, T., Yamaguchi, M., Mori, K. & Kageyama, R. (2011) Continuous neurogenesis in the adult forebrain is required for innate olfactory responses. *Proceedings of the National Academy of Sciences of the United States of America*, **108**, 8479-8484.

Sakayori, N., Maekawa, M., Numayama-Tsuruta, K., Katura, T., Moriya, T. & Osumi, N. (2011) Distinctive effects of arachidonic acid and docosahexaenoic acid on neural stem /progenitor cells. *Genes to cells : devoted to molecular & cellular mechanisms*, **16**, 778-790.

Saltiel, A.R. & Kahn, C.R. (2001) Insulin signalling and the regulation of glucose and lipid metabolism. *Nature*, **414**, 799-806.

Samuel, W., Terry, R.D., DeTeresa, R., Butters, N. & Masliah, E. (1994) Clinical correlates of cortical and nucleus basalis pathology in Alzheimer dementia. *Arch Neurol*, **51**, 772-778.

Sanai, N., Tramontin, A.D., Quinones-Hinojosa, A., Barbaro, N.M., Gupta, N., Kunwar, S., Lawton, M.T., McDermott, M.W., Parsa, A.T., Manuel-Garcia Verdugo, J., Berger, M.S. & Alvarez-Buylla, A. (2004) Unique astrocyte ribbon in adult human brain contains neural stem cells but lacks chain migration. *Nature*, **427**, 740-744.

Santarelli, L., Saxe, M., Gross, C., Surget, A., Battaglia, F., Dulawa, S., Weisstaub, N., Lee, J., Duman, R., Arancio, O., Belzung, C. & Hen, R. (2003) Requirement of hippocampal neurogenesis for the behavioral effects of antidepressants. *Science*, **301**, 805-809.

Sanz-Blasco, S., Valero, R.A., Rodriguez-Crespo, I., Villalobos, C. & Nunez, L. (2008) Mitochondrial Ca2+ overload underlies Abeta oligomers neurotoxicity providing an unexpected mechanism of neuroprotection by NSAIDs. *PloS one*, **3**, e2718.

Saunders, N.R., Daneman, R., Dziegielewska, K.M. & Liddelow, S.A. (2013) Transporters of the blood-brain and blood-CSF interfaces in development and in the adult. *Molecular aspects of medicine*, **34**, 742-752.

Sawamoto, K., Wichterle, H., Gonzalez-Perez, O., Cholfin, J.A., Yamada, M., Spassky, N., Murcia, N.S., Garcia-Verdugo, J.M., Marin, O., Rubenstein, J.L., Tessier-Lavigne, M., Okano, H. & Alvarez-Buylla, A. (2006) New neurons follow the flow of cerebrospinal fluid in the adult brain. *Science*, **311**, 629-632.

Schaefer, E.J., Bongard, V., Beiser, A.S., Lamon-Fava, S., Robins, S.J., Au, R., Tucker, K.L., Kyle, D.J., Wilson, P.W. & Wolf, P.A. (2006) Plasma phosphatidylcholine docosahexaenoic acid content and risk of dementia and Alzheimer disease: the Framingham Heart Study. *Archives of neurology*, **63**, 1545-1550.

Schaeffer, E.L., Forlenza, O.V. & Gattaz, W.F. (2009) Phospholipase A2 activation as a therapeutic approach for cognitive enhancement in early-stage Alzheimer disease. *Psychopharmacology*, **202**, 37-51.

Schmidt-Strassburger, U., Schips, T.G., Maier, H.J., Kloiber, K., Mannella, F., Braunstein, K.E., Holzmann, K., Ushmorov, A., Liebau, S., Boeckers, T.M. & Wirth, T. (2012) Expression of constitutively active FoxO3 in murine forebrain leads to a loss of neural progenitors. *FASEB journal : official publication of the Federation of American Societies for Experimental Biology*, **26**, 4990-5001.

Selkoe, D.J. (1991) The molecular pathology of Alzheimer's disease. *Neuron*, **6**, 487-498.

Selkoe, D.J. & Wolfe, M.S. (2000) In search of gamma-secretase: presenilin at the cutting edge. *Proceedings of the National Academy of Sciences of the United States of America*, **97**, 5690-5692.

Seri, B., Garcia-Verdugo, J.M., Collado-Morente, L., McEwen, B.S. & Alvarez-Buylla, A. (2004) Cell types, lineage, and architecture of the germinal zone in the adult dentate gyrus. *The Journal of comparative neurology*, **478**, 359-378.

Seri, B., Garcia-Verdugo, J.M., McEwen, B.S. & Alvarez-Buylla, A. (2001) Astrocytes give rise to new neurons in the adult mammalian hippocampus. *The Journal of neuroscience : the official journal of the Society for Neuroscience*, **21**, 7153-7160.

Sharon, R., Bar-Joseph, I., Frosch, M.P., Walsh, D.M., Hamilton, J.A. & Selkoe, D.J. (2003) The formation of highly soluble oligomers of alpha-synuclein is regulated by fatty acids and enhanced in Parkinson's disease. *Neuron*, **37**, 583-595.

Shen, Q., Goderie, S.K., Jin, L., Karanth, N., Sun, Y., Abramova, N., Vincent, P., Pumiglia, K. & Temple, S. (2004) Endothelial cells stimulate self-renewal and expand neurogenesis of neural stem cells. *Science*, **304**, 1338-1340.

Shen, Q., Wang, Y., Kokovay, E., Lin, G., Chuang, S.M., Goderie, S.K., Roysam, B. & Temple, S. (2008) Adult SVZ stem cells lie in a vascular niche: a quantitative analysis of niche cell-cell interactions. *Cell stem cell*, **3**, 289-300.

Shibata, M., Yamada, S., Kumar, S.R., Calero, M., Bading, J., Frangione, B., Holtzman, D.M., Miller, C.A., Strickland, D.K., Ghiso, J. & Zlokovic, B.V. (2000) Clearance of Alzheimer's amyloid-ss(1-40) peptide from brain by LDL receptor-related protein-1 at the blood-brain barrier. *The Journal of clinical investigation*, **106**, 1489-1499.

Shors, T.J., Miesegaes, G., Beylin, A., Zhao, M., Rydel, T. & Gould, E. (2001) Neurogenesis in the adult is involved in the formation of trace memories. *Nature*, **410**, 372-376.

Siegenthaler, J.A., Sohet, F. & Daneman, R. (2013) 'Sealing off the CNS': cellular and molecular regulation of blood-brain barriergenesis. *Current opinion in neurobiology*, **23**, 1057-1064.

Sierra, A., Encinas, J.M., Deudero, J.J., Chancey, J.H., Enikolopov, G., Overstreet-Wadiche, L.S., Tsirka, S.E. & Maletic-Savatic, M. (2010) Microglia shape adult hippocampal neurogenesis through apoptosis-coupled phagocytosis. *Cell stem cell*, **7**, 483-495.

Singla, V. & Reiter, J.F. (2006) The primary cilium as the cell's antenna: signaling at a sensory organelle. *Science*, **313**, 629-633.

Smith, E.E. & Greenberg, S.M. (2009) Beta-amyloid, blood vessels, and brain function. *Stroke; a journal of cerebral circulation*, **40**, 2601-2606.

Smyth, G.K., Michaud, J. & Scott, H.S. (2005) Use of within-array replicate spots for assessing differential expression in microarray experiments. *Bioinformatics*, **21**, 2067-2075.

Snyder, J.S., Kee, N. & Wojtowicz, J.M. (2001) Effects of adult neurogenesis on synaptic plasticity in the rat dentate gyrus. *Journal of neurophysiology*, **85**, 2423-2431.

Song, H., Stevens, C.F. & Gage, F.H. (2002a) Astroglia induce neurogenesis from adult neural stem cells. *Nature*, **417**, 39-44.

Song, H.J., Stevens, C.F. & Gage, F.H. (2002b) Neural stem cells from adult hippocampus develop essential properties of functional CNS neurons. *Nature neuroscience*, **5**, 438-445.

Song, J., Zhong, C., Bonaguidi, M.A., Sun, G.J., Hsu, D., Gu, Y., Meletis, K., Huang, Z.J., Ge, S., Enikolopov, G., Deisseroth, K., Luscher, B., Christian, K.M., Ming, G.L. & Song, H. (2012) Neuronal circuitry mechanism regulating adult quiescent neural stem-cell fate decision. *Nature*, **489**, 150-154.

Sotthibundhu, A., Li, Q.X., Thangnipon, W. & Coulson, E.J. (2009) Abeta(1-42) stimulates adult SVZ neurogenesis through the p75 neurotrophin receptor. *Neurobiology of aging*, **30**, 1975-1985.

Spalding, K.L., Bergmann, O., Alkass, K., Bernard, S., Salehpour, M., Huttner, H.B., Bostrom, E., Westerlund, I., Vial, C., Buchholz, B.A., Possnert, G., Mash, D.C., Druid, H. & Frisen, J. (2013) Dynamics of hippocampal neurogenesis in adult humans. *Cell*, **153**, 1219-1227.

Spassky, N., Merkle, F.T., Flames, N., Tramontin, A.D., Garcia-Verdugo, J.M. & Alvarez-Buylla, A. (2005) Adult ependymal cells are postmitotic and are derived from radial glial cells during embryogenesis. *The Journal of neuroscience : the official journal of the Society for Neuroscience*, **25**, 10-18.

Spires-Jones, T.L. & Hyman, B.T. (2014) The intersection of amyloid beta and tau at synapses in Alzheimer's disease. *Neuron*, **82**, 756-771.

Steinhauer, J. & Treisman, J.E. (2009) Lipid-modified morphogens: functions of fats. *Current opinion in genetics & development*, **19**, 308-314.

Storch, J. & McDermott, L. (2009) Structural and functional analysis of fatty acid-binding proteins. *Journal of lipid research*, **50 Suppl**, S126-131.

Strittmatter, W.J. & Roses, A.D. (1996) Apolipoprotein E and Alzheimer's disease. *Annual review of neuroscience*, **19**, 53-77.

Struhl, G. & Greenwald, I. (1999) Presenilin is required for activity and nuclear access of Notch in Drosophila. *Nature*, **398**, 522-525.

Stump, G., Durrer, A., Klein, A.L., Lutolf, S., Suter, U. & Taylor, V. (2002) Notch1 and its ligands Delta-like and Jagged are expressed and active in distinct cell populations in the postnatal mouse brain. *Mechanisms of development*, **114**, 153-159.

Suh, H., Deng, W. & Gage, F.H. (2009) Signaling in adult neurogenesis. *Annual review of cell and developmental biology*, **25**, 253-275.

Suhara, T., Magrane, J., Rosen, K., Christensen, R., Kim, H.S., Zheng, B., McPhie, D.L., Walsh, K. & Querfurth, H. (2003) Abeta42 generation is toxic to endothelial cells and inhibits eNOS function through an Akt/GSK-3beta signaling-dependent mechanism. *Neurobiology of aging*, **24**, 437-451.

Sultan, S., Mandairon, N., Kermen, F., Garcia, S., Sacquet, J. & Didier, A. (2010) Learning-dependent neurogenesis in the olfactory bulb determines long-term olfactory memory. *FASEB journal : official publication of the Federation of American Societies for Experimental Biology*, **24**, 2355-2363.

Sultan, S., Rey, N., Sacquet, J., Mandairon, N. & Didier, A. (2011) Newborn neurons in the olfactory bulb selected for long-term survival through olfactory learning are prematurely suppressed when the olfactory memory is erased. *The Journal of neuroscience : the official journal of the Society for Neuroscience*, **31**, 14893-14898.

Suter, O.C., Sunthorn, T., Kraftsik, R., Straubel, J., Darekar, P., Khalili, K. & Miklossy, J. (2002) Cerebral hypoperfusion generates cortical watershed microinfarcts in Alzheimer disease. *Stroke; a journal of cerebral circulation*, **33**, 1986-1992.

Szodorai, A., Kuan, Y.H., Hunzelmann, S., Engel, U., Sakane, A., Sasaki, T., Takai, Y., Kirsch, J., Muller, U., Beyreuther, K., Brady, S., Morfini, G. & Kins, S. (2009) APP anterograde transport requires Rab3A GTPase activity for assembly of the transport vesicle. *The Journal of neuroscience : the official journal of the Society for Neuroscience*, **29**, 14534-14544.

Takada, R., Satomi, Y., Kurata, T., Ueno, N., Norioka, S., Kondoh, H., Takao, T. & Takada, S. (2006) Monounsaturated fatty acid modification of Wnt protein: its role in Wnt secretion. *Developmental cell*, **11**, 791-801.

Tanzi, R.E. (2012) The genetics of Alzheimer disease. *Cold Spring Harbor perspectives in medicine*, **2**.

Tanzi, R.E., Kovacs, D.M., Kim, T.W., Moir, R.D., Guenette, S.Y. & Wasco, W. (1996) The gene defects responsible for familial Alzheimer's disease. *Neurobiology of disease*, **3**, 159-168.

Tarkowski, E., Blennow, K., Wallin, A. & Tarkowski, A. (1999) Intracerebral production of tumor necrosis factor-alpha, a local neuroprotective agent, in Alzheimer disease and vascular dementia. *Journal of clinical immunology*, **19**, 223-230.

Tashiro, A., Zhao, C. & Gage, F.H. (2006) Retrovirus-mediated single-cell gene knockout technique in adult newborn neurons in vivo. *Nature protocols*, **1**, 3049-3055.

Tavazoie, M., Van der Veken, L., Silva-Vargas, V., Louissaint, M., Colonna, L., Zaidi, B., Garcia-Verdugo, J.M. & Doetsch, F. (2008) A specialized vascular niche for adult neural stem cells. *Cell stem cell*, **3**, 279-288.

Tayebati, S.K. & Amenta, F. (2013) Choline-containing phospholipids: relevance to brain functional pathways. *Clinical chemistry and laboratory medicine : CCLM / FESCC*, **51**, 513-521.

Teunissen, C.E., de Vente, J., Steinbusch, H.W. & De Bruijn, C. (2002) Biochemical markers related to Alzheimer's dementia in serum and cerebrospinal fluid. *Neurobiology of aging*, **23**, 485-508.

Teunissen, C.E., Veerhuis, R., De Vente, J., Verhey, F.R., Vreeling, F., van Boxtel, M.P., Glatz, J.F. & Pelsers, M.A. (2011) Brain-specific fatty acid-binding protein is elevated in serum of patients with dementia-related diseases. *European journal of neurology : the official journal of the European Federation of Neurological Societies*, **18**, 865-871.

Thal, D.R., Capetillo-Zarate, E., Larionov, S., Staufenbiel, M., Zurbruegg, S. & Beckmann, N. (2009) Capillary cerebral amyloid angiopathy is associated with vessel occlusion and cerebral blood flow disturbances. *Neurobiology of aging*, **30**, 1936-1948.

Thinakaran, G., Teplow, D.B., Siman, R., Greenberg, B. & Sisodia, S.S. (1996) Metabolism of the "Swedish" amyloid precursor protein variant in neuro2a (N2a) cells. Evidence that cleavage at the "beta-secretase" site occurs in the golgi apparatus. *The Journal of biological chemistry*, **271**, 9390-9397.

Thomas, A., Charbonneau, J.L., Fournaise, E. & Chaurand, P. (2012) Sublimation of new matrix candidates for high spatial resolution imaging mass spectrometry of lipids: enhanced information in both positive and negative polarities after 1,5-diaminonapthalene deposition. *Analytical chemistry*, **84**, 2048-2054.

Tosto, G. & Reitz, C. (2013) Genome-wide association studies in Alzheimer's disease: a review. *Current neurology and neuroscience reports*, **13**, 381.

Tozuka, Y., Fukuda, S., Namba, T., Seki, T. & Hisatsune, T. (2005) GABAergic excitation promotes neuronal differentiation in adult hippocampal progenitor cells. *Neuron*, **47**, 803-815.

Traiffort, E., Charytoniuk, D.A., Faure, H. & Ruat, M. (1998) Regional distribution of Sonic Hedgehog, patched, and smoothened mRNA in the adult rat brain. *Journal of neurochemistry*, **70**, 1327-1330.

Tremblay, C., Pilote, M., Phivilay, A., Emond, V., Bennett, D.A. & Calon, F. (2007) Biochemical characterization of Abeta and tau pathologies in mild cognitive impairment and Alzheimer's disease. *Journal of Alzheimer's disease : JAD*, **12**, 377-390.

Tropepe, V., Craig, C.G., Morshead, C.M. & van der Kooy, D. (1997) Transforming growth factor-alpha null and senescent mice show decreased neural progenitor cell proliferation in the forebrain subependyma. *The Journal of neuroscience : the official journal of the Society for Neuroscience*, **17**, 7850-7859.

Uchida, N., Buck, D.W., He, D., Reitsma, M.J., Masek, M., Phan, T.V., Tsukamoto, A.S., Gage, F.H. & Weissman, I.L. (2000) Direct isolation of human central nervous system stem cells. *Proceedings of the National Academy of Sciences of the United States of America*, **97**, 14720-14725.

Ullian, E.M., Christopherson, K.S. & Barres, B.A. (2004) Role for glia in synaptogenesis. *Glia*, **47**, 209-216.

Urist, M.R. (1965) Bone: formation by autoinduction. *Science*, **150**, 893-899.

Uryu, S., Tokuhiro, S. & Oda, T. (2003) beta-Amyloid-specific upregulation of stearoyl coenzyme A desaturase-1 in macrophages. *Biochemical and biophysical research communications*, **303**, 302-305.

Van Nostrand, W.E., Melchor, J.P. & Ruffini, L. (1998) Pathologic amyloid beta-protein cell surface fibril assembly on cultured human cerebrovascular smooth muscle cells. *Journal of neurochemistry*, **70**, 216-223.

Van Nostrand, W.E., Wagner, S.L., Shankle, W.R., Farrow, J.S., Dick, M., Rozemuller, J.M., Kuiper, M.A., Wolters, E.C., Zimmerman, J., Cotman, C.W. & et al. (1992) Decreased levels of soluble amyloid beta-protein precursor in cerebrospinal fluid of live Alzheimer disease patients. *Proceedings of the National Academy of Sciences of the United States of America*, **89**, 2551-2555.

van Praag, H., Kempermann, G. & Gage, F.H. (1999) Running increases cell proliferation and neurogenesis in the adult mouse dentate gyrus. *Nature neuroscience*, **2**, 266-270.

van Praag, H., Schinder, A.F., Christie, B.R., Toni, N., Palmer, T.D. & Gage, F.H. (2002) Functional neurogenesis in the adult hippocampus. *Nature*, **415**, 1030-1034.

Van Zant, G. & Liang, Y. (2003) The role of stem cells in aging. *Exp Hematol*, **31**, 659-672.

Vassar, R. (2004) BACE1: the beta-secretase enzyme in Alzheimer's disease. *Journal of molecular neuroscience : MN*, **23**, 105-114.

Veena, J., Rao, B.S. & Srikumar, B.N. (2011) Regulation of adult neurogenesis in the hippocampus by stress, acetylcholine and dopamine. *Journal of natural science, biology, and medicine*, **2**, 26-37.

Vescovi, A.L., Reynolds, B.A., Fraser, D.D. & Weiss, S. (1993) bFGF regulates the proliferative fate of unipotent (neuronal) and bipotent (neuronal/astroglial) EGF-generated CNS progenitor cells. *Neuron*, **11**, 951-966.

Veyrac, A., Sacquet, J., Nguyen, V., Marien, M., Jourdan, F. & Didier, A. (2009) Novelty determines the effects of olfactory enrichment on memory and neurogenesis through noradrenergic mechanisms. *Neuropsychopharmacology : official publication of the American College of Neuropsychopharmacology*, **34**, 786-795.

Villeda, S.A., Luo, J., Mosher, K.I., Zou, B., Britschgi, M., Bieri, G., Stan, T.M., Fainberg, N., Ding, Z., Eggel, A., Lucin, K.M., Czirr, E., Park, J.S., Couillard-Despres, S., Aigner, L., Li, G., Peskind, E.R., Kaye, J.A., Quinn, J.F., Galasko, D.R., Xie, X.S., Rando, T.A. & Wyss-Coray, T. (2011) The ageing systemic milieu negatively regulates neurogenesis and cognitive function. *Nature*, **477**, 90-94.

Walker, M.R., Patel, K.K. & Stappenbeck, T.S. (2009) The stem cell niche. *The Journal of pathology*, **217**, 169-180.

Wallin, A.K., Blennow, K., Andreasen, N. & Minthon, L. (2006) CSF biomarkers for Alzheimer's Disease: levels of beta-amyloid, tau, phosphorylated tau relate to clinical symptoms and survival. *Dementia and geriatric cognitive disorders*, **21**, 131-138.

Walter, A., Korth, U., Hilgert, M., Hartmann, J., Weichel, O., Hilgert, M., Fassbender, K., Schmitt, A. & Klein, J. (2004) Glycerophosphocholine is elevated in cerebrospinal fluid of Alzheimer patients. *Neurobiology of aging*, **25**, 1299-1303.

Wang, R., Dineley, K.T., Sweatt, J.D. & Zheng, H. (2004) Presenilin 1 familial Alzheimer's disease mutation leads to defective associative learning and impaired adult neurogenesis. *Neuroscience*, **126**, 305-312.

Wang, Z., Liu, D., Zhang, Q., Wang, J., Zhan, J., Xian, X., Du, Z., Wang, X. & Hao, A. (2014) Palmitic acid affects proliferation and differentiation of neural stem cells in vitro. *Journal of neuroscience research*, **92**, 574-586.

Weickert, C.S., Webster, M.J., Colvin, S.M., Herman, M.M., Hyde, T.M., Weinberger, D.R. & Kleinman, J.E. (2000) Localization of epidermal growth factor receptors and putative neuroblasts in human subependymal zone. *The Journal of comparative neurology*, **423**, 359-372.

Weiss, S., Dunne, C., Hewson, J., Wohl, C., Wheatley, M., Peterson, A.C. & Reynolds, B.A. (1996) Multipotent CNS stem cells are present in the adult mammalian spinal cord and ventricular neuroaxis. *The Journal of neuroscience : the official journal of the Society for Neuroscience*, **16**, 7599-7609.

Weller, R.O., Subash, M., Preston, S.D., Mazanti, I. & Carare, R.O. (2008) Perivascular drainage of amyloid-beta peptides from the brain and its failure in cerebral amyloid angiopathy and Alzheimer's disease. *Brain Pathol*, **18**, 253-266.

Willert, K., Brown, J.D., Danenberg, E., Duncan, A.W., Weissman, I.L., Reya, T., Yates, J.R., 3rd & Nusse, R. (2003) Wnt proteins are lipid-modified and can act as stem cell growth factors. *Nature*, **423**, 448-452.

Winner, B., Cooper-Kuhn, C.M., Aigner, R., Winkler, J. & Kuhn, H.G. (2002) Long-term survival and cell death of newly generated neurons in the adult rat olfactory bulb. *The European journal of neuroscience*, **16**, 1681-1689.

Winner, B., Kohl, Z. & Gage, F.H. (2011) Neurodegenerative disease and adult neurogenesis. *The European journal of neuroscience*, **33**, 1139-1151.

Wirenfeldt, M., Dalmau, I. & Finsen, B. (2003) Estimation of absolute microglial cell numbers in mouse fascia dentata using unbiased and efficient stereological cell counting principles. *Glia*, **44**, 129-139.

Wyss-Coray, T. & Mucke, L. (2002) Inflammation in neurodegenerative disease--a double-edged sword. *Neuron*, **35**, 419-432.

Xie, L., Kang, H., Xu, Q., Chen, M.J., Liao, Y., Thiyagarajan, M., O'Donnell, J., Christensen, D.J., Nicholson, C., Iliff, J.J., Takano, T., Deane, R. & Nedergaard, M. (2013) Sleep drives metabolite clearance from the adult brain. *Science*, **342**, 373-377.

Xu, J., Chen, S., Ku, G., Ahmed, S.H., Xu, J., Chen, H. & Hsu, C.Y. (2001) Amyloid beta peptide-induced cerebral endothelial cell death involves mitochondrial dysfunction and caspase activation. *Journal of cerebral blood flow and metabolism : official journal of the International Society of Cerebral Blood Flow and Metabolism*, **21**, 702-710.

Xu, Q., Bernardo, A., Walker, D., Kanegawa, T., Mahley, R.W. & Huang, Y. (2006) Profile and regulation of apolipoprotein E (ApoE) expression in the CNS in mice with targeting of green fluorescent protein gene to the ApoE locus. *The Journal of neuroscience : the official journal of the Society for Neuroscience*, **26**, 4985-4994.

Yamada, K., Kono, K., Umegaki, H., Yamada, K., Iguchi, A., Fukatsu, T., Nakashima, N., Nishiwaki, H., Shimada, Y., Sugita, Y. & et al. (1995) Decreased interleukin-6 level in the cerebrospinal fluid of patients with Alzheimer-type dementia. *Neuroscience letters*, **186**, 219-221.

Yamaguchi, M. & Mori, K. (2005) Critical period for sensory experience-dependent survival of newly generated granule cells in the adult mouse olfactory bulb. *Proceedings of the National Academy of Sciences of the United States of America*, **102**, 9697-9702.

Yang, C.P., Gilley, J.A., Zhang, G. & Kernie, S.G. (2011) ApoE is required for maintenance of the dentate gyrus neural progenitor pool. *Development*, **138**, 4351-4362.

Yeo, H., Lyssiotis, C.A., Zhang, Y., Ying, H., Asara, J.M., Cantley, L.C. & Paik, J.H. (2013) FoxO3 coordinates metabolic pathways to maintain redox balance in neural stem cells. *The EMBO journal*, **32**, 2589-2602.

Yuan, Q., Zhao, S., Wang, F., Zhang, H., Chen, Z.J., Wang, J., Wang, Z., Du, Z., Ling, E.A., Liu, Q. & Hao, A. (2013) Palmitic acid increases apoptosis of neural stem cells via activating c-Jun N-terminal kinase. *Stem cell research*, **10**, 257-266.

Zappaterra, M.W. & Lehtinen, M.K. (2012) The cerebrospinal fluid: regulator of neurogenesis, behavior, and beyond. *Cellular and molecular life sciences : CMLS*, **69**, 2863-2878.

Zechner, R., Zimmermann, R., Eichmann, T.O., Kohlwein, S.D., Haemmerle, G., Lass, A. & Madeo, F. (2012) FAT SIGNALS--lipases and lipolysis in lipid metabolism and signaling. *Cell metabolism*, **15**, 279-291.

Zhang, R., Zhang, Z., Wang, L., Wang, Y., Gousev, A., Zhang, L., Ho, K.L., Morshead, C. & Chopp, M. (2004a) Activated neural stem cells contribute to stroke-induced neurogenesis and neuroblast migration toward the infarct boundary in adult rats. *Journal of cerebral blood flow and metabolism : official journal of the International Society of Cerebral Blood Flow and Metabolism*, **24**, 441-448.

Zhang, R., Zhang, Z., Zhang, C., Zhang, L., Robin, A., Wang, Y., Lu, M. & Chopp, M. (2004b) Stroke transiently increases subventricular zone cell division from asymmetric to symmetric and increases neuronal differentiation in the adult rat. *The Journal of neuroscience : the official journal of the Society for Neuroscience*, **24**, 5810-5815.

Zhang, R.L., Chopp, M., Roberts, C., Liu, X., Wei, M., Nejad-Davarani, S.P., Wang, X. & Zhang, Z.G. (2014) Stroke increases neural stem cells and angiogenesis in the neurogenic niche of the adult mouse. *PloS one*, **9**, e113972.

Zhao, C., Teng, E.M., Summers, R.G., Jr., Ming, G.L. & Gage, F.H. (2006) Distinct morphological stages of dentate granule neuron maturation in the adult mouse hippocampus. *The Journal of neuroscience : the official journal of the Society for Neuroscience*, **26**, 3-11.

Zheng, W., Nowakowski, R.S. & Vaccarino, F.M. (2004) Fibroblast growth factor 2 is required for maintaining the neural stem cell pool in the mouse brain subventricular zone. *Developmental neuroscience*, **26**, 181-196.

Zhou, Z.D., Chan, C.H., Ma, Q.H., Xu, X.H., Xiao, Z.C. & Tan, E.K. (2011) The roles of amyloid precursor protein (APP) in neurogenesis: Implications to pathogenesis and therapy of Alzheimer disease. *Cell adhesion & migration*, **5**, 280-292.

Ziabreva, I., Perry, E., Perry, R., Minger, S.L., Ekonomou, A., Przyborski, S. & Ballard, C. (2006) Altered neurogenesis in Alzheimer's disease. *Journal of psychosomatic research*, **61**, 311-316.

Zlokovic, B.V. (2008) The blood-brain barrier in health and chronic neurodegenerative disorders. *Neuron*, **57**, 178-201.

APPENDIX A

CONTRIBUTION TO THE ARTICLES

For the first article "Widespread deficits in neurogenesis precede plaque and tangle formation in the 3xTg mouse model of Alzheimer's disease" (Chapter 2), I played a key role in the acquisition, analysis and interpretation of the data. I performed the tissue preparation, immunohistochemistry, quantifications and western blotting. We collaborated with Carl Julien and the lab of Dr. Frédéric Calon to obtain 3xTg-AD mice at 11- and 18-months of age. The study was principally conceived by my supervisor and we wrote the article together.

For the second article "Elevated oleic acid levels within the forebrain niche suppress neural stem cell activation in Alzheimer's disease" (Chapter 3), I developed the concepts, carried out the experiments, analysed data and co-wrote the paper. We provided the sections for the collaboration with Martin Dufresne and the lab of Pierre Chaurand who developed and carried out IMS experiments and analysed data. Sandra Joppé helped with neurogenesis experiments and flow cytometry. Sarah Petryszyn and the lab of Martin Parent provided us with human Alzheimer's disease brains and age-matched controls. Sarah and I carried out the Oil red O staining on human tissues. I collected the samples and extracted the lipids for the LC-MS. Alexandra Furtos and I optimized the LC-MS protocol and Alexandra analyzed the data. I collected the samples and extracted the RNA for the microarray that was run at the genomics platform at IRIC and took part in the data analysis. Frederic Calon provided the 3xTg-AD mice. My supervisor developed the concept, analyzed data, performed the surgeries and co-wrote the paper.

APPENDIX B

REVIEW ARTICLE: "AGING AND NEUROGENESIS IN THE ADULT FOREBRAIN: WHAT WE HAVE LEARNED AND WHERE WE SHOULD GO FROM HERE"

EJN fens European Journal of Neuroscience

European Journal of Neuroscience, Vol. 37, pp. 1978–1986, 2013 doi:10.1111/ejn.12207

Aging and neurogenesis in the adult forebrain: what we have learned and where we should go from here

Laura K. Hamilton, Sandra E. Joppé, Loïc M. Cochard and Karl J. L. Fernandes
Department of Pathology and Cell Biology, Groupe de recherche sur le système nerveux central (GRSNC), Centre of Excellence in Neuroscience of the Université de Montréal (CENUM), Université de Montréal, Montréal, Canada

Keywords: Alzheimer's disease, neural stem cells, neurospheres, quiescence, rodent, senescence

Abstract

In the brains of adult vertebrates, including humans, neurogenesis occurs in restricted niches where it maintains cellular turnover and cognitive plasticity. In virtually all species, however, aging is associated with a significant decline in adult neurogenesis. Moreover, an acceleration of neurogenic defects is observed in models of Alzheimer's disease and other neurodegenerative diseases, suggesting an involvement in aging- and disease-associated cognitive deficits. To gain insights into when, how and why adult neurogenesis decreases in the aging brain, we critically reviewed the scientific literature on aging of the rodent subventricular zone, the neurogenic niche of the adult forebrain. Our analysis revealed that deficits in the neurogenic pathway are largely established by middle age, but that there remains striking ambiguity in the underlying mechanisms, especially at the level of stem and progenitor cells. We identify and discuss several challenging issues that have contributed to these key gaps in our current knowledge. In the future, addressing these issues should help untangle the interactions between neurogenesis, aging and aging-associated diseases.

Introduction

Aging is associated with a generalized reduction in the ability of adult tissues to maintain and repair themselves. At the cellular level, this decline in homeostatic and regenerative capacity can be attributed to both time-dependent ('chronological aging') and division-dependent ('replicative aging') mechanisms (Rando, 2006; Liu & Rando, 2011). Adult stem cells are unique in that they need to resist both chronological and long-term replicative aging processes. In the adult brain, the subventricular zone (SVZ) of the forebrain lateral ventricles represents the principal reservoir of neural stem cells (NSCs). NSCs of the SVZ continue to generate new neurons and glial cells during adulthood, contributing to the ongoing turnover of olfactory bulb interneurons and forebrain glial cell populations (Menn *et al.*, 2006; Lledo *et al.*, 2008; Imayoshi *et al.*, 2010). In response to brain injury, migrating NSC-derived progeny are also re-routed to areas of degeneration, where they can serve as a target for therapeutic manipulations (Kolb *et al.*, 2007; de Chevigny *et al.*, 2008; Erlandsson *et al.*, 2011). However, NSC-derived neurogenesis undergoes a marked decline over the course of aging, resulting in reduced tissue function; in rodents, for instance, olfactory bulb neuronal replacement is an early target of aging, affecting olfactory recognition, discrimination and identification tasks (Enwere *et al.*, 2004; Rey *et al.*, 2012). Furthermore, certain neurodegenerative conditions such as Alzheimer's and Parkinson's disease also show defective SVZ neurogenesis and an acceleration of aging-associated olfactory deficits, suggesting that declining neurogenesis may ultimately contribute to age-related cognitive diseases (Mesholam *et al.*, 1998; Winner *et al.*, 2011). To increase the ability of NSCs to maintain and repair the aging brain, it is essential to achieve a clearer understanding of when, how and why the aging process intersects with the regulation of adult neurogenesis.

Correspondence: Dr K. Fernandes, as above.

Received 14 December 2012, revised 20 February 2013, accepted 28 February 2013

Development and aging of the neurogenic lineage

Prior to adopting their mature adult phenotype, NSCs evolve through several distinct developmental stages during which they possess different properties and perform different biological functions (Alvarez-Buylla *et al.*, 2001) (see Fig. 1).

During embryonic development of the central nervous system (CNS), the main biological function of the early precursors of NSCs is tissue growth. In their first phase, the precursors of NSCs correspond to primitive neuroepithelial cells (NEPs). NEPs span the one-cell-layer thick neural tube, contacting both the inner ventricular surface and the outer pial surface, and they divide symmetrically to rapidly expand their population. The onset of asymmetric cell divisions initiates a second phase, when the accumulation of differentiated progeny and consequent thickening of the neural tube cause NEPs to transition into radial glial cells (RGCs). Once thought to mainly serve a scaffolding function, it is now recognized that RGCs generate the neurons, oligodendrocytes and astrocytes of the developing CNS, either directly or indirectly via intermediate progenitor cells (IPCs) (Noctor *et al.*, 2004; Kriegstein & Alvarez-Buylla, 2009; Hansen *et al.*, 2010). In the final stages of development, a subpopulation of RGCs begins assembling the SVZ niche that will

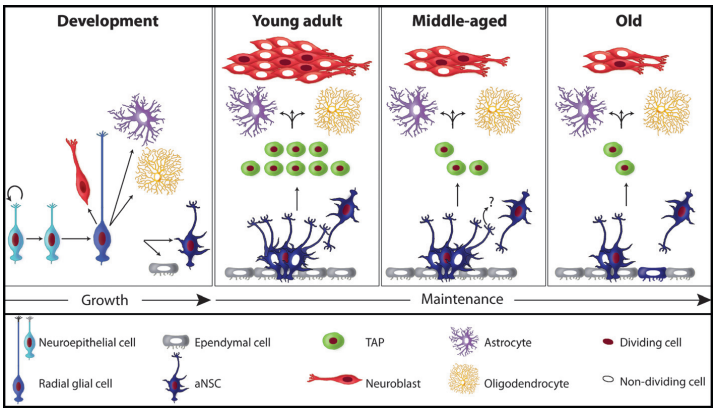

FIG. 1. Changes in neural stem cells and neurogenesis during development and aging. Prior to adulthood and during the developmental period of central nervous system (CNS) growth, adult neural stem cells (aNSCs) pass through three morphologically and functionally distinct phases. Initially, neuroepithelial stem cells are dividing symmetrically to expand their numbers. When neuroepithelial cells begin dividing asymmetrically to generate neurons and glial cells, they transition into radial glial cells. As formation of the main populations of differentiated neural cell types nears completion, forebrain radial glial cells retract their peripheral radial process and differentiate into either ventricle-contacting subventricular zone (SVZ) astrocytes or ventricle-lining ependymal cells, setting up the SVZ niche. SVZ astrocytes are aNSCs of the postnatal and adult forebrain. During adulthood, aNSC function shifts to forebrain maintenance; aNSCs primarily divide asymmetrically, maintaining the size of the stem cell pool while generating new neuroblasts and glioblasts. As adulthood continues into Middle-age and Old age, neurogenic output decreases dramatically. Visible changes include alterations within the aNSC pool (comprising fewer ventricle-contacting SVZ astrocytes and some conversion of astrocytes into ependymal cells), a reduction of total numbers of transiently amplifying progenitors (TAPs), neuroblasts, and proliferating cells (including aNSCs, TAPs, and some neuroblasts). The question mark reflects that it is unknown whether ventricle-contacting astrocytes disappear or simply withdraw their ventricle contacting process.

maintain NSCs during adulthood. They do so by retracting their apical processes while maintaining ventricular contact at their basal surface, subsequently converting into either ventricle-lining ependymal cells or ventricle-contacting SVZ astrocytes (Merkle *et al.*, 2004; Spassky *et al.*, 2005).

The biological function of NSCs undergoes a major change when they begin shifting into a mode dedicated to tissue maintenance. This maintenance phase begins in the postnatal period and continues throughout adulthood. In the forebrain, SVZ astrocytes continue functioning as postnatal and adult NSCs (aNSCs) (Doetsch *et al.*, 1999; Imura *et al.*, 2003; Morshead *et al.*, 2003). These aNSCs are highly quiescent, dividing only once every 2–3 weeks (Morshead *et al.*, 1994) to generate highly proliferative, transiently amplifying progenitors (TAPs) that give rise to migratory, fate-committed neuroblasts and glioblasts (Suzuki & Goldman, 2003). Neuroblasts born in the SVZ migrate along the rostral migratory stream and differentiate into olfactory bulb interneurons (Lois & Alvarez-Buylla, 1994) that are critical for odour recognition (Breton-Provencher *et al.*, 2009; Mouret *et al.*, 2009) and short-term olfactory memory (Breton-Provencher *et al.*, 2009). Forebrain ependymal cells rarely divide, but remain capable of neurogenesis under pathological conditions (Carlen *et al.*, 2009).

aNSCs are ideally positioned within the niche to be dynamically regulated by environmental signals. Their basal processes contact the lateral ventricle at the center of spirals of ependymal cells termed pinwheels (Mirzadeh *et al.*, 2008; Nam & Benezra, 2009), while their apical processes contact SVZ blood vessels (Shen *et al.*, 2008; Tavazoie *et al.*, 2008). Combinatorial extrinsic signals arising from adjacent aNSCs, TAPs, neuroblasts, ependymal cells, extracellular matrix molecules, the cerebrospinal fluid (CSF) and the vasculature interact with cell-intrinsic mechanisms to control proliferation, self-renewal capacity, fate determination, migration, differentiation and survival (Fuchs *et al.*, 2004; Morrison & Spradling, 2008; Suh *et al.*, 2009; Walker *et al.*, 2009). Under basal conditions, aNSCs mainly divide asymmetrically, allowing them to maintain the stem cell pool while also generating rapidly dividing TAPs (Morshead *et al.*, 1998). Moreover, aNSCs also retain the ability to return to a symmetric mode of division to expand stem cell numbers after injury (Parent *et al.*, 1997; Zhang *et al.*, 2004; Lugert *et al.*, 2010). In spite of having this ability, adult neurogenesis still declines during aging (Fig. 1). A significant number of studies have investigated this decline–so what have we learned about the underlying mechanisms of SVZ aging?

Aging and SVZ neurogenesis: what do we really know?

We surveyed the scientific literature for published peer-reviewed studies on the topic of age-related impairments in forebrain neurogenesis, and found 20 articles that have investigated this issue using rodent models. Comparison of the assumptions, experimental designs, methods, primary data, interpretations and conclusions revealed considerable heterogeneity and inconsistencies across these parameters. To begin developing a clearer picture, we therefore divided adulthood into three age ranges, identified here as *Young adult* (2–6 months of age), *Middle-aged* (6–14 months), and *Old* (greater than 14 months) (see Fig. 2). According to these criteria, we found that of the 20 studies examining age-related changes in SVZ neurogenesis, 15/20 compared Young adult with Old stages (Kuhn *et al.*, 1996; Tropepe *et al.*, 1997; Jin *et al.*, 2003; Enwere *et al.*, 2004; Maslov *et al.*, 2004; Luo *et al.*, 2006; Molofsky *et al.*, 2006; Belluardo *et al.*, 2008; Ahlenius *et al.*, 2009; Acosta *et al.*, 2010; Frinchi *et al.*, 2010; Stoll *et al.*, 2011a,b; McGinn *et al.*, 2012; Shook *et al.*, 2012), 8/20 made Young adult to Middle-age comparisons (Kippin *et al.*, 2005; Chen *et al.*, 2006; Luo *et al.*, 2006; Molofsky *et al.*, 2006; Tanaka *et al.*, 2007; Medrano *et al.*, 2009; Bouab *et al.*, 2011; Shook *et al.*, 2012), and 3/20 compared

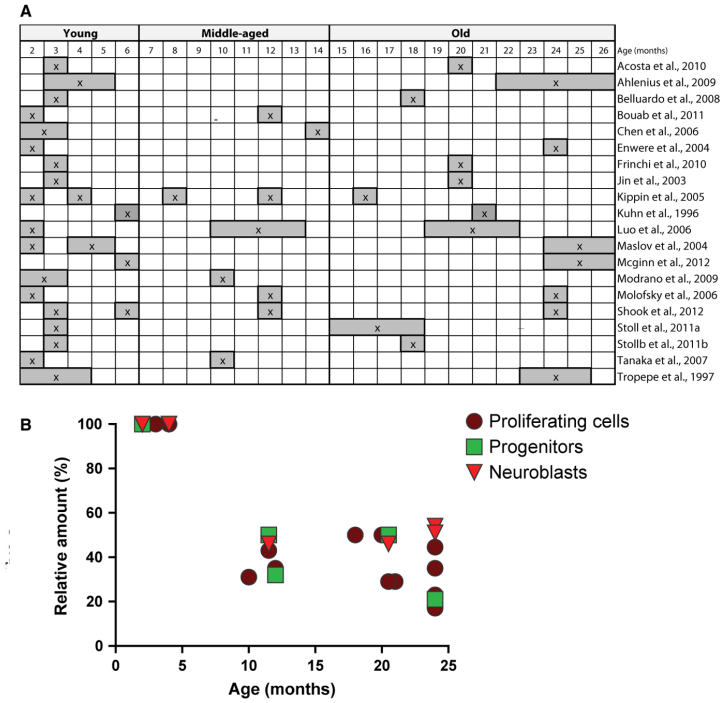

FIG. 2. Survey of published studies on aging-associated changes in neurogenesis in the rodent SVZ. (A) Table summarizing the 20 articles that have studied SVZ neurogenesis in adult to aged rodents. Rodent ages are divided into Young adult (2–6 months), Middle-aged (7–14 months) and Old (15 months and greater) age groups. There were 15/20 studies that examined Young adult to Old time-points, 8/20 that examined Young adult to Middle-aged time-points, and only three studies compared all three age groups. (B) Graph of the data compiled from the studies listed in A, plotted as the amount relative to the young adult age group. Categories of data are Proliferating cells ($PH3^+$, $BrdU^+$ or $Ki67^+$), transiently amplifying progenitors (TAPs) ($Mash1^+$) and Neuroblasts (DCX^+ or $PSA\text{-}NCAM^+$). Note that for all of these stages of the neurogenic pathway, the main decrease occurs by Middle-age and is only slightly worsened by Old age.

Young adult, Middle-aged and Old stages in parallel (Luo *et al.*, 2006; Molofsky *et al.*, 2006; Shook *et al.*, 2012). Analysing the data in this manner allowed us to draw three main conclusions.

Forebrain neurogenesis is drastically reduced in the brains of Old rodents

Compared with Young adults, Old rodents exhibit a marked decrease in virtually all stages of SVZ neurogenesis. Cell proliferation is reduced by 50–80% as measured by acute incorporation of bromodeoxyuridine (BrdU) or staining for phospho-histone-3 (PH3) or Ki67 (Tropepe *et al.*, 1997; Jin *et al.*, 2003; Enwere *et al.*, 2004; Luo *et al.*, 2006; Ahlenius *et al.*, 2009; Acosta *et al.*, 2010). This results in a 40–80% reduction in neuroblasts labeled with PSA-NCAM (Enwere *et al.*, 2004), doublecortin (DCX) (Ahlenius *et al.*, 2009) or BrdU+Tbr2 (Stoll *et al.*, 2011b), and a downstream 50–80% decrease in BrdU+ cells within the rostral migratory stream and olfactory bulbs (Enwere *et al.*, 2004). Collectively, the entire SVZ–olfactory bulb neurogenesis pathway is found to be decreased by at least 50%.

At the level of the aNSCs and TAPs themselves, alterations that have been reported include (i) a 50% reduction in expression of Nestin (expressed by both aNSCs and TAPs) (Ahlenius *et al.*, 2009); (ii) a 45% reduction in long-term BrdU-retaining cells (Shook *et al.*, 2012) (a measure of the number of surviving aNSCs that divided within the time frame of BrdU treatment); (iii) a 78% decrease in pinwheels along the surface of the lateral ventricles (Shook *et al.*, 2012) and (iv) a 86% decrease in the number of ventricle-contacting SVZ astrocytes (Shook *et al.*, 2012). Results of the widely used colony-forming neurosphere assay (used as a measure of cells having stem cell potential) were inconclusive, as one study found no change (Tropepe *et al.*, 1997) and three studies reported 22–77% decreases (Enwere *et al.*, 2004; Maslov *et al.*, 2004; Ahlenius *et al.*, 2009). Cell cycle alterations in the aging SVZ are complex and remain only partially understood. Shook *et al.* (2012) identified a decrease in the total number of ventricle-contacting $GFAP^+$ aNSCs, but no change in the number that are proliferating. TAPs exhibit a decreased cell cycle length *in vivo* (as measured by BrdU/^{3}H-thymidine double-labelling) (Tropepe *et al.*, 1997) but an increased propensity to divide *in vitro* (CldU/IdU incorporation experiments) (Stoll *et al.*, 2011b); this suggests that TAPs either become increasingly resistant to proliferative signals *in vivo* or that the surrounding niche becomes less supportive.

The steepest decline in neurogenesis occurs between Young adult and Middle-age

Interestingly, the major neurogenic defects observed in Old rodents were found to have already taken place by middle-age. For example, there is good consensus that SVZ cell proliferation is decreased by

50–70% (Ki67, BrdU) at 10–14 months of age (Luo *et al.*, 2006; Tanaka *et al.*, 2007; Belluardo *et al.*, 2008; Bouab *et al.*, 2011), resulting in a downstream 76% decrease in BrdU+ neurons that are contributed to the olfactory bulbs (Bouab *et al.*, 2011), and both these results match findings obtained using Old mice (above).

At the level of aNSCs and TAPs, (i) immuno-labelling and electron microscopy studies indicate a 65–75% reduction in TAPs (Luo *et al.*, 2006; Bouab *et al.*, 2011); (ii) the number of label-retaining slowly dividing cells decreases by about 67% (Bouab *et al.*, 2011); (iii) the number of pinwheels decreases by about 68% (Shook *et al.*, 2012) and (iv) the number of ventricle-contacting astrocytes (GFAP/gamma-tubulin-expressing cells) decreases by 73% (Shook *et al.*, 2012). In the case of the neurosphere assay, the data generally indicate that there is no major difference in numbers of neurosphere-forming cells. However, as discussed further in the following section, experimental differences such as neurosphere assay parameters and mouse strains that were used preclude reliable comparison of data across these studies (Tropepe *et al.*, 1997; Kippin *et al.*, 2005; Chen *et al.*, 2006; Medrano *et al.*, 2009; Bouab *et al.*, 2011).

Collectively, comparison of the Middle-age and Old data reveals that all the neurogenesis parameters tested remained relatively stable after Middle-age in rodents. This is illustrated in Fig. 2B, which shows a compilation of the age-related differences in numbers of proliferating cells, TAPs and neuroblasts described above.

We still do not know what is occurring at the aNSC and TAP stages

Despite the compelling data showing that adult forebrain neurogenesis is highly diminished between Young adult and Middle-age time-points (above), the causes, mechanisms and exact nature of the changes occurring at the levels of the aNSC and TAP populations remain strikingly nebulous. For example: Are aNSCs decreased in number or is their activity compromised? Are TAPs not produced or are they generated but fail to amplify in number? Are changes in the aNSC and/or TAP populations caused by cell-autonomous mechanisms or are they the result of aging of the local and systemic environments? There are numerous reasons for the continued uncertainty surrounding such key questions, as discussed further in the following section.

Why haven't we learned more about the causes of neurogenic impairments during aging?

Our review of the literature revealed at least two recurrent and problematic issues in the field of aging and neurogenesis. These issues have made it impossible to extract a more complete picture of the cellular events taking place in the aging SVZ (and particularly at the level of the aNSCs and TAPs) using the currently published data.

Problem 1: the assumption that aging = old

The first obvious problem stems from the fact that aging is a vaguely defined process for which there are few known measurable features, leading to a wide disparity in study conditions. This can be contrasted with disorders such as Alzheimer's disease, which is defined by specific pathological hallmarks, spatial and temporal patterns of progression, and functional criteria, facilitating consensus on key study parameters. To study aging in a rigorous scientific manner, it is therefore essential to define its biological features more clearly.

A principal biological feature of aging is a reduction in the ability of adult tissues to maintain and repair themselves. When does this reduced capacity for adult tissue homeostasis begin? On the one hand, some aspects of the aging process may start the moment our first cell is born. However, considering the overwhelming importance of proper embryonic development for organismal survival, it is likely that strong evolutionary pressure ensures homeostatic integrity during the critical development period. Moreover, it would be challenging to distinguish deleterious aging-associated events from the rapid and profound cellular changes that normally occur during development (i.e. Fig. 1). To establish a more practical framework for studying the aging process, it is therefore useful to define it as a process that (i) begins once a cell has completed its rapid developmental changes and first reaches the stable phenotype that it will maintain throughout adulthood; (ii) occurs at a rate related to chronological age but is also regulated by factors such as epigenetics and cell–cell interactions and (iii) continues progressing until death. Three informative predictions emerge when these criteria are applied to the study of adult neurogenesis.

(i) Aging of aNSCs may begin very early

As illustrated in Fig. 1, adult neurogenesis is compromised long before reaching an Old age. Interestingly, cognitive decline in humans may also begin as early as the 20 s (Salthouse, 2009). If a biological 'clock' controls aNSC replicative aging and the onset of the decline in neurogenesis, it is likely that we would be able to detect it even as soon as the early postnatal period, when aNSCs have transitioned through their developmental neuroepithelial and radial glial stages and have begun adopting their quiescent adult phenotype, i.e. when their biological function shifts from tissue *growth* to tissue *maintenance* (Fig. 1).

(ii) Aging may occur at different rates across tissues and cell types

There are large variations in both the basal rates of cell production and the lifespan of differentiated cells across different tissues, particularly between high turnover tissues such as the epidermis, intestinal epithelium and hematopoietic system, and low turnover tissues such as the brain and spinal cord. To avoid being misled, aging-related studies should be designed using tissue-specific criteria.

(iii) Focusing on Old time-points could be deceptive

As aging is a progressive process, the most logical approach to analysing it would be to study multiple time-points that are prior to or within the actual period of neurogenic decline. The tendency to study Old time-points has allowed us to identify the *consequences* of the aging process; however, focusing on the remnants of neurogenesis that are left after decline has already occurred does not provide insight into the *causes* of the process, and could incorporate additional sources of variability, such as aging-related diseases and 'survivor bias'.

As seen in the previous section, it is clear that aging does *not* equal Old in terms of adult neurogenesis. If we are to successfully identify the mechanisms that are responsible for the age-related decline in neurogenesis, it will be essential to define the cellular and molecular events that are occurring prior to the appearance of age-related declines in neurogenesis.

Problem 2: the blurred line between NSCs and progenitors

Accurate interpretation of many of the studies cited here required careful re-evaluation of the primary data, due to an unfortunate

tendency in the literature to interchangeably use such terms as stem cells, progenitor cells, stem-progenitors and precursors (Seaberg & van der Kooy, 2003). This problem originates largely from the current inability to accurately identify aNSCs and to precisely delineate between the early aNSC and TAP stages of neurogenesis.

aNSCs *in vivo* are rare in the adult, and spend most of their time in quiescence, rendering them a challenge to detect and study even in young adults. aNSCs are found within the GFAP-expressing astrocyte population (Doetsch *et al.*, 1999; Imura *et al.*, 2003; Morshead *et al.*, 2003) and TAPs express Dlx2, Mash1 and/or Olig2 (Doetsch *et al.*, 2002; Aguirre & Gallo, 2004; Parras *et al.*, 2004; Menn *et al.*, 2006); however, these markers are not *specific*, and there is a lack of widely accepted markers that can enable discrimination of the early lineage stages. Division-based labeling approaches, such as cell cycle-based markers and long-term label retention approaches, will be inherently imprecise in the context of aging as there are changes in cell cycle lengths or the frequency of exit from quiescence. Furthermore, changes in S-phase nucleotide incorporation are a reflection of changes in proliferative activity rather than cell numbers. Even changes in the number of morphologically defined cell types (such as ventricle-contacting $GFAP^+$ astrocytes, putative aNSCs) are complicated by the caveat that the cells may remain present and retain aNSC function or capability, but have simply retracted their ventricle-contacting process.

Evidence for aNSCs initially came from *in vitro* studies showing that isolated cells from the adult CNS can respond to growth factors to generate neurospheres, which can then be induced to differentiate into neuronal and glial lineages upon growth factor withdrawal (Reynolds & Weiss, 1992). The neurosphere assay subsequently emerged as an informative and powerful approach for gaining insights into the biology of aNSCs and TAPs; however, it requires meticulous care and attention to technical details to obtain results that are valid, reproducible and interpretable (Coles-Takabe *et al.*, 2008; Pastrana *et al.*, 2011). As described earlier, however, there has been little consensus among studies concerning changes in neurosphere numbers with aging, and this variability probably stems from the methodological inconsistencies evident in the experimental protocols used. Moreover, there are important questions pertaining to the interpretation of results obtained with the neurosphere assay, particularly in aging studies. For instance, to what extent can non-aNSCs (such as early TAP cells) be reprogrammed to generate self-renewing neurospheres *in vitro* (Doetsch *et al.*, 2002)? And will aNSCs always grow into neurospheres *in vitro*, regardless of their state *in vivo* (activated vs. quiescent vs. senescent)?

In light of the current technical limitations and challenges, great care should be taken to make precise conclusions that take into account the limitations of the methods used, and to avoid using all-encompassing terms that mis-identify or blur the cell types implicated (Seaberg & van der Kooy, 2003). Thus, at present, our understanding of the changes occurring to aNSCs vs. TAPs during aging remains limited.

Possible mechanisms leading to age-related decline in neurogenesis

Tissue aging is mediated by at least two forms of cellular aging. *Chronological* aging affects all cells and refers to the time-dependent deterioration in cellular functioning that occurs as a result of normal 'wear and tear'. Proliferating cells are additionally subject to *replicative* aging, the deterioration in proliferative capacity resulting from division-coupled telomere shortening and DNA damage (Rando, 2006; Liu & Rando, 2011; Longo *et al.*, 2012). Such aging processes lead to a mitotic 'clock', a finite number of possible cell divisions after which cells become senescent (the 'Hayflick limit'; Hayflick, 1965). In the case of adult neurogenesis, age-related impairments could therefore be the result of (i) cell-autonomous aging mechanisms occurring within the aNSC lineage itself; (ii) non-cell-autonomous aging mechanisms occurring within the local and systemic regulatory environments, or a combination of these two processes. Cell-autonomous and/or non-cell-autonomous aging processes can then ultimately impact upon any level(s) of the multi-step neurogenic pathway, such as (i) cell cycle properties of aNSCs and TAPs; (ii) expansion capacity of the TAP population; (iii) cell death at any stage of the neurogenic pathway and (iv) lineage specification and fate choice (Fig. 3).

Cell autonomous causes?

Cells are generally believed to possess two main control systems to restrict their proliferative potential: telomere shortening and cyclin-dependent kinase inhibitors (Mandal *et al.*, 2011). These control systems act by increasing the cell cycle length and by promoting entry into reversible quiescence or irreversible senescence. Such cell cycle control is likely to be particularly beneficial at younger ages, preventing oncogenic transformation within the stem cell population, but may be detrimental for neurogenic plasticity at later ages. In particular, as described below, there is striking evidence that circumventing these systems can help to prevent and/or reverse the effects of aging on adult neurogenesis.

Telomerase is a reverse transcriptase that is highly expressed in immortal embryonic stem cells and whose enzymatic activity counteracts the telomere-shortening effects of cell division. Increasing telomerase activity in cultured cells confers the ability for unlimited proliferation, enabling them to avoid senescence (Bodnar *et al.*, 1998). Telomerase is generally absent within the adult brain, but it remains detectable in the SVZ–olfactory system (Caporaso *et al.*, 2003). In late-generation telomerase knockout mice, there is widespread acceleration of tissue aging, including suppression of SVZ neurogenesis (Wong *et al.*, 2003; Ferron *et al.*, 2004). Remarkably, these changes (including deficits in SVZ neurogenesis and olfaction) can actually be *reversed* by restoring telomerase expression in the knockout mice (Jaskelioff *et al.*, 2011).

Cyclin-dependent kinase inhibitors are classified into two branches: the INK4 family ($P16^{INK4a}$, $p15^{INK4b}$, $p18^{INK4c}$, $p19^{INK4d}$) and the Cip/Kip family ($p21^{Waf1/Cip}$, $p27^{Kip1}$ and $p57^{Kip2}$) (Sherr & Roberts, 1999; Kim & Sharpless, 2006). The INK4 tumour suppression pathway is activated during aging in many tissues including the bone marrow, liver, heart and renal cortex (Krishnamurthy *et al.*, 2004; Burd *et al.*, 2013) and brain (Molofsky *et al.*, 2006). Studies have used $p16^{INK4a}$-deficient and $p16^{INK4a}$-overexpressing mice to assess the impact on self-renewal in hematopoietic stem cells, neural stem cells and pancreatic islets and have concluded that $p16^{INK4a}$ expression is one cause of aging in these tissues (Janzen *et al.*, 2006; Krishnamurthy *et al.*, 2006; Molofsky *et al.*, 2006). In all three cell types, $p16^{INK4a}$ deficiency partially abrogated the age-induced decline in proliferation. Expression of the INK4 family is normally repressed by factors such Bmi1 and Hmga2. The transcription factor Bmi1 promotes cell proliferation and self-renewal by inhibiting INK4a/Arf, and Bmi-1-deficient mice show widespread deficits, including inhibited proliferation in the postnatal SVZ (Molofsky *et al.*, 2003, 2006). The transcriptional modulator Hmga2 is a negative regulator of $p16^{INK4a}$ and $p19^{ARF}$ during development, but is itself negatively regulated by the let-7 family of microRNAs, whose expression increases during aging (Nishino *et al.*, 2008).

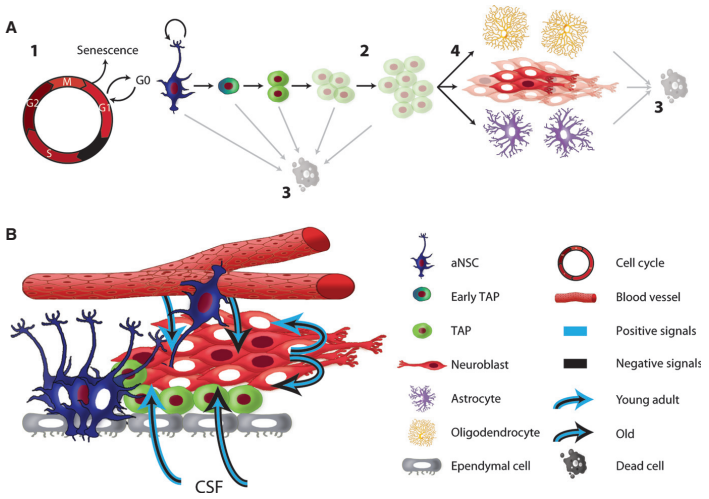

FIG. 3. Possible mechanisms underlying impaired neurogenesis during aging. (A) Reduced neurogenic output could occur by alterations occurring at multiple stages of the neurogenic pathway, including (1) changes in cell cycle dynamics that cause irreversible senescence, reversible quiescence or lengthening of the cell cycle, (2) decreased expansion of the transiently amplifying progenitor (TAP) pool, (3) increased cell death and/or (4) altered neuronal lineage specification. (B) The above mechanisms of neurogenesis impairment could be due to aging of the adult neural stem cell (aNSC) lineage itself (cell-autonomous), aging of the local or systemic environment (non-cell-autonomous), or both. In the case of non-cell-autonomous changes, the underlying causes would be a decrease in neurogenesis-promoting factors or an increase in neurogenesis-inhibiting factors (arrows). The sources of such factors could be the systemic milieu [via blood or cerebrospinal fluid (CSF)], support cells of the subventricular zone niche (such as ventricle-lining ependymal cells or blood vessel endothelial cells) or cells of the neurogenic lineage themselves (aNSCs, TAPs or neuroblasts).

Expression of the Cip/Kip family member, p21, is likewise elevated during aging in the cerebellum (Legrier *et al.*, 2001), and p21-knockout mice show an initial increase in proliferation followed by a premature exhaustion of proliferation (Kippin *et al.*, 2005).

One caveat to the interpretation of these studies on telomerase and cell cycle regulators is that, although they demonstrate a role in preventing and/or reversing aging-related changes in proliferation and neurogenesis, it nevertheless remains uncertain whether age-related changes to these systems are themselves involved in the aging process (Burd *et al.*, 2013). Studies have yet to provide direct evidence for which cell types express altered levels of these proteins during aging, as changes in cell cycle dynamics could impact expansion of aNSCs and/or the TAP cells (Fig. 3A). Also, studies that have looked at the effects of over-expressing or inhibiting these pathways have rarely used more recently developed tissue-specific or temporally controlled methods, and thus induce widespread deficits that make it difficult to interpret the exact mechanism of the observed effects.

Non-cell-autonomous causes?

The potential non-cell-autonomous causes of neurogenesis impairments can conceptually be divided into reduced neurogenesis-promoting signals and increased neurogenesis-inhibiting signals (Fig. 3B). Within the young adult SVZ, a growing list of secreted factor families has now been implicated in stem cell regulation and neurogenesis, including (but not limited to) Ephrins (Conover *et al.*, 2000), Shh (Ahn & Joyner, 2005; Balordi & Fishell, 2007a,b), EGFs (Kuhn *et al.*, 1997; Doetsch *et al.*, 2002; Pastrana *et al.*, 2009), FGFs (Kuhn *et al.*, 1997; Frinchi *et al.*, 2008), TNF-α (Tropepe *et al.*, 1997), Notch-Delta (Carlen *et al.*, 2009; Imayoshi *et al.*, 2010), Noggin (Lim *et al.*, 2000; Peretto *et al.*, 2004), BMPs (Lim *et al.*, 2000; Peretto *et al.*, 2004; Colak *et al.*, 2008) and Wnts (Adachi *et al.*, 2007), making it easy to envisage that a de-regulation of such factors could lead to impaired neurogenesis with age. Exogenous application of some of these factors has been shown to increase neurogenesis in older brains (Jin *et al.*, 2003; Enwere *et al.*, 2004; Paliouras *et al.*, 2012), showing that the ability of the SVZ to respond to extrinsic signals is at least partially preserved during aging. However, this does not prove that altered levels of these factors play a role during aging. To the contrary, the data investigating whether endogenous quantities of these factors actually changes in the SVZ during aging are mixed (Enwere *et al.*, 2004; Frinchi *et al.*, 2010; Werry *et al.*, 2010). Moreover, although declining receptor levels for some factors have been reported (Enwere *et al.*, 2004), such reductions are probably secondary to the age-related loss of the SVZ cells themselves.

Given the lack of information concerning actual changes occurring with age, it appears that greater emphasis should be placed on identifying aging-associated changes that take place within the neurogenic environment and assessing their significance for adult neurogenesis. For example, some insight has recently been provided by a study using a parabiosis approach to link the circulatory systems of young adult and old mice, demonstrating that age-related changes in blood-borne factors contribute to decreasing neurogenesis (Villeda *et al.*, 2011). Several other changes have also recently been documented within the aging neurogenic environment, including alterations in the composition of the CSF (Zhang *et al.*, 2005; Baird *et al.*, 2012), ependymal cell loss from stenosis of the ventricle walls (Shook *et al.*, 2012) and accumulation of lipid droplets within the aging ependyma (Bouab *et al.*, 2011). Importantly, aging of neural precursors and of their

surrounding SVZ niche are likely to be inter-related events, and it remains to be established whether such changes within the niche contribute to, or are themselves caused by, age-related decreases in neurogenesis.

Does irreversible stem cell exhaustion/loss/senescence occur in the aging SVZ?

This key question remains to be answered due to the lack of consensus amongst published findings and the current technical hurdles in reliably identifying aNSCs described earlier. It is noteworthy, however, that alterations in the proliferation and/or cell cycle properties of aNSCs and TAPs have been identified (Tropepe *et al.*, 1997; Ahlenius *et al.*, 2009; Bouab *et al.*, 2011; Shook *et al.*, 2012) and that experiments de-regulating either cell-autonomous or non-cell-autonomous control mechanisms have shown that functional exhaustion of SVZ stem cell activity can in principle occur (Kippin *et al.*, 2005; Imayoshi *et al.*, 2010). Interestingly, radial glial-like neurogenic precursors in the dentate gyrus have been found to undergo a terminal astrocytic differentiation, leading to the proposal of a 'disposable' model of neural stem cell (Encinas *et al.*, 2011).

The implications of when, how and why SVZ neurogenesis declines with age

Evolutionary theories of aging make the distinction between chronological age (measured in time) and biological age (measured in terms of cellular function). Until now, studies of age-related declines in adult neurogenesis have focused on chronological aging, and have clearly established many of the *consequences* of the aging process on adult neurogenesis: reduced cellular proliferation in the niche, decreased numbers of progenitors and neuroblasts, and reduced olfactory function. While these studies have left unresolved the issue of upstream changes in aNSC and progenitor biology, they have nevertheless established that the *when* of the biological aging of adult neurogenesis occurs sometime between early adulthood and middle-age, and significantly before rodents are 'old'. To uncover the upstream cellular events and molecular mechanisms (i.e. the *how* of declining neurogenesis), the experimental design of future studies will need to be significantly re-oriented towards younger ages, so that more light is shed on the *process* of aging rather than its consequences.

Given the functional importance of adult neurogenesis for cognitive plasticity and brain maintenance, the *why* of age-related declines in neurogenesis remains unknown. Evolutionarily, because natural selection is largely geared towards improving reproductive fitness, one possibility is that there is simply insufficient evolutionary pressure to select for individuals that maintain high levels of adult neurogenesis after reproductive age; indeed, in the hippocampus of various species, proliferation declines rapidly after the age of first reproduction (Kirkwood & Rose, 1991; Amrein *et al.*, 2011). A second possibility is that the cellular mechanisms restricting neurogenesis as we get older are actually protective, preventing tumor development and/or stem cell exhaustion from occurring at earlier ages. Thus, different therapeutic objectives may ultimately be desirable depending on one's biological age: reducing aNSC activity to the minimal amount necessary at early ages to preserve the replicative life and genomic integrity of aNSCs, vs. activating aNSCs at later ages to restore a minimal level of adult neurogenesis in the old brain. The answers to these questions may have significant implications for the design of future therapeutic strategies.

Acknowledgements

We thank members of the Fernandes laboratory for helpful discussion and critiques. L.H. is funded by studentships from the Alzheimer Society of Canada and the Fonds de recherche de Québec en Santé (FRQS). K.F. is the recipient of a Canada Research Chair in Neural Stem Cell Biology. This work has been supported by the Canadian Institutes of Health Research (CIHR). The authors declare no competing interests.

Abbreviations

aNSC, adult neural stem cell; BrdU, 2-bromodeoxyuridine; CNS, central nervous system; CSF, cerebrospinal fluid; DCX, doublecortin; IPC, intermediate progenitor cells; NEP, neuroepithelial cell; NSC, neural stem cell; RGC, radial glial cell; SVZ, subventricular zone; TAP, transiently amplifying progenitor.

Reference

Acosta, S., Jernberg, J., Sanberg, C.D., Sanberg, P.R., Small, B.J., Gemma, C. & Bickford, P.C. (2010) NT-020, a natural therapeutic approach to optimize spatial memory performance and increase neural progenitor cell proliferation and decrease inflammation in the aged rat. *Rejuv. Res.*, **13**, 581–588.

Adachi, K., Mirzadeh, Z., Sakaguchi, M., Yamashita, T., Nikolcheva, T., Gotoh, Y., Peltz, G., Gong, L., Kawase, T., Alvarez-Buylla, A., Okano, H. & Sawamoto, K. (2007) Beta-catenin signaling promotes proliferation of progenitor cells in the adult mouse subventricular zone. *Stem Cells*, **25**, 2827–2836.

Aguirre, A. & Gallo, V. (2004) Postnatal neurogenesis and gliogenesis in the olfactory bulb from NG2-expressing progenitors of the subventricular zone. *J. Neurosci.*, **24**, 10530–10541.

Ahlenius, H., Visan, V., Kokaia, M., Lindvall, O. & Kokaia, Z. (2009) Neural stem and progenitor cells retain their potential for proliferation and differentiation into functional neurons despite lower number in aged brain. *J. Neurosci.*, **29**, 4408–4419.

Ahn, S. & Joyner, A.L. (2005) In vivo analysis of quiescent adult neural stem cells responding to Sonic hedgehog. *Nature*, **437**, 894–897.

Alvarez-Buylla, A., Garcia-Verdugo, J.M. & Tramontin, A.D. (2001) A unified hypothesis on the lineage of neural stem cells. *Nat. Rev. Neurosci.*, **2**, 287–293.

Amrein, I., Isler, K. & Lipp, H.P. (2011) Comparing adult hippocampal neurogenesis in mammalian species and orders: influence of chronological age and life history stage. *Eur. J. Neurosci.*, **34**, 978–987.

Baird, G.S., Nelson, S.K., Keeney, T.R., Stewart, A., Williams, S., Kraemer, S., Peskind, E.R. & Montine, T.J. (2012) Age-dependent changes in the cerebrospinal fluid proteome by slow off-rate modified aptamer array. *Am. J. Pathol.*, **180**, 446–456.

Balordi, F. & Fishell, G. (2007a) Hedgehog signaling in the subventricular zone is required for both the maintenance of stem cells and the migration of newborn neurons. *J. Neurosci.*, **27**, 5936–5947.

Balordi, F. & Fishell, G. (2007b) Mosaic removal of hedgehog signaling in the adult SVZ reveals that the residual wild-type stem cells have a limited capacity for self-renewal. *J. Neurosci.*, **27**, 14248–14259.

Belluardo, N., Mudo, G., Bonomo, A., Di Liberto, V., Frinchi, M. & Fuxe, K. (2008) Nicotine-induced fibroblast growth factor-2 restores the age-related decline of precursor cell proliferation in the subventricular zone of rat brain. *Brain Res.*, **1193**, 12–24.

Bodnar, A.G., Ouellette, M., Frolkis, M., Holt, S.E., Chiu, C.P., Morin, G.B., Harley, C.B., Shay, J.W., Lichtsteiner, S. & Wright, W.E. (1998) Extension of life-span by introduction of telomerase into normal human cells. *Science*, **279**, 349–352.

Bouab, M., Paliouras, G.N., Aumont, A., Forest-Berard, K. & Fernandes, K.J. (2011) Aging of the subventricular zone neural stem cell niche: evidence for quiescence-associated changes between early and mid-adulthood. *Neuroscience*, **173**, 135–149.

Breton-Provencher, V., Lemasson, M., Peralta, M.R. 3rd. & Saghatelyan, A. (2009) Interneurons produced in adulthood are required for the normal functioning of the olfactory bulb network and for the execution of selected olfactory behaviors. *J. Neurosci.*, **29**, 15245–15257.

Burd, C.E., Sorrentino, J.A., Clark, K.S., Darr, D.B., Krishnamurthy, J., Deal, A.M., Bardeesy, N., Castrillon, D.H., Beach, D.H. & Sharpless, N.E. (2013) Monitoring tumorigenesis and senescence in vivo with a p16 (INK4a)-luciferase model. *Cell*, **152**, 340–351.

Caporaso, G.L., Lim, D.A., Alvarez-Buylla, A. & Chao, M.V. (2003) Telomerase activity in the subventricular zone of adult mice. *Mol. Cell. Neurosci.*, **23**, 693–702.
Carlen, M., Meletis, K., Goritz, C., Darsalia, V., Evergren, E., Tanigaki, K., Amendola, M., Barnabe-Heider, F., Yeung, M.S., Naldini, L., Honjo, T., Kokaia, Z., Shupliakov, O., Cassidy, R.M., Lindvall, O. & Frisen, J. (2009) Forebrain ependymal cells are Notch-dependent and generate neuroblasts and astrocytes after stroke. *Nat. Neurosci.*, **12**, 259–267.
Chen, J., Zacharek, A., Li, Y., Li, A., Wang, L., Katakowski, M., Roberts, C., Lu, M. & Chopp, M. (2006) N-cadherin mediates nitric oxide-induced neurogenesis in young and retired breeder neurospheres. *Neuroscience*, **140**, 377–388.
de Chevigny, A., Cooper, O., Vinuela, A., Reske-Nielsen, C., Lagace, D.C., Eisch, A.J. & Isacson, O. (2008) Fate mapping and lineage analyses demonstrate the production of a large number of striatal neuroblasts after transforming growth factor alpha and noggin striatal infusions into the dopamine-depleted striatum. *Stem Cells*, **26**, 2349–2360.
Colak, D., Mori, T., Brill, M.S., Pfeifer, A., Falk, S., Deng, C., Monteiro, R., Mummery, C., Sommer, L. & Gotz, M. (2008) Adult neurogenesis requires Smad4-mediated bone morphogenic protein signaling in stem cells. *J. Neurosci.*, **28**, 434–446.
Coles-Takabe, B.L., Brain, I., Purpura, K.A., Karpowicz, P., Zandstra, P.W., Morshead, C.M. & van der Kooy, D. (2008) Don't look: growing clonal versus nonclonal neural stem cell colonies. *Stem Cells*, **26**, 2938–2944.
Conover, J.C., Doetsch, F., Garcia-Verdugo, J.M., Gale, N.W., Yancopoulos, G.D. & Alvarez-Buylla, A. (2000) Disruption of Eph/ephrin signaling affects migration and proliferation in the adult subventricular zone. *Nat. Neurosci.*, **3**, 1091–1097.
Doetsch, F., Caille, I., Lim, D.A., Garcia-Verdugo, J.M. & Alvarez-Buylla, A. (1999) Subventricular zone astrocytes are neural stem cells in the adult mammalian brain. *Cell*, **97**, 703–716.
Doetsch, F., Petreanu, L., Caille, I., Garcia-Verdugo, J.M. & Alvarez-Buylla, A. (2002) EGF converts transit-amplifying neurogenic precursors in the adult brain into multipotent stem cells. *Neuron*, **36**, 1021–1034.
Encinas, J.M., Michurina, T.V., Peunova, N., Park, J.H., Tordo, J., Peterson, D.A., Fishell, G., Koulakov, A. & Enikolopov, G. (2011) Division-coupled astrocytic differentiation and age-related depletion of neural stem cells in the adult hippocampus. *Cell Stem Cell*, **8**, 566–579.
Enwere, E., Shingo, T., Gregg, C., Fujikawa, H., Ohta, S. & Weiss, S. (2004) Aging results in reduced epidermal growth factor receptor signaling, diminished olfactory neurogenesis, and deficits in fine olfactory discrimination. *J. Neurosci.*, **24**, 8354–8365.
Erlandsson, A., Lin, C.H., Yu, F. & Morshead, C.M. (2011) Immunosuppression promotes endogenous neural stem and progenitor cell migration and tissue regeneration after ischemic injury. *Exp. Neurol.*, **230**, 48–57.
Ferron, S., Mira, H., Franco, S., Cano-Jaimez, M., Bellmunt, E., Ramirez, C., Farinas, I. & Blasco, M.A. (2004) Telomere shortening and chromosomal instability abrogates proliferation of adult but not embryonic neural stem cells. *Development*, **131**, 4059–4070.
Frinchi, M., Bonomo, A., Trovato-Salinaro, A., Condorelli, D.F., Fuxe, K., Spampinato, M.G. & Mudo, G. (2008) Fibroblast growth factor-2 and its receptor expression in proliferating precursor cells of the subventricular zone in the adult rat brain. *Neurosci. Lett.*, **447**, 20–25.
Frinchi, M., Di Liberto, V., Olivieri, M., Fuxe, K., Belluardo, N. & Mudo, G. (2010) FGF-2/FGFR1 neurotrophic system expression level and its basal activation do not account for the age-dependent decline of precursor cell proliferation in the subventricular zone of rat brain. *Brain Res.*, **1358**, 39–45.
Fuchs, E., Tumbar, T. & Guasch, G. (2004) Socializing with the neighbors: stem cells and their niche. *Cell*, **116**, 769–778.
Hansen, D.V., Lui, J.H., Parker, P.R. & Kriegstein, A.R. (2010) Neurogenic radial glia in the outer subventricular zone of human neocortex. *Nature*, **464**, 554–561.
Hayflick, L. (1965) The limited in vitro lifetime of human diploid cell strains. *Exp. Cell Res.*, **37**, 614–636.
Imayoshi, I., Sakamoto, M., Yamaguchi, M., Mori, K. & Kageyama, R. (2010) Essential roles of Notch signaling in maintenance of neural stem cells in developing and adult brains. *J. Neurosci.*, **30**, 3489–3498.
Imura, T., Kornblum, H.I. & Sofroniew, M.V. (2003) The predominant neural stem cell isolated from postnatal and adult forebrain but not early embryonic forebrain expresses GFAP. *J. Neurosci.*, **23**, 2824–2832.
Janzen, V., Forkert, R., Fleming, H.E., Saito, Y., Waring, M.T., Dombkowski, D.M., Cheng, T., DePinho, R.A., Sharpless, N.E. & Scadden, D.T. (2006) Stem-cell ageing modified by the cyclin-dependent kinase inhibitor p16INK4a. *Nature*, **443**, 421–426.
Jaskelioff, M., Muller, F.L., Paik, J.H., Thomas, E., Jiang, S., Adams, A.C., Sahin, E., Kost-Alimova, M., Protopopov, A., Cadinanos, J., Horner, J.W., Maratos-Flier, E. & Depinho, R.A. (2011) Telomerase reactivation reverses tissue degeneration in aged telomerase-deficient mice. *Nature*, **469**, 102–106.
Jin, K., Sun, Y., Xie, L., Batteur, S., Mao, X.O., Smelick, C., Logvinova, A. & Greenberg, D.A. (2003) Neurogenesis and aging: FGF-2 and HB-EGF restore neurogenesis in hippocampus and subventricular zone of aged mice. *Aging Cell*, **2**, 175–183.
Kim, W.Y. & Sharpless, N.E. (2006) The regulation of INK4/ARF in cancer and aging. *Cell*, **127**, 265–275.
Kippin, T.E., Martens, D.J. & van der Kooy, D. (2005) p21 loss compromises the relative quiescence of forebrain stem cell proliferation leading to exhaustion of their proliferation capacity. *Gene. Dev.*, **19**, 756–767.
Kirkwood, T.B. & Rose, M.R. (1991) Evolution of senescence: late survival sacrificed for reproduction. *Philos. T. Roy. Soc. B.*, **332**, 15–24.
Kolb, B., Morshead, C., Gonzalez, C., Kim, M., Gregg, C., Shingo, T. & Weiss, S. (2007) Growth factor-stimulated generation of new cortical tissue and functional recovery after stroke damage to the motor cortex of rats. *J. Cerebr. Blood F. Met.*, **27**, 983–997.
Kriegstein, A. & Alvarez-Buylla, A. (2009) The glial nature of embryonic and adult neural stem cells. *Annu. Rev. Neurosci.*, **32**, 149–184.
Krishnamurthy, J., Torrice, C., Ramsey, M.R., Kovalev, G.I., Al-Regaiey, K., Su, L. & Sharpless, N.E. (2004) Ink4a/Arf expression is a biomarker of aging. *J. Clin. Invest.*, **114**, 1299–1307.
Krishnamurthy, J., Ramsey, M.R., Ligon, K.L., Torrice, C., Koh, A., Bonner-Weir, S. & Sharpless, N.E. (2006) p16INK4a induces an age-dependent decline in islet regenerative potential. *Nature*, **443**, 453–457.
Kuhn, H.G., Dickinson-Anson, H. & Gage, F.H. (1996) Neurogenesis in the dentate gyrus of the adult rat: age-related decrease of neuronal progenitor proliferation. *J. Neurosci.*, **16**, 2027–2033.
Kuhn, H.G., Winkler, J., Kempermann, G., Thal, L.J. & Gage, F.H. (1997) Epidermal growth factor and fibroblast growth factor-2 have different effects on neural progenitors in the adult rat brain. *J. Neurosci.*, **17**, 5820–5829.
Legrier, M.E., Ducray, A., Propper, A. & Kastner, A. (2001) Region-specific expression of cell cycle inhibitors in the adult brain. *NeuroReport*, **12**, 3127–3131.
Lim, D.A., Tramontin, A.D., Trevejo, J.M., Herrera, D.G., Garcia-Verdugo, J.M. & Alvarez-Buylla, A. (2000) Noggin antagonizes BMP signaling to create a niche for adult neurogenesis. *Neuron*, **28**, 713–726.
Liu, L. & Rando, T.A. (2011) Manifestations and mechanisms of stem cell aging. *J. Cell Biol.*, **193**, 257–266.
Lledo, P.M., Merkle, F.T. & Alvarez-Buylla, A. (2008) Origin and function of olfactory bulb interneuron diversity. *Trends Neurosci.*, **31**, 392–400.
Lois, C. & Alvarez-Buylla, A. (1994) Long-distance neuronal migration in the adult mammalian brain. *Science*, **264**, 1145–1148.
Longo, V.D., Shadel, G.S., Kaeberlein, M. & Kennedy, B. (2012) Replicative and chronological aging in Saccharomyces cerevisiae. *Cell Metab.*, **16**, 18–31.
Lugert, S., Basak, O., Knuckles, P., Haussler, U., Fabel, K., Gotz, M., Haas, C.A., Kempermann, G., Taylor, V. & Giachino, C. (2010) Quiescent and active hippocampal neural stem cells with distinct morphologies respond selectively to physiological and pathological stimuli and aging. *Cell Stem Cell*, **6**, 445–456.
Luo, J., Daniels, S.B., Lennington, J.B., Notti, R.Q. & Conover, J.C. (2006) The aging neurogenic subventricular zone. *Aging Cell*, **5**, 139–152.
Mandal, P.K., Blanpain, C. & Rossi, D.J. (2011) DNA damage response in adult stem cells: pathways and consequences. *Nat. Rev. Mol. Cell Bio.*, **12**, 198–202.
Maslov, A.Y., Barone, T.A., Plunkett, R.J. & Pruitt, S.C. (2004) Neural stem cell detection, characterization, and age-related changes in the subventricular zone of mice. *J. Neurosci.*, **24**, 1726–1733.
McGinn, M.J., Colello, R.J. & Sun, D. (2012) Age-related proteomic changes in the subventricular zone and their association with neural stem/progenitor cell proliferation. *J. Neurosci. Res.*, **90**, 1159–1168.
Medrano, S., Burns-Cusato, M., Atienza, M.B., Rahimi, D. & Scrable, H. (2009) Regenerative capacity of neural precursors in the adult mammalian brain is under the control of p53. *Neurobiol. Aging*, **30**, 483–497.
Menn, B., Garcia-Verdugo, J.M., Yaschine, C., Gonzalez-Perez, O., Rowitch, D. & Alvarez-Buylla, A. (2006) Origin of oligodendrocytes in the subventricular zone of the adult brain. *J. Neurosci.*, **26**, 7907–7918.
Merkle, F.T., Tramontin, A.D., Garcia-Verdugo, J.M. & Alvarez-Buylla, A. (2004) Radial glia give rise to adult neural stem cells in the subventricular zone. *Proc. Natl. Acad. Sci. USA*, **101**, 17528–17532.

Mesholam, R.I., Moberg, P.J., Mahr, R.N. & Doty, R.L. (1998) Olfaction in neurodegenerative disease: a meta-analysis of olfactory functioning in Alzheimer's and Parkinson's diseases. *Arch. Neurol.*, **55**, 84–90.
Mirzadeh, Z., Merkle, F.T., Soriano-Navarro, M., Garcia-Verdugo, J.M. & Alvarez-Buylla, A. (2008) Neural stem cells confer unique pinwheel architecture to the ventricular surface in neurogenic regions of the adult brain. *Cell Stem Cell*, **3**, 265–278.
Molofsky, A.V., Pardal, R., Iwashita, T., Park, I.K., Clarke, M.F. & Morrison, S.J. (2003) Bmi-1 dependence distinguishes neural stem cell self-renewal from progenitor proliferation. *Nature*, **425**, 962–967.
Molofsky, A.V., Slutsky, S.G., Joseph, N.M., He, S., Pardal, R., Krishnamurthy, J., Sharpless, N.E. & Morrison, S.J. (2006) Increasing p16INK4a expression decreases forebrain progenitors and neurogenesis during ageing. *Nature*, **443**, 448–452.
Morrison, S.J. & Spradling, A.C. (2008) Stem cells and niches: mechanisms that promote stem cell maintenance throughout life. *Cell*, **132**, 598–611.
Morshead, C.M., Craig, C.G. & van der Kooy, D. (1998) In vivo clonal analyses reveal the properties of endogenous neural stem cell proliferation in the adult mammalian forebrain. *Development*, **125**, 2251–2261.
Morshead, C.M., Garcia, A.D., Sofroniew, M.V. & van Der Kooy, D. (2003) The ablation of glial fibrillary acidic protein-positive cells from the adult central nervous system results in the loss of forebrain neural stem cells but not retinal stem cells. *Eur. J. Neurosci.*, **18**, 76–84.
Morshead, C.M., Reynolds, B.A., Craig, C.G., McBurney, M.W., Staines, W.A., Morassutti, D., Weiss, S. & van der Kooy, D. (1994) Neural stem cells in the adult mammalian forebrain: a relatively quiescent subpopulation of subependymal cells. *Neuron*, **13**, 1071–1082.
Mouret, A., Lepousez, G., Gras, J., Gabellec, M.M. & Lledo, P.M. (2009) Turnover of newborn olfactory bulb neurons optimizes olfaction. *J. Neurosci.*, **29**, 12302–12314.
Nam, H.S. & Benezra, R. (2009) High levels of Id1 expression define B1 type adult neural stem cells. *Cell Stem Cell*, **5**, 515–526.
Nishino, J., Kim, I., Chada, K. & Morrison, S.J. (2008) Hmga2 promotes neural stem cell self-renewal in young but not old mice by reducing p16Ink4a and p19Arf Expression. *Cell*, **135**, 227–239.
Noctor, S.C., Martinez-Cerdeno, V., Ivic, L. & Kriegstein, A.R. (2004) Cortical neurons arise in symmetric and asymmetric division zones and migrate through specific phases. *Nat. Neurosci.*, **7**, 136–144.
Paliouras, G.N., Hamilton, L.K., Aumont, A., Joppe, S.E., Barnabe-Heider, F. & Fernandes, K.J. (2012) Mammalian target of rapamycin signaling is a key regulator of the transit-amplifying progenitor pool in the adult and aging forebrain. *J. Neurosci.*, **32**, 15012–15026.
Parent, J.M., Yu, T.W., Leibowitz, R.T., Geschwind, D.H., Sloviter, R.S. & Lowenstein, D.H. (1997) Dentate granule cell neurogenesis is increased by seizures and contributes to aberrant network reorganization in the adult rat hippocampus. *J. Neurosci.*, **17**, 3727–3738.
Parras, C.M., Galli, R., Britz, O., Soares, S., Galichet, C., Battiste, J., Johnson, J.E., Nakafuku, M., Vescovi, A. & Guillemot, F. (2004) Mash1 specifies neurons and oligodendrocytes in the postnatal brain. *EMBO J.*, **23**, 4495–4505.
Pastrana, E., Cheng, L.C. & Doetsch, F. (2009) Simultaneous prospective purification of adult subventricular zone neural stem cells and their progeny. *Proc. Natl. Acad. Sci. USA*, **106**, 6387–6392.
Pastrana, E., Silva-Vargas, V. & Doetsch, F. (2011) Eyes wide open: a critical review of sphere-formation as an assay for stem cells. *Cell Stem Cell*, **8**, 486–498.
Peretto, P., Dati, C., De Marchis, S., Kim, H.H., Ukhanova, M., Fasolo, A. & Margolis, F.L. (2004) Expression of the secreted factors noggin and bone morphogenetic proteins in the subependymal layer and olfactory bulb of the adult mouse brain. *Neuroscience*, **128**, 685–696.
Rando, T.A. (2006) Stem cells, ageing and the quest for immortality. *Nature*, **441**, 1080–1086.
Rey, N.L., Sacquet, J., Veyrac, A., Jourdan, F. & Didier, A. (2012) Behavioral and cellular markers of olfactory aging and their response to enrichment. *Neurobiol. Aging*, **33**, 626.e9–626.e23.
Reynolds, B.A. & Weiss, S. (1992) Generation of neurons and astrocytes from isolated cells of the adult mammalian central nervous system. *Science*, **255**, 1707–1710.
Salthouse, T.A. (2009) When does age-related cognitive decline begin? *Neurobiol. Aging*, **30**, 507–514.
Seaberg, R.M. & van der Kooy, D. (2003) Stem and progenitor cells: the premature desertion of rigorous definitions. *Trends Neurosci.*, **26**, 125–131.
Shen, Q., Wang, Y., Kokovay, E., Lin, G., Chuang, S.M., Goderie, S.K., Roysam, B. & Temple, S. (2008) Adult SVZ stem cells lie in a vascular niche: a quantitative analysis of niche cell-cell interactions. *Cell Stem Cell*, **3**, 289–300.
Sherr, C.J. & Roberts, J.M. (1999) CDK inhibitors: positive and negative regulators of G1-phase progression. *Gene. Dev.*, **13**, 1501–1512.
Shook, B.A., Manz, D.H., Peters, J.J., Kang, S. & Conover, J.C. (2012) Spatiotemporal changes to the subventricular zone stem cell pool through aging. *J. Neurosci.*, **32**, 6947–6956.
Spassky, N., Merkle, F.T., Flames, N., Tramontin, A.D., Garcia-Verdugo, J.M. & Alvarez-Buylla, A. (2005) Adult ependymal cells are postmitotic and are derived from radial glial cells during embryogenesis. *J. Neurosci.*, **25**, 10–18.
Stoll, E.A., Cheung, W., Mikheev, A.M., Sweet, I.R., Bielas, J.H., Zhang, J., Rostomily, R.C. & Horner, P.J. (2011a) Aging neural progenitor cells have decreased mitochondrial content and lower oxidative metabolism. *J. Biol. Chem.*, **286**, 38592–38601.
Stoll, E.A., Habibi, B.A., Mikheev, A.M., Lasiene, J., Massey, S.C., Swanson, K.R., Rostomily, R.C. & Horner, P.J. (2011b) Increased re-entry into cell cycle mitigates age-related neurogenic decline in the murine subventricular zone. *Stem Cells*, **29**, 2005–2017.
Suh, H., Deng, W. & Gage, F.H. (2009) Signaling in adult neurogenesis. *Annu. Rev. Cell Dev. Bi.*, **25**, 253–275.
Suzuki, S.O. & Goldman, J.E. (2003) Multiple cell populations in the early postnatal subventricular zone take distinct migratory pathways: a dynamic study of glial and neuronal progenitor migration. *J. Neurosci.*, **23**, 4240–4250.
Tanaka, A., Watanabe, Y., Kato, H. & Araki, T. (2007) Immunohistochemical changes related to ageing in the mouse hippocampus and subventricular zone. *Mech. Ageing Dev.*, **128**, 303–310.
Tavazoie, M., Van der Veken, L., Silva-Vargas, V., Louissaint, M., Colonna, L., Zaidi, B., Garcia-Verdugo, J.M. & Doetsch, F. (2008) A specialized vascular niche for adult neural stem cells. *Cell Stem Cell*, **3**, 279–288.
Tropepe, V., Craig, C.G., Morshead, C.M. & van der Kooy, D. (1997) Transforming growth factor-alpha null and senescent mice show decreased neural progenitor cell proliferation in the forebrain subependyma. *J. Neurosci.*, **17**, 7850–7859.
Villeda, S.A., Luo, J., Mosher, K.I., Zou, B., Britschgi, M., Bieri, G., Stan, T.M., Fainberg, N., Ding, Z., Eggel, A., Lucin, K.M., Czirr, E., Park, J.S., Couillard-Despres, S., Aigner, L., Li, G., Peskind, E.R., Kaye, J.A., Quinn, J.F., Galasko, D.R., Xie, X.S., Rando, T.A. & Wyss-Coray, T. (2011) The ageing systemic milieu negatively regulates neurogenesis and cognitive function. *Nature*, **477**, 90–94.
Walker, M.R., Patel, K.K. & Stappenbeck, T.S. (2009) The stem cell niche. *J. Pathol.*, **217**, 169–180.
Werry, E.L., Enjeti, S., Halliday, G.M., Sachdev, P.S. & Double, K.L. (2010) Effect of age on proliferation-regulating factors in human adult neurogenic regions. *J. Neurochem.*, **115**, 956–964.
Winner, B., Kohl, Z. & Gage, F.H. (2011) Neurodegenerative disease and adult neurogenesis. *Eur. J. Neurosci.*, **33**, 1139–1151.
Wong, K.K., Maser, R.S., Bachoo, R.M., Menon, J., Carrasco, D.R., Gu, Y., Alt, F.W. & DePinho, R.A. (2003) Telomere dysfunction and Atm deficiency compromises organ homeostasis and accelerates ageing. *Nature*, **421**, 643–648.
Zhang, J., Goodlett, D.R., Peskind, E.R., Quinn, J.F., Zhou, Y., Wang, Q., Pan, C., Yi, E., Eng, J., Aebersold, R.H. & Montine, T.J. (2005) Quantitative proteomic analysis of age-related changes in human cerebrospinal fluid. *Neurobiol. Aging*, **26**, 207–227.
Zhang, R., Zhang, Z., Wang, L., Wang, Y., Gousev, A., Zhang, L., Ho, K.L., Morshead, C. & Chopp, M. (2004) Activated neural stem cells contribute to stroke-induced neurogenesis and neuroblast migration toward the infarct boundary in adult rats. *J. Cerebr. Blood F. Met.*, **24**, 441–448.

APPENDIX C

MASTER'S PROJECT ARTICLE: "CELLULAR ORGANIZATION OF THE CENTRAL CANAL EPENDYMAL ZONE, A NICHE OF LATENT NEURAL STEM CELLS IN THE ADULT MAMMALIAN SPINAL CORD"

Neuroscience 164 (2009) 1044–1056

CELLULAR ORGANIZATION OF THE CENTRAL CANAL EPENDYMAL ZONE, A NICHE OF LATENT NEURAL STEM CELLS IN THE ADULT MAMMALIAN SPINAL CORD

L. K. HAMILTON, M. K. V. TRUONG, M. R. BEDNARCZYK, A. AUMONT AND K. J. L. FERNANDES*

Département de pathologie et biologie cellulaire, Groupe de recherche sur le système nerveux central (GRSNC), and Centre d'excellence en neuromique de l'Université de Montréal (CENUM), Université de Montréal, Montréal, Canada

Abstract—A stem cell's microenvironment, or "niche," is a critical regulator of its behaviour. In the adult mammalian spinal cord, central canal ependymal cells possess latent neural stem cell properties, but the ependymal cell niche has not yet been described. Here, we identify important similarities and differences between the central canal ependymal zone and the forebrain subventricular zone (SVZ), a well-characterized niche of neural stem cells. First, direct immunohistochemical comparison of the spinal cord ependymal zone and the forebrain SVZ revealed distinct patterns of neural precursor marker expression. In particular, ependymal cells in the spinal cord were found to be bordered by a previously uncharacterized sub-ependymal layer, which is relatively less elaborate than that of the SVZ and comprised of small numbers of astrocytes, oligodendrocyte progenitors and neurons. Cell proliferation surrounding the central canal occurs in close association with blood vessels, but unlike in the SVZ, involves mainly ependymal rather than sub-ependymal cells. These proliferating ependymal cells typically self-renew rather than produce transit-amplifying progenitors, as they generate doublets of progeny that remain within the ependymal layer and show no evidence of a lineage relationship to sub-ependymal cells. Interestingly, the dorsal pole of the central canal was found to possess a sub-population of tanycyte-like cells that express markers of both ependymal cells and neural precursors, and their presence correlates with higher numbers of dorsally proliferating ependymal cells. Together, these data identify key features of the spinal cord ependymal cell niche, and suggest that dorsal ependymal cells possess the potential for stem cell activity. This work provides a foundation for future studies aimed at understanding ependymal cell regulation under normal and pathological conditions.

Key words: mouse, sub-ependymal cells, differentiation, proliferation, precursors, tanycytes.

Adult neural stem cells are responsible for maintaining and repairing central nervous system (CNS) tissues. These crucial functions are controlled by the stem cell's "niche," that is, its adjacent cells, extracellular matrix molecules, diffusible factors and circulating signals, which together regulate stem cell survival, proliferation and differentiation (Fuchs et al., 2004; Morrison and Spradling, 2008; Walker et al., 2009). Understanding how neural stem cells and their niches interact is critical for determining why stem cells are highly neurogenic in some regions of the adult nervous system and quiescent in others, for promoting tissue regeneration following injury and disease, and for re-establishing appropriate stem cell regulation in cancer or in aging.

Neural stem cells possess an astrocytic phenotype in the subventricular zone (SVZ) of the forebrain, which is the most well-characterized stem cell niche in the adult CNS (Chojnacki et al., 2009). The SVZ stem cell niche is comprised of quiescent ependymal cells, which line the lateral ventricles, and a heterogenous mixture of sub-ependymal cells that includes astrocytes, transit-amplifying progenitors, neuroblasts, tanycytes, microglia, and blood vessels (Doetsch et al., 1997; Shen et al., 2008; Tavazoie et al., 2008; Pastrana et al., 2009). Sub-ependymal astrocytes are neural stem cells in the SVZ; they generate transit-amplifying progenitors, which produce migratory neuroblasts that replenish olfactory bulb interneurons (Lois and Alvarez-Buylla, 1994; Doetsch et al., 1999; Imura et al., 2003; Morshead et al., 2003). Astrocytic stem cells in the SVZ retain an apical contact with the lateral ventricle and a basal process that extends towards local vasculature (Mirzadeh et al., 2008; Shen et al., 2008; Tavazoie et al., 2008). They normally divide slowly, but following experimental depletion of SVZ cells, are capable of reconstituting the principal SVZ cell populations (Morshead et al., 1994; Doetsch et al., 1999).

Neural stem cells have also been isolated from the ependymal zone surrounding the central canal of the spinal cord (Weiss et al., 1996; Johansson et al., 1999; Martens et al., 2002). In the spinal cord, there is no defined sub-ependymal layer, there is no neurogenesis, and ependymal cells rather than astrocytes are the primary source of *in vitro* stem cell activity (Meletis et al., 2008). Little is known about the spinal cord ependymal cell niche, but cuboidal, tanycytic and radial classes of lumen-contacting, ciliated ependymal cells have been identified (Bruni and Reddy, 1987; Meletis et al., 2008). The antigenic and functional differences between these three classes of ependymal cells are unclear. However, ependymal cells are rapidly activated following spinal cord injury, proliferating and undergoing multi-lineage differentiation to

Abbreviations: BrdU, bromodeoxyuridine; CNS, central nervous system; d, day(s); DAB, 3,3-diaminobenzidine; DIV, days *in vitro*; E, embryonic; EGF, epidermal growth factor; FGF2, fibroblast growth factor-2; GFAP, glial fibrillary acidic protein; P, postnatal; SVZ, sub-ventricular zone.

0306-4522/09 $ - see front matter
doi:10.1016/j.neuroscience.2009.09.006

contribute astrocytes and oligodendrocytes to the injured tissue. Thus, at least a sub-population of spinal cord ependymal cells has latent neural stem cell properties (Johansson et al., 1999; Namiki and Tator, 1999; Meletis et al., 2008).

In the present study, we investigated whether key features of the well-defined forebrain stem cell niche exist surrounding the central canal. This detailed study of the spinal cord ependymal zone revealed that important elements of the SVZ stem cell niche are conserved surrounding the central canal, but with a distinct organization. Identifying the cellular organization of the ependymal cell niche will facilitate future efforts to understand and modify ependymal cell regulation under normal and pathological conditions.

EXPERIMENTAL PROCEDURES

Animals

Experiments were conducted in accordance with the guidelines of the Canadian Council of Animal Care and were approved by the institutional Animal Care committee. A total of 70 two-month-old CD1 mice (Charles River Laboratories, St. Constant, QC, Canada) were used. For bromodeoxyuridine (BrdU) incorporation experiments, mice were administered three 100 μl intraperitoneal injections of BrdU (Sigma, 1.5 mg/injection) at 3 hour intervals, and were sacrificed either 1 or 21 days later.

Neurosphere cultures from the adult spinal cord

Mice were given a lethal dose of chloral hydrate (7%) and a 12–16 mm segment from each lumbar spinal cord was dissected into ice cold HBSS (Wisent). Spinal cords were dissociated to single cells using papain (Worthington). Cells were re-suspended in 30 ml of DMEM/F12 (3:1) (Invitrogen) supplemented with 1% Penicillin/Streptomycin (Wisent), 1 μg/ml Fungizone (Invitrogen), 2% B27 (Invitrogen), 20 ng/ml epidermal growth factor (EGF) (Sigma) and 25 ng/ml fibroblast growth factor-2 (FGF2) (Sigma). The medium was replenished with EGF and FGF2 every 3–4 days and with B27 every week. To assess self-renewal and obtain greater numbers of neurospheres, primary spheres grown for 14 days were passaged by centrifugation, the pellet dissociated by trituration, and the cells re-plated under the same conditions.

To differentiate neurospheres for Western blotting and immunocytochemistry, secondary neurospheres were gently triturated and plated onto poly-L-lysine-coated dishes (0.02 mg/mL in sterile water; Sigma) in medium consisting of DMEM/F12 (3:1) (Invitrogen) supplemented with 1% Penicillin/Streptomycin (Wisent), 1 μg/ml Fungizone (Invitrogen), 2% B27 (Invitrogen), 1% fetal bovine serum (Wisent), 2 ng/ml EGF (Sigma) and 2 ng/ml FGF2 (Sigma). Differentiated cells were either lysed for Western blotting or fixed in 4% paraformaldehyde for 15 min for immunocytochemistry. Secondary spheres were characterized by plating them as above and processing them for immunocytochemistry after 4–6 hours.

Western blotting

For biochemical analyses, spinal cord-derived neurospheres were lysed using Ripa Buffer (1 M Tris pH 8, 5 M NaCl, NP-40 10%, SDS 10%, Sodium Desoxycholate 10% in dH_20) supplemented with sodium vanadate (25 μl/5 ml Ripa Buffer, Fisher) and protease inhibitors (Complete Mini, Roche Diagnostics). Protein concentrations were determined using the bicinchoninic acid assay (Pierce). Twenty-five micrograms of protein from each sample was boiled in sample buffer (0.5 M Tris–HCl pH 6.8, glycerol, SDS 10%, Bromophenol blue, β-mercaptoethanol), separated using SDS-PAGE (10% acrylamide), and transferred onto a Nitrocellulose membrane (0.45 μm, Bio-Rad). Membranes were immersed in Ponceau Red (0.2% Ponceau S (Fisher) in 11% trichloroacetic acid (Fisher)) to visualize the proteins, washed in Tris–buffered saline containing 0.2% Tween (TBS-T) and blocked in 5% skim milk powder (Carnation). They were then incubated overnight at 4 °C with primary antibody. The following antibodies were used: mouse anti-rat βIII tubulin (1:1000, Covance), mouse anti-human CNPase (1:1000, Chemicon), rabbit anti-cow GFAP (1:1000, Dako), and mouse anti-Xenopus β-actin (1:10 000, Abcam). HRP-conjugated secondary antibodies, diluted in blocking solution, were used as follows: anti-mouse IgG (1:5000, Bio-Rad) or anti-rabbit IgG (1:5000, Chemicon). Secondary antibodies were detected using the ECL chemiluminescence reagent kit (GE Health Care) and X-Omat Blue film (Kodak). Membranes were subsequently stripped with Re-Blot Plus Mild (Millipore), re-blocked and re-probed as described above.

Immunohistochemistry

Tissue processing and basic immunohistochemical procedures were performed as detailed in Bednarczyk et al. (Bednarczyk et al., in press).

The primary antibodies used were mouse anti-human Ki67 (1:200, BD Biosciences), mouse anti-mouse NeuN (1:200, Chemicon), chicken anti-Vimentin (1:1000, Chemicon), rabbit anti-mouse Olig2 (1:500, Chemicon), rabbit anti-rat NG2 (1:200, Chemicon), mouse anti-rat βIII tubulin (1:500, Covance), rabbit anti-human GAD65 (1:1000, Chemicon), rabbit anti-human Sox2 (1:1000, Chemicon), mouse anti-rat Mash-1 (1:100, BD Biosciences), mouse anti-human CNPase (1:500, Chemicon), rabbit anti-cow GFAP (1:1000, Dako), mouse anti-pig GFAP (1:1000, Chemicon), mouse anti-rat Nestin (1:400, BD Biosciences), chicken anti-Nestin (1:5000, Novus), rabbit anti-cow S100β (1:1000, Sigma), mouse anti-cow S100, β subunit (1:1000, Sigma), rat anti-mouse PECAM (1:300, BD Pharmingen) and rat anti-BrdU (1:200, AbD Serotec).

For bright-field immunohistochemistry, primary antibodies bound to sections were detected using the species-appropriate biotinylated secondary antibody (Jackson ImmunoResearch, PA, USA), the signal was amplified using the avidin–biotin-peroxidase system (VectaStain ABC Kit, Vector Laboratories), and revealed using a 3,3-diaminobenzidine (DAB)-containing solution (Bednarczyk et al., in press). For fluorescence immunohistochemistry, primary antibodies were detected using species-appropriate secondary antibodies that were conjugated to either CY3 (1:400, Jackson ImmunoResearch), Alexa 488 (1:1000, Invitrogen) or Alexa 647 (1:1000, Invitrogen). Nuclear counterstaining was performed using either Hoechst 33342 (0.2 μM, Sigma) or TOPRO-3 (1 μM, Invitrogen). For fluorescence double-labelling using anti-Ki67 and anti-Nestin antibodies, which were both raised in mouse, we used a sequential immunofluorescence procedure. Briefly, the same procedure was followed except that after the application of the Nestin primary antibody and detection using the anti-mouse CY3 secondary antibody, the sections were re-blocked for 30 min prior to incubation with the anti-Ki67 antibody. Fluorescence triple-labelling of BrdU, Ki67 and Vimentin was as described in (Bednarczyk et al., in press).

Microscopy was performed using either a motorized Olympus IX81 microscope equipped with a black and white CCD camera or a Leica SP1 laser-scanning confocal microscope. To generate multi-channel images, black and white images were colorized and merged using Adobe Photoshop. Image manipulations were limited to Brightness/Contrast, and were performed in a standardized manner to all images. Images were assembled into figures using Adobe Illustrator.

Resin-embedded semi-thin sections

Some sections processed for bright-field immunohistochemistry were further sectioned to 1 μm thickness to improve resolution of the signal. Following application of the DAB solution, sections were rinsed in phosphate buffer, fixed with 1% osmic acid (Electron Microscopy Science) for 30 min, dehydrated in a graded series of ethanols and propylene oxide (Fisher) and then embedded in electron microscopy grade Resin (Durcapan ACM, Sigma). Resin-embedded sections were cut at 1 micron thickness on an ultramicrotome (Ultracut E, Reichert Jung), counterstained with 0.5–1% toluidine blue and mounted on slides. They were then coverslipped using Permount, and examined using bright-field illumination.

Quantification of proliferating cells surrounding the central canal

The distribution of Ki67(+) cells surrounding the central canal was quantified following DAB-based and fluorescence-based immunohistochemistry. Diagrams were prepared in which the ependymal layer and sub-ependymal region of the central canal were each divided into dorsal, dorsomedial, ventral and ventromedial zones. Following DAB-immunohistochemistry, the ependymal layer was identified morphologically under phase-contrast illumination and the locations of Ki67(+) cells were recorded from 28–38 coronal sections from each of five animals. For fluorescence immunohistochemistry, the ependymal layer was identified based on Vimentin expression and the locations of Ki67(+) cells were recorded from 32–36 coronal sections from each of four additional animals. Cells were considered to belong to the region where the majority of the cell was located. For each animal, 100% was set to the total number of Ki67(+) cells, and the percentage of cells in each of the eight zones was calculated. Using both methods, summary diagrams were built by averaging the percentage of Ki67(+) cells per zone from all animals.

Quantification of blood vessels surrounding the central canal

The distribution of blood vessels surrounding the central canal and their proximity to proliferating ependymal cells was quantified following triple-label immunofluorescence for Ki67 and Vimentin and the endothelial marker PECAM. The central canal ependymal zone was again identified based on Vimentin expression. Diagrams were prepared where the central canal ependymal and sub-ependymal zones had three horizontal lines drawn through them; the first line was drawn directly through the midline and the other two were drawn at the dorsal and ventral extremities of the central canal. The quantification of PECAM (+) blood vessels was achieved by counting the number of times a blood vessel intersected either the dorsal, medial or ventral horizontal lines. The total number of blood vessel intersections with dorsal, medial and ventral lines was compiled from 10 coronal sections from each of three animals. Ki67(+) cells were simultaneously recorded as above.

RESULTS

Isolation and characterization of neurospheres from the adult mouse lumbar spinal cord

Multipotent neurospheres can be cultured from the adult mouse spinal cord (Weiss et al., 1996; Meletis et al., 2008). We were able to generate neurosphere cultures from the adult mouse lumbar spinal cord (Fig. 1) that expanded rapidly *in vitro* (Fig. 1a–d) and expressed typical neural stem cell markers such as Nestin, Sox2 and CD133 (Fig. 1e–j). Although neurogenesis does not occur in the adult spinal cord, spinal cord-derived neurospheres differentiated into neurons, astrocytes and oligodendrocytes *in vitro* (Fig. 1k–m), including GABAergic neurons (Fig. 1n–p). These experiments confirmed that multipotent, neurogenically competent neural stem cells can be isolated from the adult spinal cord. To better understand the *in vivo* regulation of spinal cord-derived stem cells, we characterized the ependymal cell niche, which is the origin of multipotent, self-renewing spinal cord-derived neurospheres (Johansson et al., 1999; Martens et al., 2002; Meletis et al., 2008).

SVZ-associated neural precursor markers are expressed surrounding the central canal

Immunohistochemical comparison of the forebrain SVZ and spinal cord ependymal zone showed that markers of SVZ-associated cell lineages are also found surrounding the central canal (Fig. 2). Ependymal cells of both the forebrain SVZ and the spinal cord central canal expressed Vimentin and S100β (Fig. 2a, b). Transit amplifying type C progenitor cells in the forebrain SVZ are located sub-ependymally and express NG2 and the nuclear transcription factors Olig2 (Fig. 2c, d) and/or Mash1 (not shown) (Doetsch et al., 1997; Aguirre et al., 2004). In the spinal cord, small numbers of NG2 and Olig2-expressing cells were likewise present directly adjacent to the ependymal cells, as well as scattered throughout the parenchyma (Fig. 2c, d). Mash1, which is associated with neurogenic SVZ progenitors, was not detected in the spinal cord (data not shown). Type B astrocytes and astrocytic stem cells in the forebrain SVZ are located sub-ependymally and express glial fibrillary acidic protein (GFAP) (Fig. 2e) (Doetsch et al., 1999). Surrounding the central canal, we observed (i) frequent GFAP-immunoreactive fibers of sub-ependymal astrocytes that extended into the ependymal layer and (ii) rare GFAP-immunoreactive cell bodies within the dorsal ependymal layer itself that possessed dorsally projecting processes (Fig. 2e). Ki67-immunoreactive proliferating cells, which are restricted to the sub-ependymal layer of the forebrain SVZ, were less common surrounding the central canal and found within the ependymal layer itself (Fig. 2f). Both sub-ependymal and ependymal cells in the forebrain SVZ express Nestin and the transcription factor Sox2 (Fig. 2g, h). Within the spinal cord, Nestin immunoreactivity was not detected in the majority of ependymal cells, but it was prominently expressed by a sub-population of cells at the dorsal pole of the ependymal zone (Fig. 2g). These dorsal Nestin-expressing cells possessed long Nestin-immunoreactive filaments that extended along the dorsal midline. Similar fibers were sometimes seen extending from the ventral pole and occasionally from the lateral ependymal zone (Fig. 2g), but these displayed far weaker Nestin immunoreactivity. Sox2, unlike Nestin, was highly expressed throughout the ependymal zone of the central canal (Fig. 2h), as well as in some sub-ependymal cells.

Together, this comparison revealed that several markers of SVZ-associated neural precursor lineages are also expressed in the ependymal and/or sub-ependymal zones of the adult spinal cord. To understand the composition of the ependymal cell niche, we investigated these observations in greater detail.

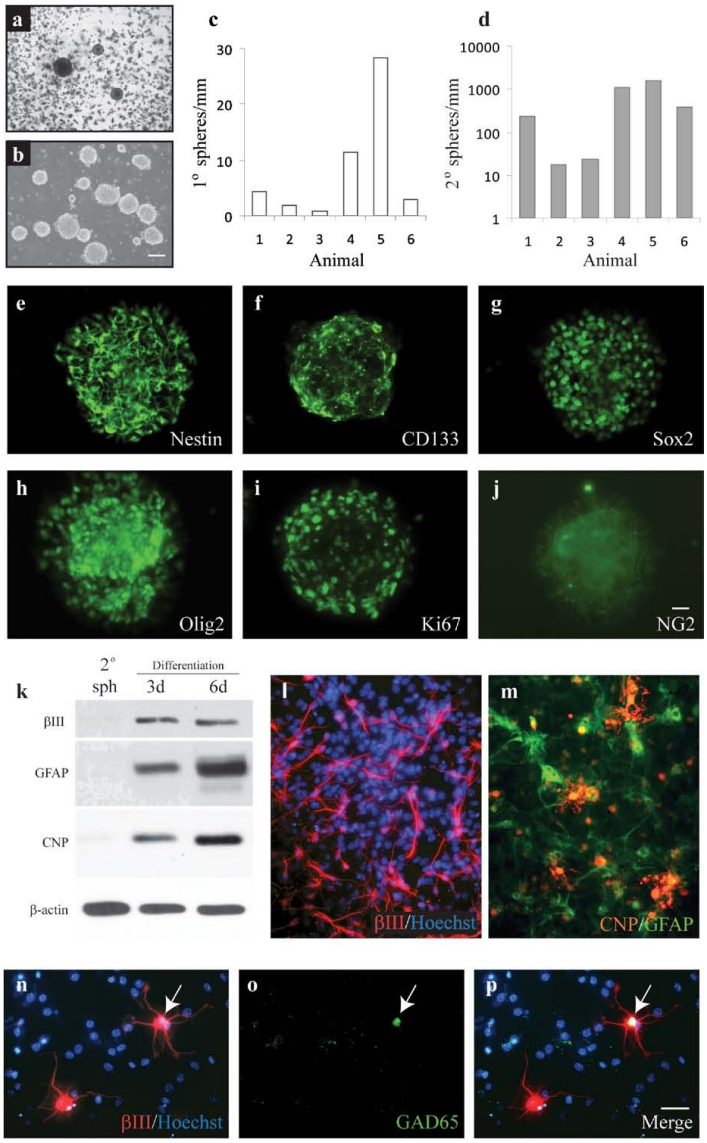

Fig. 1. Isolation and characterization of neurospheres from the adult mouse lumbar spinal cord. Lumbar spinal cords of adult mice were dissected, dissociated and plated using standard neurosphere forming conditions. Small spheres were visible after 1 week and reached full size after 14 days *in vitro* (DIV) (Fig. 1a), at which time they were similar in size and morphology to 7 DIV forebrain neurospheres (not shown). Passaged primary (1°) neurospheres generated secondary (2°) neurospheres after 7 DIV (Fig. 1b). Quantification of the total number of 1° (c) and 2° (d) neurospheres obtained per mm of spinal cord showed that up to 30 1° spheres were grown per mm of lumbar spinal cord; upon passaging, these spheres generated up to 1600 2° spheres/mm. Using the same culture conditions, approximately 800 primary spheres are typically generated from a single adult striatal SVZ (data not shown) Note that the cellular debris from the spinal cord seen in 1° cultures (a) was removed upon passaging (b). Immunohistochemistry for various stem/progenitor/proliferation markers on 2° neurospheres (e–j), illustrating that Nestin, CD133, Sox2, Olig2 and Ki67 were abundantly expressed (e–i) while NG2 was not present at detectable levels (j). 2° neurospheres were differentiated and assessed for multipotentiality by Western blot analysis and immunocytochemistry using antibodies against neurons (βIII tubulin), astrocytes (GFAP) and oligodendrocytes (CNP) (k–m). Analysis by Western blotting revealed the absence of neuron, astrocyte and oligodendrocyte markers in undifferentiated 2° spheres and their appearance after as little as 3 days (d) of differentiation (k). After 9 d of differentiation, cells displaying the appropriate morphologies for all three neural cell types were detectable by immunocytochemistry (l, m). After 18 d of differentiation, a sub-population of βIII tubulin-expressing neurons co-expressed the GABAergic marker GAD65 (arrow, n–p). Differentiated cultures were counterstained with Hoechst 33342 to identify nuclei (l, n, p). Scale bar in b=120 μm (for a, b), in j=20 μm (for e–j), in p=10 μm (for l–p).

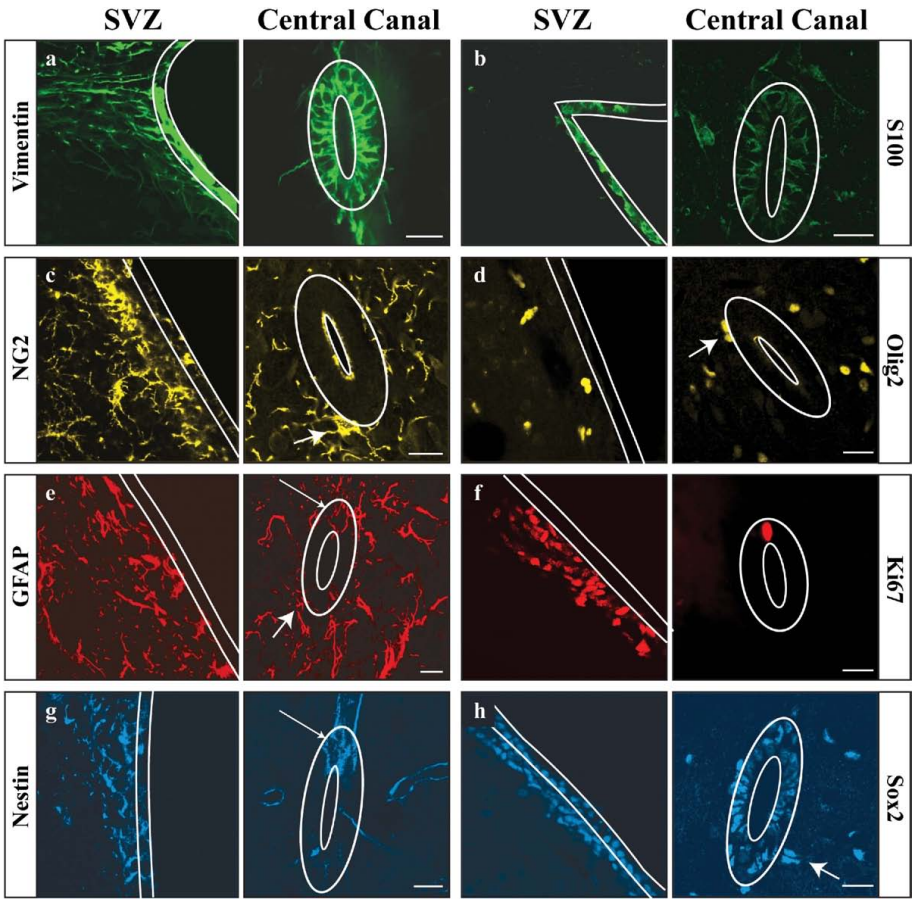

Fig. 2. Comparison of neural precursor marker expression within the forebrain subventricular zone (SVZ) and the spinal cord ependymal zone. Fluorescence immunohistochemistry was performed on 40 μm sections of the forebrain SVZ and spinal cord central canal. Forebrain ependymal cell markers Vimentin (a) and S100β (b) were expressed by ependymal cells lining the central canal. The forebrain progenitor markers NG2 (c) and Olig2 (d) were not expressed within the ependymal layer of the spinal cord, but were often present adjacent to the ependymal layer (short arrows). GFAP (e), a marker of forebrain neural stem cells and astrocytes, was expressed by sub-ependymal astrocytes immediately adjacent to the spinal cord ependymal layer (e, short arrow), and GFAP immunoreactivity was also observed at the dorsal pole of the central canal ependymal layer (e, long arrow). Ki67 (f), a marker of proliferating cells, was exclusively expressed sub-ependymally in the forebrain but was concentrated within the ependymal layer surrounding the central canal. Nestin (g), a marker of undifferentiated stem cells and progenitors throughout the forebrain SVZ, was expressed at the poles of the spinal cord ependymal layer (long arrow) and displayed long, dorsally directed projections. Sox2 (h), a second neural stem cell and progenitor marker in the forebrain SVZ, was expressed by all the ependymal cells of the central canal as well as by some sub-ependymal cells just outside of this zone (short arrow). In all panels, white lines illustrate the approximate borders of the ependymal layer. Scale bars=15 μm.

The central canal possesses a rudimentary sub-ependymal zone

Unlike the forebrain SVZ, the central canal lacks a distinct layer of sub-ependymal cells. Given the expression of neural precursor markers surrounding the central canal, we used two different approaches to assess the possibility that small numbers of sub-ependymal cells may nevertheless be present. First, we performed immunofluorescence for the ependymal cell marker Vimentin and counter-stained with the general nuclear marker TOPRO-3 (Fig. 3a). Using this approach together with confocal microscopy, we identified the nuclei of numerous Vimentin(–) cells that were tightly apposed to the Vimentin-expressing ependymal layer. We confirmed this observation on 1 μm semi-thin sections using DAB-based immunohistochemistry for a second ependymal cell marker, S100β and counter-stained with toluidine blue (Fig. 3b); again, we observed the nuclei of numerous S100β(−) cells juxta-

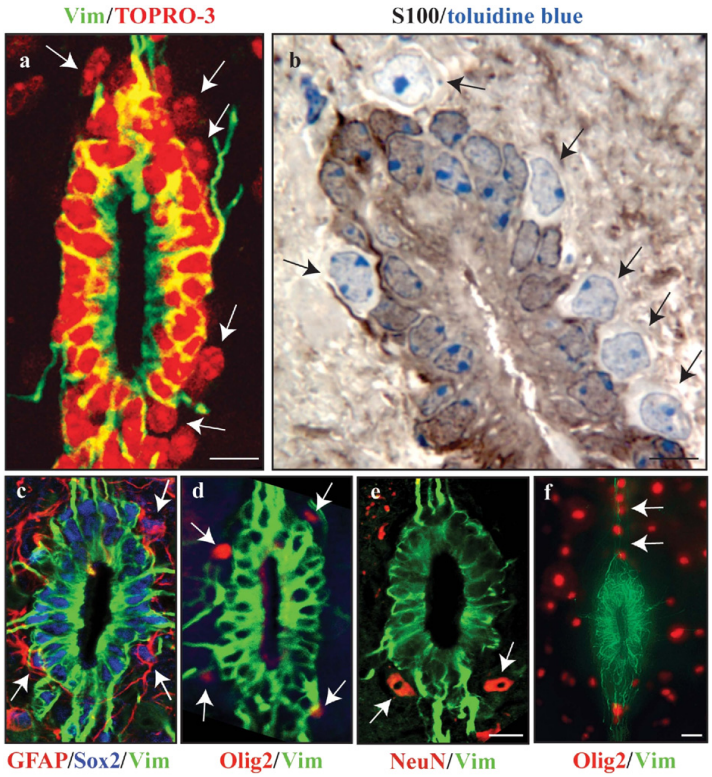

Fig. 3. Detection of sub-ependymal cells in close apposition to the ependymal cell layer of the central canal. Confocal image of immunofluorescence for the ependymal cell marker Vimentin and the general nuclear marker TOPRO-3 (a). Multiple unlabelled nuclei are found directly adjacent to the Vimentin(+) ependymal cells (arrows). 1 μm semi-thin section stained for the ependymal cell marker S100β using DAB-immunohistochemistry and counterstained with toluidine blue (b). The nuclei of several S100β(−) cells (arrows) are closely apposed to the S100β(+) ependymal cell layer. Immunohistochemical characterization of sub-ependymal cells (c–e). Sub-populations of Vimentin(–) sub-ependymal cells were observed that were either GFAP(+)Sox2(+) (c), Olig2(+) (d) or NeuN(+) (e) (arrows). Olig2(+) cells could also be observed along the radial fibers of Vimentin(+) dorsal ependymal cells (f) (arrows). Scale bars in a, b, e (for c–e) and f=10 μm.

posed against the S100β(+) ependymal cells. Cells that were in close contact with the ependymal layer were surprisingly abundant using both these approaches, as we typically observed about 6 cells/1 μm cross-section through the central canal. To determine the antigenic profile of these sub-ependymal cells we used multi-label immunofluorescence. These experiments revealed multiple cell types within the immediate microenvironment of ependymal cells, including GFAP(+)Sox2(+) astrocytes, Olig2(+) oligodendrocyte progenitors and NeuN(+) neurons (Fig. 3c–e). In addition, Olig2(+) cells were often observed along the basal processes of ependymal cells (Fig. 3f). Thus, the ependymal cell niche includes several sub-ependymal cell types that closely border the ependymal layer.

Proliferating ependymal cells are concentrated dorsally

Previous work has used BrdU incorporation into the DNA of dividing cells to reveal the existence of small numbers of constitutively proliferating spinal cord ependymal cells (Horner et al., 2000). To identify and characterize the cells proliferating surrounding the central canal in greater detail, we performed immunohistochemistry for Ki67, a marker expressed by actively proliferating cells at all stages of their cell cycle (Fig. 4). Proliferating cells were identified throughout the grey and white matter, as well as surrounding the central (Fig. 4a). Between zero and nine Ki67(+) cells were observed in the ependymal/sub-ependymal layers per section (Fig. 4b, c).

To assess the distribution of proliferating cells surrounding the central canal, spinal cord cross-sections were analyzed for Ki67 expression using DAB immunohistochemistry and phase-contrast microscopy (Fig. 4d–g). Ki67(+) cells were primarily found in the ependymal layer, however a small number of proliferating cells appeared to have a sub-ependymal localization (Fig. 4d, e). Quantification of the dorso-ventral distribution of Ki67(+) cells

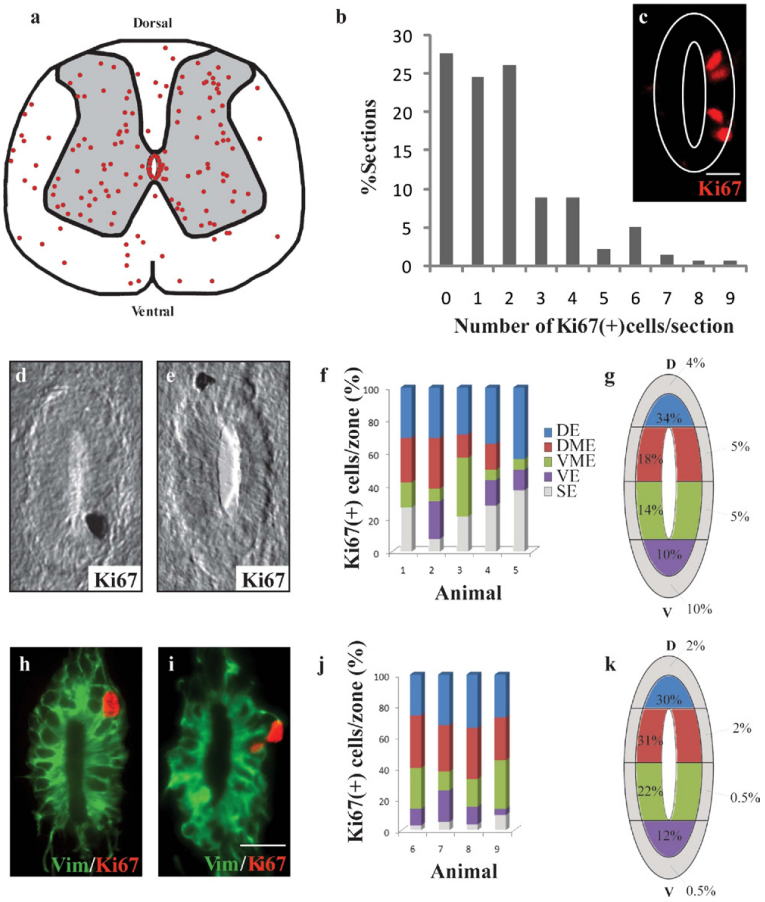

Fig. 4. Proliferating ependymal cells are concentrated dorsally. Schematic showing the distribution of proliferating cells throughout the grey and white matter of the spinal cord (a). The locations of Ki67 immunoreactive cells were compiled from 20–25 coronal sections from each of three animals. Quantification of the number of Ki67(+) ependymal and sub-ependymal cells per sections (b). Between 0 and 9 cells were counted per section. A representative image of Ki67(+) cells in the ependymal zone is shown in (c). The dorsal-ventral and ependymal/sub-ependymal distributions of proliferating cells surrounding the central canal were determined using both DAB-immunohistochemistry for Ki67 (d–g) and fluorescence immunohistochemistry for Ki67 and Vimentin (h–k). The ependymal (E) and sub-ependymal (SE) regions were each sub-divided into four zones along the dorso-ventral axis: dorsal, dorsomedial, ventromedial and ventral. Using both DAB and fluorescence immunohistochemical approaches, the majority of Ki67(+) proliferating cells were found to be located in the ependymal layer (d, h). Ki67(+) nuclei were also infrequently detected in cells located adjacent to the ependymal layer (e, i). Individualized data of the percentage of Ki67(+) cells found within the dorsal ependymal (DE), dorsomedial ependymal (DME), ventromedial ependymal (VME), ventral ependymal (VE), and total SE zones using each immunohistochemical method is shown in (f, j), and summary diagrams of the group percentages of Ki67(+) cells/zone is shown in (g, k). Note that both approaches revealed that higher numbers of Ki67(+) proliferating ependymal cells are located dorsally. For DAB-immunohistochemistry, data were compiled from 28–38 sections/animal, 13–32 cells/animal, $n=5$ animals. For fluorescence immunohistochemistry, data were compiled from 32–36 sections/animal, 51–79 cells/animal, $n=4$ animals. Scale bar in c=10 μm and i=15 μm (for d, e, h, i).

revealed that all five animals examined possessed a greater number of Ki67(+) cells at the dorsal pole compared to the ventral pole, and in four of the five animals this difference was at least two-three fold (Fig. 4f). Group analysis revealed a dorsal-to-ventral proliferation gradient in the ependymal layer with more than three times as many proliferating cells found within the dorsal ependymal zone (33.6±2.41%) when compared to the ventral ependymal zone (10.2±4.04%) (Fig. 4g).

To verify the dorsal concentration of ependymal cell proliferation, as well as to more reliably distinguish between ependymal and sub-ependymal cells, we performed double-label immunofluorescence with Ki67 and Vimentin and repeated the above analysis using four additional

animals (Fig. 4h–k). The vast majority of proliferating cells were found to be Vimentin(+) ependymal cells (Fig. 4h), however a small number of Vimentin(–) proliferating cells were also observed sub-ependymally (Fig. 4i). When the dorsal-ventral analysis was repeated as above, approximately 95% of proliferating cells surrounding the central canal were found to be Vimentin(+) ependymal cells and 5% were Vimentin(–) sub-ependymal cells (Fig. 4j, k). The number of sub-ependymal cells identified with this approach may be an underestimation, as cells were only classified as sub-ependymal when they were clearly not co-labelled with Vimentin. Using this more stringent classification strategy, all animals again possessed a greater number of Ki67(+) cells at the dorsal pole compared to the ventral pole, with individual dorsal-ventral pole differences ranging from 1.5 to 10 fold (Fig. 4j). Group data confirmed a dorsal concentration of Ki67(+) proliferating ependymal cells, with 30.0±1.67% of proliferating cells within the dorsal ependymal zone versus 11.6±2.90% in the ventral ependymal zone (Fig. 4k).

Together, these results reveal an asymmetric distribution of ependymal cell proliferation surrounding the central canal, with higher numbers of proliferating ependymal cells located at the dorsal pole.

Proliferating central canal ependymal cells undergo self-renewing divisions in close proximity to local vasculature

Recent studies indicate that neural precursor proliferation in both the forebrain SVZ and the hippocampal subgranular zone occurs in close association with blood vessels (Palmer et al., 2000; Shen et al., 2008; Tavazoie et al., 2008). To assess whether proliferating ependymal cells possess a similar relationship with blood vessels, sections of the spinal cord were processed for fluorescence immunohistochemistry for Vimentin, Ki67 and platelet endothelial cell adhesion molecule (PECAM), an endothelial cell marker. This analysis failed to provide evidence for a clear relationship between blood vessels and ependymal cell proliferation, as proliferating ependymal cells were often non-existent when vessels projected into the ependymal layer itself (Fig. 5a, b). Since the relationship between neural precursor proliferation and the vasculature in the SVZ was likewise not evident until examined in the rostrocaudal longitudinal direction (Shen et al., 2008; Tavazoie et al., 2008), we also analyzed longitudinal sections of the spinal cord (Fig. 5c, d). Ki67(+)Vimentin(+) ependymal cells were found at regular intervals along the rostrocaudal axis and were visualized almost exclusively in doublets (Fig. 5c, d), in contrast to what was observed using coronal sections (Fig. 4b). Moreover, the examination of these longitudinal sections revealed that doublets of Ki67(+)Vimentin(+) cells surrounding the central canal were consistently located within approximately 12 microns of the PECAM-immunolabelled blood vessels (Fig. 5d). While Ki67(+) cells were concentrated dorsally (Fig. 4), quantification showed no evidence for a differential distribution of blood vessels between dorsal, medial and ventral regions of the central canal (1.1±0.14, 1.2±0.22, and 1.03±0.24 blood vessel intersections/section, respectively). Taken together, these data indicate that ependymal cell proximity to blood vessels is necessary but not sufficient to stimulate their proliferation.

While proliferation in the forebrain SVZ is mediated by rapidly dividing transit-amplifying progenitors, proliferating ependymal cells did not show evidence of producing such transit-amplifying progenitors under normal conditions. Dividing cells were tagged by administering BrdU to a group of animals that were sacrificed either 1 or 21 days post-injection (Fig. 5e–i). As expected from the Ki67 results (above), virtually all ependymal cells that incorporated BrdU 1 day earlier were found in doublets (97.5±1.25%) and still expressed Ki67 (97.6±1.94%). The vast majority of BrdU-retaining cells remained in doublets even after 21 days (90.2±5.95%). The small fraction of single BrdU-retaining cells may simply represent doublets that were divided upon sectioning of the tissue. Of the 21 day BrdU-retaining cells, only 51.4±3.84% remained proliferative (i.e. double-labelled with Ki67) (Fig. 5h, i). There were no cases of BrdU(+) doublets composed of one Ki67(−) cell and one Ki67(+) cell, and all BrdU(+) doublets were composed of Vimentin(+) ependymal cells. Thus, unlike astrocytic forebrain stem cells, dividing spinal cord ependymal cells do not produce rapidly dividing transit amplifying progenitors under normal conditions. The fact that both daughter cells remain within the ependyma is suggestive of symmetrical ependymal cell division, and implies that the primary function of ependymal cell proliferation under normal circumstances is ependymal cell maintenance.

Neural precursor markers are expressed at the dorsal pole of the central canal

In the forebrain SVZ, Nestin and GFAP are markers of undifferentiated neural precursors and astrocyte-like neural stem cells, respectively. Given the concentration of ependymal cell proliferation at the dorsal pole of the central canal, we studied the Nestin and GFAP immunoreactivity that was previously observed in this dorsal area (Fig. 2) in greater detail.

Multiple approaches demonstrated that dorsal ependymal cells preferentially express Nestin. Using DAB-immunohistochemistry, Nestin-immunoreactive fibers could be observed extending from the dorsal ependymal layer and spanning the entire distance of the grey matter to the dorsal columns (Fig. 6a). At higher magnification, similar fibers displaying much weaker Nestin immunoreactivity could also be detected extending from the ventral ependymal layer (Fig. 6b). This pattern of Nestin immunoreactivity was confirmed using two separate antibodies to Nestin (not shown). On 1 μm semi-thin sections, Nestin immunoreactivity was detected in the apical cytoplasm and basal processes of cells whose nuclei were located within the dorsal ependymal layer (Fig. 6c). Moreover, when sections were triple-labelled using immunofluorescence for Nestin and the ependymal markers Vimentin and Sox2, analysis by confocal microscopy confirmed that the Nestin(+) dorsal cells express ependymal cell markers (Fig. 6d). In order to determine if the Nestin(+) dorsal ependymal cells con-

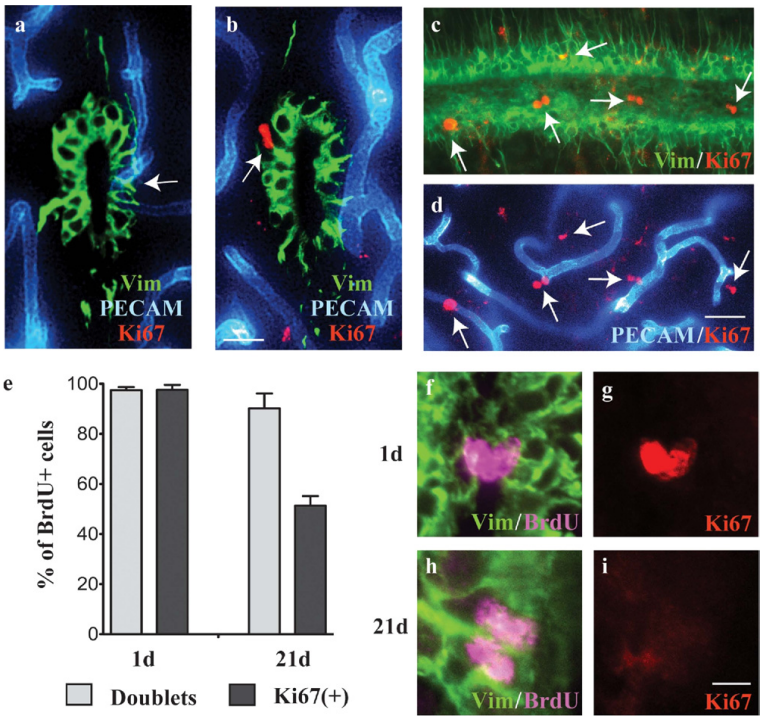

Fig. 5. Ependymal cells divide near the surface of blood vessels and do not produce transit-amplifying progenitors. Triple-label immunofluorescence for Vimentin, Ki67 and PECAM on coronal (a, b) and longitudinal (c, d) sections through the spinal cord ependymal zone. Ki67(+) proliferating ependymal cells do not exhibit a consistent relationship with PECAM(+) blood vessels on coronal sections, as they were often absent when vessels passed through the ependymal layer (a, arrow) and were often present at locations not immediately adjacent to blood vessels (b, arrow). When examined on longitudinal sections, however, Ki67(+) proliferating cells within the Vimentin(+) ependymal zone were typically found in doublets (c, d arrows) and were invariably associated with blood vessels (d, arrows). To assess the fate of proliferating ependymal cells, fluorescence immunohistochemistry was performed for BrdU, Ki67 and Vimentin on longitudinal spinal cord sections of mice treated with BrdU either 1 day (d) or 21 d earlier (e–h). Vimentin immunoreactivity was used to locate the regions containing the ependymal layer. Quantification of the percentage of BrdU-incorporating cells found in doublets or expressing Ki67 after 1 d (n=3) and 21 d (n=3) (e). Virtually all BrdU(+) cells were found in doublets at both time points, indicating that transit-amplifying progenitors are not produced (e). Doublets were almost all Ki67(+) at 1 d (e, f, g) but 50% of these doublets were no longer Ki67(+) after 21 d (e, h, i). Errors bars represent the standard error of the mean (SEM) of these data. Scale bar in b=10 μm (for a, b), d=35 μm (for c, d) and in i=6 μm (for f–i).

tributed to the dorsal concentration of proliferation that we previously observed (Fig. 4), we double-labelled sections for Ki67 and Nestin. Proliferating cells in the dorsal ependymal layer typically expressed Nestin and had a basal process (Fig. 6e). Thus, dorsal ependymal cells are strongly immunoreactive for a marker of undifferentiated neural precursors, Nestin, and proliferating cells in this dorsal region are part of the Nestin(+) population.

The same immunohistochemical analyses were carried out to evaluate GFAP immunoreactivity within the dorsal ependymal layer (Fig. 6f–j). Under epi-fluorescence illumination, GFAP-immunoreactive processes were commonly observed projecting into the ependymal layer (Fig. 2e), however it was not always apparent whether the cell bodies of origin were ependymal cells or sub-ependymal astrocytes. When using DAB-immunohistochemistry, GFAP-immunoreactive cell bodies could be observed within the ependymal layer itself (Fig. 6g, h). These cells were mainly located at the dorsal pole of the ependymal zone, and possessed both a lumen-contacting apical process and a dorsally-projecting basal process on semi-thin sections (Fig. 6h). Confocal microscopy of triple-labelling with GFAP, Vimentin (which under normal conditions is solely expressed by ependymal cells, and not by GFAP-expressing astrocytes, Fig. 3c) and Sox2 (which is expressed by both ependymal cells and astrocytes, Fig. 3c) indicated that the GFAP-expressing cells are antigenically consistent with being ependymal cells (Fig. 6i). The same findings were made using two separate GFAP antibodies (not shown). Quantification of GFAP(+)Vimentin(+) cells revealed an average of 1.91±0.54 cells/section (n=3 animals, 15 sections/animal). These cells had a dorsal-to-ventral gradient with 82.2±19.5% located dorsally, 11.4±13.2% medially, and 6.38±6.32% ventrally. Interestingly, when we per-

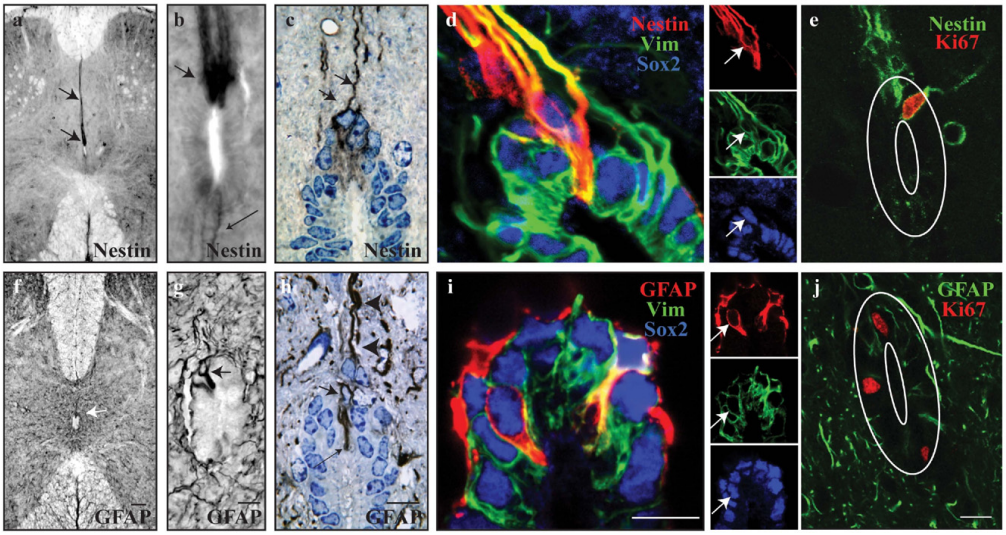

Fig. 6. Expression of Nestin and GFAP within the dorsal ependymal layer. DAB immunohistochemistry for Nestin (a–c) and GFAP (f–h) on spinal cord cross-sections. At low magnification, Nestin-expressing cells were apparent within the dorsal ependymal zone and displayed prominent dorsally projecting fibers. These fibers extended the entire length of the dorsal median grey matter (a, short arrows). At higher magnification, pronounced Nestin expression was detected within the cells of the dorsal ependymal zone and their dorsally projecting fibers (b, short arrow). Ventrally projecting fibers that were less Nestin immunoreactive were also visible projecting from the ventral pole (b, long arrow). Toluidine blue counterstaining of 1 μm semi-thin sections showed Nestin expression within the cytoplasm and dorsally projecting fibers of cells in the dorsal ependymal zone (c, short arrows). At low magnification, GFAP-expressing astrocytes were scattered throughout the parenchyma but GFAP immunoreactivity could also be observed within the ependymal zone (f, white arrow). At higher magnifications (g) and on toluidine blue-counterstained semi-thin sections (h), 1–2 GFAP-immunoreactive cell bodies consistently appeared to be present within the dorsal ependymal layer (short arrows). Note the GFAP immunoreactivity within the perinuclear cytoplasm (short arrow), the apical cytoplasm that contacts the lumen of the central canal (long arrow), and within dorsally projecting basal fibers (arrowheads) (h). Triple-label immunofluorescence was performed for the ependymal cell markers Vimentin and Sox2, together with either Nestin (d) or GFAP (i). Both the Nestin-expressing and GFAP-expressing cells were found to co-express the ependymal cell markers (d, i, short arrows). Immunofluorescence for Ki67 and either Nestin (e) or GFAP (j), illustrating that Ki67(+) ependymal cells usually co-express Nestin (e) but not GFAP (j). Scale bar in f=70 μm (for a, f), in g=15 μm (for b, g), in h=10 μm (for c, h), in i=10 μm (for d, i) and in j=10 μm (for e, j).

formed double-labelling for GFAP and Ki67, we did not observe proliferating GFAP(+) cells within the ependymal layer (Fig. 6j), indicating either that GFAP(+)Vimentin(+) cells do not proliferate or that they proliferate only rarely. However, it is intriguing that the distribution of GFAP(+) immunoreactive cells directly correlates with the proliferation gradient previously observed (Fig. 4).

Collectively, the selective expression of Nestin and GFAP by cells in the dorsal ependymal zone contributes to an unexpected degree of cellular heterogeneity within the ependymal cell niche, as summarized in a model in Fig. 7.

DISCUSSION

Unlike the highly neurogenic astrocyte-like stem cells of the forebrain SVZ, ependymal cells of the spinal cord are normally relatively quiescent, only displaying stem cell properties following tissue injury or in culture (Frisen et al., 1995; Johansson et al., 1999; Martens et al., 2002; Meletis et al., 2008). In the present study, we analyzed the cellular organization of the spinal cord ependymal cell niche. We show that the spinal cord ependymal zone possesses many key features of the SVZ stem cell niche, however with a distinct organization. The model of the ependymal cell niche provided by this work (Fig. 7) will facilitate further investigation of the cellular and molecular mechanisms controlling the stem cell properties of spinal cord ependymal cells.

A rudimentary sub-ependymal layer surrounds the central canal

Although the central canal is known to lack a distinct sub-ependymal layer, we identified small numbers of sub-ependymal cells that were situated immediately adjacent to the ependymal layer and that were antigenically distinct from ependymal cells. These cells expressed markers of astrocytes, oligodendrocyte progenitors and neuronal cells, which are likewise found (in higher numbers) within the forebrain SVZ. It is important to note that, despite similarities in the composition of sub-ependymal cell types in the SVZ and spinal cord, there are fundamental differences. Within the SVZ, sub-ependymal cells constitute a direct lineage, from astrocyte-like stem cells to transit-amplifying progenitors to migratory neuroblasts and glioblasts. This highly neurogenic astrocytic stem cell-derived

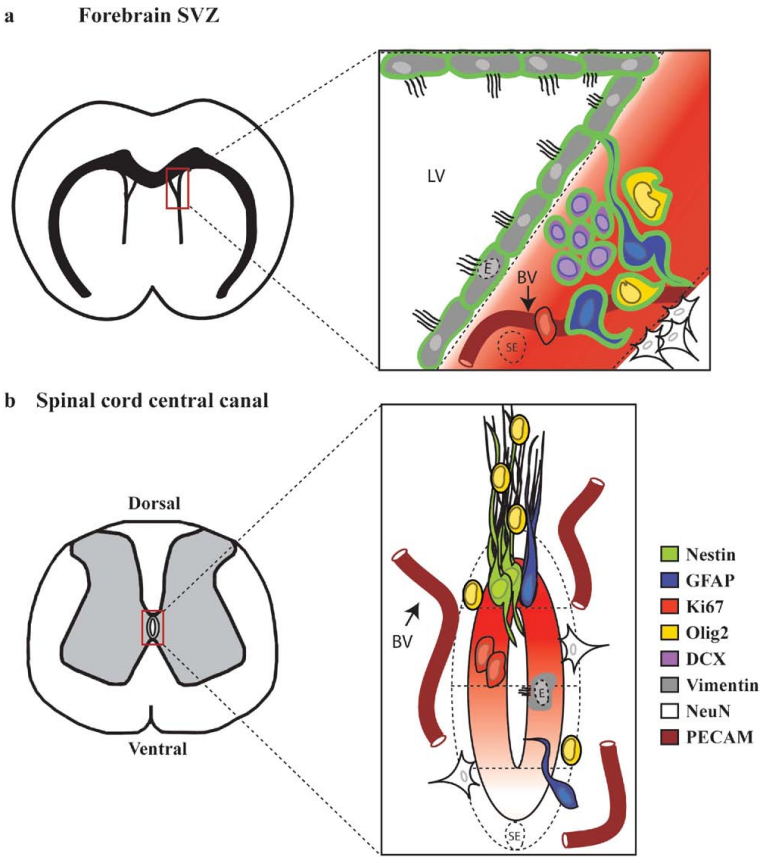

Fig. 7. Comparison of the key features of the forebrain SVZ stem cell niche and spinal cord ependymal cell niche. In the forebrain (a), the lateral ventricles (LV) are lined with ciliated ependymal cells (E) that express Vimentin (grey) and Nestin (green). Ki67(+) proliferating cells (red) are solely sub-ependymal and are invariably found closely apposed to PECAM-expressing blood vessels (Shen et al., 2008; Tavazoie et al., 2008) (BV, dark red). Within the sub-ependymal zone (SE), there are GFAP-expressing astrocytes (blue), Olig2-expressing progenitors (yellow) and DCX-expressing neuroblasts (violet) which all co-express Nestin. NeuN-expressing neurons (white) are located beneath the sub-ependymal zone and do not proliferate. In the spinal cord (b), the central canal is lined with ciliated ependymal cells that likewise express Vimentin. Ki67(+) proliferating cells are primarily found within the ependymal rather than sub-ependymal zone and are distributed in a dorsal to ventral gradient (red gradient). Rare sub-ependymal proliferation is also detected (not illustrated). Proliferating cells are found in doublets and are always closely apposed to PECAM-expressing blood vessels (however, this association is not clearly evident on coronal sections). There are Nestin-expressing and GFAP-expressing Vimentin(+) cells at the dorsal pole that possess extensive basal projections. Within the sub-ependymal layer, there are GFAP(+) astrocytes, NeuN(+) neurons and Olig2(+) oligodendrocyte progenitors. Olig2(+) cells are often observed along the basal processes of dorsal ependymal cells.

lineage results in the formation of a prominent sub-ependymal zone of proliferating cells. Thus, sub-ependymal astrocytic stem cells are capable of replenishing all principal SVZ cell types, including the forebrain ependymal cells (Morshead et al., 1994; Doetsch et al., 1999; Luo et al., 2008). There is no evidence for such a lineage relationship among the cells surrounding the non-neurogenic central canal, where the vast majority of proliferation occurs ependymally, there is only a rudimentary sub-ependymal layer, and sub-ependymal neurons are actually mature NeuN(+) neurons rather than Doublecortin(+) neuroblasts. Since previous lineage tracing experiments have shown that all neurosphere-forming capacity in the adult spinal cord originates from ependymal cells (Meletis et al., 2008), it is likely that sub-ependymal astrocytes, oligodendrocyte progenitors and neurons that directly surround the central canal act as regulatory influences within the ependymal cell niche.

A dorsal concentration of self-renewing ependymal cells

We detected a consistent dorsal-to-ventral gradient of proliferating ependymal cells. This gradient may be due to

intrinsic dorsal-to-ventral differences between ependymal cells or to a dorsal concentration of mitotic signals. Proliferating ependymal cells were almost always found in doublets when examined along the rostro-caudal axis and they were closely associated with the vasculature. The close proximity of Ki67(+) proliferating ependymal cells to blood vessels has similarities to recent observations in the forebrain SVZ (Shen et al., 2008; Tavazoie et al., 2008). Interestingly, in both the SVZ and the spinal cord ependymal zone, the relationship between proliferation and vasculature was ambiguous when examined on cross-sections, and only became apparent when longitudinal/sagittal sections were analyzed. In the case of the central canal, we did not detect a dorso-ventral difference in blood vessel density surrounding the central canal, suggesting that proximity to vasculature is necessary but not sufficient for ependymal cell proliferation. The close association of proliferating ependymal cells with blood vessels raises the possibility of ependymal cell regulation by systemically-mediated hormonal changes and/or pharmacological treatments (Tavazoie et al., 2008).

Our findings indicate that proliferating central canal ependymal cells normally divide symmetrically rather than generate transit-amplifying progenitors. Unlike in the forebrain SVZ, where astrocytic stem cells generate rapidly dividing Type C progenitors, central canal ependymal cells that had incorporated BrdU continued to be found in doublets after 21 days, indicating (i) that they do not produce a transit-amplifying daughter cell, and (ii) that neither daughter cell migrates out of the ependymal cell layer. Thus, under normal conditions, it appears that proliferating ependymal cells primarily produce ependymal cell progeny that remain resident in the ependymal layer. Previous studies suggest that the mode of ependymal cell division is drastically altered following spinal cord injury. Injury induces a rapid and marked increase in the proportion of ependymal cells that are proliferating, and ependymally-derived cells infiltrate the entire injury site, generating at least astrocytes and oligodendrocytes (Frisen et al., 1995; Namiki and Tator, 1999; Mothe and Tator, 2005; Meletis et al., 2008; Cizkova et al., 2009). Elucidation of the molecular signals underlying this symmetric-to-asymmetric transition in ependymal cell division is an important future objective.

A sub-population of cells at the dorsal pole of the central canal co-expresses ependymal and neural precursor markers

Nestin, a marker of undifferentiated neural cells in both the developing and adult nervous systems, was found to be highly expressed in a dorsal population of central canal ependymal cells. These dorsal ependymal cells possessed filamentous processes that extended along the dorsal midline to the dorsal column white matter. Weaker Nestin immunoreactivity was also present at the ventral pole. Dorsal cells that were proliferating were also found to co-express Nestin. Thus, Nestin expression may define a more immature ependymal cell phenotype. Interestingly, we also identified relatively rare (1–2 cells/section) cells at the dorsal pole that express GFAP. GFAP is expressed by astrocytes throughout the nervous system, but also by primitive neural stem cells in the forebrain SVZ (Doetsch et al., 1999; Imura et al., 2003; Morshead et al., 2003). In the present study, we found that the GFAP-expressing cells at the dorsal pole co-expressed Vimentin, a marker solely expressed by ependymal cells under normal conditions. Further work will be required to evaluate the nature of these cells.

Based on their long, basally projecting fibers, Nestin-expressing cells correspond to tanycytic or radial ependymal cells. Cells having the distinctive morphology of the Nestin-expressing cells described here appear to derive from “ependymoglial cells” that originate early during embryonic spinal cord development. Following closure of the neural tube and fusion of the dorsal walls of the central canal, at approximately E15 in the mouse, the neuroepithelial-derived ependymoglial cells persist at the dorsal and ventral midlines, maintaining long filament-rich fibers that can still be observed extending all the way to the pia at E18 (Sturrock, 1981). The dorsal fibers of these cells can be traced along the dorsal grey matter even into adulthood, but by P5 their trajectory within the dorsal columns is obscured by white matter (Sturrock, 1981). The functions of these cells during development and adulthood have yet to be identified.

Antigenic differences between cuboidal, tanycytic and radial classes of ependymal cells have not been previously described, and the presence of intermediate phenotypes has led to the suggestion that these classes may actually represent a spectrum (Meletis et al., 2008). The fact that the neural precursor markers Nestin and GFAP are expressed by a sub-population of Vimentin(+) cells raises the possibility of heterogeneity in ependymal cell functions *in vivo*. Although it is established that the neurosphere-forming capacity in the adult spinal cord is derived from ependymal cells (Meletis et al., 2008), it is unclear whether all spinal cord ependymal cells have equivalent stem cell potential. Previous studies have shown that spinal cord injury increases the proportion of ependymal cells that are proliferating (Mothe and Tator, 2005; Meletis et al., 2008), induces ependymal expression of Nestin and to a lesser extent GFAP (Meletis et al., 2008), and stimulates an increase in the number of neurospheres that can be cultured (Xu et al., 2006). We therefore favour the idea that the Nestin(+) dorsal population of ependymal cells is more undifferentiated within the normal *in vivo* context, but that the wider ependymal cell population is capable of entering a stem cell-like state under the appropriate circumstances, that is following *in vitro* culturing or *in vivo* injury.

CONCLUSION

Spinal cord ependymal cells have neural stem cell potential both *in vitro* and following tissue injury *in vivo*. Here, we found that they do not display multilineage potential or the ability to produce transit amplifying progenitors under normal conditions. Analysis of the ependymal cell niche revealed a previously unrecognized level of cellular hetero-

geneity and complexity, and indicated that many of the key elements of the forebrain stem cell niche are in fact present. However, these elements are organized in a distinct fashion. Determining the molecular basis of the cellular interactions occurring within the spinal cord ependymal zone may help us to unlock the stem cell potential of ependymal cells to promote spinal cord repair.

Acknowledgments—This work was supported by funds from the Canadian Foundation for Innovation and the Université de Montréal. KF is a Canada Research Chair in Stem Cell Neurobiology. The authors are grateful to Meriem Bouab for helpful comments, to Dr. Fanie Barnabé-Heider for critical reading of the manuscript, and to Dr. Mustapha Riad and Dr. Laurent Descarries for technical advice.

REFERENCES

Aguirre AA, Chittajallu R, Belachew S, Gallo V (2004) NG2-expressing cells in the subventricular zone are type C-like cells and contribute to interneuron generation in the postnatal hippocampus. J Cell Biol 165:575–589.

Bednarczyk MR, Aumont A, Decary S, Bergeron R, Fernandes KJ (in press) Prolonged voluntary wheel-running stimulates neural precursors in the hippocampus and forebrain of adult CD1 mice. Hippocampus, in press.

Bruni JE, Reddy K (1987) Ependyma of the central canal of the rat spinal cord: a light and transmission electron microscopic study. J Anat 152:55–70.

Chojnacki AK, Mak GK, Weiss S (2009) Identity crisis for adult periventricular neural stem cells: subventricular zone astrocytes, ependymal cells or both? Nat Rev 10:153–163.

Cizkova D, Nagyova M, Slovinska L, Novotna I, Radonak J, Cizek M, Mechirova E, Tomori Z, Hlucilova J, Motlik J, Sulla I Jr, Vanicky I (2009) Response of ependymal progenitors to spinal cord injury or enhanced physical activity in adult rat. Cell Mol Neurobiol 29: 999–1013.

Doetsch F, Caille I, Lim DA, Garcia-Verdugo JM, Alvarez-Buylla A (1999) Subventricular zone astrocytes are neural stem cells in the adult mammalian brain. Cell 97:703–716.

Doetsch F, Garcia-Verdugo JM, Alvarez-Buylla A (1997) Cellular composition and three-dimensional organization of the subventricular germinal zone in the adult mammalian brain. J Neurosci 17: 5046–5061.

Frisen J, Johansson CB, Torok C, Risling M, Lendahl U (1995) Rapid, widespread, and longlasting induction of nestin contributes to the generation of glial scar tissue after CNS injury. J Cell Biol 131: 453–464.

Fuchs E, Tumbar T, Guasch G (2004) Socializing with the neighbors: stem cells and their niche. Cell 116:769–778.

Horner PJ, Power AE, Kempermann G, Kuhn HG, Palmer TD, Winkler J, Thal LJ, Gage FH (2000) Proliferation and differentiation of progenitor cells throughout the intact adult rat spinal cord. J Neurosci 20:2218–2228.

Imura T, Kornblum HI, Sofroniew MV (2003) The predominant neural stem cell isolated from postnatal and adult forebrain but not early embryonic forebrain expresses GFAP. J Neurosci 23:2824–2832.

Johansson CB, Momma S, Clarke DL, Risling M, Lendahl U, Frisen J (1999) Identification of a neural stem cell in the adult mammalian central nervous system. Cell 96:25–34.

Lois C, Alvarez-Buylla A (1994) Long-distance neuronal migration in the adult mammalian brain. Science (New York, NY) 264:1145–1148.

Luo J, Shook BA, Daniels SB, Conover JC (2008) Subventricular zone-mediated ependyma repair in the adult mammalian brain. J Neurosci 28:3804–3813.

Martens DJ, Seaberg RM, van der Kooy D (2002) In vivo infusions of exogenous growth factors into the fourth ventricle of the adult mouse brain increase the proliferation of neural progenitors around the fourth ventricle and the central canal of the spinal cord. Eur J Neurosci 16:1045–1057.

Meletis K, Barnabe-Heider F, Carlen M, Evergren E, Tomilin N, Shupliakov O, Frisen J (2008) Spinal cord injury reveals multilineage differentiation of ependymal cells. PLoS Biol 6:e182.

Mirzadeh Z, Merkle FT, Soriano-Navarro M, Garcia-Verdugo JM, Alvarez-Buylla A (2008) Neural stem cells confer unique pinwheel architecture to the ventricular surface in neurogenic regions of the adult brain. Cell Stem Cell 3:265–278.

Morrison SJ, Spradling AC (2008) Stem cells and niches: mechanisms that promote stem cell maintenance throughout life. Cell 132: 598–611.

Morshead CM, Garcia AD, Sofroniew MV, van Der Kooy D (2003) The ablation of glial fibrillary acidic protein-positive cells from the adult central nervous system results in the loss of forebrain neural stem cells but not retinal stem cells. Eur J Neurosci 18:76–84.

Morshead CM, Reynolds BA, Craig CG, McBurney MW, Staines WA, Morassutti D, Weiss S, van der Kooy D (1994) Neural stem cells in the adult mammalian forebrain: a relatively quiescent subpopulation of subependymal cells. Neuron 13:1071–1082.

Mothe AJ, Tator CH (2005) Proliferation, migration, and differentiation of endogenous ependymal region stem/progenitor cells following minimal spinal cord injury in the adult rat. Neuroscience 131:177–187.

Namiki J, Tator CH (1999) Cell proliferation and nestin expression in the ependyma of the adult rat spinal cord after injury. J Neuropathol Exp Neurol 58:489–498.

Palmer TD, Willhoite AR, Gage FH (2000) Vascular niche for adult hippocampal neurogenesis. J Comp Neurol 425:479–494.

Pastrana E, Cheng LC, Doetsch F (2009) Simultaneous prospective purification of adult subventricular zone neural stem cells and their progeny. Proc Natl Acad Sci U S A 106:6387–6392.

Shen Q, Wang Y, Kokovay E, Lin G, Chuang SM, Goderie SK, Roysam B, Temple S (2008) Adult SVZ stem cells lie in a vascular niche: a quantitative analysis of niche cell-cell interactions. Cell Stem Cell 3:289–300.

Sturrock RR (1981) An electron microscopic study of the development of the ependyma of the central canal of the mouse spinal cord. J Anat 132:119–136.

Tavazoie M, Van Der Veken L, Silva-Vargas V, Louissaint M, Colonna L, Zaidi B, Garcia-Verdugo JM, Doetsch F (2008) A specialized vascular niche for adult neural stem cells. Cell Stem Cell 3: 279–288.

Walker MR, Patel KK, Stappenbeck TS (2009) The stem cell niche. J Pathol 217:169–180.

Weiss S, Dunne C, Hewson J, Wohl C, Wheatley M, Peterson AC, Reynolds BA (1996) Multipotent CNS stem cells are present in the adult mammalian spinal cord and ventricular neuroaxis. J Neurosci 16:7599–7609.

Xu Y, Kitada M, Yamaguchi M, Dezawa M, Ide C (2006) Increase in bFGF-responsive neural progenitor population following contusion injury of the adult rodent spinal cord. Neurosci Lett 397:174–179.

(Accepted 1 September 2009)
(Available online 9 September 2009)